United States
Environmental Protection
Agency

Office of Air Quality
Planning and Standards
Research Triangle Park NC 27711

EPA-450/4-80-031
November 1980

Air

EPA

Workbook for Estimating Visibility Impairment

EPA-450/4-80-031

Workbook for Estimating Visibility Impairment

by

Douglas A. Latimer and Robert G. Ireson

Systems Applications, Inc.
950 Northgate Drive
San Rafael, California 94903

Contract No. 68-02-0337

Prepared for

U.S. ENVIRONMENTAL PROTECTION AGENCY
Office of Air, Noise, and Radiation
Office of Air Quality Planning and Standards
Research Triangle Park, North Carolina 27711

November 1980

This report is issued by the Environmental Protection Agency to report technical data of interest to a limited number of readers. Copies are available - in limited quantities - from the Library Services Office (MD-35), U.S. Environmental Protection Agency, Research Triangle Park, North Carolina 27711; or, for a fee, from the National Technical Information Service, 5285 Port Royal Road, Springfield, Virginia 22161.

Publication No. EPA-450/4-80-031

Preface

This workbook provides screening techniques for assessing visibility impairment from a single emissions source. EPA believes these techniques are at a point where the results should now be employed to assist decision-makers in their assessments. The approach is through a hierarchy of three levels of analysis, somewhat analogous to that in EPA's "Guideline for Air Quality Maintenance Planning and Analysis Volume 10 (Revised): Procedures for Evaluating the Air Quality Impact of New Stationary Sources," EPA-450/4-79-001. Frequent consultation between users and decision-makers is encouraged so that difficulties, misapplications or unjustified interpretations can be avoided.

One option in the level-2 analysis and the level-3 analysis are based on the Plume Visibility Model (PLUVUE) and examples/applications are provided based on output from this model. EPA has also published the "User's Manual for the Plume Visibility Model (PLUVUE),"EPA-450/4-80-032. However, the Agency has not yet recommended any visibility model for routine use in regulatory applications.

ACKNOWLEDGMENTS

The guidance, helpful comments, and the idea for the screening analyses approach contributed by the EPA Project Officers, Steven Eigsti and James Dicke, are much appreciated. William Malm of the EPA's Environ--mental Monitoring and Support Laboratory at Las Vegas deserves thanks for his suggestions regarding the use of contrast and contrast reduction as the basis for this workbook.

The efforts of the authors of the workbook, Douglas A. Latimer and Robert G. Ireson, under Contract No. 68-02-3337 with Systems Applications, Inc., San Rafael, California, are gratefully acknowledged. Also at SAI, Robert Bergstrom and Thomas Ackerman provided the computations based on Mie scattering theory, which are the basis of many of the tables and figures in this report, while Hoi-Ying Holman and Clark Johnson exercised the visibility computer model for the reference tables and figures provided in the appendix.

CONTENTS

Figures..... vi
Tables..... x
Nomenclature..... xiii

1 INTRODUCTION..... 1
1.1 Classes of Visibility Impairment..... 2
1.2 Approach Used in This Workbook..... 4

2 GENERAL CONCEPTS..... 7
2.1 Physical Concepts Related to Visibility Impairment..... 7
2.1.1 Visual Perception..... 7
2.1.2 Fundamental Causes of Visibility Impairment..... 8
2.1.3 Atmospheric Optics..... 11
2.1.4 Plume Visual Impacts..... 16
2.1.5 Characterizing Visibility Impairment..... 19
2.2 Plume-Observer Geometry..... 27
2.3 Characterizing the Frequency Distribution of Plume Visibility Impacts..... 35
2.3.1 Wind Speed..... 39
2.3.2 Wind Direction..... 39
2.3.3 Atmospheric Stability..... 43
2.3.4 Background Ozone Concentration..... 44
2.3.5 Background Visual Range..... 44
2.3.6 Study Area Topography..... 45
2.3.7 Season and Time of Day..... 45
2.3.8 Model Runs..... 45

3 LEVEL-1 VISIBILITY SCREENING ANALYSIS..... 47
3.1 Derivation of Level-1 Screening Analysis..... 47
3.1.1 Impacts of Particulate and NO_x Emissions..... 50
3.1.2 Impacts of SO_2 Emissions..... 53
3.2 Instructions for Level-1 Screening Analysis..... 56
3.3 Example Applications of the Level-1 Analysis..... 61
3.3.1 Example 1..... 61
3.3.2 Example 2..... 63

4	LEVEL-2 VISIBILITY SCREENING ANALYSIS	65
4.1	Identification of Worst-Case Conditions	65
4.1.1	Location of Emissions Source and Class I Area(s)	66
4.1.2	Meteorological Conditions	68
4.1.3	Background Ozone Concentration	89
4.1.4	Background Visual Range	91
4.2	Hand Calculation of Worst-Case Visual Impacts	92
4.2.1	Determining the Geometry of Plume, Observer, Viewing Background, and Sun	93
4.2.2	Calculating Plume Optical Depth	99
4.2.3	Calculating Phase Functions	111
4.2.4	Calculating Plume Contrast and Contrast Reduction	117
4.3	Use of Reference Tables for NO_2 Impacts	119
4.4	Use of Reference Figures for Power Plants	121
4.5	Use of the Computer Model	121
4.6	Example Calculations	121
4.7	Summary of Level-1 and Level-2 Procedures	122
5	SUGGESTIONS FOR DETAILED VISIBILITY IMPACT ANALYSES (LEVEL-3)	131
5.1	Frequency of Occurrence of Impact	132
5.2	Appearance of Impacts	133
5.3	Impacts on Scenic Beauty	141
5.4	Impacts of Existing Emissions Sources	143
5.5	Regional Impacts	144

APPENDIXES

A	CHARACTERIZING GENERAL HAZE	147
A.1	Wavelength Dependence	147
A.2	The Contrast Formula	148
A.3	Quantifying Increases in Atmospheric Haze	149
A.3.1	Plume Impacts	150
A.3.2	Regional Haze Impacts	153
A.4	The Effect of Increased Haze on the Contrast of Landscape Features	153
A.5	Summary	156
B	PHASE FUNCTIONS	161
C	PLUME DISCOLORATION PARAMETERS FOR VARIOUS NO_2 LINE-OF-SIGHT INTEGRALS AND BACKGROUND CONDITIONS	189
D	REFERENCE FIGURES AND TABLES FOR POWER PLANT VISUAL IMPACTS	241

E TWO EXAMPLE APPLICATIONS OF THE LEVEL-1 AND LEVEL-2 ANALYSES..... 323
E.1 Example 1--Coal-Fired Power Plant..... 323
E.1.1 Level-1 Analysis..... 323
E.1.2 Level-2 Analysis..... 326
E.1.3 Calculation of Plume Optical Depth..... 342
E.1.4 Phase Function Calculations..... 348
E.1.5 Calculating Plume Contrasts..... 352
E.1.6 Calculating Reduction in Sky/Terrain Contrast Caused by Plume..... 355
E.1.7 General Haze Effects..... 356
E.1.8 Comparison of Results with Reference Tables..... 357
E.2 Example 2--Cement Plant and Related Operations..... 359
E.2.1 Level-1 Analysis..... 359
E.2.2 Level-2 Analysis..... 362

REFERENCES..... 371

FIGURES

1	Schematic of Visibility Screening Analysis Procedure.....	5
2	Effect of an Atmosphere on the Perceived Light Intensity of Objects.....	13
3	Object-Observer Geometry with Plume.....	17
4	Five Basic Situations in Which Air Pollution is Visually Perceptible.....	20
5	Plan View of Observer-Plume Geometry.....	28
6	Elevation View of Observer-Plume Geometry.....	29
7	Plan View of Four Possible Plume Parcel Trajectories That Would Transport Emissions from a Source to Affect a Vista in a Class I Area.....	34
8	Example of a Frequency Distribution of Visual Impact.....	37
9	Schematic Diagram Showing Plume-Observer Geometry for Two Wind Directions.....	41
10	Two Types of Plume Visibility Impairment Considered in the Level-1 Visibility Screening Analysis.....	48
11	Geometry of Plume, Observer, and Line of Sight Used in Level-1 Visibility Screening Analysis.....	48
12	Vertical Dispersion Coefficient (σ_z) as a Function of Downwind Distance from the Source.....	57
13	Regional Background Visual Range Values (r_{v0}) for Use in Level-1 Visibility Screening Analysis.....	59
14	Example of Map Showing Emissions Source, Class I Areas, and Stable Plume Trajectories.....	69

15 Examples of Terrain Elevation Plots..... 70

16 Joint Frequency Distribution Tables Required to Estimate Worst-Case Meteorological Conditions for Plume Discoloration..... 75

17 Schematic Diagram Showing Emissions Source, Observer Locations, and Wind Direction Sectors..... 77

18 Joint Frequency Distribution Tables Required to Estimate Worst-Case Meteorological Conditions for Visibility Impairment Due to SO_2 Emissions..... 83

19 Example Map Showing Class I Areas in Region Around Emissions Source and Wind Direction/Speed Sectors..... 86

20 A Schematic of the Vertical O_3 Structure and Its Diurnal and Seasonal Variations at Remote Sites..... 90

21 Locus of Plume Centerlines within Worst-Case Wind Direction Sector..... 94

22 Observer-Plume Orientation for Level-2 Visibility Screening Analysis..... 96

23 Plan View of Assumed Plume-Observer Geometry for Level-2 Visibility Screening Calculations..... 93

24 Scattering-to-Volume Ratios for Various Size Distributions..... 101

25 Wavelength Dependence of Light Absorption of Nitrogen Dioxide..... 108

26 Phase Functions for Various Particle Size Distributions..... 113

27 Logic Flow Diagram for Level-1 Analysis..... 123

28 Logic Flow Diagram for Level-2 Analysis..... 124

29 Examples of Predicted Frequency of Occurrence of Plume Discoloration Perceptible from a Class I Area: Number of Mornings in the Designated Season with an Impact Greater than the Indicated Value..... 134

30 Examples of Predicted Frequency of Occurrence of Haze (Visual Range Reduction) in a Class I Area: Number of Afternoons in the Desginated Season with an Impact Greater than the Indicated Value..... 135

31 Examples of Calculated Plume Visibility Impairment Dependent on Wind Direction, Azimuth of Line of Sight, and Viewing Background..... 136

32 Example of Black and White Plume-Terrain Perspective..... 142

A-1 Two Types of Spatial Distributions of Extra Extinction..... 151

A-2 Change in Sky/Terrain Contrast as a Function of Fractional Increase in Extinction Coefficient for Various Observer-Terrain Distances..... 157

A-3 Change in Sky/Terrain Contrast as a Function of Fractional Decrease in Visual Range for Various Observer-Terrain Distances..... 158

A-4 Change in Sky/Terrain Contrast as a Function of Plume Optical Thickness for Various Observer-Terrain Distances..... 159

E-1 Relative Location of the Proposed Power Plant and Class I Area for Example 1..... 324

E-2 Significant Terrain Features and Possible Plume Trajectories..... 329

E-3 Terrain Elevation Plots..... 330

E-4 Class I Areas within 48-Hour Transport Range at Wind Speeds up to 8 m/s..... 333

E-5 Worksheet for the Calculation of Wind Speed and Mixing Depth Joint Frequency Distribution..... 335

E-6 Observer-Plume Orientations..... 337

E-7 Plan View of Assumed Geometries for Views 1 and 2..... 338

E-8 Plan View of Assumed Geometry for View 3..... 339

TABLES

1	Example Table Showing Worst-Case Meteorological Conditions for Plume Discoloration Calculations.....	78
2	Example Table Showing Worst-Case Limited Mixing Conditions for Haze Calculations.....	84
3	Example Tables Showing Computations of Days in a Five-Year Period with the Given Limited Mixing Condition.....	88
4	Wavelength Dependence of Scattering Coefficient as a Function of Particle Size Distribution.....	104
5	Example Table Showing Background Atmosphere Phase Functions and Scattering Coefficients.....	116
6	Example Summary of the Frequency of Occurrence of Power Plant Plume Discoloration Perceptible from a Class I Area.....	139
7	Example Summary of Frequency of Occurrence of Increased Haze (Visual Range Reduction) in a Class I Area Due to Power Plant Emissions.....	140
A-1	Summary of Relationships among Parameters Used for Quantifying Increased Atmospheric Haze.....	160
E-1	Frequency of Occurrence of SW and WSW Winds by Dispersion Condition and Time of Day.....	332
E-2	Frequency of Episode Days by Mixing Depth and Wind Speed.....	334
E-3	Values of Θ_{ij}.....	343
E-4	Phase Functions and Scattering Coefficients for Background and Plume.....	351

E-5 Comparison of Example Power Plant Emissions and Appendix D Power Plant Emissions..... 357

E-6 Comparison of Selected Scenario Descriptors..... 357

E-7 Example 2--Cement Plant and Related Operations..... 360

E-8 Background and Plume atmosphere Phase Functions and Scattering Coefficients..... 368

E-9 Projected Plume Contrast and Contrast Reduction for Example 2..... 370

NOMENCLATURE

A -- Azimuth angle of line of sight, relative to north

b_{abs} -- Light absorption coefficient of the air parcel, proportional to concentrations of nitrogen dioxide (NO_2) and aerosol (like soot) that absorb visible radiation (m^{-1})

b_{ext} -- Light extinction coefficient of an air parcel, the sum of absorption and scattering coefficients (m^{-1})

b_R -- Light scattering coefficient of particle-free air caused by Rayleigh scatter from air molecules (m^{-1})

b_{scat} -- Light scattering coefficient resulting from Rayleigh scatter (air molecules) and Mie scatter (particles), the sum of b_R and b_{sp} (m^{-1})

(b_{scat}/V) -- Light scattering efficiency per unit aerosol volume concentration (m^{-1})

b_{sp} -- Light scattering coefficient caused by particles only (m^{-1})

C -- Contrast at a given wavelength of two colored objects, like plume/sky or sky/terrain

C_{haze} -- Contrast of a haze layer against the sky above it

C_{min} -- Contrast that is just perceptible, a threshold contrast

C_{plume} -- Contrast of a plume against a viewing background like the sky on a terrain feature

C_r -- Contrast of a terrain feature at distance r against the sky

ΔC_r -- Change in sky/terrain contrast caused by a plume or extra extinction

C_0 -- Intrinsic contrast of a terrain feature against the sky. The sky/terrain contrast at $r = 0$. For a black object, $C_0 = -1$.

D -- Stack diameter (m)

$\Delta E(L^*a^*b^*)$ -- Color difference parameter used to characterize the perceptibility of the difference between two colors. In the context of this workbook, it is used to characterize the perceptibility of a plume on the basis of the color difference between the plume and a viewing background like the sky, a cloud, or a terrain feature. Color differences are due to differences in three dimensions: brightness (L^*) and color hue and saturation (a^*b^*)

F -- Buoyancy flux of flue gas emissions from a stack ($m^4 s^{-3}$)

F_s -- Solar insolation or flux incident on an air parcel within a given wavelength band (watt m^{-2} μm^{-1})

f_{obj} -- Fraction of total plume optical thickness between an observer and a viewed object

g -- Gravitational acceleration ($\cong 9.8$ m s^{-2})

H -- Plume altitude above the ground (m)

H_m -- Height of a mixed layer above the ground (m)

h_{stack} -- Height of a stack (m)

Δh -- Plume rise (m)

I -- Light intensity or radiance for a given line of sight and wavelength band (watt $m^{-2} sr^{-1} \mu m^{-1}$). Subscripts t and h refer to terrain and horizon, respectively.

I_{obj} -- Light intensity reflected from an object like a terrain feature (watt $m^{-2} sr^{-1} \mu m^{-1}$)

k_d -- Rate constant for surface deposition (s^{-1})

k_f -- Rate constant for SO_2-to-$SO_4^=$ conversion (s^{-1})

p -- Atmospheric dispersion parameter used in the level-1 analysis to calculate the horizontal line-of-sight integral of a plume concentration (s m^{-2})

$p(\lambda,\Theta)$ -- Phase function, a parameter that relates the portion of total scattered light of a given wavelength λ that is scattered in a given direction specified by the scattering angle Θ

Q -- Emission rate of a species, such as SO_2, or plume flux at a given downwind distance, which may be less than the emission rate because of surface deposition and chemical conversion (g s^{-1}). Subscripts refer to species considered (e.g., SO_2, $SO_4^=$, and particulate)

Q_{scat} -- Plume flux of the scattering coefficient above background ($m^2 s^{-1}$). Subscripts refer to species considered (e.g., $SO_4^=$, primary particulate)

R -- Blue-red ratio used in visibility impairment calculations to characterize the coloration of a plume relative to the viewing background

RH -- Relative background humidity (percent)

r -- Distance along the line of sight from the viewed object to the observer (m)

r_o -- Object-observer distance (m)

r_p -- Distance from observer to centroid of plume material (m)

r_q -- Distance from viewed object to centroid of plume material (m)

r_v -- Visual range, a parameter characteristic of the clarity of the atmosphere, inversely proportional to the extinction coefficient. H is farthest distance at which a black object is perceptible against the horizon sky (m)

r_{vO} -- Background visual range without plume (m)

T -- Temperature in degrees absolute

t -- Time (s)

u -- Wind speed (m s^{-1})

$\dot{V}$ -- Flue gas volumetric flow rate ($m^3 s^{-1}$)

$\bar{v}$ -- Wind velocity vector (m s^{-1})

ΔV-- Percentage visual range reduction

v_d -- Deposition velocity (m s^{-1})

WD -- Wind direction

x -- Downwind distance from emissions source (m)

y -- Cross-wind direction from plume centerline (m)

Z_{site} -- Elevation of a site above mean sea level (m)

Z_{block} -- Elevation of the terrain above mean sea level that can be assumed to block the flow of emissions (m)

Z_s -- Solar zenith angle, the angle between the sun and the normal to the earth's surface

z -- Distance above ground (m)

λ -- Wavelength of light (m)

ρ -- Density of a particle (g m^{-3})

α -- Horizontal angle between a line of sight and the plume centerline

β -- Vertical angle between a line of sight and the horizontal

χ -- Concentration of a given species in an air parcel (g m^{-3})

τ -- Optical thickness of a plume, the line-of-sight integral of the extinction coefficient. Subscripts refer to the component of the total or plume optical thickness (e.g., particulate, $SO_4^=$, NO_2)

[ ] -- Denotes the concentration of the species within brackets

ω -- Albedo of the plume or background atmosphere, the ratio of the scattering coefficient to the extinction coefficient

θ -- Scattering angle, the angle between direct solar radiation and the line of sight. If the observer were looking directly at the sun, θ would equal 0°. If the observer looked away from the sun, θ would equal 180°.

Q -- Emission rate of a species, such as SO_2, or plume flux at a given downwind distance, which may be less than the emission rate because of surface deposition and chemical conversion (g s^{-1}). Subscripts refer to species considered (e.g., SO_2, $SO_4^=$, and particulate)

Q_{scat} -- Plume flux of the scattering coefficient above background ($m^2 s^{-1}$). Subscripts refer to species considered (e.g., $SO_4^=$, primary particulate)

R -- Blue-red ratio used in visibility impairment calculations to characterize the coloration of a plume relative to the viewing background

RH -- Relative background humidity (percent)

r -- Distance along the line of sight from the viewed object to the observer (m)

r_o -- Object-observer distance (m)

r_p -- Distance from observer to centroid of plume material (m)

r_q -- Distance from viewed object to centroid of plume material (m)

r_v -- Visual range, a parameter characteristic of the clarity of the atmosphere, inversely proportional to the extinction coefficient. H is farthest distance at which a black object is perceptible against the horizon sky (m)

r_{vO} -- Background visual range without plume (m)

T -- Temperature in degrees absolute

t -- Time (s)

u -- Wind speed (m s^{-1})

$\dot{V}$ -- Flue gas volumetric flow rate ($m^3 s^{-1}$)

$\bar{v}$ -- Wind velocity vector (m s^{-1})

ΔV-- Percentage visual range reduction

v_d -- Deposition velocity (m s^{-1})

WD -- Wind direction

x -- Downwind distance from emissions source (m)

y -- Cross-wind direction from plume centerline (m)

Z_{site} -- Elevation of a site above mean sea level (m)

Z_{block} -- Elevation of the terrain above mean sea level that can be assumed to block the flow of emissions (m)

Z_s -- Solar zenith angle, the angle between the sun and the normal to the earth's surface

z -- Distance above ground (m)

λ -- Wavelength of light (m)

ρ -- Density of a particle (g m^{-3})

α -- Horizontal angle between a line of sight and the plume centerline

β -- Vertical angle between a line of sight and the horizontal

χ -- Concentration of a given species in an air parcel (g m^{-3})

τ -- Optical thickness of a plume, the line-of-sight integral of the extinction coefficient. Subscripts refer to the component of the total or plume optical thickness (e.g., particulate, $SO_4^=$, NO_2)

[ ] -- Denotes the concentration of the species within brackets

ω -- Albedo of the plume or background atmosphere, the ratio of the scattering coefficient to the extinction coefficient

θ -- Scattering angle, the angle between direct solar radiation and the line of sight. If the observer were looking directly at the sun, θ would equal 0°. If the observer looked away from the sun, θ would equal 180°.

Q -- Emission rate of a species, such as SO_2, or plume flux at a given downwind distance, which may be less than the emission rate because of surface deposition and chemical conversion (g s^{-1}). Subscripts refer to species considered (e.g., SO_2, $SO_4^=$, and particulate)

Q_{scat} -- Plume flux of the scattering coefficient above background ($m^2 s^{-1}$). Subscripts refer to species considered (e.g., $SO_4^=$, primary particulate)

R -- Blue-red ratio used in visibility impairment calculations to characterize the coloration of a plume relative to the viewing background

RH -- Relative background humidity (percent)

r -- Distance along the line of sight from the viewed object to the observer (m)

r_o -- Object-observer distance (m)

r_p -- Distance from observer to centroid of plume material (m)

r_q -- Distance from viewed object to centroid of plume material (m)

r_v -- Visual range, a parameter characteristic of the clarity of the atmosphere, inversely proportional to the extinction coefficient. H is farthest distance at which a black object is perceptible against the horizon sky (m)

r_{vO} -- Background visual range without plume (m)

T -- Temperature in degrees absolute

t -- Time (s)

u -- Wind speed (m s^{-1})

$\dot{V}$ -- Flue gas volumetric flow rate ($m^3 s^{-1}$)

$\bar{v}$ -- Wind velocity vector (m s^{-1})

ΔV-- Percentage visual range reduction

v_d -- Deposition velocity (m s^{-1})

WD -- Wind direction

x -- Downwind distance from emissions source (m)

y -- Cross-wind direction from plume centerline (m)

Z_{site} -- Elevation of a site above mean sea level (m)

Z_{block} -- Elevation of the terrain above mean sea level that can be assumed to block the flow of emissions (m)

Z_s -- Solar zenith angle, the angle between the sun and the normal to the earth's surface

z -- Distance above ground (m)

λ -- Wavelength of light (m)

ρ -- Density of a particle (g m^{-3})

α -- Horizontal angle between a line of sight and the plume centerline

β -- Vertical angle between a line of sight and the horizontal

χ -- Concentration of a given species in an air parcel (g m^{-3})

τ -- Optical thickness of a plume, the line-of-sight integral of the extinction coefficient. Subscripts refer to the component of the total or plume optical thickness (e.g., particulate, $SO_4^=$, NO_2)

[ ] -- Denotes the concentration of the species within brackets

ω -- Albedo of the plume or background atmosphere, the ratio of the scattering coefficient to the extinction coefficient

θ -- Scattering angle, the angle between direct solar radiation and the line of sight. If the observer were looking directly at the sun, θ would equal 0°. If the observer looked away from the sun, θ would equal 180°.

Q -- Emission rate of a species, such as SO_2, or plume flux at a given downwind distance, which may be less than the emission rate because of surface deposition and chemical conversion (g s^{-1}). Subscripts refer to species considered (e.g., SO_2, $SO_4^=$, and particulate)

Q_{scat} -- Plume flux of the scattering coefficient above background ($m^2 s^{-1}$). Subscripts refer to species considered (e.g., $SO_4^=$, primary particulate)

R -- Blue-red ratio used in visibility impairment calculations to characterize the coloration of a plume relative to the viewing background

RH -- Relative background humidity (percent)

r -- Distance along the line of sight from the viewed object to the observer (m)

r_o -- Object-observer distance (m)

r_p -- Distance from observer to centroid of plume material (m)

r_q -- Distance from viewed object to centroid of plume material (m)

r_v -- Visual range, a parameter characteristic of the clarity of the atmosphere, inversely proportional to the extinction coefficient. H is farthest distance at which a black object is perceptible against the horizon sky (m)

r_{vO} -- Background visual range without plume (m)

T -- Temperature in degrees absolute

t -- Time (s)

u -- Wind speed (m s^{-1})

$\dot{V}$ -- Flue gas volumetric flow rate ($m^3 s^{-1}$)

$\bar{v}$ -- Wind velocity vector (m s^{-1})

ΔV-- Percentage visual range reduction

v_d -- Deposition velocity (m s^{-1})

WD -- Wind direction

x -- Downwind distance from emissions source (m)

y -- Cross-wind direction from plume centerline (m)

Z_{site} -- Elevation of a site above mean sea level (m)

Z_{block} -- Elevation of the terrain above mean sea level that can be assumed to block the flow of emissions (m)

Z_s -- Solar zenith angle, the angle between the sun and the normal to the earth's surface

z -- Distance above ground (m)

λ -- Wavelength of light (m)

ρ -- Density of a particle (g m^{-3})

α -- Horizontal angle between a line of sight and the plume centerline

β -- Vertical angle between a line of sight and the horizontal

χ -- Concentration of a given species in an air parcel (g m^{-3})

τ -- Optical thickness of a plume, the line-of-sight integral of the extinction coefficient. Subscripts refer to the component of the total or plume optical thickness (e.g., particulate, $SO_4^=$, NO_2)

[ ] -- Denotes the concentration of the species within brackets

ω -- Albedo of the plume or background atmosphere, the ratio of the scattering coefficient to the extinction coefficient

θ -- Scattering angle, the angle between direct solar radiation and the line of sight. If the observer were looking directly at the sun, θ would equal 0°. If the observer looked away from the sun, θ would equal 180°.

Q -- Emission rate of a species, such as SO_2, or plume flux at a given downwind distance, which may be less than the emission rate because of surface deposition and chemical conversion (g s^{-1}). Subscripts refer to species considered (e.g., SO_2, $SO_4^=$, and particulate)

Q_{scat} -- Plume flux of the scattering coefficient above background ($m^2 s^{-1}$). Subscripts refer to species considered (e.g., $SO_4^=$, primary particulate)

R -- Blue-red ratio used in visibility impairment calculations to characterize the coloration of a plume relative to the viewing background

RH -- Relative background humidity (percent)

r -- Distance along the line of sight from the viewed object to the observer (m)

r_o -- Object-observer distance (m)

r_p -- Distance from observer to centroid of plume material (m)

r_q -- Distance from viewed object to centroid of plume material (m)

r_v -- Visual range, a parameter characteristic of the clarity of the atmosphere, inversely proportional to the extinction coefficient. H is farthest distance at which a black object is perceptible against the horizon sky (m)

r_{vO} -- Background visual range without plume (m)

T -- Temperature in degrees absolute

t -- Time (s)

u -- Wind speed (m s^{-1})

$\dot{V}$ -- Flue gas volumetric flow rate ($m^3 s^{-1}$)

$\bar{v}$ -- Wind velocity vector (m s^{-1})

ΔV-- Percentage visual range reduction

v_d -- Deposition velocity (m s^{-1})

WD -- Wind direction

x -- Downwind distance from emissions source (m)

y -- Cross-wind direction from plume centerline (m)

Z_{site} -- Elevation of a site above mean sea level (m)

Z_{block} -- Elevation of the terrain above mean sea level that can be assumed to block the flow of emissions (m)

Z_s -- Solar zenith angle, the angle between the sun and the normal to the earth's surface

z -- Distance above ground (m)

λ -- Wavelength of light (m)

ρ -- Density of a particle (g m^{-3})

α -- Horizontal angle between a line of sight and the plume centerline

β -- Vertical angle between a line of sight and the horizontal

χ -- Concentration of a given species in an air parcel (g m^{-3})

τ -- Optical thickness of a plume, the line-of-sight integral of the extinction coefficient. Subscripts refer to the component of the total or plume optical thickness (e.g., particulate, $SO_4^=$, NO_2)

[ ] -- Denotes the concentration of the species within brackets

ω -- Albedo of the plume or background atmosphere, the ratio of the scattering coefficient to the extinction coefficient

θ -- Scattering angle, the angle between direct solar radiation and the line of sight. If the observer were looking directly at the sun, θ would equal 0°. If the observer looked away from the sun, θ would equal 180°.

Q -- Emission rate of a species, such as SO_2, or plume flux at a given downwind distance, which may be less than the emission rate because of surface deposition and chemical conversion (g s^{-1}). Subscripts refer to species considered (e.g., SO_2, $SO_4^=$, and particulate)

Q_{scat} -- Plume flux of the scattering coefficient above background ($m^2 s^{-1}$). Subscripts refer to species considered (e.g., $SO_4^=$, primary particulate)

R -- Blue-red ratio used in visibility impairment calculations to characterize the coloration of a plume relative to the viewing background

RH -- Relative background humidity (percent)

r -- Distance along the line of sight from the viewed object to the observer (m)

r_o -- Object-observer distance (m)

r_p -- Distance from observer to centroid of plume material (m)

r_q -- Distance from viewed object to centroid of plume material (m)

r_v -- Visual range, a parameter characteristic of the clarity of the atmosphere, inversely proportional to the extinction coefficient. H is farthest distance at which a black object is perceptible against the horizon sky (m)

r_{vO} -- Background visual range without plume (m)

T -- Temperature in degrees absolute

t -- Time (s)

u -- Wind speed (m s^{-1})

$\dot{V}$ -- Flue gas volumetric flow rate ($m^3 s^{-1}$)

$\bar{v}$ -- Wind velocity vector (m s^{-1})

ΔV-- Percentage visual range reduction

v_d -- Deposition velocity (m s^{-1})

WD -- Wind direction

x -- Downwind distance from emissions source (m)

y -- Cross-wind direction from plume centerline (m)

Z_{site} -- Elevation of a site above mean sea level (m)

Z_{block} -- Elevation of the terrain above mean sea level that can be assumed to block the flow of emissions (m)

Z_s -- Solar zenith angle, the angle between the sun and the normal to the earth's surface

z -- Distance above ground (m)

λ -- Wavelength of light (m)

ρ -- Density of a particle (g m^{-3})

α -- Horizontal angle between a line of sight and the plume centerline

β -- Vertical angle between a line of sight and the horizontal

χ -- Concentration of a given species in an air parcel (g m^{-3})

τ -- Optical thickness of a plume, the line-of-sight integral of the extinction coefficient. Subscripts refer to the component of the total or plume optical thickness (e.g., particulate, $SO_4^=$, NO_2)

[ ] -- Denotes the concentration of the species within brackets

ω -- Albedo of the plume or background atmosphere, the ratio of the scattering coefficient to the extinction coefficient

θ -- Scattering angle, the angle between direct solar radiation and the line of sight. If the observer were looking directly at the sun, θ would equal 0°. If the observer looked away from the sun, θ would equal 180°.

Q -- Emission rate of a species, such as SO_2, or plume flux at a given downwind distance, which may be less than the emission rate because of surface deposition and chemical conversion (g s^{-1}). Subscripts refer to species considered (e.g., SO_2, $SO_4^=$, and particulate)

Q_{scat} -- Plume flux of the scattering coefficient above background ($m^2 s^{-1}$). Subscripts refer to species considered (e.g., $SO_4^=$, primary particulate)

R -- Blue-red ratio used in visibility impairment calculations to characterize the coloration of a plume relative to the viewing background

RH -- Relative background humidity (percent)

r -- Distance along the line of sight from the viewed object to the observer (m)

r_o -- Object-observer distance (m)

r_p -- Distance from observer to centroid of plume material (m)

r_q -- Distance from viewed object to centroid of plume material (m)

r_v -- Visual range, a parameter characteristic of the clarity of the atmosphere, inversely proportional to the extinction coefficient. H is farthest distance at which a black object is perceptible against the horizon sky (m)

r_{vO} -- Background visual range without plume (m)

T -- Temperature in degrees absolute

t -- Time (s)

u -- Wind speed (m s^{-1})

$\dot{V}$ -- Flue gas volumetric flow rate ($m^3 s^{-1}$)

$\bar{v}$ -- Wind velocity vector (m s^{-1})

ΔV-- Percentage visual range reduction

v_d -- Deposition velocity (m s^{-1})

WD -- Wind direction

x -- Downwind distance from emissions source (m)

y -- Cross-wind direction from plume centerline (m)

Z_{site} -- Elevation of a site above mean sea level (m)

Z_{block} -- Elevation of the terrain above mean sea level that can be assumed to block the flow of emissions (m)

Z_s -- Solar zenith angle, the angle between the sun and the normal to the earth's surface

z -- Distance above ground (m)

λ -- Wavelength of light (m)

ρ -- Density of a particle (g m^{-3})

α -- Horizontal angle between a line of sight and the plume centerline

β -- Vertical angle between a line of sight and the horizontal

χ -- Concentration of a given species in an air parcel (g m^{-3})

τ -- Optical thickness of a plume, the line-of-sight integral of the extinction coefficient. Subscripts refer to the component of the total or plume optical thickness (e.g., particulate, $SO_4^=$, NO_2)

[ ] -- Denotes the concentration of the species within brackets

ω -- Albedo of the plume or background atmosphere, the ratio of the scattering coefficient to the extinction coefficient

θ -- Scattering angle, the angle between direct solar radiation and the line of sight. If the observer were looking directly at the sun, θ would equal 0°. If the observer looked away from the sun, θ would equal 180°.

Q -- Emission rate of a species, such as SO_2, or plume flux at a given downwind distance, which may be less than the emission rate because of surface deposition and chemical conversion (g s^{-1}). Subscripts refer to species considered (e.g., SO_2, $SO_4^=$, and particulate)

Q_{scat} -- Plume flux of the scattering coefficient above background ($m^2 s^{-1}$). Subscripts refer to species considered (e.g., $SO_4^=$, primary particulate)

R -- Blue-red ratio used in visibility impairment calculations to characterize the coloration of a plume relative to the viewing background

RH -- Relative background humidity (percent)

r -- Distance along the line of sight from the viewed object to the observer (m)

r_o -- Object-observer distance (m)

r_p -- Distance from observer to centroid of plume material (m)

r_q -- Distance from viewed object to centroid of plume material (m)

r_v -- Visual range, a parameter characteristic of the clarity of the atmosphere, inversely proportional to the extinction coefficient. H is farthest distance at which a black object is perceptible against the horizon sky (m)

r_{vO} -- Background visual range without plume (m)

T -- Temperature in degrees absolute

t -- Time (s)

u -- Wind speed (m s^{-1})

$\dot{V}$ -- Flue gas volumetric flow rate ($m^3 s^{-1}$)

$\bar{v}$ -- Wind velocity vector (m s^{-1})

ΔV-- Percentage visual range reduction

v_d -- Deposition velocity (m s^{-1})

WD -- Wind direction

x -- Downwind distance from emissions source (m)

y -- Cross-wind direction from plume centerline (m)

Z_{site} -- Elevation of a site above mean sea level (m)

Z_{block} -- Elevation of the terrain above mean sea level that can be assumed to block the flow of emissions (m)

Z_s -- Solar zenith angle, the angle between the sun and the normal to the earth's surface

z -- Distance above ground (m)

λ -- Wavelength of light (m)

ρ -- Density of a particle (g m^{-3})

α -- Horizontal angle between a line of sight and the plume centerline

β -- Vertical angle between a line of sight and the horizontal

χ -- Concentration of a given species in an air parcel (g m^{-3})

τ -- Optical thickness of a plume, the line-of-sight integral of the extinction coefficient. Subscripts refer to the component of the total or plume optical thickness (e.g., particulate, $SO_4^=$, NO_2)

[ ] -- Denotes the concentration of the species within brackets

ω -- Albedo of the plume or background atmosphere, the ratio of the scattering coefficient to the extinction coefficient

θ -- Scattering angle, the angle between direct solar radiation and the line of sight. If the observer were looking directly at the sun, θ would equal 0°. If the observer looked away from the sun, θ would equal 180°.

Q -- Emission rate of a species, such as SO_2, or plume flux at a given downwind distance, which may be less than the emission rate because of surface deposition and chemical conversion (g s^{-1}). Subscripts refer to species considered (e.g., SO_2, $SO_4^=$, and particulate)

Q_{scat} -- Plume flux of the scattering coefficient above background ($m^2 s^{-1}$). Subscripts refer to species considered (e.g., $SO_4^=$, primary particulate)

R -- Blue-red ratio used in visibility impairment calculations to characterize the coloration of a plume relative to the viewing background

RH -- Relative background humidity (percent)

r -- Distance along the line of sight from the viewed object to the observer (m)

r_o -- Object-observer distance (m)

r_p -- Distance from observer to centroid of plume material (m)

r_q -- Distance from viewed object to centroid of plume material (m)

r_v -- Visual range, a parameter characteristic of the clarity of the atmosphere, inversely proportional to the extinction coefficient. H is farthest distance at which a black object is perceptible against the horizon sky (m)

r_{vO} -- Background visual range without plume (m)

T -- Temperature in degrees absolute

t -- Time (s)

u -- Wind speed (m s^{-1})

$\dot{V}$ -- Flue gas volumetric flow rate ($m^3 s^{-1}$)

$\bar{v}$ -- Wind velocity vector (m s^{-1})

ΔV-- Percentage visual range reduction

v_d -- Deposition velocity (m s^{-1})

WD -- Wind direction

x -- Downwind distance from emissions source (m)

y -- Cross-wind direction from plume centerline (m)

Z_{site} -- Elevation of a site above mean sea level (m)

Z_{block} -- Elevation of the terrain above mean sea level that can be assumed to block the flow of emissions (m)

Z_s -- Solar zenith angle, the angle between the sun and the normal to the earth's surface

z -- Distance above ground (m)

λ -- Wavelength of light (m)

ρ -- Density of a particle (g m^{-3})

α -- Horizontal angle between a line of sight and the plume centerline

β -- Vertical angle between a line of sight and the horizontal

χ -- Concentration of a given species in an air parcel (g m^{-3})

τ -- Optical thickness of a plume, the line-of-sight integral of the extinction coefficient. Subscripts refer to the component of the total or plume optical thickness (e.g., particulate, $SO_4^=$, NO_2)

[ ] -- Denotes the concentration of the species within brackets

ω -- Albedo of the plume or background atmosphere, the ratio of the scattering coefficient to the extinction coefficient

θ -- Scattering angle, the angle between direct solar radiation and the line of sight. If the observer were looking directly at the sun, θ would equal 0°. If the observer looked away from the sun, θ would equal 180°.

Q -- Emission rate of a species, such as SO_2, or plume flux at a given downwind distance, which may be less than the emission rate because of surface deposition and chemical conversion (g s^{-1}). Subscripts refer to species considered (e.g., SO_2, $SO_4^=$, and particulate)

Q_{scat} -- Plume flux of the scattering coefficient above background ($m^2 s^{-1}$). Subscripts refer to species considered (e.g., $SO_4^=$, primary particulate)

R -- Blue-red ratio used in visibility impairment calculations to characterize the coloration of a plume relative to the viewing background

RH -- Relative background humidity (percent)

r -- Distance along the line of sight from the viewed object to the observer (m)

r_o -- Object-observer distance (m)

r_p -- Distance from observer to centroid of plume material (m)

r_q -- Distance from viewed object to centroid of plume material (m)

r_v -- Visual range, a parameter characteristic of the clarity of the atmosphere, inversely proportional to the extinction coefficient. H is farthest distance at which a black object is perceptible against the horizon sky (m)

r_{vO} -- Background visual range without plume (m)

T -- Temperature in degrees absolute

t -- Time (s)

u -- Wind speed (m s^{-1})

$\dot{V}$ -- Flue gas volumetric flow rate ($m^3 s^{-1}$)

$\bar{v}$ -- Wind velocity vector (m s^{-1})

ΔV-- Percentage visual range reduction

v_d -- Deposition velocity (m s^{-1})

WD -- Wind direction

x -- Downwind distance from emissions source (m)

y -- Cross-wind direction from plume centerline (m)

Z_{site} -- Elevation of a site above mean sea level (m)

Z_{block} -- Elevation of the terrain above mean sea level that can be assumed to block the flow of emissions (m)

Z_s -- Solar zenith angle, the angle between the sun and the normal to the earth's surface

z -- Distance above ground (m)

λ -- Wavelength of light (m)

ρ -- Density of a particle (g m^{-3})

α -- Horizontal angle between a line of sight and the plume centerline

β -- Vertical angle between a line of sight and the horizontal

χ -- Concentration of a given species in an air parcel (g m^{-3})

τ -- Optical thickness of a plume, the line-of-sight integral of the extinction coefficient. Subscripts refer to the component of the total or plume optical thickness (e.g., particulate, $SO_4^=$, NO_2)

[ ] -- Denotes the concentration of the species within brackets

ω -- Albedo of the plume or background atmosphere, the ratio of the scattering coefficient to the extinction coefficient

θ -- Scattering angle, the angle between direct solar radiation and the line of sight. If the observer were looking directly at the sun, θ would equal 0°. If the observer looked away from the sun, θ would equal 180°.

1 INTRODUCTION

The Clean Air Act Amendments of 1977 require evaluation of new and existing emissions sources to determine potential impacts on visibility in class I areas.* These source evaluations are to be used as part of a regulatory program to prevent future and remedy existing impairment of visibility in mandatory class I federal areas that results from man-made air pollution.

This workbook is designed to provide the air pollution analyst with technical guidance in determining the potential impacts of an emissions source on class I area visibility. It should be useful in siting studies, emissions control specification, environmental impact statements, and new source reviews, and it may also be used in conjunction with measurements of existing emissions sources to assess the potential requirements for emissions control retrofit technology. It is beyond the scope of this document to address the cumulative impacts of multiple sources on regional haze. Rather, the emphasis is on the incremental visual impact of a single emissions source.

Although this workbook can be used independently, we highly recommend that the analyst read the following documents:

> U.S. Environmental Protection Agency (October 1979), "Protecting Visibility: An EPA Report to Congress," EPA-450/5-79-008, U.S. Environmental Protection Agency, Research Triangle Park, North Carolina.

> Latimer, D. A., et al. (September 1978), "The Development of Mathematical Models for the Prediction of Anthropogenic Visibility Impairment," EPA-450/3-78-110a,b,c, U.S.

*Class I area as used in this document means Federal Class I area.

Environmental Protection Agency, Research Triangle Park, North Carolina.

> Turner, D. B. (1969), "Workbook of Atmospheric Dispersion

Other guidance documents on visibility, including those below, should also be consulted:

> User's Manual for the Plume Visibility Model (PLUVUE), EPA-450/4-30-032.

> Interim Guidance for Visibility Monitoring, EPA-450/2-80-082

> Guidelines for Determining Best Available Retrofit Technology for Coal-Fired Power Plants and Other Major Stationary Sources, EPA-450/3-80-0096.

1.1 CLASSES OF VISIBILITY IMPAIRMENT

Two separate classes of visibility impairment are of concern in this workbook:

> Atmospheric discoloration.

> Visual range reduction (increased haze).

Plumes from power plants or other combustion sources may be discolored because of NO_x emissions that are converted in the atmosphere to the reddish-brown gas, nitrogen dioxide. However, particle emissions and secondary aerosols formed from gaseous precursor emissions may also discolor the atmosphere. Increased haze is caused principally by primary particulate emissions and secondary aerosols, such as sulfate.

Worst-case impacts associated with these two classes of visibility impairment occur during two distinctly different kinds of atmospheric conditions. On one hand, atmospheric discoloration is greatest during periods of stable, light winds that occur after periods of nighttime transport. These conditions result in maximum particle and NO_2 line-of-

sight integrals that could cause maximum plume coloration. However, because a plume remains intact during such conditions, discoloration would be limited to a shallow vertical layer in the atmosphere. General atmospheric clarity would not be impaired, but the plume or layer could have an adverse visual impact, degrading the scenic beauty of a vista. The plume might be perceptible and discolored enough to interfere with a visitor's enjoyment of a class I area.

On the other other hand, increased general haze (decreased visual range) is greatest during light wind, limited mixing, or stagnation conditions after daytime transport, because conversion of gaseous precursor emissions to secondary aerosol is more rapid during these conditions, when an individual plume or discolored layer may not be perceptible at all. Rather, the impact would be manifested by an increased haze and loss of clarity in landscape features. Also, since the impact of any one emissions source may be small when compared to regional emissions, incremental impacts must be considered in light of the magnitude and frequency of increased haze caused by other natural and man-made emissions sources in the region. Increased haze may be a particularly severe problem in areas where ventilation is limited by terrain obstacles such as canyon walls, mountain ranges, plateaus, and river valleys. In such areas, emissions could accumulate over a period of a few days. Diurnal upslope and downslope (drainage) winds can cause a "sloshing" air motion that could trap emissions in a valley. Although ground-level contaminant concentrations might be very low in such a situation, increased haze could be a problem.

EPA has published regulations concerning the protection of visibility as Subpart P of Part 51 Title 40 of the Code of Federal Regulations. The regulations define "visibility impairment" to mean any humanly perceptible change in visibility (visual range, contrast, coloration) from that which would have existed under natural conditions. Definitions for "adverse impact on visibility" and "significant impairment" are also provided in the regulations. States are required to establish procedures for use in conducting visibility impact analyses. An important part of a visibility impact analysis is to determine the

frequency of occurrence and magnitude of visual impact in or within view of a class I area.*

1.2 APPROACH USED IN THIS WORKBOOK

This workbook outlines a screening procedure that will expedite the analysis of an emissions source. Figure 1 shows a schematic diagram of this screening procedure. Potentially, one could analyze a given source at any one of three basic levels of detail. A level-1 analysis involves a series of conservative screening tests that permit the analyst to eliminate sources with little potential for adverse or significant visibility impairment. A simple screening calculation, requiring only a few minutes of an analyst's time, indicates whether a source could cause significant impairment during hypothetical, worst-case meteorological conditions. If not, further analysis is unnecessary. If impairment is indicated, a level-2 analysis would be performed. The level-2 screening procedure is similar to the level-1 analysis in that its purpose is to estimate impacts during worst-case meteorological conditions; however, more specific information regarding the source, topography, regional visual range, and meteorological conditions is assumed to be available. A frequency-of-occurrence analysis is performed to determine conditions representative of the worst day in a year. Whereas the level-1 analysis requires only a few minutes, the level-2 analysis may require several days. In this workbook several options are recommended for performing a level-2 analysis: (1) use of hand calculations based on the formulas, tables, and graphs presented here, (2) use of reference tables and figures presented in the appendixes, and (3) use of the computer-based plume visibility model.

Finally, if both the level-1 and level-2 analyses indicate the possibility of significant or adverse visibility impairment, a more detailed

---

* It is important to note that emissions may not have to be transported into a class I area to cause visual impact in a class 1 area. If a vista within a class I area has views of landscape features outside that area that are considered by the federal land manager to be an integral part of the class I area experience, that vista may be protected.

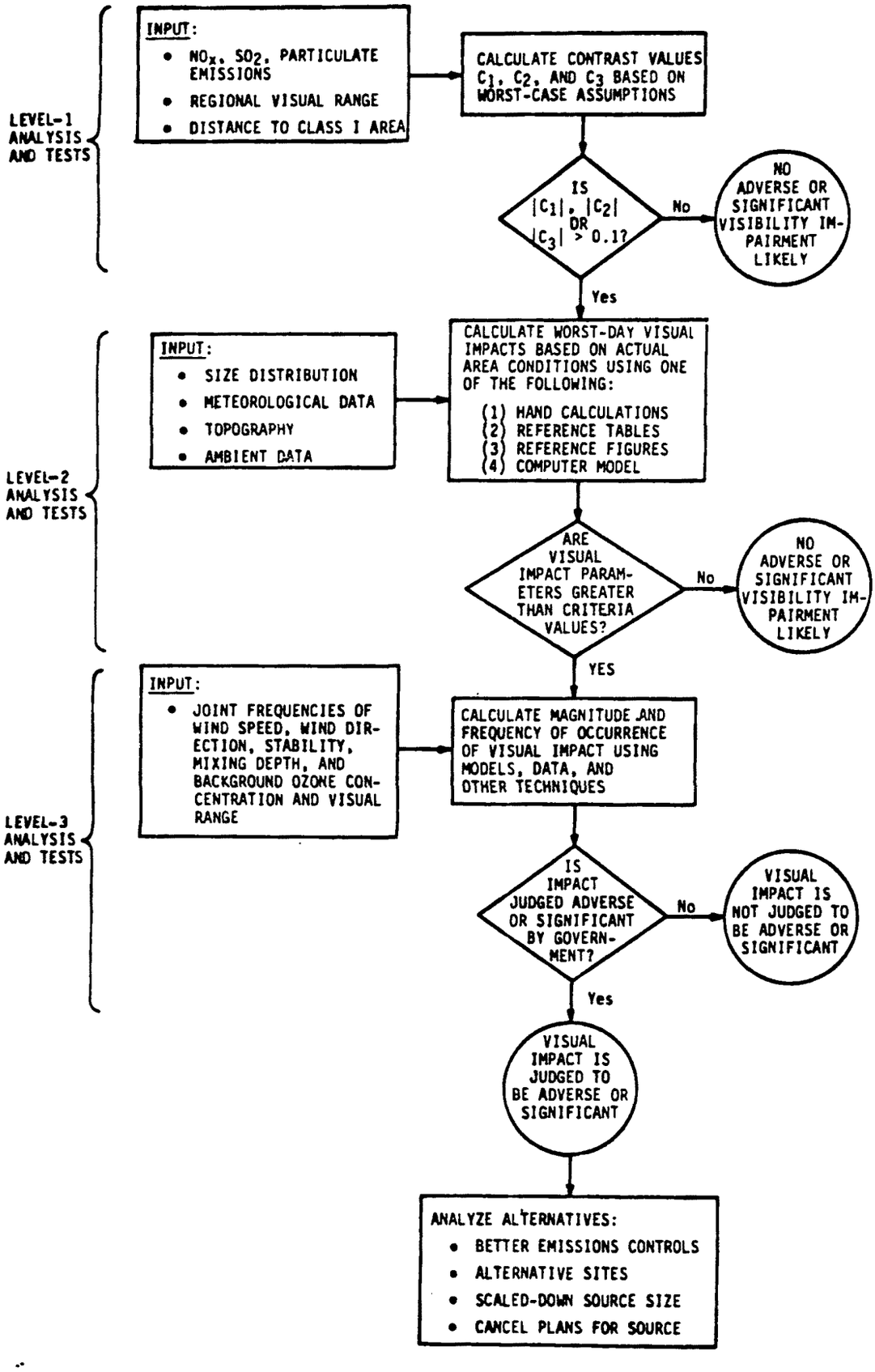

Figure 1. Schematic of visibility screening analysis procedure. The numerical meaning of the terms "significant" and "adverse" differ on a case-by-case basis and will be defined after an in-depth policy analysis of each case.

level-3 analysis is recommended. The purpose of a level-3 analysis is to provide an accurate description of the magnitude and frequency of occurrence of impact. For this level of analysis, a visibility model is used. The number of days per year and season in which a given magnitude of impact occurs are calculated from joint frequency tables of wind speed, wind direction, stability, mixing depth, ozone concentration, and visual range in the area. Computer graphics can be used to display the appearance of plumes or haze layers in black and white or in color. Detailed analyses of the spatial and temporal distribution of windfields and the effect on visual impacts may be made. For existing sources, measurements of visual impacts can be used in place of, or in combination with, the model calculations.

As shown in figure 1, there are tests that the analyst can apply after the level-1 and level-2 analyses to determine if there is a potential for adverse or significant impairment. If these tests show little potential for adverse or significant impacts, the analyst may choose to make a recommendation on the basis of these less detailed analyses. In some situations, however, even though the level-1 or level-2 test shows that impacts are not likely to be adverse or significant, the analyst may choose to use more detailed analytic procedures such as those suggested for the level-3 analysis. This might be the case if the emissions source barely passes the level-1 or level-2 test. Also, special meteorological conditions such as stagnation, terrain-influenced dispersion, and complex photochemistry (if the source emits reactive hydrocarbons, is located in an urban area, or is affected by an urban plume) may require further detailed analysis.

We have attempted to make this workbook a straightforward, easy-to-use reference manual; however, before we present the details of the visibility screening analysis procedures, we feel it is necessary to describe some of the concepts and theories upon which they are based. These are presented in chapter 2. The level-1 and level-2 analyses and tests are presented in chapters 3 and 4. Suggestions for more detailed analyses (level-3) are presented in chapter 5.

2 GENERAL CONCEPTS

In this chapter we present the general conceptual approach used throughout this workbook. We recommend that the user of this document read this chapter and the reference material cited in chapter 1 before using the procedures presented in the following three chapters for the level-1, -2, and -3 visibility screening analyses. Here we discuss the following subjects:

- Atmospheric optics and visibility impairment.
- Plume-observer geometry.
- Characterization of the frequency of occurrence of visual impacts.

2.1 PHYSICAL CONCEPTS RELATED TO VISIBILITY IMPAIRMENT

2.1.1 Visual Perception

Human visual perception occurs when the eye is exposed to light (i.e., electromagnetic radiation within the visible spectrum, 0.4 to 0.7 μm). Furthermore, the eye must be exposed to light of different intensities or wavelength mixtures before one perceives objects in the outside world. Since objects are usually viewed through the atmosphere (unless the observer is under water or in outer space), atmospheric contaminants can affect what one perceives visually. This is the crux of the visibility impairment issue: what impact does air pollution have on our visual perception, particularly of scenic areas?

Through recent perceptual research, Land (1977) has found that the eye-brain mechanism responds to objects within the field of view using a

comparison procedure. We compare light intensities of different objects at different wavelengths in the visual field. Through this comparison we perceive whether an object is visible, whether it is lighter or darker than neighboring objects, and whether it is more or less blue, green, or red than neighboring objects. A convenient way to describe this light intensity comparison is by a ratio such as

$$\frac{I_1(\lambda)}{I_2(\lambda)}$$

where I_1 and I_2 are the spectral radiances (light intensities) of two objects, 1 and 2, at wavelength λ in the visible spectrum ($0.4 < \lambda < 0.7$ μm).

Another way to describe this comparison of light intensities is to use contrast:

$$C(\lambda) = \frac{I_1(\lambda) - I_2(\lambda)}{I_2(\lambda)} = \frac{I_1(\lambda)}{I_2(\lambda)} - 1$$

Note that if $C(\lambda) = 0$ for all wavelengths λ, then $I_1 = I_2$ and there would be no perceptible difference in the two objects defined by I_1 and I_2. When we say there is much contrast in a given scene, then at least for some wavelengths, $C(\lambda) \neq 0$. Air pollution is visually perceptible only if it changes the contrast of objects at different wavelengths in the visible spectrum.

2.1.2 Fundamental Causes of Visibility Impairment

The effects of air pollution are visually perceptible as a result of the following interactions in the atmosphere:

> Light scattering
  - By molecules of air
  - By particles
> Light absorption
  - By gases
  - By particles.

Light scattering by gaseous molecules of air (Rayleigh scattering), which causes the blue color of the atmosphere, is dominant when the air is relatively free of aerosols and light-absorbing gases. Light scattering by particles is the most important cause of visual range reduction. Fine solid or liquid particulates, whose diameters range from 0.1 to 1.0 μm, are most effective per unit mass in scattering light.

Light absorption by gases is particularly important in the discussion of anthropogenic visibility impairment since nitrogen dioxide, a major constituent of power plant plumes, absorbs light. Nitrogen dioxide is reddish-brown because it absorbs strongly at the blue end of the visible spectrum while allowing light at the red end to pass through. Light absorption by particles is important when black soot (finely divided carbon) is present.

Anthropogenic contributions to visibility impairment result from the emission of primary particulate matter (such as fly ash, acid and water droplets, soot, and fugitive dust) and of pollutant precursors that are converted in the atmosphere into the following secondary species:

> Nitrogen dioxide (NO_2) gas from emissions of nitric oxide (NO).
> Sulfate ($SO_4^=$) particles from SO_x emissions.
> Nitrate (NO_3^-) particles from NO_x emissions.
> Organic particles from hydrocarbon emissions.

Before particulate control technology was commonly employed, primary particulate matter, such as smoke, windblown dust, or soot, was a major

contributor to visibility impairment, because emissions sources emit primary particles of fly ash and combustion-generated particulates to the atmosphere. If such sources are equipped with efficient abatement equipment, the emission rate of primary particles may be small. However, some emissions escape the control equipment and do contribute to the ambient particulate concentration and hence to general visibility impairment. If the emission rate of primary particulates is sufficiently large, the plume itself may be visible.

In the past, many older emissions sources generated conspicuous, visible plumes resulting from the large emission rates of primary particulate matter. New plants and old plants still in operation have benefited from more efficient particulate abatement equipment and a state of the art in which particulate removal efficiencies in excess of 99.5 percent are commonly specified and achieved. In addition, with the installation of flue gas desulfurization systems (scrubbers), and with combustion modifications, sulfur dioxide and nitrogen oxide emissions have also been reduced. As a result, the visual impact of emissions has been sharply reduced, as evidenced by the nearly invisible plumes under most conditions of modern coal-fired power plants. Unfortunately, however, the contribution to visibility impairment of the secondary pollutants--nitrogen dioxide gas and sulfate, nitrate, and organic aerosol--is now becoming increasingly evident and is of growing concern.

Since nitrogen dioxide absorbs light selectively, it can discolor the atmosphere, causing a yellow or brown plume when present in sufficient concentrations. Almost all of the nitrogen oxide emitted from emissions sources is nitric oxide, a colorless gas. But chemical reactions in the atmosphere can oxidize a substantial portion of the colorless NO to the reddish-brown NO_2.

Secondary sulfate, nitrate, and organic particles have a dominating effect on visual range in many situations because these particles range in size from 0.1 to 1.0 μm in diameter, which is the most efficient size per unit mass for light scattering. As is discussed later, submicron aerosol

(with diameters in the range from 0.1 to 1.0 μm) is 10 times more effective in light scattering than the same mass of coarse (> 1 μm) aerosol. Also, because secondary aerosol forms slowly in the atmosphere, maximum aerosol concentrations and associated visibility impairment may occur at large distances from emissions sources.

2.1.3 Atmospheric Optics

The effect of the intervening atmosphere on the visibility and coloration of a viewed object (e.g., the horizon sky, a mountain, a cloud) can be calculated by solving the radiation transfer equation along the line of sight. As we noted earlier, the effects of air pollution are visually perceptible because of contrast. Thus, visibility impairment can be quantified by comparing the intensity or the coloration of two objects (e.g., a distant mountain against the horizon sky). The effect of the intervening atmosphere on the light intensity of the viewed object can be determined if the concentration and characteristics of air molecules, aerosol, and nitrogen dioxide are known along the line of sight.

The change in spectral light intensity or spectral radiance $I(\lambda)$ as a function of distance along the sight path at any point in the atmosphere can be calculated (neglecting multiple scattering*) as follows:

$$\frac{dI(\lambda)}{dr} = -b_{ext}(\lambda)I(\lambda) + \frac{p(\lambda,\Theta)}{4\pi} b_{scat}(\lambda)F_s(\lambda) \quad , \qquad (1)$$

---

* Multiple scattered radiation is scattered (or reflected) more than once. Although the plume visibility model treats multiple scattering, it is beyond the scope of the hand calculations presented in this workbook to do so. Reasonably accurate solutions are obtained for the contrast parameters used to characterize visibility impairment in this workbook even if multiple scattering is ignored.

where

r = the distance along the sight path from the object to the observer,

$p(\theta)$ = the scattering distribution or phase function for scattering angle θ [see figure 2(a) for definitions],

F_s = the solar flux (watt/m^2/μm) incident on the atmosphere,

b_{scat} = the scattering coefficient, which is the sum of the Rayleigh scattering (due to air molecules), b_R, and the scattering due to particles, b_{sp}:

$$b_{scat}(\lambda) = b_R(\lambda) + b_{sp}(\lambda) \quad , \tag{2}$$

b_{ext} = the sum of the scattering, b_{sp}, and absorption coefficients, b_{abs}:

$$b_{ext}(\lambda) = b_{scat}(\lambda) + b_{abs}(\lambda) \quad . \tag{3}$$

On the right-hand side of equation (1), the first term represents light absorbed or scattered out of the line of sight; the second term represents light scattered into the line of sight. The values of b_{scat} and b_{abs} can be evaluated if the aerosol and NO_2 concentrations and such characteristics as the refractive index and the size distribution of the aerosol are known. Except in the cleanest atmospheres, b_{scat} is dominated by b_{sp}; also, unless soot is present, b_{abs} is dominated by the absorption coefficient due to NO_2. Scattering and absorption are wavelength-dependent, and effects are greatest at the blue end ($\lambda = 0.4$ μm) of the visible spectrum ($0.4 < \lambda < 0.7$ μm). The Rayleigh scattering coefficient b_R is proportional to λ^{-4}; the scattering coefficient caused by particles is generally proportional to λ^{-n}, where $0 < n < 2$. Also, NO_2 absorption is greatest at the blue end. This wavelength dependence causes the discoloration of the atmosphere.

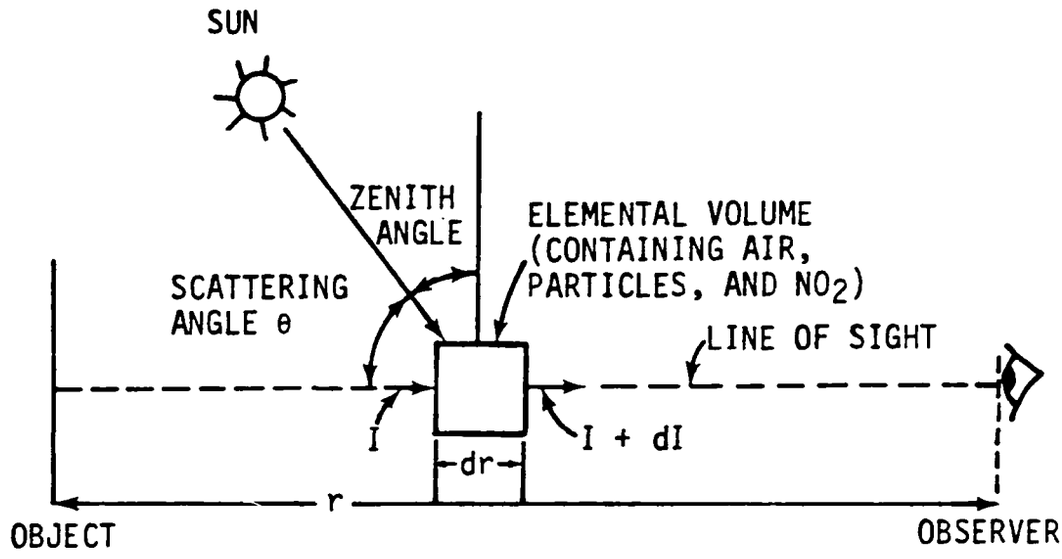

(a) Geometry

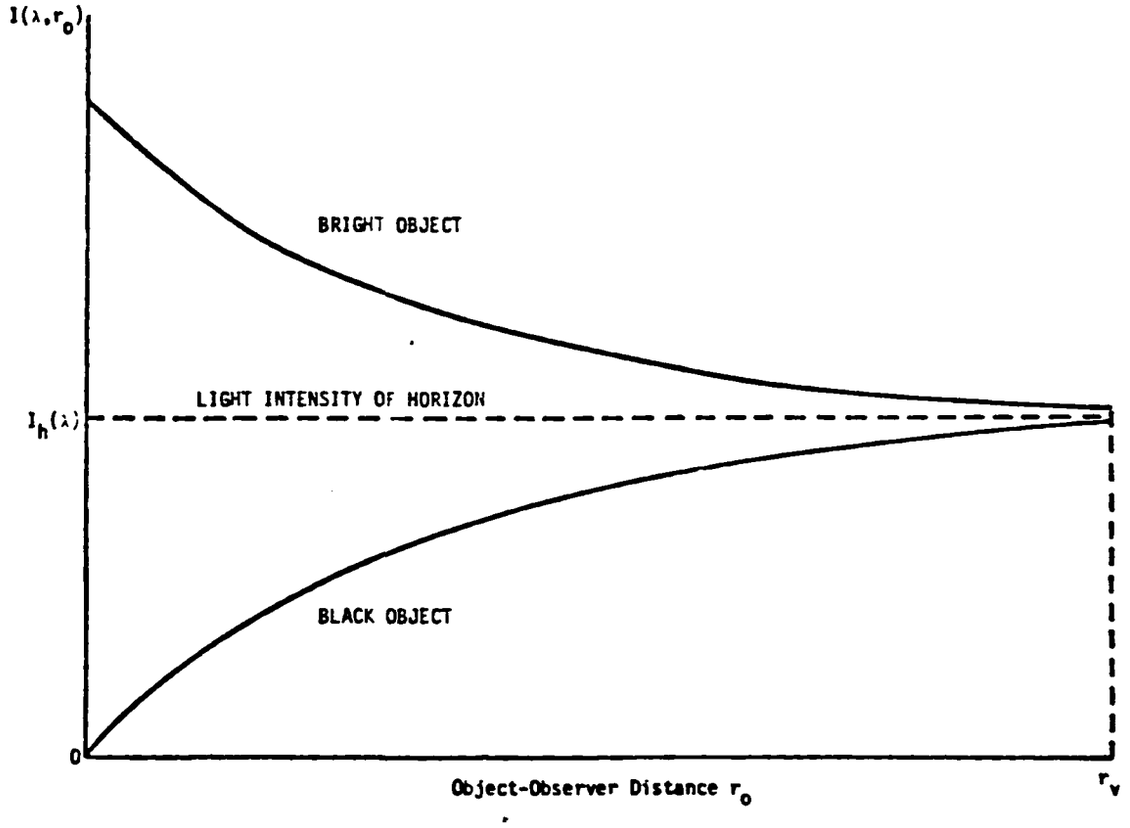

(b) Visual Range r_V (Homogeneous Atmosphere)

Figure 2. Effect of an atmosphere on the perceived light intensity of objects.

For a uniform atmosphere, without inhomogeneities caused by plumes (where b_{scat} and b_{ext} do not vary with distance r along the line of sight), equation (1) can be solved to find the intensity and coloration of the horizon sky (neglecting multiple scattering):

$$I_h(\lambda) = \frac{p(\lambda,\Theta)}{4\pi} \frac{b_{scat}(\lambda)}{b_{ext}(\lambda)} F_s(\lambda) \quad . \tag{4}$$

The perceived intensity of distant bright and dark objects will approach this intensity as an asymptote, as illustrated by figure 2(b).

The visual range r_v is the distance at which a black object is barely perceptible against the horizon sky, which occurs when the perceived light intensity of the black object is $(1 + C_{min})I_h$, where C_{min} is the liminal (barely perceptible) contrast, commonly assumed to be -0.02. When equation (1) is solved for r_v, for a uniform atmosphere, r_v is independent of $p(\Theta)$ and $F_s(\lambda)$ and can be calculated using Koschmieder's equation:

$$r_v = \frac{-\ln(C_{min})}{b_{ext}(\lambda)} = \frac{3.912}{b_{ext}(\lambda)} \quad , \tag{5}$$

where $b_{ext}(\lambda)$ is evaluated at the middle of the visible spectrum (to which the human eye is most sensitive) and where $\lambda = 0.55$ μm. The visual range for a nonuniform atmosphere (e.g., a plume case) must be calculated by evaluating equation (1) for the appropriate conditions of the given situation.

Atmospheric coloration is determined by the wavelength-dependent scattering and absorption in the atmosphere. The spectral distribution of $I(\lambda)$ for λ over the visible spectrum determines the perceived color and light intensity of the viewed object. The relative contributions of scattering (aerosols plus air) and absorption (NO_2) to coloration can be illustrated by rearranging equation (1):

$$\frac{1}{I(\lambda)} \frac{dI(\lambda)}{dr} = b_{scat}(\lambda) \left[\frac{\frac{p(\lambda,\theta)}{4\pi} F_s(\lambda)}{I(\lambda)} - 1 \right] - b_{abs}(\lambda) \quad . \tag{6}$$

Note from equation (4) that when light absorption is negligible compared with light scattering, the clear horizon intensity is simply (if multiple scattering is ignored):

$$I_{h0}(\lambda) = \frac{p(\lambda,\theta)\ F_s(\lambda)}{4\pi} \quad . \tag{7}$$

We now can rewrite equation (6):

$$\frac{1}{I(\lambda)} \frac{dI(\lambda)}{dr} = b_{scat}(\lambda) \left[\frac{I_{h0}(\lambda)}{I(\lambda)} - 1 \right] - b_{abs}(\lambda) \quad . \tag{8}$$

Equation (8) is thus an expression relating the effects of light scattering and light absorption to the change in spectral light intensity with distance along a sight path. On the right-hand side of equation (8), the first term is the effect of light scattering, and the second term is the effect of light absorption (NO_2). As noted previously, since b_{scat} and b_{abs} (due to NO_2) are strong functions of wavelength and are greater at the blue end (λ = 0.4 μm), atmospheric coloration can result.

Equation (8) makes clear that NO_2 always tends to cause a decrease in light intensity and a yellow-brown coloration by preferentially absorbing blue light, whereas particles may cause a blue-white or a yellow-brown coloration, depending on the value of the quantity in the brackets. If, at a given point along the sight path, $I(\lambda)$ is greater than the clean horizon sky intensity $I_{h0}(\lambda)$, then the quantity in brackets in the first term on the right-hand side of equation (8) will be negative, which means that the net effect of scattering will be to remove predominantly blue

light from the line of sight. This effect would occur if a bright, white cloud or distant snowbank were observed through an aerosol that did not contain NO_2; scattering would cause a yellow-brown coloration. If, however, $I(\lambda)$ is less than $I_{h0}(\lambda)$, then the quantity in brackets in equation (8) will be positive, which means that the net effect of scattering will be to add predominantly blue light into the line of sight. This effect would occur if a distant, dark mountain were observed through an aerosol that did not contain NO_2; scattering would cause the mountain to appear lighter and bluish. Only light absorption can cause $I(\lambda)$ to be less than $I_{h0}(\lambda)$, and whenever $I(\lambda) < I_{h0}(\lambda)$, scattering will add light to the sight path, thereby masking the coloration caused by NO_2 light absorption.

The mathematical expressions used in this workbook are simply solutions to equation (1) for different boundary conditions and for different values of b_{scat}, b_{ext}, $p(\Theta)$ and F_s as they are affected by natural and man-made light scatterers and absorbers. The plume visibility model uses similar formulations, but it also accounts for multiple scattering effects.

2.1.4 Plume Visual Impacts

Let us consider now the geometry shown in figure 3, namely, the case of a plume embedded in an otherwise uniform, background atmosphere. Equation (1) can be solved for the spectral radiance at the observer location P_o as follows:

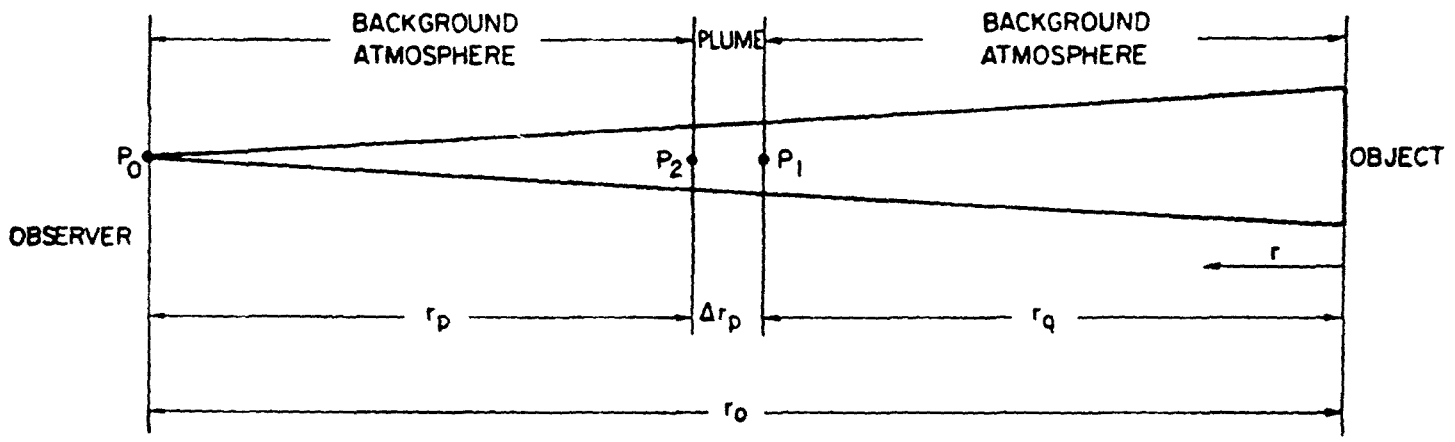

Figure 3. Object-observer geometry with plume.

$$I(\lambda,r_o) = I_h \left[1 - \exp\left(-b_{ext} r_p\right)\right]$$

$$+ \frac{F_s}{4\pi} \bar{p}_{plume}\, \bar{\omega}_{plume} \left[1 - \exp(-\tau_{plume})\right] \left[\exp(-b_{ext} r_p)\right]$$

$$+ I_h \left[1 - \exp(-b_{ext} r_q)\right] \left[\exp(-\tau_{plume})\right] \left[\exp(-b_{ext} r_p)\right]$$

$$+ I_{obj} \left[\exp(-b_{ext} r_q)\right] \left[\exp(-\tau_{plume})\right] \left[\exp(-b_{ext} r_p)\right] \qquad (9)$$

where

$I(\lambda,r_o)$ ≡ spectral radiance at observer point P_o,

I_h ≡ horizon sky radiance, assuming the atmosphere is uniform and optically thick (i.e., earth curvature can be ignored); see equation (4) and figure 2(b),

r_p ≡ plume-observer distance; see figure 3,

$\bar{p}_{plume}$ ≡ average plume phase function, corrected for multiple scattering effects albedo,

$\bar{\omega}_{plume}$ ≡ average plume albedo

$$= \frac{\int b_{scat} dr}{\int b_{ext} dr} \quad ,$$

τ_{plume} ≡ plume optical thickness (increment above background)

$$= \int_{plume} b_{ext} dr = \int_{plume} (b_{scat} + b_{abs}) dr \quad ,$$

r_q ≡ distance between viewed object and plume; see figure 3,

r_o ≡ total distance from viewed object and observer; see figure 3. If the plume is treated as a point, then $r_o = r_p + r_q$.

Note that other variables were defined previously and that all the optical variables (F_s, I_h, b_{scat}, b_{ext}, $\bar{p}_{plume}$, $\bar{\omega}_{plume}$, and τ_{plume}) are functions of wavelength λ. Further, note that I_h and $\bar{p}_{plume}$ are dependent on the scattering angle Θ (see figure 2(a) for a definition). Each term on the right-hand side of equation (9) has a physical meaning. The first term represents light scattered into the line of sight by the background atmosphere between points P_2 and P_0. The second term represents the light scattered into the line of sight by the plume material. The third term represents the light scattered into the line of sight by the background atmosphere between the object and P_1. The fourth and last term represents the light reflected from the object and transmitted to the observer.

2.1.5 Characterizing Visibility Impairment

Figure 4 illustrates five situations in which air pollution is visually perceptible. There are two basic kinds of visibility impacts. In one case, of which figures 4(b), (c), and (e) are examples, air pollution is perceptible as a result of the comparison of two objects viewed simultaneously by an observer. The haze layer and plume in figures 4(b) and (c), for example, are perceptible because they contrast with the background atmosphere. The plume in figure 4(e) is perceptible because it contrasts with the viewed objects; in other words, it is brighter or darker or colored differently from the viewed object. In the other case, of which figures 4(a) and (d) are examples, perception of pollution results from the difference between the presently observed scene and the scene remembered under clear conditions. For example, the haze in figure 4(c) may be perceptible because it is colored differently from what is considered normal sky color; it appears white, gray, yellow, or brown instead of blue. The situation shown in figure 4(d) is similar. The scene may appear hazy because the contrast of viewed objects is decreased from that observed on a clear day.

Each of these situations can be described either by a set of single contrast values for different wavelengths or by a set of contrast differences for different wavelengths; the cases shown in figures 4(a), (b), and

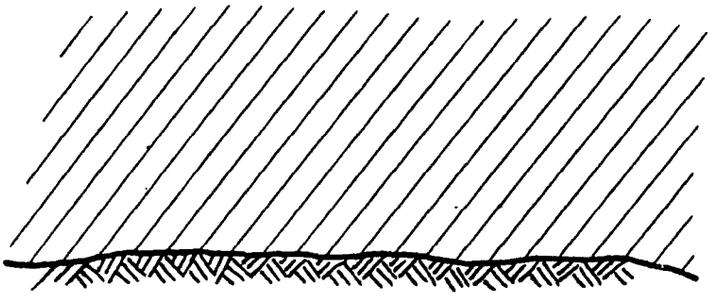

(a) General, uniformly discolored haze

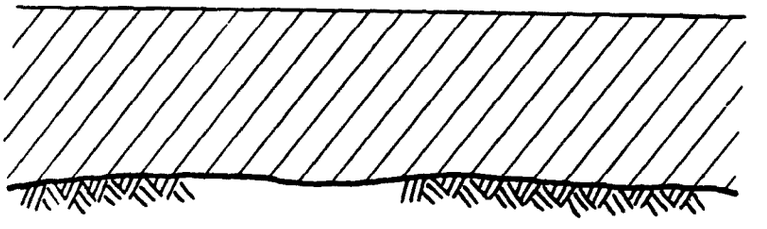

(b) Surface-based haze layer contrasting with background atmosphere above

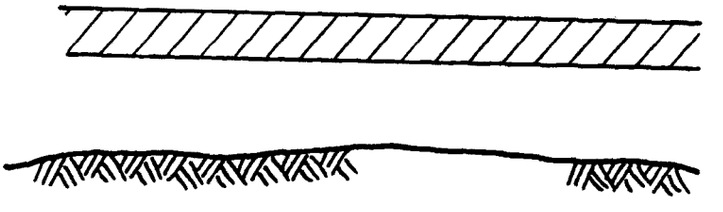

(c) Elevated plume or haze layer contrasting with background atmosphere above and below

Figure 4. Five basic situations in which air pollution is visually perceptible.

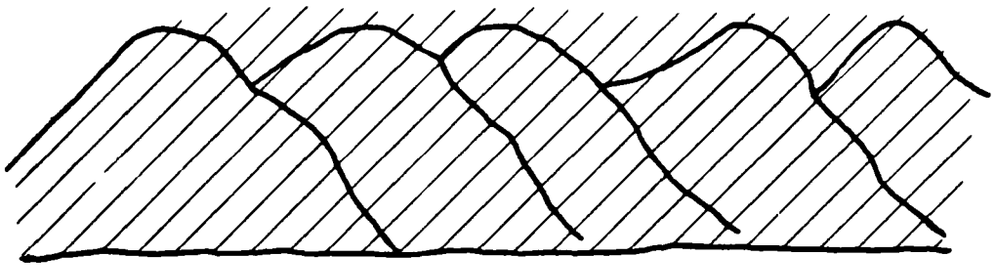

(d) General haze reducing contrast of viewed objects

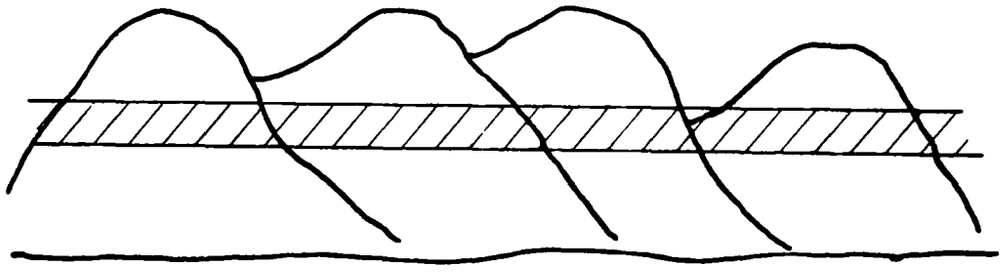

(e) Elevated plume or ground-based or elevated haze layer reducing contrast of a portion of a viewed object

Figure 4 (Concluded)

(c) can be characterized by contrast, whereas those shown in figures 4(d) and (e) can be characterized by contrast differences.

We can use equation (9) to calculate contrast values or contrast differences so as to characterize each of the situations shown in figure 4. First, let us consider the situations in which the effect of air pollution is perceptible against the sky, as shown in figures 4(a), (b), and (c). If the atmosphere is relatively hazy, the atmosphere along a horizontal line of sight is optically thick. In such a situation, for the case without a plume ($\tau_{plume} = 0$), it can be shown that equation (9) reduces to equation (4) [see the asymptote in figure 2(b)].

The contrast between the plume and the horizon sky background as observed at point P_o is evaluated from equation (9) as follows:

$$C_{plume} = \frac{I_{h\text{-}plume} - I_h}{I_h}$$

$$= \left[\frac{(\bar{p}\,\bar{\omega})_{plume}}{(\bar{p}\,\bar{\omega})_{background}} - 1\right]\left[1 - \exp(-\tau_{plume})\right]\left[\exp(-b_{ext}r_p)\right] \quad . \tag{10}$$

Note that, depending on whether the product of the phase function and the albedo ($\bar{p}\bar{\omega}$) for the plume or haze layer is larger or smaller than that for the background, the plume or haze layer will be brighter ($C > 0$) or darker ($C < 0$) than the background horizon sky. Also note that the contrast is dependent on the plume optical thickness (τ_{plume}); as τ_{plume} approaches zero, C_{plume} approaches zero. Plume contrast also diminishes as the plume-observer distance increases.

For the case in which the haze is homogeneous and optically thick, it can be shown that:

$$C_{haze} = \left[\frac{(\bar{p}\bar{\omega})_{haze}}{(\bar{p}\bar{\omega})_{background}} - 1 \right] \quad . \tag{11}$$

These formulas can be used to evaluate impacts of the type shown in figures 4(a), (b), and (c). It should be noted, however, that in very clean areas where background conditions approach Rayleigh conditions, the assumption that the atmosphere along the horizontal line of sight is optically thick is no longer valid, and these formulas are only approximations. In these situations, visibility model calculations are needed for more accurate solutions.

To characterize the types of visibility impairment represented in figures 4(d) and (e), we need to calculate a change in sky/terrain contrast caused by a plume or haze layer:

$$\Delta C_r = C_r\Big|_{\text{with plume}} - C_r\Big|_{\text{without plume}}$$

where

$$C_r\Big|_{\text{with plume}}' = \frac{I_{t\text{-plume}} - I_{h\text{-plume}}}{I_{h\text{-plume}}}$$

$$C_r\Big|_{\text{without plume}} = \frac{I_t - I_h}{I_h} \quad .$$

For simplicity we assume that the terrain that is viewed behind the plume has an intrinsic radiance, I_{obj}, which is a function of the horizon sky radiance I_h, namely, $I_{obj} = (1 + C_0)I_h$. C_0 is the intrinsic contrast. If the terrain were black, C_0 would equal -1. With this assumption we again use equation (9) to evaluate the following spectral radiance values:

$$I_t = I_h \left[1 + C_0 \exp(-b_{ext} r_o)\right] \quad ,$$

$$I_{t\text{-plume}} = I_{h\text{-plume}} + C_0 I_h \left[\exp(-b_{ext} r_o)\right]\left[\exp(-\tau_{plume})\right] \quad . \tag{12}$$

The sky/terrain contrast values with and without the plume are:

$$C_r\Big|_{\text{without plume}} = C_0 \exp(-b_{ext} r_o) \quad ,$$

$$C_r\Big|_{\text{with plume}} = C_0 \frac{I_h}{I_{h\text{-plume}}} \left[\exp(-b_{ext} r_o)\right]\left[\exp(-\tau_{plume})\right] \quad . \tag{13}$$

The change in contrast caused by the plume or haze is then:

$$\Delta C_r = -C_0 \left[\exp(-b_{ext} r_o)\right]\left[1 - \left(\frac{I_h}{I_{h\text{-plume}}}\right) \exp(-\tau_{plume})\right] \quad . \tag{14}$$

It should be noted that the visual range and visual range reduction can be calculated from equations (12), (13), and (14). The visual range is defined as the distance r_v from the observer to a black object such that the sky/target contrast $C_r = -0.02$ at $\lambda = 0.55$ μm. By solving equations (12), (13), and (14) for $r_o = r_v$ such that $C_r = -0.02$, we can obtain the following formulas:

$$r_{v0} = \frac{3.912}{b_{ext}} \tag{15}$$

for a homogeneous atmosphere without a plume and

$$r_v = \frac{1}{b_{ext}} \left[3.912 - \ln\left(\frac{I_{h\text{-plume}}}{I_h}\right) - \tau_{plume}\right] \quad . \tag{16}$$

The fractional visual range reduction is simply

$$-\frac{\Delta r_v}{r_{v0}} = -\frac{(r_v - r_{v0})}{r_{v0}} = \frac{\ln\left(\frac{I_{h\text{-plume}}}{I_h}\right) + \tau_{plume}}{3.912} \quad . \tag{17}$$

Further discussion of the relationships between plume optical thickness, extinction coefficient, visual range, and sky/terrain contrast is presented in appendix A.

Equations (10) and (14) are the basic formulas upon which this workbook is based. Because of the assumptions previously noted, these equations are approximate; more exact solutions can be obtained using the computer-based plume visibility model. Equations (10) through (14) can be used to determine contrasts at different wavelengths in the visible spectrum. This workbook describes how calculations can be made at λ = 0.40, 0.55, and 0.70 μm. The contrast at λ = 0.55 μm is used as an overall indication of relative brightness of a plume or haze layer. The contrasts at λ = 0.40 and 0.70 μm are used to determine the coloration of the plume or haze layer relative to the background. The blue-red ratio, indicative of coloration, is calculated from these contrast values as follows:

$$R = \frac{1 + C(\lambda = 0.4\ \mu m)_{plume}}{1 + C(\lambda = 0.7\ \mu m)_{plume}} \tag{18}$$

The visibility model uses many parameters to characterize plume visual impact; however, the following four parameters are particularly important:

> Visual range reduction [see equation (17)]

- Plume blue-red ratio [see equation (18)]
- Plume contrast [see equation (10)]
- Plume perceptibility parameter $\Delta E(L^*a^*b^*)$.

We have already described the first three parameters. The fourth parameter, the plume perceptibility ΔE value, characterizes the extent of color difference between the plume and a viewing background. Whereas visual range reduction and plume contrast values are calculated at one wavelength ($\lambda = 0.55$ μm) and blue-red ratio at two wavelengths ($\lambda = 0.4$ and 0.7 μm), the ΔE value is calculated across the visible spectrum ($0.4 < \lambda < 0.7$ μm). The ΔE parameter is particularly useful to characterize plume perceptibility because it is a function of the difference in coloration between the plume and a viewing background in terms of both brightness difference and color (chromaticity) difference. Because the spectral radiances [$I(\lambda)$] have to be calculated at several wavelengths to determine ΔE, the ΔE parameter is not appropriate for use in hand calculations.

We are not aware of any studies that have specifically addressed the question of what the standards for visibility impairment should be in terms of these quantitative specifications. A very well defined, reasonably large target, with sharp edges that contrast with a viewing background, probably has a threshold of detectability corresponding to a contrast of ±0.02 and a ΔE value of about 1. Figure 4 shows the five basic viewing situations in which air pollution might be visually perceptible. A direct comparison of two adjacent colors is only possible when the plume or haze layer contrasts with a viewing background. In most situations, however, the boundary between a plume and a viewing background is not distinct, but diffused, because of the nature of plume dispersion. This is particularly true at large distances from the emissions source. A general haze can only be detected by comparison with the memory of clearer conditions on previous days. Thus, there is no clear set of threshold values to characterize visibility impairment.

The situation is made even more complicated by the fact that the

magnitude of visual impact caused in a class I area by a given emissions source varies significantly over the course of a year. Although impacts may be visible during the worst day in a year, they may not be visible most of the year. For this workbook, we have adopted the following criteria for use in level-1 and -2 tests. If the absolute value of either plume contrast (C_{plume}) or the change in sky/terrain contrast (ΔC_r) is greater than 0.1, or if plume $\Delta E(L^*a^*b^*)$ is greater than 4 for the worst-day impact case, then the possibility that the visual impact would be judged adverse or significant cannot be ruled out.

2.2 PLUME-OBSERVER GEOMETRY

Figures 5 and 6 show plan and elevation views, respectively, of an arbitrary plume-observer geometry defined by elevation angle β, the horizontal angle α between the line of sight and the plume centerline, the distance x downwind from the emissions source of the plume parcel being observed, and the distance r_p from the observer to this plume parcel. Although the visibility model offers the option of specifying any arbitrary angle β, for most real-world problems $\beta \cong 0$ since plumes are usually not observed at close range. Thus, for the sake of simplicity, the formulas presented in this workbook are based on the assumption that the line of sight is horizontal ($\beta = 0$).

In the previous section we showed that plume visual effects are dependent on the plume optical thickness τ, which is proportional to the integrals of NO_2 and particle concentrations along the line of sight. For a horizontal line of sight ($\beta = 0$) through a Gaussian plume, these integrals can be calculated using the following approximate formulas.

For a fixed plume orientation and observer location, as shown in figure 5, the magnitude of plume optical thickness (τ) in equations (10) and (14) is a function of the direction of view (i.e., the angle α). Although the optical thickness τ of the plume is a minimum at $\alpha = 90°$, the plume-observer distance r_p is at its minimum value also since

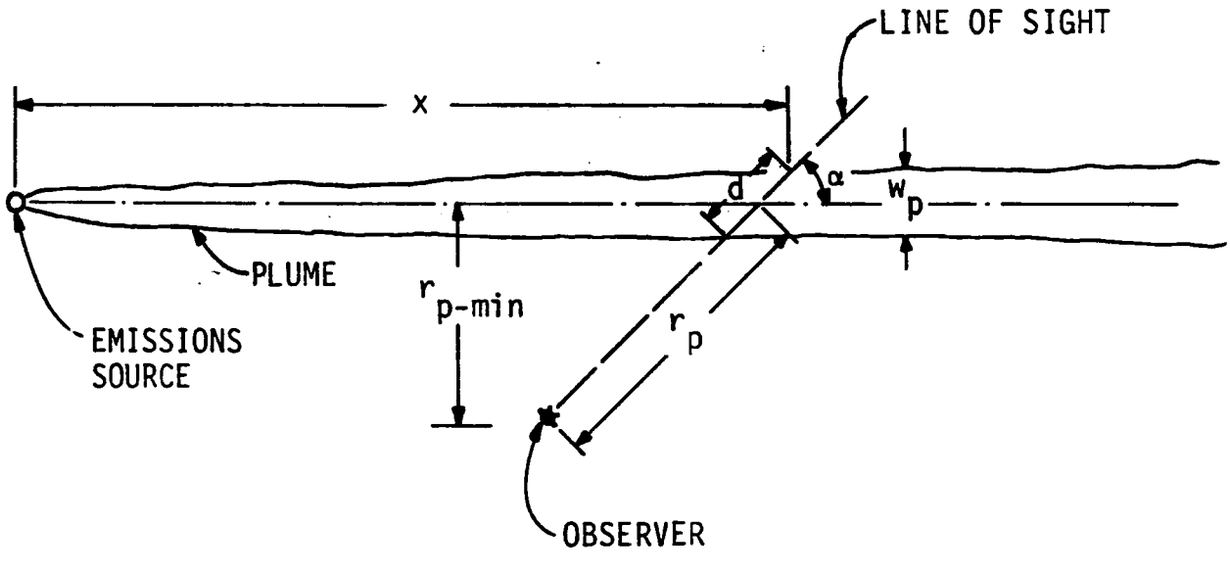

Figure 5. Plan view of observer-plume geometry.

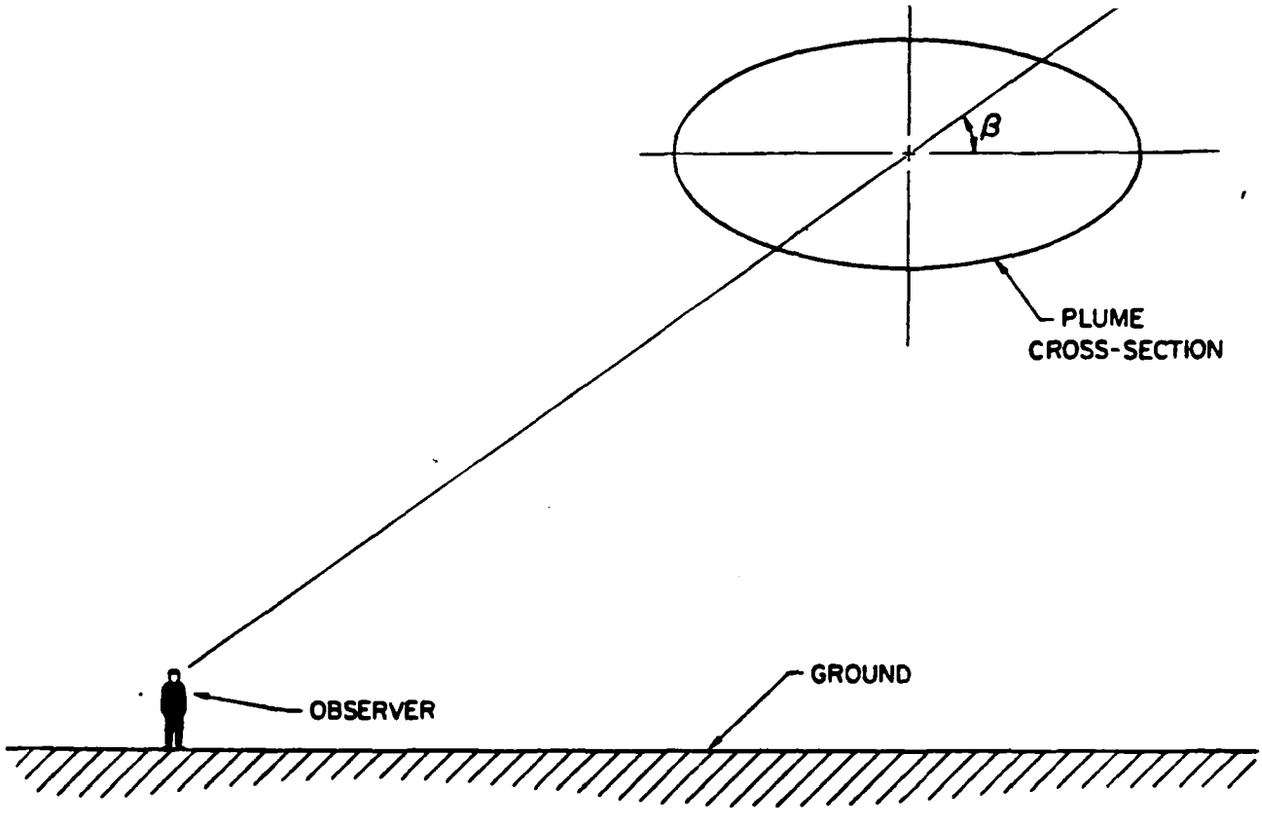

Figure 6. Elevation view of observer-plume geometry.

$$r_{p\alpha} = \frac{r_{p\text{-}min}}{\sin \alpha} \quad .$$

Thus, there are two counterbalancing effects of α. Although the optical thickness of the plume is larger for small αs, the distance between the plume and the observer is larger, the magnitude of plume effects is correspondingly smaller, and the apparent size of the plume is smaller. In very clear background areas, if the observer is close to the source, impact magnitudes will be largest for lines of sight with small αs, though the plume will appear smaller as noted above. However, in most situations visual effects are maximum or close to maximum when the line of sight is perpendicular to the plume ($\alpha = 90°$) such that $r_p = r_{p\text{-}min}$. Because of this, we recommend, for this workbook, that plume effects be evaluated for lines of sight perpendicular to the plume centerline.

The optical thickness of a plume is proportional to

$$\int_{-\infty}^{\infty} \chi \, dy = \frac{Q}{(2\pi)^{1/2} \sigma_z u \sin \alpha} \left\{ \exp \left[-\frac{1}{2} \left(\frac{H + z}{\sigma_z} \right)^2 \right] \right.$$

$$\left. + \exp \left[-\frac{1}{2} \left(\frac{H - z}{\sigma_z} \right)^2 \right] \right\} \quad . \tag{19}$$

For lines of sight directly through the center of a Gaussian plume, we have simply

$$\int_{-\infty}^{\infty} \chi \, dy = \frac{Q}{(2\pi)^{1/2} \sigma_z u \sin \alpha} \quad . \tag{20}$$

When the plume is uniformly mixed in the vertical between the ground and an elevated stable layer of height, H_m, we have

$$\int_{-\infty}^{\infty} \chi \, dy = \frac{Q}{H_m u \sin \alpha} \quad . \tag{21}$$

Note that these formulas no longer apply as α approaches 0. If the observer were within the plume, the integral along the plume centerline ($\alpha = 0°$) would have to be calculated numerically from the Gaussian equation. As we discuss in a later subsection of this section, the probability of an observer's being within the plume is exceedingly small, so that a quite adequate general description of plume-observer geometry is as shown in figure 5 (i.e., lines of sight oblique to the plume centerline).

It should be understood from the foregoing discussion that visual impacts are a function of the following parameters:

> NO_2 and aerosol plume loading (Q)
> Wind speed (u)
> Vertical extent of plume mixing (σ_z or H_m)
> Distance between the plume and observer (r_p)
> Background extinction coefficient (b_{ext}).

Thus, the visual impacts will increase with:

> Increasing NO_x, particulate, and aerosol precursor emission rates.
> Increasing NO_2 and aerosol formation rates in the atmosphere from precursors.
> Decreasing wind speed.
> Decreasing vertical mixing.
> Decreasing plume-observer distance (i.e., the wind direction is such that plume transport is toward the observer).
> Increasing background visual range (i.e., decreasing extinction coefficient, the lower bound being the Rayleigh scattering coefficient of particle-free air).

The largest visual impacts for a given emissions source and observer location (in a class I area) occur when a plume is transported relatively close to the observer, with light winds and little vertical mixing. Thus, to estimate worst-case impacts, it is necessary to identify reasonable worst-case meteorological conditions such as light-wind, stable conditions; light-wind, limited-mixing conditions; and stagnation conditions. These worst-case conditions are dependent on meteorological conditions in the area and the distance between the emissions source and the class I area. For example, although an F stability and a 1 m/s wind speed may be reasonable worst-case conditions for visual impacts close to a source, they certainly are not for observer locations 100 to 200 km from the source. At 1 m/s, it would require 28 to 56 hours for a plume to be transported 100 to 200 km. Typically, stable (F stability) conditions would not be likely to persist for more than 12 hours.* If we assume that a stable plume would remain intact for no longer than 12 hours, the worst-case wind speeds for the observer locations 100 and 200 km from the emissions source would be 2.3 and 4.6 m/s, respectively. In this workbook we use this assumption regarding persistence of stable conditions.

Another consideration is that of variability in wind speed and wind direction, and of its impact on plume dispersion and transport to within view of an observer in a class I area. The location of a plume parcel relative to the emissions source at any time t_f is dependent on the spatially- and temporally-varying windfield, the time of emission from the source t_0, and the transport time $\Delta t = t_f - t_0$:

$$\bar{r} = \int_{t_0}^{t_f} \bar{v}(x,y,z,t)\, dt \quad . \qquad (22)$$

---

* It should be noted that, during winter or at high latitudes, stable conditions (E or F stability) could persist longer than 12 hours. The analyst may wish to use a different assumption regarding persistence if appropriate to a given application.

If the displacement vector $\bar{r}$ is within a given radius of the observer point in a class I area, one might expect a visual impact, depending on the dilution of the plume parcel. Thus, we could have transport from the emissions source to the observer locations in any number of possible trajectories, as shown by the examples in figure 7. If one had a set of spatially- and temporally-resolved wind data, one could perform the vector integration shown in equation (22) and determine the frequency of occurrence of transport toward a class I area. Usually, however, wind data are not available for more than one location in a region, and one must make assumptions regarding the variability of wind in time and space.

Uncertainty in the meteorological conditions used for input is probably the most important source of error in visibility impact calculations. The level of sophistication of an air quality or visibility impact analysis is most often limited, not by theoretical or analytic concerns, but by the lack of a detailed meteorological data base for the region of interest, with spatial and temporal resolution appropriate for the task.

The level-1 visibility screening analysis is based on assumptions regarding worst-case meteorological conditions. The level-2 visibility screening analysis is based on the assumption that the joint frequency of occurrence of meteorological conditions, at plume height, at a point within a region, is representative of all points within the region. It is also assumed that plume geometry can be approximated by a straight plume trajectory, as shown by trajectory 1 in figure 7. This assumption will be conservative in most situations (i.e., overestimate impacts). However, in other situations, such as during a stagnation condition in a valley, the assumption may cause underestimation of impacts because wind reversals could cause a buildup of emissions as shown by trajectory 2 in figure 7. For level-3 analyses more detailed representations of the windfield could be used as the basis for visibility impact calculations, depending on the availability of meteorological data.

2.3 CHARACTERIZING THE FREQUENCY DISTRIBUTION OF PLUME VISIBILITY IMPACTS

In this workbook, the purpose of level-1 and -2 screening analyses is to estimate the worst-case visual impacts that might occur on about one day per year. For the level-3 analysis, the frequency of occurrence of impact of different magnitudes can be calculated, as well as the worst-day impacts. It is important to determine the frequency of occurrence of visual impact, because the adversity or significance of impact is dependent on how frequently an impact of a given magnitude occurs. For example, if a plume is perceptible from a class I area a third of the time, the impact would be considered much more significant than if it were perceptible only one day per year. The assessment of frequency of occurrence of impact should be an integral part of a visibility impact assessment.

In this subsection we discuss how one can determine both the magnitude and frequency of occurrence of visual impact. This procedure entails making several model runs for different values of the following important input parameters:

- Emission rates (particulate, SO_2, NO_x).
- Wind speed.
- Wind direction.
- Atmospheric stability.
- Mixing depth.
- Background ozone concentration.
- Background visual range.
- Time of day and season.
- Orientation of observer, plume, and sun.
- Viewing background (whether it is sky, cloud, or snow-covered, sunlit, or shaded terrain).

Because of the large number of variables important to a visual impact

calculation, several calculations are needed to assess the magnitude and frequency of occurrence of visual impact. It is recommended that a computer model be used for level-3 analysis because of the large number of scenarios and calculations involved. It would be ideal to calculate hourly impacts over the course of a year or more using hourly values of the above variables. However, such an extensive data base is rarely available for use. Even if it were available, the computing costs involved would be prohibitive. It is therefore preferable to select a few representative, discrete values for each of these variables to represent the range (i.e., the magnitude and frequency of occurrence) of visual impact over a given period of time, such as a season or year. One can start with conditions that cause the worst impacts and then assess the frequency of occurrence, in a season or year, of all the variables having worst-case values simultaneously.

It is possible to imagine a worst-case impact condition that would never occur in the real atmosphere; this condition could be represented on a cumulative frequency plot, such as that of figure 8, as point A. The impact is great, but it almost never occurs. If another worst-case situation less extreme than point A were selected, the magnitude of impact would be less, but it might occur with some nonzero frequency, about one day per year, for example (the reasonable worst-case impacts for level-1 and level-2 analyses). It is possible to select various values of all the important input variables and to assess the frequency with which those conditions resulting in impacts worse than a given impact would occur. By this process, several points necessary to specify the frequency distribution could be obtained (for example, points B, C, and D in figure 8). With average (50-percentile) conditions, a negligible impact, as shown at point E in figure 8, might be found. In figure 8, the ordinate could be any of the parameters used to characterize visibility impairment, such as visual range reduction, plume contrast, blue-red ratio, or ΔE, and the abscissa could represent cumulative frequency over a season or a year.

In a visual impact assessment, it is recommended that one select various combinations of upper-air wind speed, wind direction, and atmos-

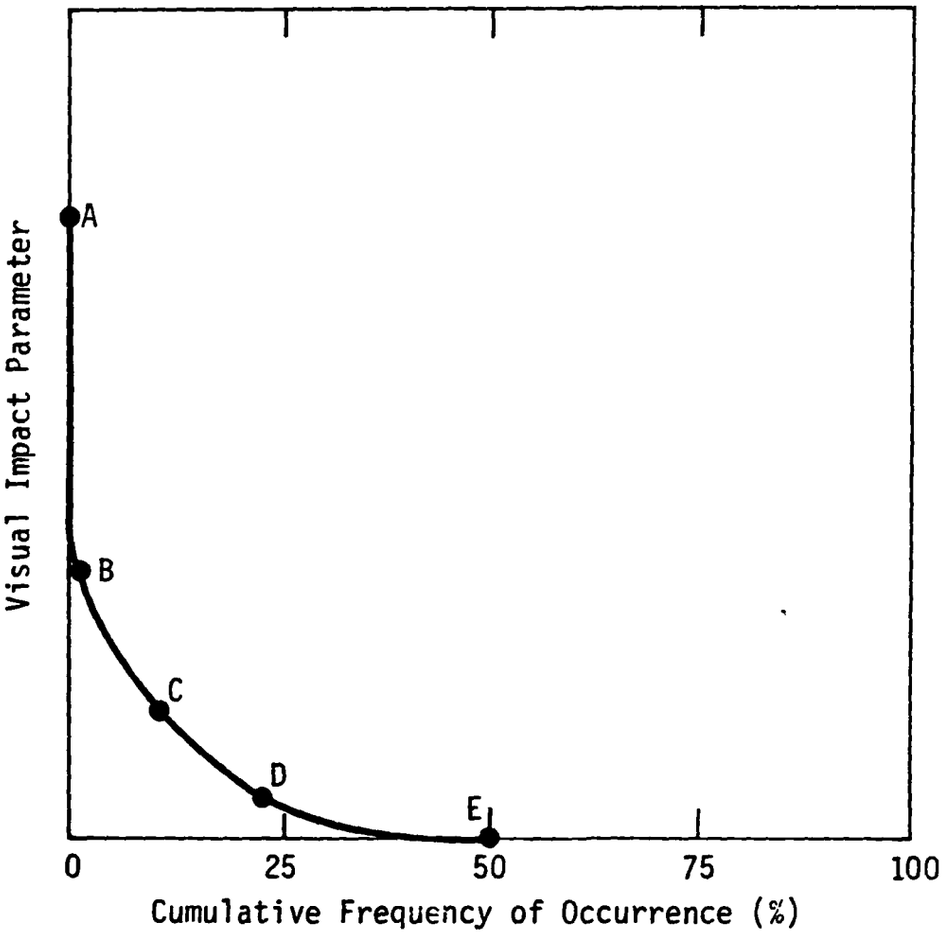

Figure 8. Example of a frequency distribution of visual impact.

pheric stability; background ozone concentration; and background visual range to specify the frequency distribution of visual impact. If one has a large, concurrent data base of all five of these variables, it would be desirable to calculate a five-way joint-probability distribution matrix and to use these joint probabilities to calculate frequency of occurrence of impact. However, in most situations, such a data base is not available, and one must treat the various worst-case events as independent probabilities. With this assumption, the probability of worst-case impacts can be calculated by multiplying the independent probabilities. This can be represented as follows:

$$f(y > y') = \prod_i f(x_i > x_i') \quad ,$$

where $f(y > y')$ is the cumulative frequency of impact y greater than y', and $f(x_i > x_i')$ is the cumulative frequency of variable x_i having values that would cause greater impact than the value x_i'.

In such an application, one might obtain an estimate of cumulative frequency by using the joint frequency distribution of upper-air wind speed and wind direction and the separate frequency distributions of upper-air stability, ozone concentration, and visual range. For example, the plume perceptibility parameter ΔE has a cumulative frequency distribution that can be estimated as follows:

$$f(\Delta E > \Delta E') = f(u < u', WD < WD') \cdot f(s > s') \cdot f([O_3] > [O_3]') \cdot f(r_v > r_v') \quad ,$$

where

$f(\Delta E > \Delta E')$ = the frequency of occurrence of ΔE values greater than $\Delta E'$. $\Delta E'$ is calculated on the basis of a wind speed u', wind direction WD', stability s', ozone concentration $[O_3]'$, and visual range r_v'.

$f(u < u', WD < WD')$ = the frequency of occurrence of wind speeds

less than u' associated within a specified value (WD') of the worst-case wind direction.

$f(s > s')$ = the frequency of occurrence of stabilities greater than s'.

$f([O_3] > [O_3]')$ = the frequency of occurrence of background ozone concentrations greater than $[O_3]'$.

$f(r_v > r_v')$ = the frequency of occurrence of background visual range values greater than r_v'.

Each of the input parameters that are important to the visibility model calculation varies significantly over the period of a year, and all are discussed in the following paragraphs.

2.3.1 Wind Speed

Wind speed affects plume visual impact strongly because plume centerline concentrations and plume line-of-sight integrals are inversely proportional to wind speed. Greater impact would be expected during light-wind stagnation conditions than during strong-wind, well-ventilated conditions. Also, since the age of a plume parcel at a given distance downwind from a power plant is inversely proportional to wind speed, more time is available at low wind speeds for the chemical conversion of primary emissions. A well-aged plume parcel is more likely to cause a reduction in visual range than is a younger one. However, the time necessary to transport emissions a given distance toward a class I area increases with decreasing wind speed. Thus, during light-wind conditions, several hours of persistent conditions may be needed to transport emissions to a class I area where they could cause visual impact.

2.3.2 Wind Direction

Wind direction also affects plume visual impact, because the direction of plume parcel transport affects the orientation of the plume with respect to the observer. If the plume is transported directly toward an

observer, the observer's line of sight directly along the center of the plume is significantly affected. As noted previously, if the observer's line of sight is oblique to or along the plume axis, plume optical thickness will be greater than if the line of sight is normal to the plume axis. However, there is a compensating effect; the direction of plume transport affects the distance (r_p) between the observer and the plume material. Plume discoloration is diminished by light scattered by the intervening, or background, atmosphere. The more distant the plume material, the less colored and less perceptible it is likely to be. This decrease in plume coloration can be expressed as follows:

$$C_{plume}(r_p) = C_{plume}(0)\exp(-3.9\ r_p/r_{v0}) \quad , \qquad (23)$$

where

$C_{plume}(r)$, $C_{plume}(0)$ = plume contrasts at plume-observer distances r and 0, respectively.

r_p = plume-observer distance.

r_{v0} = background visual range.

It should be noted that visual range reduction does not decrease with increasing distance between the plume and the observer, assuming one can still see across the plume. However, the aesthetic effects of this visual range reduction would be less, since contrast reduction (ΔC_r) would decrease exponentially, as the plume-object distance increases as shown in equation (14). Also, it should be noted that with a more distant plume, only the contrast of distant terrain objects would be affected and fewer lines of sight would be impacted. In addition, the aesthetic impact caused by plume discoloration is likely to be less if the plume is farther away, because the plume will appear smaller (i.e., fewer lines of sight will be affected).

To illustrate the effect of wind direction, figure 9(a and b) shows the positions of two plumes from a hypothetical emissions source relative to a vista in a class I area 90 km away. Plume ±2 σ_y outlines are shown

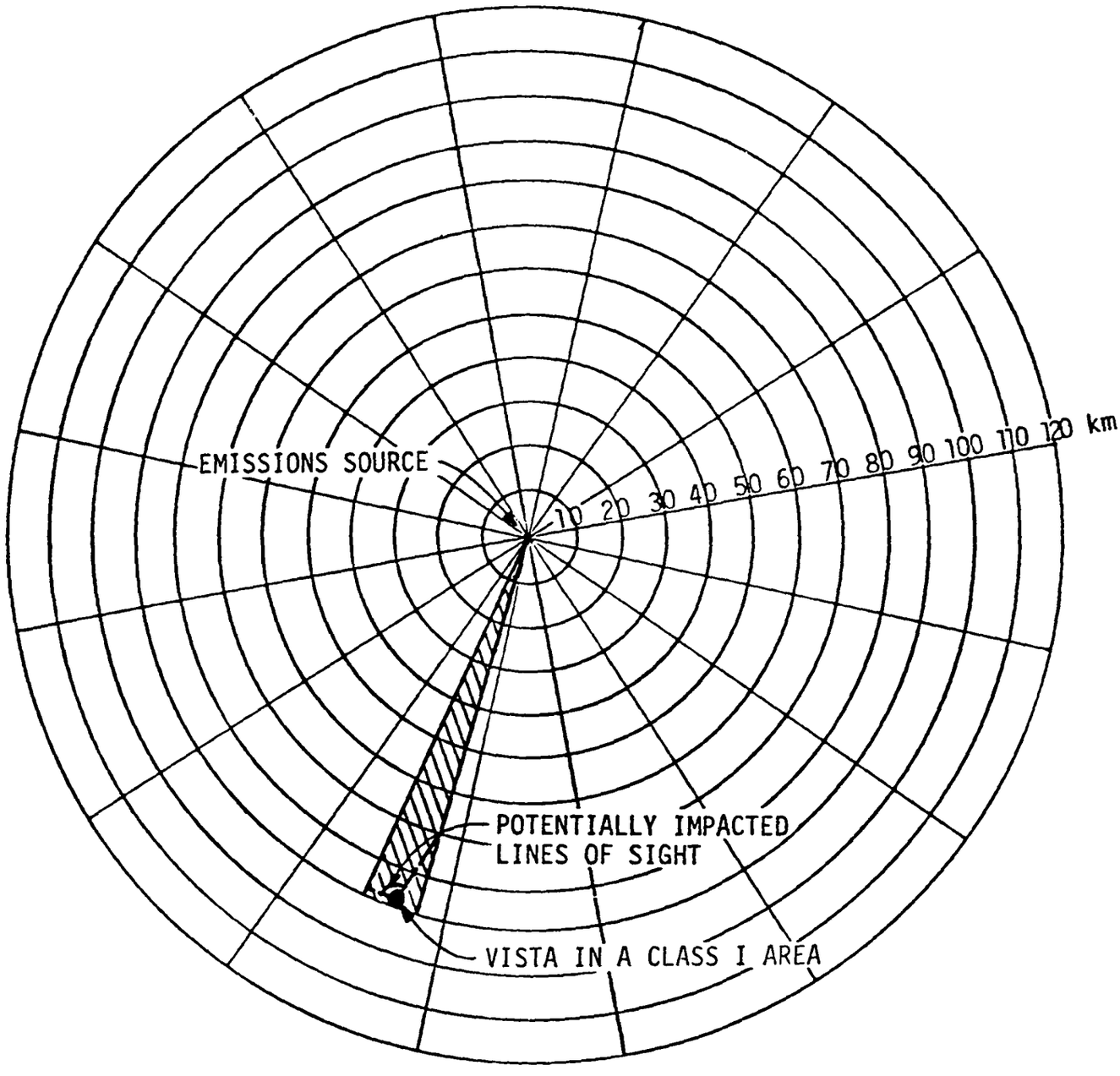

(a) Worst-Case Wind Direction

Figure 9. Schematic diagram showing plume-observer geometry for two wind directions.

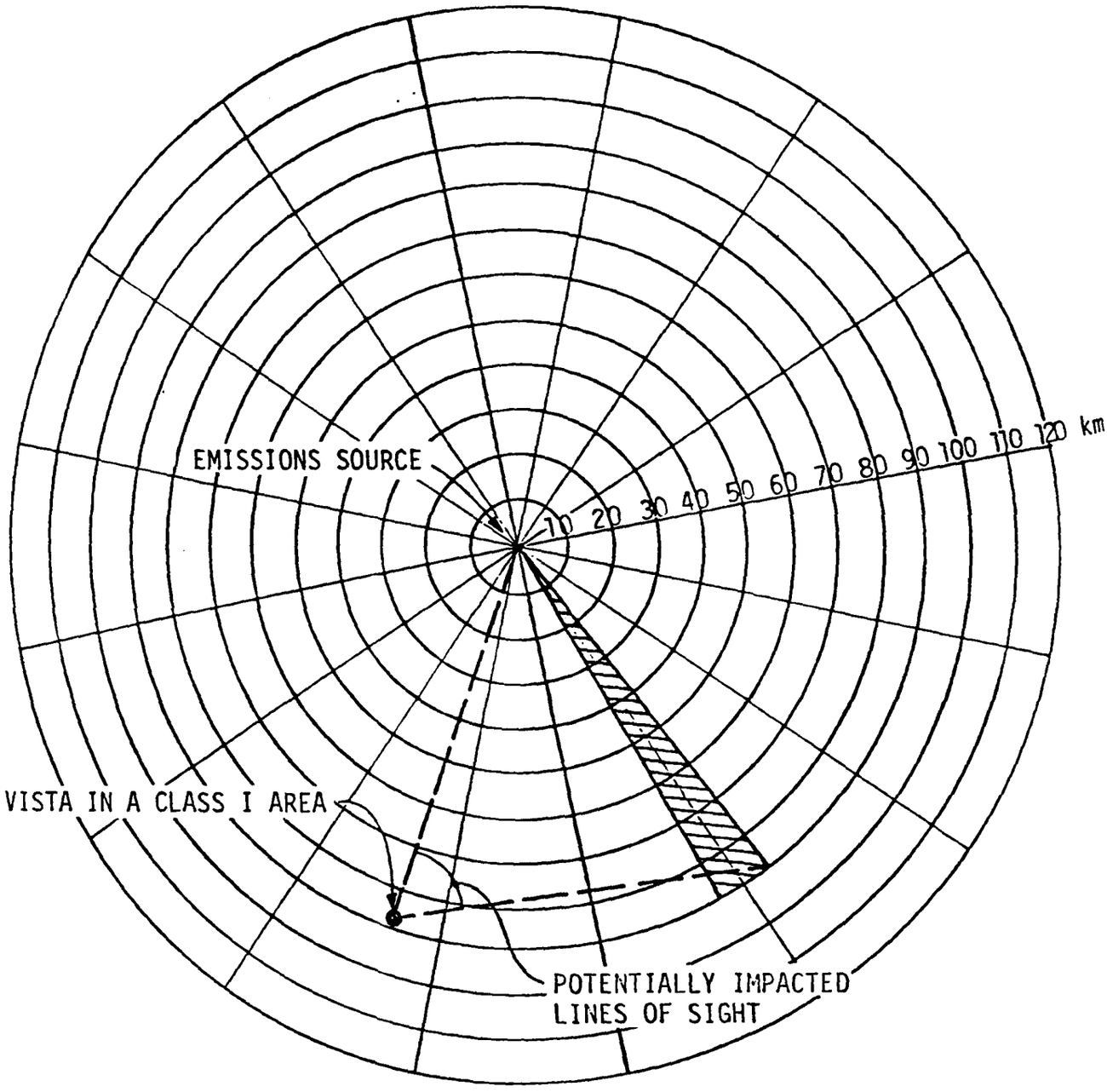

(b) Wind direction resulting in less impact than the worst case.

Figure 9 (Concluded)

to scale with σ_y values appropriate for a Pasquill E stability. Of course, actual plume trajectories would be affected by wind channeling, complex terrain, and changes in wind direction with time, so these figures are only idealized representations. Figure 9 shows trajectories that could occur with north-northwesterly and north-northeasterly winds. A plume associated with a north-northeasterly wind direction (defined by a sector 22.5° wide) could be anywhere within the extremes of the sector shown in figure 9. Thus, a wide range of impacts could occur associated with north-northeasterly winds. The worst case would be that shown in figure 9(a), in which the plume is transported directly toward the observer. Of course, the worst-case conditions of figure 9(a) would occur for only some of the periods of north-northeasterly flow. Figure 9(b) shows that, for another wind direction, plume discoloration would be considerably less, because plumes would be tens of kilometers away from the observer, and the observer's line of sight could be nearly perpendicular to the plume, not along the plume as in figure 9(a). Since the case shown in figure 9(a) is not a likely occurrence, the level-1 and level-2 analyses are not suitable for evaluating the visual impact associated with this plume-observer orientation. A level-3 analysis is required when views along the plume axis are of concern.

2.3.3 Atmospheric Stability

Upper-air stability controls the rate at which source emissions are mixed with ambient air. During stable conditions, diffusion is limited, particularly in the vertical direction, so plumes remain as ribbon-like layers. Plume discoloration is most apparent during such stable conditions, because the integral of NO_2 and particulate concentrations along the line of sight is greater. During well-mixed (neutral or unstable) conditions, plumes are rapidly diffused and not likely to be visible as plumes per se.

Stability, or the rate of plume mixing, also has an effect on chemical conversion within a plume. The conversion of nitric oxide (NO) to nitrogen dioxide (NO_2) is diffusion-limited in stable plumes, as is the

formation of sulfate and nitrate, because background ozone that effects NO_2 formation is depleted within the plume.

2.3.4 Background Ozone Concentration

An important input parameter to the visibility model is the background ozone concentration, that is, the concentration of ozone outside the plume. Ozone reacts directly with the colorless nitric oxide emitted from power plants to form the brownish gas, nitrogen dioxide, the principal plume colorant:

$$NO + O_3 \rightarrow NO_2 + O_2 \quad .$$

Ozone is also indirectly important in the oxidation of plume NO_2 and SO_2, since ultraviolet radiation photolyzes ozone to form the hydroxyl radical (OH•) that reacts with NO_2 and SO_2 to form nitric acid and sulfate aerosol.

Calculations should be made for the median (50-percentile) background ozone concentration as a minimum and possibly for the 25- and 75-percentiles also.

2.3.5 Background Visual Range

Background visual range is also an important input parameter, because the magnitude of plume discoloration visible from a given location depends on the clarity of the intervening atmosphere. Plume discoloration is much more noticeable in the extremely clear areas of the Southwest, for example, than in hazy areas. Equation (23) shows that as the background visual range (r_{v0}) decreases (i.e., the atmosphere becomes hazier), the degree of plume discoloration decreases also. Thus, one must supply one or more (e.g., 25-, 50-, and 75-percentile) values of background visual range in the study area to characterize impacts for different levels of atmospheric clarity.

2.3.6 Study Area Topography

The topography of an area also has an influence on visibility impairment. High terrain affects the transport of emissions, particularly during worst-case stable conditions. It is likely that a stable plume would be channeled by high terrain and remain in a valley. Thus, the assumption of a straight plume trajectory approaching an observer location on elevated terrain, such as is shown in figure 9(a), may never occur in some areas. The topography also affects the rate of dilution of plumes, with mechanically induced turbulence enhancing plume dilution.

Topography also affects the views from a given vista location. For example, topography can obstruct views in certain directions from a vista where plume material is located. It can also have an effect on the type of viewing background (what is visible behind the plume), which has an effect on plume discoloration.

2.3.7 Season and Time of Day

Gas-to-particle conversion is also a function of season and time of day, with higher conversion rates at times when ultraviolet flux is greatest. Also, the sun angles (i.e., azimuth, zenith, and scattering angles) are dependent on season and time of day.

2.3.8 Model Runs

If one used all the permutations of the important input variables, one could make hundreds of plume visibility model runs to characterize the frequency distribution of visual impact over a season or a year. For example, if 5 wind directions, 3 wind speeds, 2 stabilities, 3 background visual ranges, 3 background ozone concentrations, and 2 seasons are evaluated, one would have to make 540 runs (5 x 3 x 2 x 3 x 3 x 2). Furthermore, if 10 downwind distances were evaluated and 4 viewing background colorations were considered for each line-of-sight geometry, a total of 21,600 individual line-of-sight calculations would be needed. The comput-

ing costs for this many calculations would be prohibitive. To reduce costs, one can reasonably approximate the frequency distribution of impacts by using median values of background ozone concentrations and visual range and evaluating impacts for sun angles corresponding to one season (e.g., spring or fall), thus reducing the total number of runs in this example to 30.

3 LEVEL-1 VISIBILITY SCREENING ANALYSIS

The level-1 visibility screening analysis is a simple, straightforward calculation designed to identify those emissions sources that have little potential of adversely affecting visibility in a class I area. If a source passes this first screening test, it would not be likely to cause adverse visibility impairment, and further analysis of potential visibility impacts would be unnecessary. If the source fails this test, additional screening analysis would be needed to assess potential impacts.

The level-1 visibility screening analysis requires a minimal amount of information about the source and only a few minutes of an analyst's time to evaluate potential visibility impairment. The input parameters needed to evaluate potential visibility impacts with this screening analysis procedure are as follows:

- Minimum distance of the emissions source from a potentially affected class I area (in kilometers).
- Location of the emissions source and class I area.
- Particulate emission rate (in metric tons/day).
- NO_x emission rate (in metric tons/day).
- SO_2 emission rate (in metric tons/day).

3.1 DERIVATION OF LEVEL-1 SCREENING ANALYSIS

The level-1 visibility screening analysis is designed to evaluate two potential types of visibility impairment that can be caused by plumes from emissions sources. These two types of visibility impairment are caused by nitrogen oxide, particulate, and sulfur dioxide emissions. Figures 10 and 11 illustrate the two types of plume impacts. One is a discolored, dark

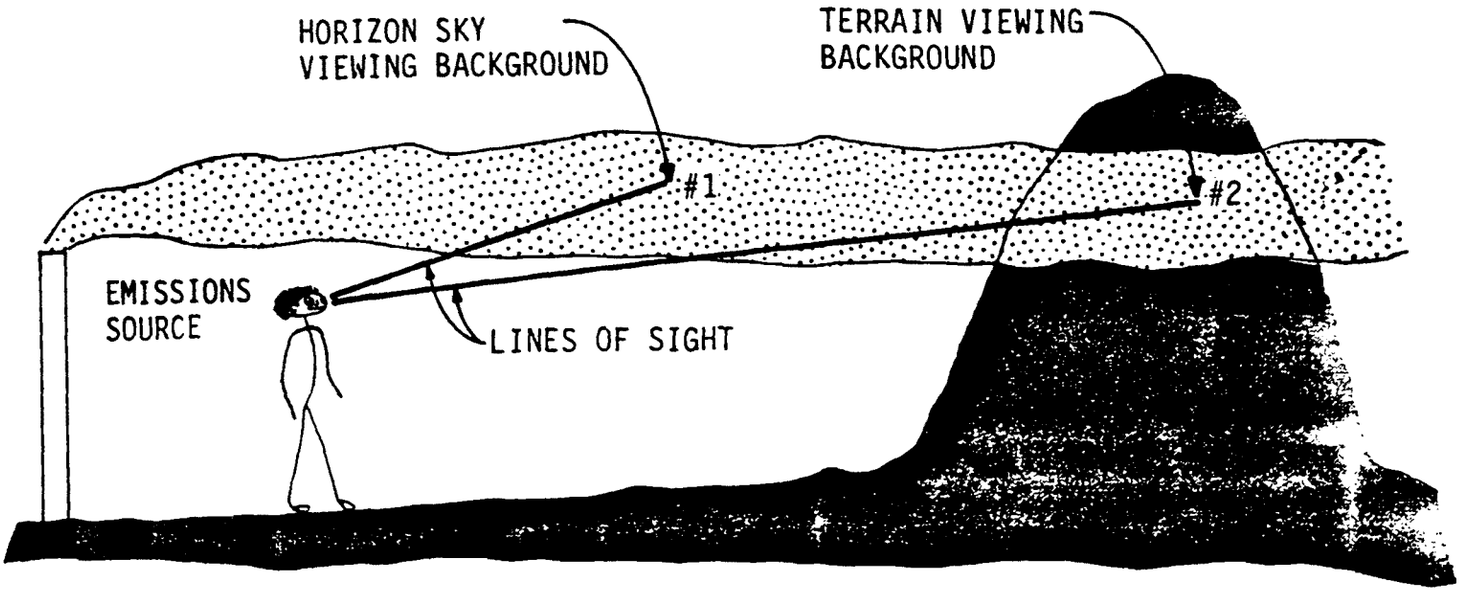

Figure 10. Two types of plume visibility impairment considered in the level-1 visibility screening analysis.

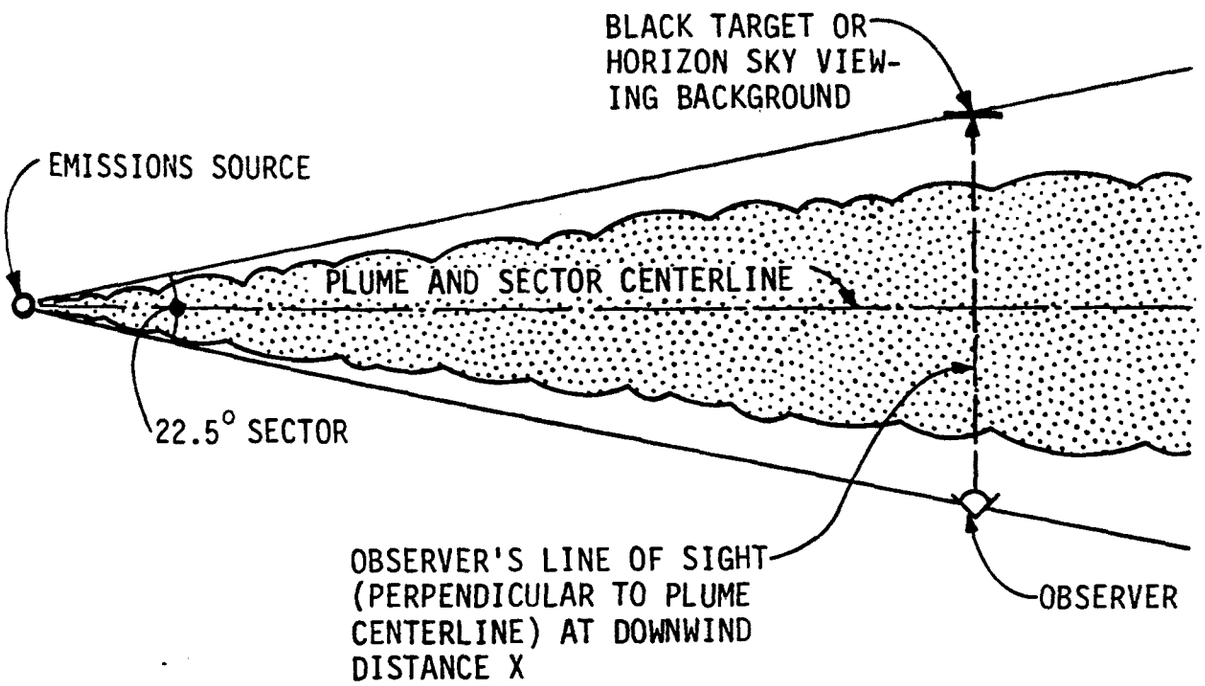

Figure 11. Geometry of plume, observer, and line of sight used in level-1 visibility screening analysis.

plume observed against a bright horizon sky (labeled 1 in figure 10). This effect is caused principally by NO_2 gas formed from NO_x emissions, though particulates can contribute in some cases. The other type is a bright plume observed against a dark terrain viewing background (labeled 2 in figure 10). This effect is caused principally by particle emissions and sulfate aerosol formed from SO_2 emissions.

Model calculations (Latimer et al., 1980a) suggest that sulfate aerosol does not form in stable plumes containing a significant amount of NO_x. Sulfate formation does not occur until emissions are diluted significantly with background air. However, the visual impacts caused by NO_x and particulate emissions are greatest when the plume material is concentrated, as in light-wind, stable conditions. For these reasons, we consider two different meteorological conditions:

- For maximum impact caused by particulate and NO_x emissions: stable (Pasquill-Gifford stability category F), light-wind conditions with a 12-hour transport time to the closest class I area.
- For maximum impact caused by SO_2 emissions: limited mixing conditions, vertically well-mixed plume within a 1000 m mixing depth, 2 m/s wind speed.

For both cases, the geometry of the plume, observer, and line of sight assumed for this screening analysis is shown in figure 11. The plume is assumed to pass very close to the observer, with its centerline half the width of a 22.5° sector away from the observer at the given downwind distance x. The observer's line of sight is assumed to be perpendicular to the plume centerline. The viewing background is assumed to be either the horizon sky or a black terrain object located on the opposite side of the plume a distance equivalent to a full sector from the observer.

3.1.1 Impacts of Particulate and NO_x Emissions

Meteorological conditions are assumed to be stable with light winds. Pasquill-Gifford F stability is used to characterize the vertical dispersion (σ_z) important in evaluating the visual impacts for horizontal lines of sight. Since such stable conditions are not likely to persist for more than 12 hours in a typical diurnal cycle, we selected a worst-case wind speed that would transport emissions from the source to a class I area in 12 hours. Thus, wind speed is determined as a function of distance x to the class I area as shown below:

$$u = \frac{(x \text{ km})(1000 \text{ m/km})}{(12 \text{ hr})(3600 \text{ sec/hr})} = 2.31 \cdot 10^{-2}(x) \text{ m/s} \quad .$$

Thus, a 2.3 m/s wind would be used to evaluate impacts in a class I area 100 km from the emissions source.

The horizontal optical thickness through the center of an elevated stable plume is

$$\tau = \frac{Q}{(2\pi)^{1/2}\sigma_z u}$$

where Q is the mass emission rate of NO_x and particles multiplied by the respective light absorption and scattering efficiencies of these two species. For the level-1 analysis we conservatively assume that there is complete conversion of NO_x emissions to NO_2 in the atmosphere.

We can calculate the absorption (NO_2) and scattering (particle) components of the plume optical thickness separately, as follows:

$$\tau_{NO_2} = b_{abs}/(\mu g/m^3)\ p\ Q_{NO_2} \quad ,$$

$$\tau_{part} = b_{scat}/(\mu g/m^3)\ p\ Q_{part} \quad ,$$

where

$$p = \frac{1}{(2\pi)^{1/2}\sigma_z u} \quad .$$

The value of p is evaluated so that the units of Q_{part} and Q_{NO_2} in the above formulas are in metric tons per day:

$$p = \frac{(10^{12}\ \mu g/\text{metric ton})(\text{day}/24\ \text{hr})(\text{hr}/3600\ \text{sec})}{(2\pi)^{1/2}(\sigma_z)(2.31 \times 10^{-2})(x)}$$

$$= \frac{2.0 \cdot 10^8}{\sigma_z x} \quad .$$

The absorption per unit mass of NO_2 is calculated for a wavelength of 0.55 μm as follows (Dixon, 1940):

$$b_{abs}/(\mu g/m^3) = \frac{(0.31\ km^{-1}/ppm)}{(1881\ \mu g/m^3/ppm)(1000\ m/km)} = 1.65 \times 10^{-7} m^{-1}/(\mu g/m^3) \quad .$$

The scattering coefficient per unit mass of aerosol for a wavelength of 0.55 μm was calculated using Mie scattering theory. A primary particle size distribution typical of a coal-fired power plant equipped with an electrostatic precipitator (Schulz, Engdahl, and Frankenberg, 1975) was assumed. This distribution has a mass median diameter of 2 μm, a geometric standard deviation of 2, and a density of 2.5 g/cm^3. For such a size distribution:

$$b_{scat}/(\mu g/m^3) = 10 \cdot 10^{-7} m^{-1}/(\mu g/m^3) \quad .$$

We can use equation (10) from chapter 2 to evaluate the sky/plume contrast resulting from NO_2 light absorption. For this level-1 analysis, we assume that the phase functions for the plume and the background atmosphere are equal. With this assumption, equation (10) reduces to the following equation:

$$C_{plume} = - \frac{\tau_{NO_2}}{\tau_{part} + \tau_{NO_2}} \left[1 - \exp\left(-\tau_{part} - \tau_{NO_2}\right)\right] \left[\exp\left(-3.912\ r_p/r_{v0}\right)\right]$$

where

$r_p \equiv$ the observer-plume distance, which, for the geometry shown in figure 11,
$= x \tan\left(\frac{22.5^\circ}{2}\right) = 0.199\ x$,

$r_{v0} \equiv$ background visual range (km),

$\tau_{NO_2}, \tau_{part} \equiv$ NO_2 and particulate components of plume optical thickness, as discussed above.

It should be noted that this equation can be simplified (valid only for small plume optical thicknesses, $\tau < 0.1$) by using the first two terms of a series expansion of the second term:

$$C_{plume} \tilde{=} - \tau_{NO_2} \exp(-3.912\ r_p/r_{v0})$$

From this approximate formula we see that the sky/plume contrast is proportional to the plume NO_2 line-of-sight integral (τ_{NO_2}) and decreases as the plume-observer distance increases.

Now let us consider the reduction in sky/terrain contrast by the same plume. If the background terrain is black, then $C_0 = -1$, and we can rewrite equation (14) as follows:

$$\Delta C_r = \left[1 - \left(\frac{1}{C_{plume} + 1}\right)\left(\exp -\tau_{part} - \tau_{NO_2}\right)\right]\left[\exp(-3.912\ r_0/r_{V0})\right]$$

where C_{plume} is as defined above, and r_0 is the observer-object distance, which, for the geometry shown in figure 11, equals $2 \cdot x \cdot \tan(22.5^{\circ}/2)$, where x is the downwind distance from the emissions source to the class I area.

3.1.2 Impacts of SO_2 Emissions

We evaluate the worst-case impacts of SO_2 emissions, assuming a multiday stagnation episode (limited mixing). Both primary particle emissions and sulfate ($SO_4^=$) aerosol formed in the atmosphere from SO_2 emissions reduce the contrast of objects viewed through the plume. However, NO_x emissions are converted to nitric acid vapor by reaction with the hydroxyl radical, the same species responsible for conversion of SO_2 to $SO_4^=$. Hence, no NO_2 is assumed to be present.

Since sulfate forms slowly in the atmosphere, the maximum impact does not necessarily occur at the class I area closest to the emissions source. Thus, for the level-1 analysis we evaluate sulfate impacts at a distance of 350 km from the source, the equivalent of two days' transport time from the emissions source for an assumed 2 m/s wind speed. Furthermore, we evaluate the sky/terrain contrast reduction of a terrain feature located one-fourth the background visual range distance. The contrast reduction of a terrain feature at this distance is a maximum for a given increase in extinction coefficient (see appendix A). Note that the plume itself would not be visible, but plume material uniformly diffused through the mixed layer could cause a reduction in sky/terrain contrast.

The sulfate mass flux at any given distance downwind is calculated by solving the following differential equations:

$$\frac{dQ_{SO_2}}{dt} = -(k_f + k_d)Q_{SO_2} \quad ,$$

$$\frac{dQ_{SO_4^=}}{dt} = 1.5\ k_f\ Q_{SO_2} \quad ,$$

where

Q_{SO_2}, $Q_{SO_4^=}$ ≡ mass flux of SO_2 and $SO_4^=$, respectively, in the plume at downwind distance corresponding to transit time t,

k_d ≡ rate of SO_2 loss due to surface deposition $= \frac{v_d}{H_m}$,

k_f ≡ rate of SO_2-to-$SO_4^=$ conversion ,

v_d ≡ deposition velocity ,

H_m ≡ mixing depth.

The solution to these equations is

$$Q_{SO_4^=} = \frac{1.5\ k_f}{(k_f + k_d)}\ Q_{SO_2} \left\{1 - \exp[(-k_f + k_d)\ t]\right\}$$

For an assumed transit time of 48 hours, mixing depth H_m of 1000 m, SO_2 deposition velocity (diurnal average) v_d of 0.5 cm/s, and SO_2-to-$SO_4^=$ conversion rate (diurnal average) k_f of 0.5 percent/hr, we find that the sulfate mass flux is:

$$Q_{SO_4^=} = 0.218\ Q_{SO_2}$$

We assume an average scattering coefficient per unit mass concentration of sulfate and primary particles of 6×10^{-6} and $1 \times 10^{-6} m^{-1}/(\mu g/m^3)$, respectively, appropriate for typical size distributions (see Latimer et al., 1978, and Schulz, Engdahl, and Frankenberg, 1975). The optical thickness due to total aerosol for this limited mixing case is then simply:

$$\tau_{aerosol} = \frac{\left(Q_{part} + 1.31\ Q_{SO_2}\right)\left(10^{-6} m^{-1}/\mu g/m^3\right)}{u\ H_m} \quad .$$

Now if we substitute the appropriate values of u and H_m, and the appropriate conversion factor from metric tons per day to μg/s, we have the following expression:

$$\tau_{aerosol} = (5.79 \cdot 10^{-3})\ (Q_{part} + 1.31\ Q_{SO_2}) \quad .$$

This is the total optical depth across a plume at a downwind distance of 350 km (transit time = 48 hr). We wish to use the optical depth between the observer and a terrain feature at the most sensitive distance, $r_o = r_{v0}/3.912$, as shown in appendix A. Thus, we must correct $\tau_{aerosol}$ accordingly. We assume the plume is uniformly mixed within a 22.5° sector, which is quite wide 350 km downwind:

$$2(x)\tan\left(\frac{22.5^\circ}{2}\right) = 2(350\ km)(0.199) = 139\ km$$

The ratio of the optical depth between the observer and the most sensitive terrain feature to the total optical depth is then

$$\frac{r_{v0}}{545\ km}$$

Thus, we end up with the following expression:

$$\tau_{aerosol} = (1.06 \times 10^{-5})(r_{v0})(Q_{part} + 1.31\ Q_{SO_2}) \quad ,$$

where r_{v0} is the background visual range in km, and Q_{part} and Q_{SO_2} are particle and SO_2 emission rates in metric tons per day.

Substituting this optical thickness into equation (14) and assuming that $C_{plume} = 0$, we have the following expression for the contrast reduction caused by sulfate aerosol and particulate emissions during a stagnation episode:

$$\Delta C_r = 0.368[1 - \exp(-\tau_{aerosol})] \quad .$$

3.2 INSTRUCTIONS FOR LEVEL-1 SCREENING ANALYSIS

The level-1 screening procedure comprises these steps:

> Determine the minimum, straight-line distance x, in kilometers, between the emissions source and the closest boundary of a class I area. Determine σ_z corresponding to this distance for Pasquill-Gifford F stability from figure 12 (Turner, 1969). If x > 100 km, set σ_z = 100 m. Compute the plume dispersion parameter p as follows:

$$p = \frac{2.0 \cdot 10^8}{\sigma_z x} \quad , \qquad (p\text{-}1)^*$$

---

* Throughout this workbook, formulas used in the level-1 or level-2 analysis procedure are indicated with a prefix p (for procedure). Those equations that are not part of a screening procedure are either not numbered or not labeled with the p prefix.

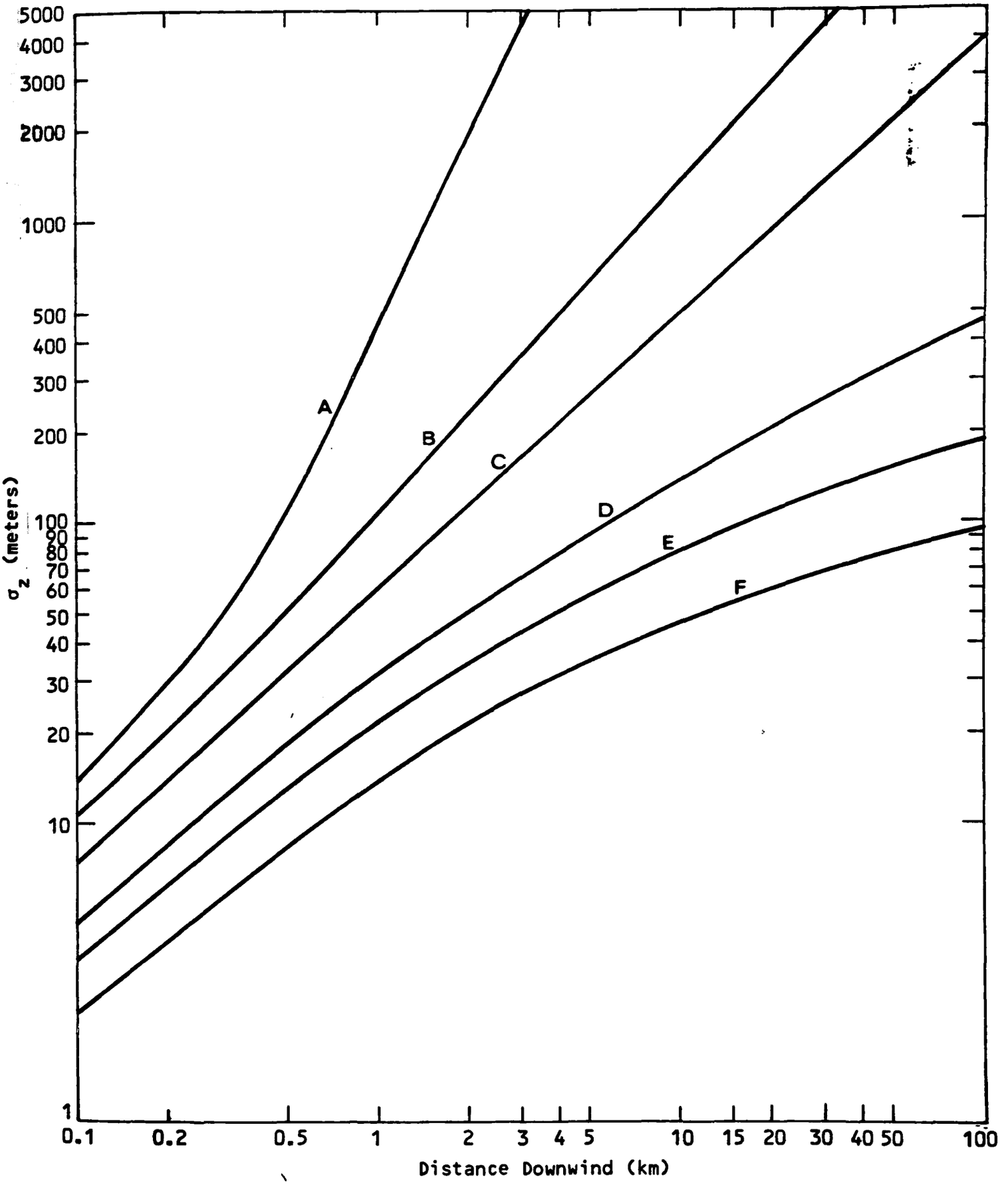

Source: Turner (1969).

Figure 12. Vertical dispersion coefficient (σ_z) as a function of downwind distance from the source

where σ_z is in meters and x is in kilometers.

> From the total mass emission rates of particulates (Q_{part}) and nitrogen oxides as NO_2 (Q_{NO_x}) in metric tons per day, calculate the following optical thicknesses:

$$\tau_{part} = 10 \cdot 10^{-7} \; p \; Q_{part} \quad , \qquad \text{(p-2)}$$

$$\tau_{NO_2} = 1.7 \cdot 10^{-7} \; p \; Q_{NO_x} \quad . \qquad \text{(p-3)}$$

> Determine locations of the emissions source and the class I area on the map shown in figure 13 and the appropriate value, r_{v0}, of the background visual range in kilometers.* If the emissions source and class I area are in different visibility regions, use the larger value of r_{v0} in subsequent calculations.

> Calculate the following optical thickness parameter for primary and secondary aerosol:

$$\tau_{aerosol} = (1.06 \times 10^{-5})(r_{v0})\left(Q_{part} + 1.31 \; Q_{SO_2}\right). \qquad \text{(p-4)}$$

> Calculate the following contrast parameters (note that C_1 is plume contrast against the sky, C_2 is plume contrast against terrain, and C_3 is a change in sky/terrain contrast caused by primary and secondary aerosol):

---

* The values of r_{v0} shown in figure 13 are estimated mean visual ranges in kilometers at 0.55 μm based on the work of Trijonis and Shapland (1979). Their values, based on human observation of terrain features at National Weather Service meteorological stations, have been increased by 50 percent to agree with mean visual range measurements made in the Southwest (Malm et al., 1979) using a telephotometer equipped with a narrow band filter at 0.55 μm. This correction was made because it is believed that the telephotometer provides more accurate measurements of visual range than those produced by human observation.

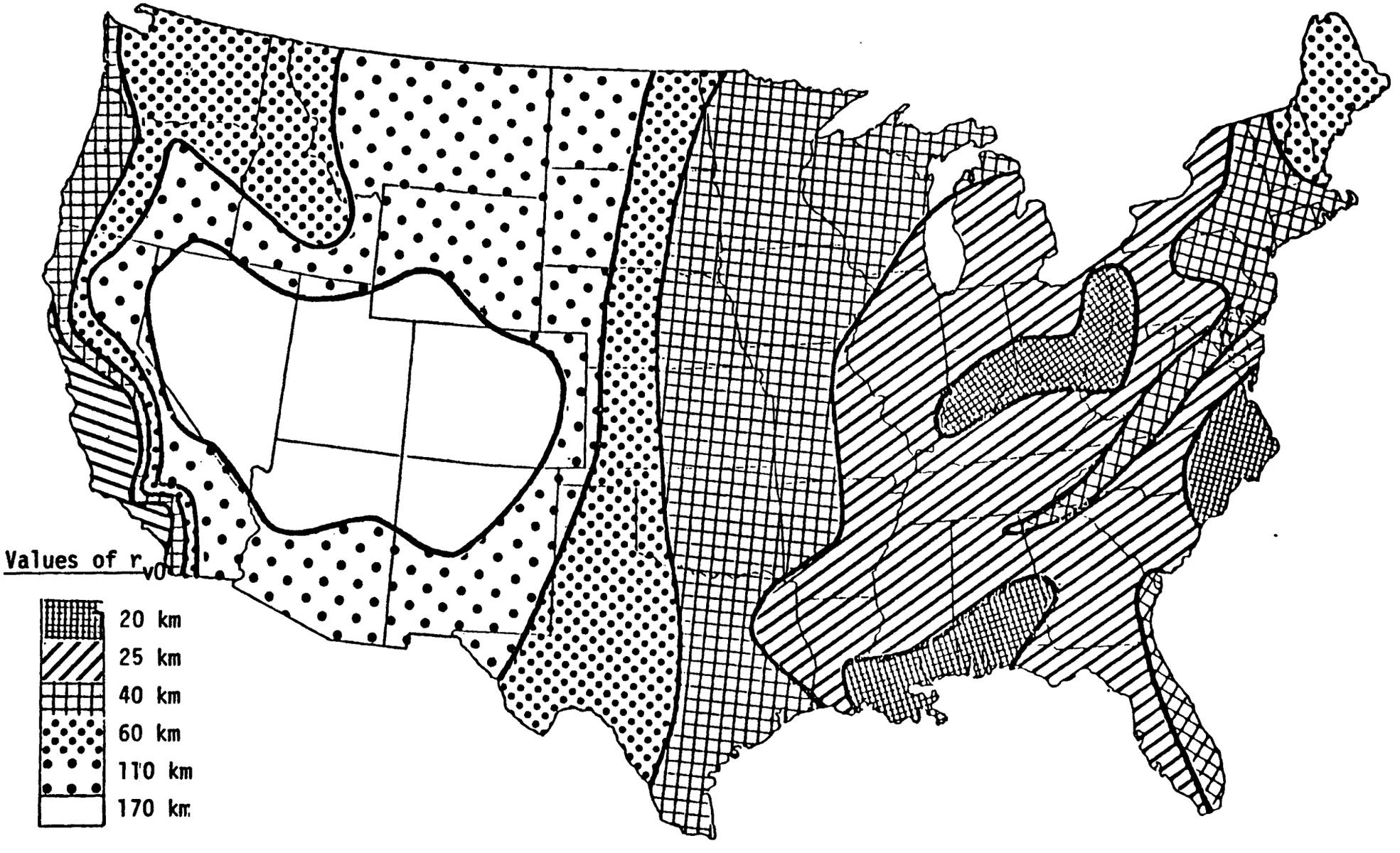

Figure 13. Regional background visual range values (r_{v0}) for use in level-1 visibility screening analysis procedure.

$$C_1 = - \frac{\tau_{NO_2}}{\tau_{part} + \tau_{NO_2}} \left[1 - \exp\left(-\tau_{part} - \tau_{NO_2}\right)\right]\left[\exp(-0.78\ x/r_{v0})\right] \quad \text{(p-5)}$$

$$C_2 = \left[1 - \left(\frac{1}{C_1 + 1}\right) \exp\left(-\tau_{part} - \tau_{NO_2}\right)\right]\left[\exp(-1.56\ x/r_{v0})\right] \quad , \quad \text{(p-6)}$$

$$C_3 = 0.368\ [1 - \exp(-\tau_{aerosol})] \quad . \quad \text{(p-7)}$$

> If the absolute value of C_1, C_2, or C_3 is greater than 0.10, the emissions source fails the level-1 visibility screening test, and further screening analysis is required to assess potential visibility impairment. If the absolute values of C_1, C_2, and C_3 are all less than 0.10, it is highly unlikely that the emissions source would cause adverse visibility impairment in class I areas; therefore, further analysis of potential visibility impacts would be unnecessary.*

---

* This screening procedure could be used as an aid in siting studies. The distance x_{min} could be determined so that the criteria for C_1 and C_2 would be met on the basis of a given regional background visual range and NO_x and particulate emissions rates. The industrial planner could use this x_{min} distance as a factor in his siting analysis. If the preferred site were at a distance $x < x_{min}$ from a class I area, further analysis (level-2 and possibly level-3) of potential visibility impacts would be needed to evaluate the acceptability of the site.

3.3 EXAMPLE APPLICATIONS OF THE LEVEL-1 ANALYSIS

3.3.1 Example 1

Suppose we evaluate a hypothetical, large power plant located 100 km from a class I area in southern Utah. The power plant emits 10 metric tons per day of particulates, 100 metric tons per day of NO_x (as NO_2), and 200 metric tons per day of SO_2.

For x = 100 km, the Pasquill-Gifford stability class F, σ_z = 90 m. Thus, we calculate the following values:

$$p = \frac{2.0 \times 10^8}{(90)(100)} = 2.22 \times 10^4 \quad ,$$

$$\tau_{part} = (10 \times 10^{-7})(2.22 \times 10^4)(10) = 0.222 \quad ,$$

$$\tau_{NO_2} = (1.7 \times 10^{-7})(2.22 \times 10^4)(100) = 0.378 \quad .$$

From figure 13 we see that the background visual range for southern Utah is 170 km.

We calculate the following parameters:

$$\tau_{aerosol} = (1.06 \cdot 10^{-5})(170)(10 + 1.31 \cdot 200) = 0.490 \quad ,$$

$$C_1 = - \frac{0.378}{0.222 + 0.378} [1 - \exp(-0.222 - 0.378)][\exp(-0.78 \cdot 100/170)]$$

$$= -0.180 \quad ,$$

$$\left[C_2 = 1 - \left(\frac{1}{1 - 0.18}\right) \exp(-0.222 - 0.378)\right]\left[\exp(-1.56 \cdot 100/170)\right]$$

$$= 0.132 \quad ,$$

$$C_3 = 0.368\,[1 - \exp(-0.490)] = 0.143 \quad .$$

Since the absolute value of each of these contrast parameters (C_1, C_2, and C_3) is greater than 0.10, we cannot rule out the possibility that this hypothetical power plant would cause adverse or significant visibility impairment in the class I area. This is not to say that the source actually does cause such impact. It means only that it does not pass the level-1 screening test. Further level-2 or level-3 analysis may show that the visual impact is not significant or adverse.

The reader can verify that if this power plant were sited at least 150 km from a class I area in the same region, it would pass the first two tests (i.e., $|C_1| < 0.10$ and $|C_2| < 0.10$); however, it would still fail the third level-1 test ($C_3 = 0.143 > 0.10$). The reader can also show that if the same plant were sited in a region with 40 km visual range at the same distance (100 km), it would easily pass the level-1 screening tests. Indeed, in such a region the source could be located as close as 70 km and still pass the level-1 tests.

Let us return to our original example and consider whether the source could meet the level-1 tests by cutting particulate and SO_2 emissions in half. By doing this, the reader can verify that, though C_2 is reduced from 0.132 to 0.097, and C_3 is reduced from 0.143 to 0.080, $|C_1|$ actually is increased from 0.180 to 0.189. Thus, even with particulate and SO_2 controls, the source would not meet the level-1 C_1 test. In order to do so, NO_x emissions would have to be reduced or the plant would have to be sited about 150 km away from the class I area.

It is interesting to note that $|C_1|$ is best reduced by NO_x emissions control, $|C_2|$ is best reduced by particulate emissions control, and $|C_3|$ is best reduced by SO_2 emissions control. Only $|C_1|$ and $|C_2|$ can be reduced by increasing the distance between the site and the class I area.

3.3.2 Example 2

Consider the impact of a proposed plant that would emit 20 metric tons per day of particulate matter and no NO_x or SO_2, and would be sited 50 km from a class I area in southern Arizona. We calculate the following parameters:

$$p = \frac{2.0 \cdot 10^8}{(78)(50)} = 5.13 \cdot 10^4 \quad ,$$

$$\tau_{part} = (10 \cdot 10^{-7})(5.13 \cdot 10^4)(20) = 1.03 \quad ,$$

$$\tau_{NO_2} = 0 \quad .$$

We see from the map shown in figure 13 that the background visual range (r_{v0}) in southern Arizona is 110 km.

$$\tau_{aerosol} = (1.06 \cdot 10^{-5})(110)(20 + 1.31 \cdot 0)$$

$$= 2.33 \cdot 10^{-2} \quad .$$

Now we calculate the contrast parameters:

$$C_1 = - \frac{0}{1.03 + 0} [1 - \exp(-1.03 - 0)][\exp(-0.78 \cdot 50/110)] = 0 \quad ,$$

$$C_2 = \left[1 - \left(\frac{1}{1 + 0}\right) \exp(-1.03 - 0)\right][\exp(-1.56 \cdot 50/110)] = 0.316 \quad ,$$

$$C_3 = 0.368\ [1 - \exp(-0.0233)] = 0.008 \quad .$$

Since C_2 is greater than 0.10, there is a potential for visibility impairment in the class I area, and further screening analysis (level-2 or level-3) would be needed. However, if particulate emissions were cut to four metric tons per day or less, the source would pass the level-1 screening test, and further analysis would be unnecessary.

4 LEVEL-2 VISIBILITY SCREENING ANALYSIS

A level-2 visibility screening analysis should be carried out when a level-1 screening analysis shows a potential for adverse or significant impairment. The level-2 analysis is based on more detailed information regarding the emissions source, regional meteorology, and other physical specifications of the site such as background visual range, ozone concentration, and topography. The primary objective of this level-2 analysis is to calculate the magnitude of visual impact that would be exceeded approximately one day per year. If the magnitude of this reasonable worst-case condition is less than some threshold value, one could be assured that an adverse or significant impact would not occur and further assessment would be unnecessary.

4.1 IDENTIFICATION OF WORST-CASE CONDITIONS

The following factors should be considered when identifying the reasonable worst-case conditions for a level-2 visibility screening analysis:

- Locations of emissions source and class I area(s)
- Wind speed
- Wind direction
- Atmospheric stability and mixing depth
- Time of day and season
- Background ozone concentration
- Background visual range
- Persistence of meteorological conditions
- Topographical effects on plume transport and diffusion.

Many of these factors have to be considered in any event when analyzing air quality impacts from a proposed emissions source in order to determine whether the source complies with ambient air quality standards and PSD increments. However, visibility impact assessments differ from air quality impact analyses in one important respect: air quality impact analyses are concerned with time-averaged, ground-level contaminant concentrations, whereas visibility analyses are concerned with instantaneous NO_2 and particle line-of-sight integrals, not necessarily at ground level.

In the following paragraphs we discuss each of these factors and the manner in which overall worst-case conditions should be selected for level-2 visibility screening analyses.

4.1.1 Location of Emissions Source and Class I Area(s)

The first step is to identify the location of the emissions source and the class I area(s) that may be affected. Some of this work will have been performed as part of the level-1 screening analysis that identified the minimum distance between the emissions source and the class I area.

The Federal Land Manager(s) of the potentially affected class I area(s) should be contacted so that important integral vistas (i.e., with views from inside to outside of the class I area) can be selected for analysis. All class I areas that may be adversely affected, as indicated by the level-1 screening test, should be considered in the level-2 analysis.

U.S. Geological Survey maps (scale 1:250,000) should be used to determine terrain elevations. These maps are recommended as a base upon which to draw the location of the emissions source, the locations at which meteorological data were collected, the boundaries of class I areas, and the particular class I area key observer points and integral vistas identified for analysis. Also, it would be helpful for later analysis to draw the boundaries of each of the 16 cardinal (22.5° wide) sectors radiating from the site of the emissions source.

Elevated terrain features that could potentially block the transport of a plume toward a class I area should be identified. (A significant terrain feature, such as a plateau, ridge, or mountain range, could prevent the direct transport of emissions toward a class I area.) A representative effective stack height of emissions should be calculated by adding to the physical stack height the plume rise for neutral conditions and the 50-percentile wind speed:

$$H = h_{stack} + \Delta h \quad . \qquad \text{(p-8)}$$

The neutral plume rise is calculated using the following Briggs plume rise formula (Briggs, 1969, 1971, 1972):

$$\Delta h = 1.6\ F^{1/3}\ (3.5\ x^{*})^{2/3}\ u^{-1} \quad , \qquad \text{(p-9)}$$

where

$\Delta h \equiv$ plume rise,

$u \equiv$ average wind speed in the layer through which the plume rises,

$F \equiv$ buoyancy flux

$$= g \frac{\dot{V}}{\pi} \left(1 - \frac{T_{ambient}}{T_{stack}} \right) \quad , \text{(values of T in degrees Kelvin)}$$

$g \equiv$ gravitational acceleration = 9.8 m/s^2,

$\dot{V} \equiv$ flue gas volumetric flow rate per stack,

$$x^{*} \equiv \begin{cases} 14\ F^{5/8} & \text{,if} \quad F < 55\ m^4 s^{-3} \\ 34\ F^{2/5} & \text{,if} \quad F > 55\ m^4 s^{-3} \end{cases} .$$

To this average effective stack height, add the elevation of the proposed site (above mean sea level) and 500 meters, which is the assumed additional terrain height that is needed to block plume transport:

$$Z_{block} = Z_{site} + H + 500 \text{ m} \quad . \qquad \text{(p-10)}$$

Shade the areas on the base map with elevations greater than this value. Trace plausible plume trajectories on this map that bypass the elevated terrain (shaded areas on the map). Examples of such plume trajectories are shown in figure 14. Note that stable plume transport directly toward observers A and B would be very unlikely. Stable flow would follow the curved trajectories shown in figure 14. Note that a stable plume would not likely be transported to observer C, although a stable plume near the emissions source might be visible to this observer. A straight-line trajectory to observer D in figure 14 is possible.

It should be noted that a plume could be transported directly toward observers A, B, and C during neutral or unstable conditions; however, mechanically induced turbulence would increase the mixing of the plume, and visual impacts would be small.

The distances along these plume trajectories will be used later as the downwind distance x to the class I area(s) for use in calculating plume transport times and diffusion.

Elevation profiles of terrain at various azimuths from key observer points in class I areas that may be affected by the emissions source (see the example in figure 15) should be prepared. These plots should extend radially from the observer location to the most distant landscape feature visible from the given location, or to the average visual range for the area, whichever is less. From these plots the distance along the line of sight to various landscape features can be calculated. These plots and distances will be used in later analyses of plume perceptibility and landscape-feature contrast reduction.

4.1.2 Meteorological Conditions

The joint frequency of occurrence of meteorological conditions at the effective stack height of the emissions is needed to estimate the worst-

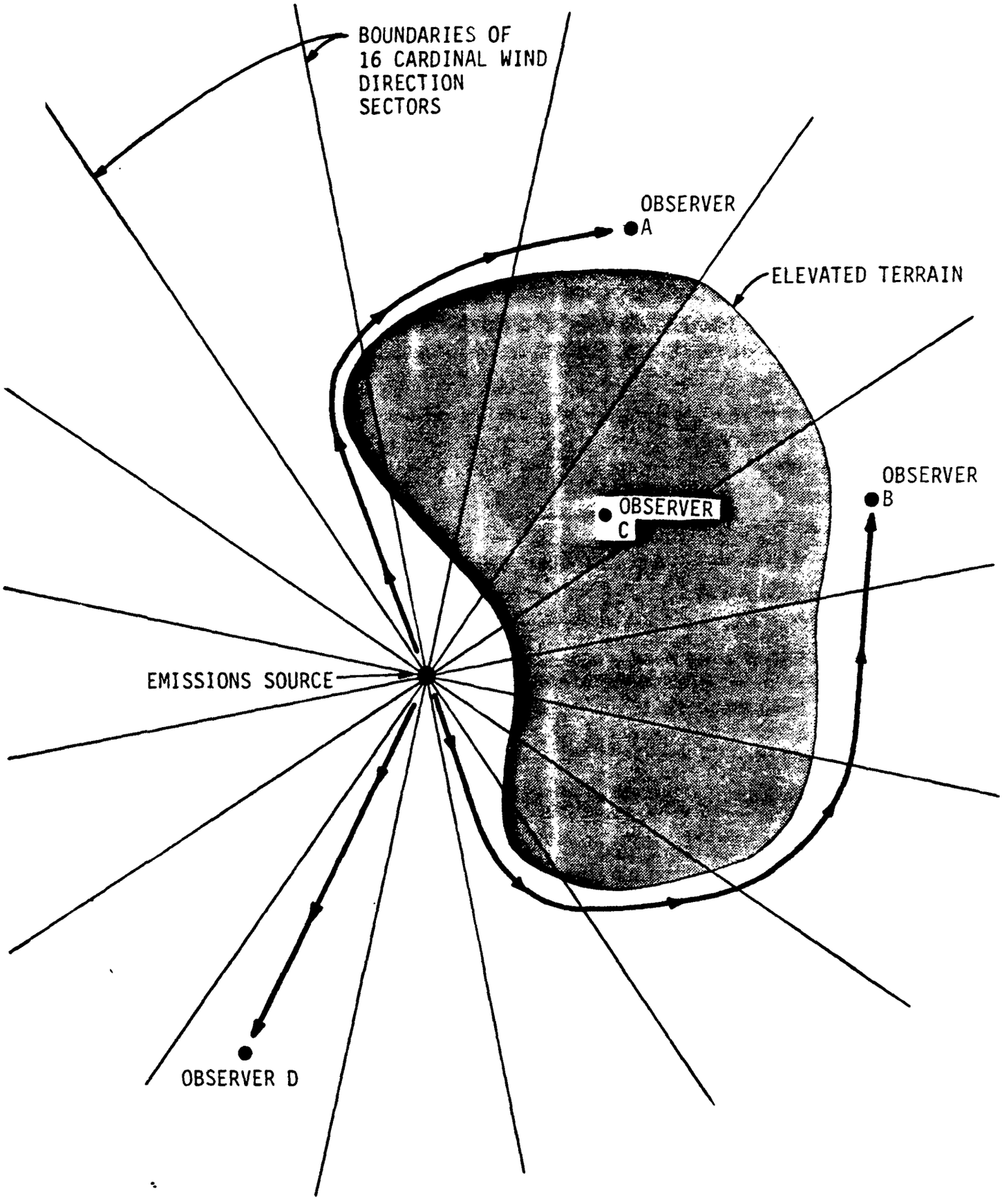

Figure 14. Example of map showing emissions source, class I areas, and stable plume trajectories.

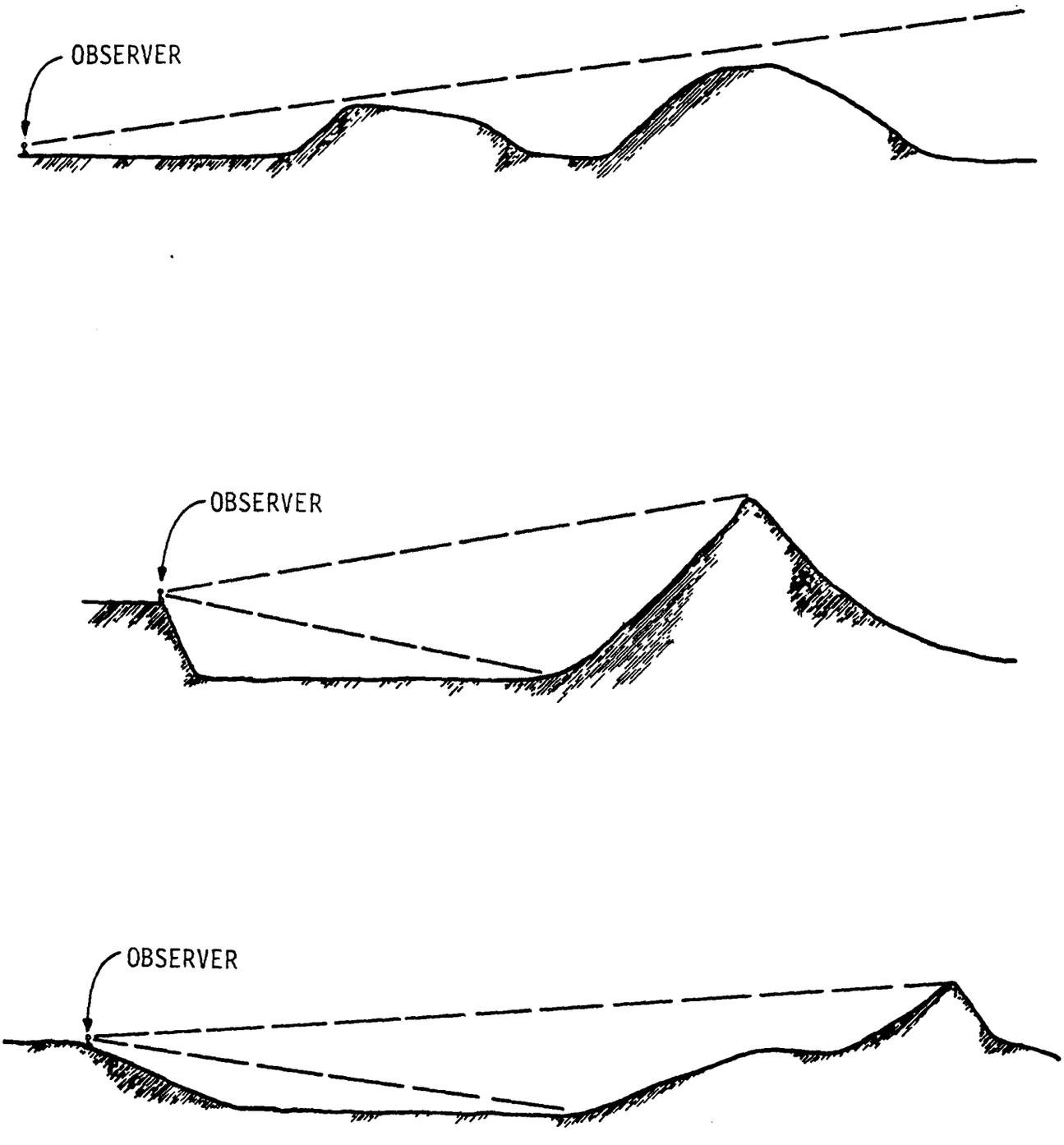

Figure 15. Examples of terrain elevation plots.

case meteorological conditions in the area associated with visual impacts that will be exceeded only about one day per year.

The important meteorological parameters are

- Wind speed
- Wind direction
- Atmospheric stability
- Mixing depth.

It is essential to consider the persistence as well as the frequency of occurrence of these conditions. For example, plume discoloration will generally be most intense during light-wind, stable conditions. However, the transport time to a class I area increases as the wind speed decreases. As the transport time approaches 24 hours, it is increasingly probable that the plume will be broken up by convective mixing and by changes in wind direction and speed; thus it will not be visible as a plume or a discolored layer. However, since increased haze often occurs because of secondary aerosols that take time to form in the atmosphere, visual range reduction may be more significant when transport times to a class I area are long. Largest increases in general haze (visual range reduction) resulting from an emissions source might occur if there is stagnation caused by synoptic meteorological conditions or topographical factors, or if there is trapping of emissions caused by upslope or downslope flow reversals.

Ideally, one would prefer to have a meteorological data base with detailed spatial and temporal coverage. However, this is rarely possible because of cost considerations. Several alternative approaches can be used to fill in missing data, but they all involve making assumptions. For example, if a complete meteorological data base is available only at the site of the proposed emissions source, one might assume that conditions at the site are representative of conditions at other locations in the region. However, in regions of complex terrain, like the example shown in figure 14, this assumption would not be appropriate. Often, data

collected at ground level are assumed to represent conditions at the effective stack height, which is a poor assumption when the plume is several hundred meters above ground or the site is located in complex terrain.

Any assessment of air quality or visibility impacts is limited by the availability of meteorological data; more detailed assessments require more detailed and extensive data bases. Detailed visibility assessments, which are discussed in the next section of this document, require spatially and temporally resolved meteorological data. The level-1 screening analysis discussed in the previous chapter requires no meteorological data; rather, conservative assumptions are made regarding worst-case stability, wind speed, and wind direction. The level-2 screening analysis assumes that the analyst has at least one year of meteorological data from the site of the proposed emissions source, a nearby site within the region, or the class I area(s) potentially affected by emissions.

The types of data bases for the level-2 analysis are listed as follows, in order of preference:

> Concurrent upper air winds and stability. The best data base would provide hourly values of vertical temperature gradients from which dispersion coefficients can be inferred and wind direction and speed vectorially averaged. If effective stack heights (physical stack height plus plume rise) are relatively low, these data can be collected from a meteorological tower. If the effective stack heights are high, these data would have to be collected using rawinsondes, tethered balloons, or Doppler acoustic radar systems. A less desirable data base would consist of upper-air meteorological data gathered twice daily, such as those collected routinely by the National Weather Service.

> Separate data sets. For some sites a good data base that consists of upper-air winds (e.g., from pibals) may be

available without concurrent lapse-rate (vertical temperature gradient) data. In such situations, one can use lapse-rate data collected from another location in the region for the same or different periods for which wind data were collected. An assumption is made that the stability at the other location is representative of the site and the class I area. If stability data are not available for the same period during which wind data were collected, the additional assumption must be made that wind frequencies and stability frequencies can be treated as independent probabilities, as discussed in chapter 2.

> Surface data. Surface data (e.g., STAR data) may be appropriate if the effective stack height of the emissions is low or zero. However, surface data may be inappropriate for evaluating the impacts of elevated releases. If no other data are available, one should use surface data with full recognition of the potential errors associated with their use; these errors may be extreme in complex terrain. If lapse-rate data are not available, one can estimate stability using the Turner method (1969).

> No data. If meteorological data are not available, the assumptions regarding meteorology used in the level-1 analysis would be used to assess impact.*

The Turner method (1969) should be used to determine stability categories that can then be used to assess plume dispersion using the σ_y and σ_z curves of Pasquill-Gifford (Turner, 1969). It should be noted that dispersion conditions at a given site may be considerably different from the idealized Pasquill-Gifford representations. Many different estimates of

---

* For the analysis of plume discoloration, these conditions are F stability and a wind speed that would transport emissions to a class I area within 12 hours. For the analysis of potential haze due to sulfate aerosol, one would assume limited mixing conditions with a mixing depth of 1000 m and a wind speed of 2 m/s.

σ_y and σ_z are available, such as the TVA, Brookhaven, and ASME curves. However, the Pasquill-Gifford curves are the most generally used and therefore have been adopted for use in this document. The Pasquill-Gifford σ_z values may either overestimate or underestimate actual vertical diffusion in a given application. If diffusion data are available from tracer studies or from similar emissions sources in the region, such data could be used to assess more accurately potential plume visual impacts.

4.1.2.1 Worst-Case Conditions for Plume Discoloration*

It should be emphasized that the vertical diffusion (σ_z) of a plume is the most important diffusion parameter for visibility impact assessments, because the optical thickness of a plume for horizontal lines of sight is inversely proportional to σ_z, as shown in equations (19) and (20). Specification of horizontal diffusion (σ_y) is less important.†

On the basis of the available data base discussed previously, tables of joint frequency of occurrence of wind speed, wind direction, and stability class should be prepared that are similar to those shown in figure 16. These tables should be stratified by time of day. If meteorological data are available at hourly intervals, it is suggested that these tables be stratified as follows: 0001-0600, 0601-1200, 1201-1800, and 1801-2400. If data are available twice daily, morning and afternoon data should be tabulated separately. With this stratification, diurnal variation in winds and stability are more easily discernible.

---

* This step can be skipped if $|C_1|$ and $|C_2|$ from the level-1 analysis are each less than 0.1.

† It should be noted that calculations of plume discoloration using the plume visibility model (PLUVUE) indicate that plume discoloration increases as plume σ_y increases because of increased NO-to-NO_2 conversion in well-mixed plumes.

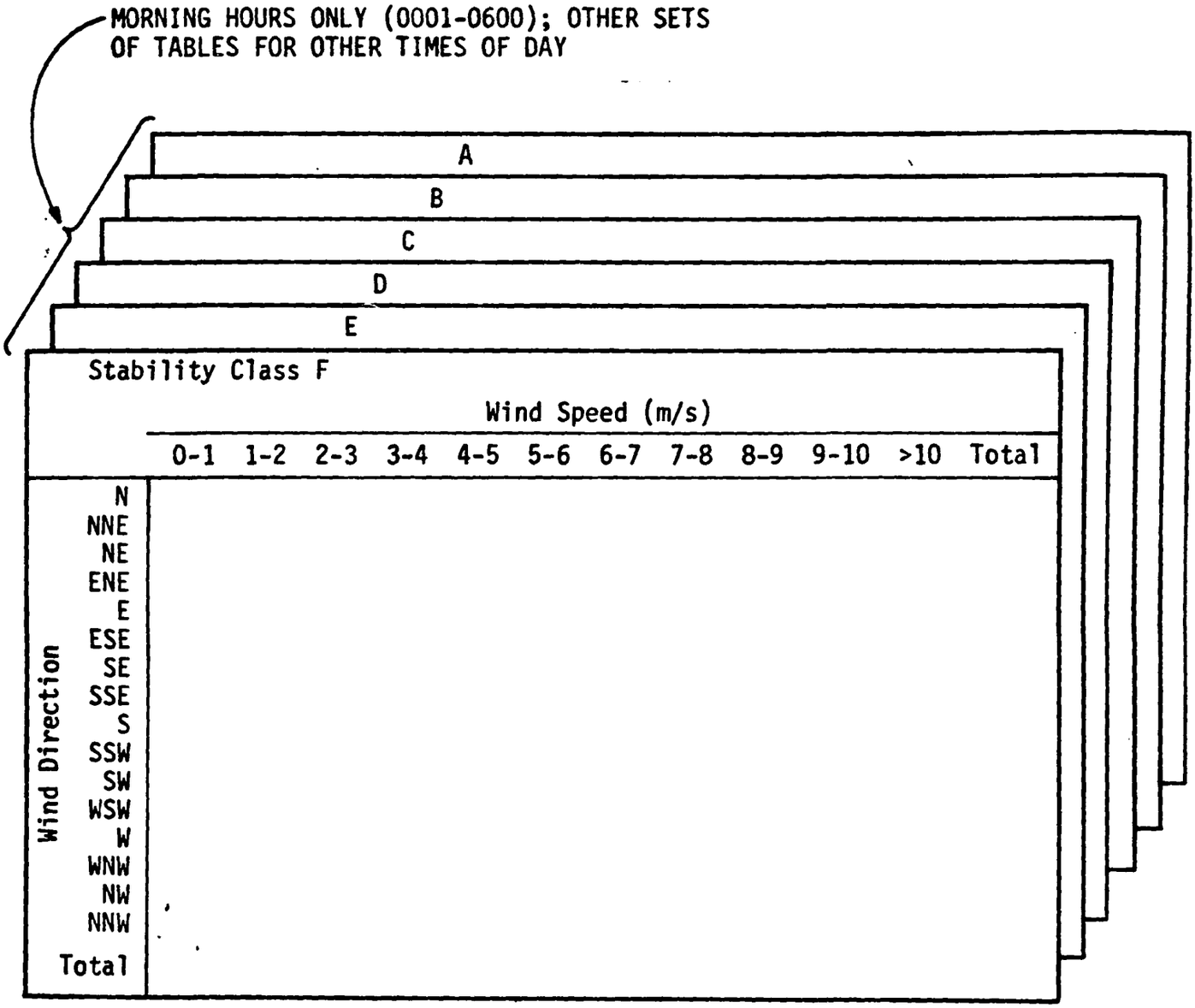

Figure 16. Joint frequency distribution tables required to estimate worst-case meteorological conditions for plume discoloration

On the basis of the maps prepared previously, the analyst should select the wind direction sector that would transport emissions closest to a given class I area observer point so that the frequency of occurrence of impact can be assessed as discussed below. For example, in the schematic diagram shown in figure 17, west winds would transport emissions closest to observer A, whereas either west-southwest or west winds would transport emissions closest to observer B. Observer C would be affected by emissions transported by west-northwest and northwest winds, but primarily by west-northwest winds.

For the situations influenced by complex terrain, such as the example shown in figure 14, the determination of this worst-case wind direction and its frequency of occurrence is much more difficult. The analyst should use professional judgment in this determination.

The determination of the worst-case wind direction and its frequency of occurrence should be made on the basis of the following factors:

> Location(s) for which meteorological data were collected relative to terrain features, emissions source, and potentially affected class I areas.
> Likely plume trajectories for each wind direction (and possibly wind speed and stability) based on either data or professional judgment. For example, potential channeling, convergence, and divergence of flows should be assessed.

The next step is to construct a table (see the example in table 1) that shows worst-case dispersion conditions ranked in order of decreasing severity and the frequency of occurrence of these conditions associated with the wind direction that could transport emissions toward the class I area. Dispersion conditions are ranked by evaluating the product $\sigma_z u$, where σ_z is the Pasquill-Gifford vertical diffusion coefficient for the given stability class and downwind distance x along the stable plume trajectory identified earlier, and u is the maximum wind speed for the given wind speed category in the joint frequency table. The dispersion condi-

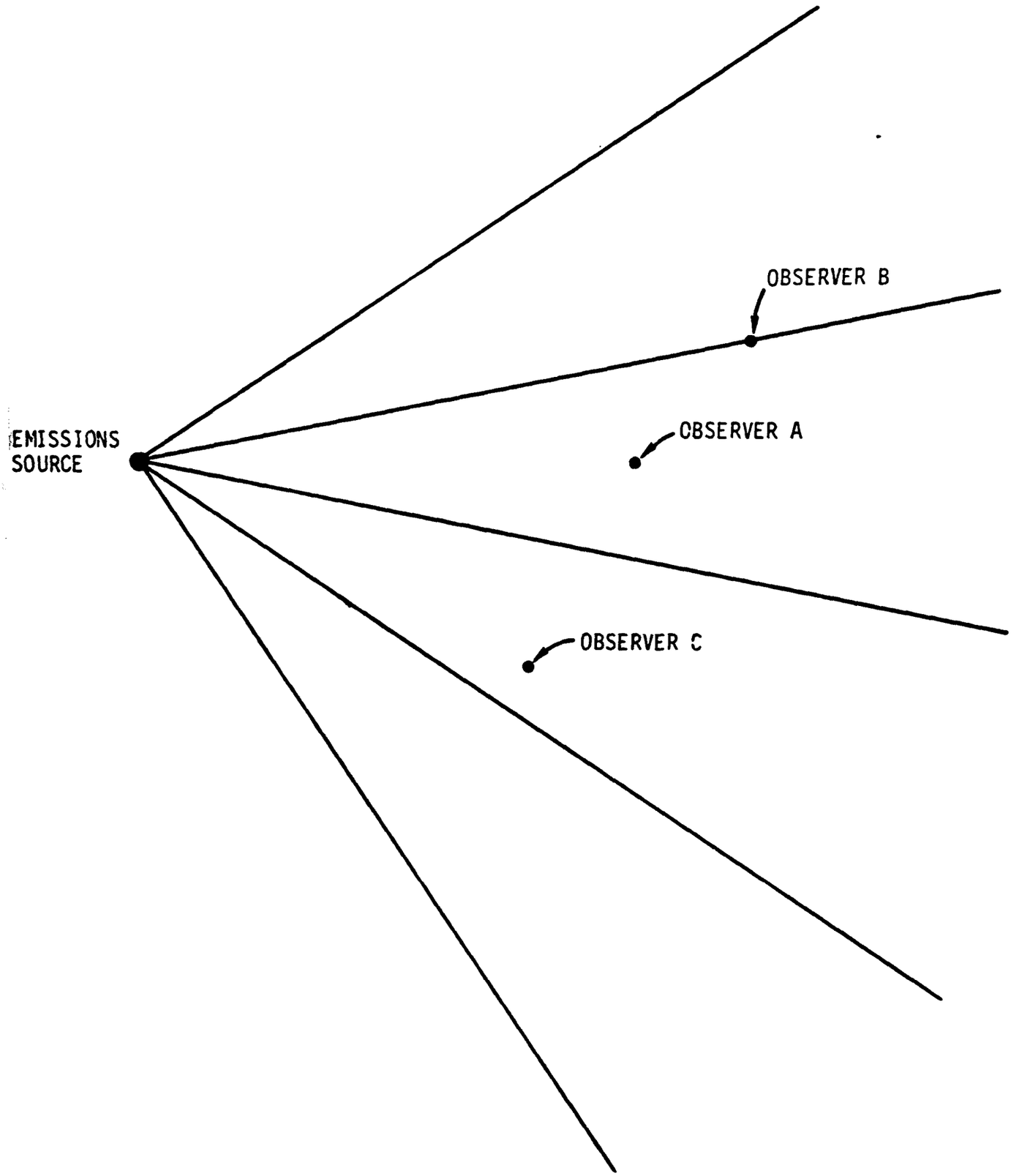

Figure 17. Schematic diagram showing emissions source, observer locations, and wind direction sectors.

TABLE 1. EXAMPLE TABLE SHOWING WORST-CASE METEOROLOGICAL CONDITIONS FOR PLUME DISCOLORATION CALCULATIONS

Dispersion Condition (Stability, wind speed)	σ_z u (m^2/s)	Transport Time (hrs)	Frequency of Occurrence of Given Dispersion Condition Associated with Worst-Case Wind Direction† for Given Time of Day (percent)				Frequency and Cumulative Frequency (percent)	
			0-6	6-12	12-18	18-24	f	cf
F, 1	90	56*	0.2	0.1	0.0	0.2	0.0	0.0
E, 1	175	56*	0.3	0.2	0.1	0.2	0.0	0.0
F, 2	180	19*	0.2	0.1	0.0	0.2	0.0	0.0
F, 3	270	11	0.2	0.2	0.0	0.2	0.2	0.2
E, 2	350	19*	0.4	0.3	0.0	0.2	0.0	0.2
F, 4	360	8	0.3	0.2	0.0	0.2	0.3	0.5
D, 1	430	56*	0.0	0.2	0.5	0.1	0.0	0.5
F, 5	450	6	0.1	0.1	0.0	0.1	0.1	0.6
E, 3	525	11	0.5	0.3	0.1	0.3	0.5	1.1

* Transport times to class I areas during these conditions are longer than 12 hours, so they are not added to the cumulative frequency summation.

† For a given class I area.

tions are then ranked in ascending order of the value $\sigma_z u$. This is illustrated with an example in table 1. The downwind distance in this hypothetical case is assumed to be 100 km. Note that F,1 (stability class F associated with wind speed class 0-1 m/s) is the worst dispersion condition, since it has the smallest value of $\sigma_z u$ (90 m^2/s). The second worst diffusion condition in this example is E,1, followed by F,2, F,3, and so on.

The next column in table 1 shows the transport time along the minimum trajectory distance from the emissions source to the class I area, based on the midpoint value of wind speed for the given wind speed category. For example, for the wind speed category, 0-1 m/s, a wind speed of 0.5 m/s should be used to evaluate transport time; for 1-2 m/s, 1.5 m/s; and so on. The times necessary for a plume parcel to be transported 100 km are 56, 19, 11, 8, and 6 hours for wind speeds of 0.5, 1.5, 2.5, 3.5, and 4.5 m/s, respectively.

For the level-2 screening analysis, we assume it is unlikely that steady-state plume conditions will persist for more than 12 hours. Thus, if a transit time of more than 12 hours is required to transport a plume parcel from the emissions source to a class I area for a given dispersion condition, we assume that plume material is more dispersed than a standard Gaussian plume model would predict. This enhanced dilution would result from daytime convective mixing and wind direction and speed changes.

The objective of this tabulation of plume dispersion conditions is to identify the worst-case meteorological conditions. The joint frequency of occurrence of these worst-case meteorological conditions, associated with high background ozone concentrations and high background visual range, would be calculated by multiplying independent probabilities as discussed in chapter 2. This would define the frequency of occurrence of worst-case visual impact conditions. To obtain the worst-case meteorological conditions, it is necessary to determine the dispersion condition (a given wind speed and stability class associated with the wind direction that would transport emissions toward the class I area) that has a $\sigma_z u$ product with a

cumulative probability of 1 percent. In other words, the dispersion condition is selected such that the sum of all frequencies of occurrence of conditions worse than this condition totals 1 percent (i.e., about four days per year). Dispersion conditions associated with transport times of more than 12 hours are not considered in this cumulative frequency for the reasons stated above.

This process is illustrated by the example shown in table 1. It is seen that the first three dispersion conditions would cause maximum plume visual impacts, because the $\sigma_z u$ products are lowest for these three conditions. However, the transport time from the emissions source to the class I area associated with each of these dispersion conditions is greater than 12 hours. With the fourth dispersion condition (F,3), emissions could be transported in less than 12 hours. The frequency of occurrence (f) of this condition is added to the cumulative frequency summation (cf). For this hypothetical example, the meteorological data are stratified into four time-of-day categories. The maximum of each of the four frequencies is used to assess the cumulative frequency. This is appropriate since we are concerned with the number of days during which, at any time, dispersion conditions are worse than or equal to a given value.

Note that the worst-case, stable, light-wind dispersion conditions occur more frequently in the nighttime hours.* In our example, the following additional worst-case dispersion conditions add to the cumulative frequency: F,4; F,5; and E,3. Dispersion conditions with wind speeds less than 2 m/s (F,1; E,1; F,2; E,2; and D,1) were not considered to cause an impact because of the long transit times to the class I area in this example. Thus, their frequencies of occurrence were not added to the cumulative frequency summation. The result of this example analysis is

---

* Nighttime visual impacts, such as obscuration of the view of the moon or the Milky Way, are not usually a concern. However, significant visual impacts could be caused in the morning after a period of nighttime transport.

that dispersion condition E,3 is associated with a cumulative frequency of 1 percent, so we would use this dispersion condition to evaluate worst-case visual impacts for the level-2 screening analysis for this example case.

It should also be noted that if the observer point in the class I area is on or near the boundary of one of the 16 cardinal wind direction sectors, it may be appropriate to interpolate the joint frequencies of wind speed, wind direction, and stability class from the two wind direction sectors, on the basis of the azimuth orientation of the observer relative to the center of the wind direction sectors.

4.1.2.2 Worst-Case Conditions for General Haze*

A similar procedure should be used to identify the potential worst-case limited mixing conditions for the region used in calculating worst-case haze increases caused by sulfate aerosol formed from SO_2 emissions. Most significant increases in general haze caused by emissions from a given source are likely to occur after a long period of transport during light-wind conditions when the vertical mixing is limited by a capping stable layer. In the level-1 analysis, we assumed that limited mixing conditions with a mixing depth of 1000 m and a wind speed of 2 m/s persisted for two days without precipitation (which would wash out particulates, SO_2 and $SO_4^=$). In the level-2 analysis, assumptions appropriate to the area being analyzed should be used.

Two alternative approaches to this analysis can be considered. The first assumes concurrent mixing depth, wind speed and wind direction data for the site or region. The second assumes the absence of these data. The first approach is more time-consuming, but presumably more accurate, than the second.

---

* This step can be skipped if $|C_3|$ from the level-1 analysis is less than 0.1.

Let us consider the first approach. If one has vertical temperature gradient data for a region, one can calculate maximum daily mixing depths in a manner similar to that used by Holzworth (1972). These data should be sorted to identify periods without precipitation for at least two days. The remaining occurrences should be used to generate joint frequency tables similar to those shown in figure 18. Occurrences are sorted into different categories of maximum 48-hour mixing depth and 48-hour vector-average wind direction and wind speed.

The vector-average wind direction and speed (i.e., the resultant wind) are defined by calculating a position vector as follows:

$$\bar{r} = \int_{t_0}^{t_0 + 48\ hr} \bar{v}\ (x,y,z,t)\ dt \quad ,$$

where $\bar{r}$ is the position vector and $\bar{v}$ (x,y,z,t) is the spatially and temporally dependent wind vector for the plume parcel emitted by the source. The vector-average wind direction is defined by the direction of the vector $\bar{r}$ and the vector-average wind speed is

$$\bar{u} = \frac{|\bar{r}|}{48\ hr} \quad .$$

The next step parallels the procedures used to identify the worst-case meteorological conditions for plume discoloration. The analyst should construct a table of worst-case limited mixing conditions ranked in decreasing order of severity (increasing product of mixing depth H_m and wind speed $\bar{u}$). Table 2(a) shows how such a table might be constructed. Different wind directions in which a class I area is located are identified in this table from a map similar to the example in figure 19. This map shows 16 wind direction sectors and circles with radii corresponding to $\bar{u}$ values of 1, 2, 3, and 4 m/s (r = 173, 346, 518, and 691 km, respectively). For each limited mixing condition ($\bar{u}$ H_m) and wind direction combination, the number of nonoverlapping 48-hour episode occurrences in a year is tabulated. If a class I area is located within the bounds

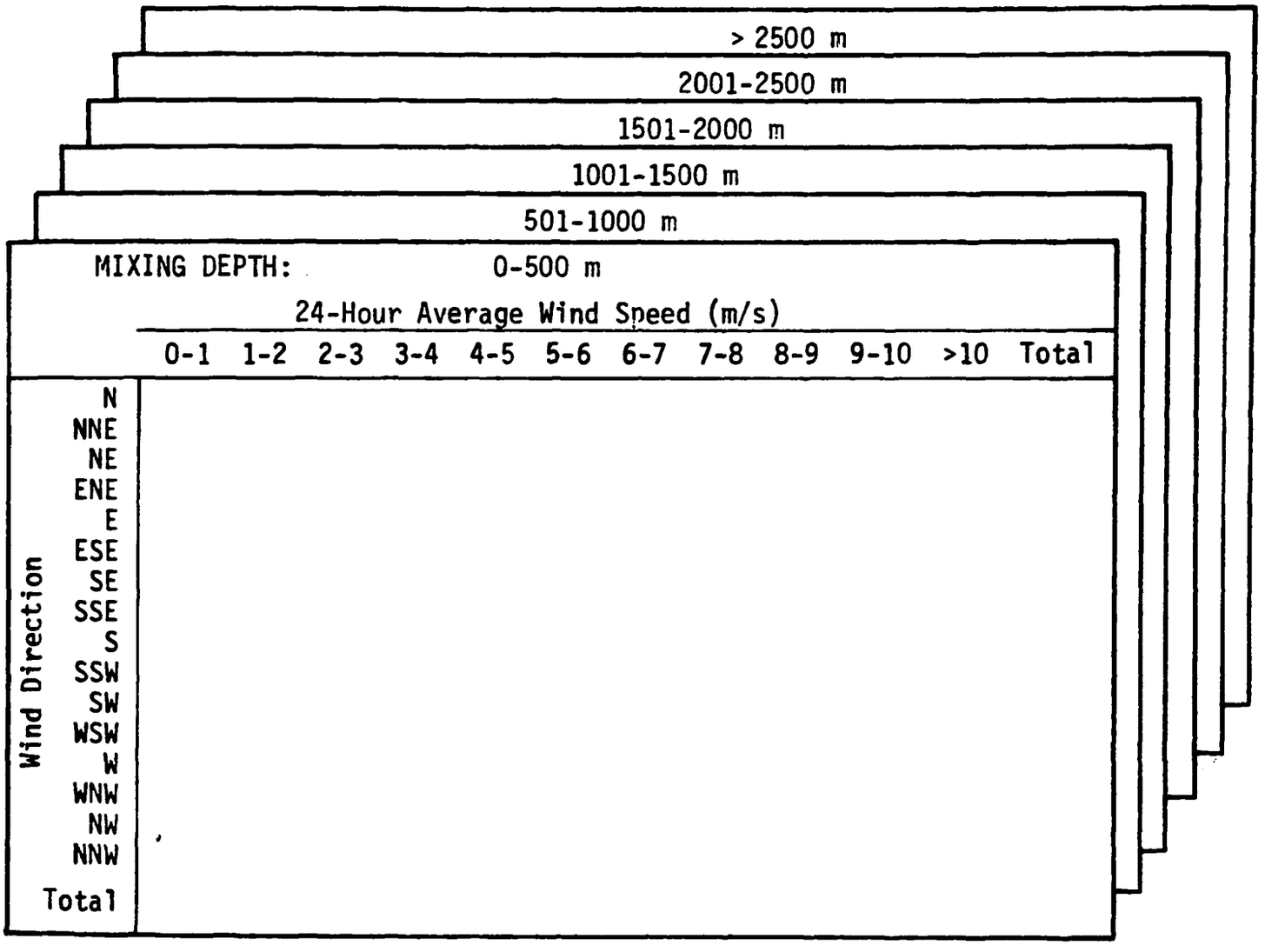

Figure 18. Joint frequency distribution tables required to estimate worst-case meteorological conditions for visibility impairment due to SO_2 emissions.

TABLE 2. EXAMPLE TABLE SHOWING WORST-CASE LIMITED MIXING CONDITIONS FOR HAZE CALCULATIONS

(a) Based on Site/Regional Data

Limited Mixing Condition (u, H_m)*	$u H_m$ (m^2/s)	Number of Occurrences of Indicated Limited Mixing Condition in a Year Associated with Wind Direction in Given Sector					Impact Frequency and Cumulative Frequency	
		SW†	W	WNW	NNW	ENE	f	cf
1; 500	500	0	0	0	0	0	0	0
2; 500	1,000	0	0	0	0	0	0	0
1; 1,000	1,000	0	0	0	0	0	0	0
3; 500	1,500	0	0	0	0	0	0	0
1; 1,500	1,500	0	0	0	0	0	0	0
2; 1,000	2,000	0	0	0	0	0	0	0
4; 500	2,000	(1)§	0	1	0	0	1	1
5; 500	2,500	0	0	0	0	0	0	1
3; 1,000	3,000	(2)§	0	0	1	0	1	2
2; 1,500	3,000	1	1	0	0	0	2	4

* In units of m/s for u and m for H_m.

† Wind direction sector is defined as the direction from which the wind blows, so areas A and B are affected by SW winds because they are located in the NE sector.

§ Parentheses indicate that, though a given combination of $\bar{u}$, H_m, and wind direction occurred, no class I areas were located within the corresponding sector-distance.

TABLE 2 (Concluded)

(b) Based on Holzworth (1972) Data (example is based on Winslow, Arizona data)

nited Mixing Condition $(u, H_m)^*$	$u\,H_m$ (m^2/s)	Episode-Days in Five-Year Period after a Minumum of 48-hours Transport	Number of Sectors with Class I Areas†	Number of Days per Year in a Class I Area Sector f§	cf
2; 500	1,000	2	4	0.10	0.10
2; 1,000	2,000	22	4	1.10	1.20
4; 500	2,000	33	3	1.24	2.44
2; 1,500	3,000	2	4	0.10	2.54
6; 500	3,000	1	2	0.03	2.57
2; 2,000	4,000	0	4	0.00	2.57
4; 1,000	4,000	80	3	3.00	2.57
4; 1,500	6,000	54	3	2.03	7.60
6; 1,000	6,000	21	2	0.53	8.13
4; 2,000	8,000	11	3	0.41	8.54
6; 1,500	9,000	21	2	0.53	9.07
6; 2,000	12,000	30	2	1.13	10.20

n units of m/s for u and m for H_m.

umber of wind direction sectors with class I areas within radii corresponding to given wind speed class (0-2, 2-4, 4-6, m/s).

ese numbers are calculated as follows:

$$= \frac{\text{(episodes/five-year period) (no. of sectors)}}{\text{(5 one-year periods/five-year period) (16 sectors)}}$$

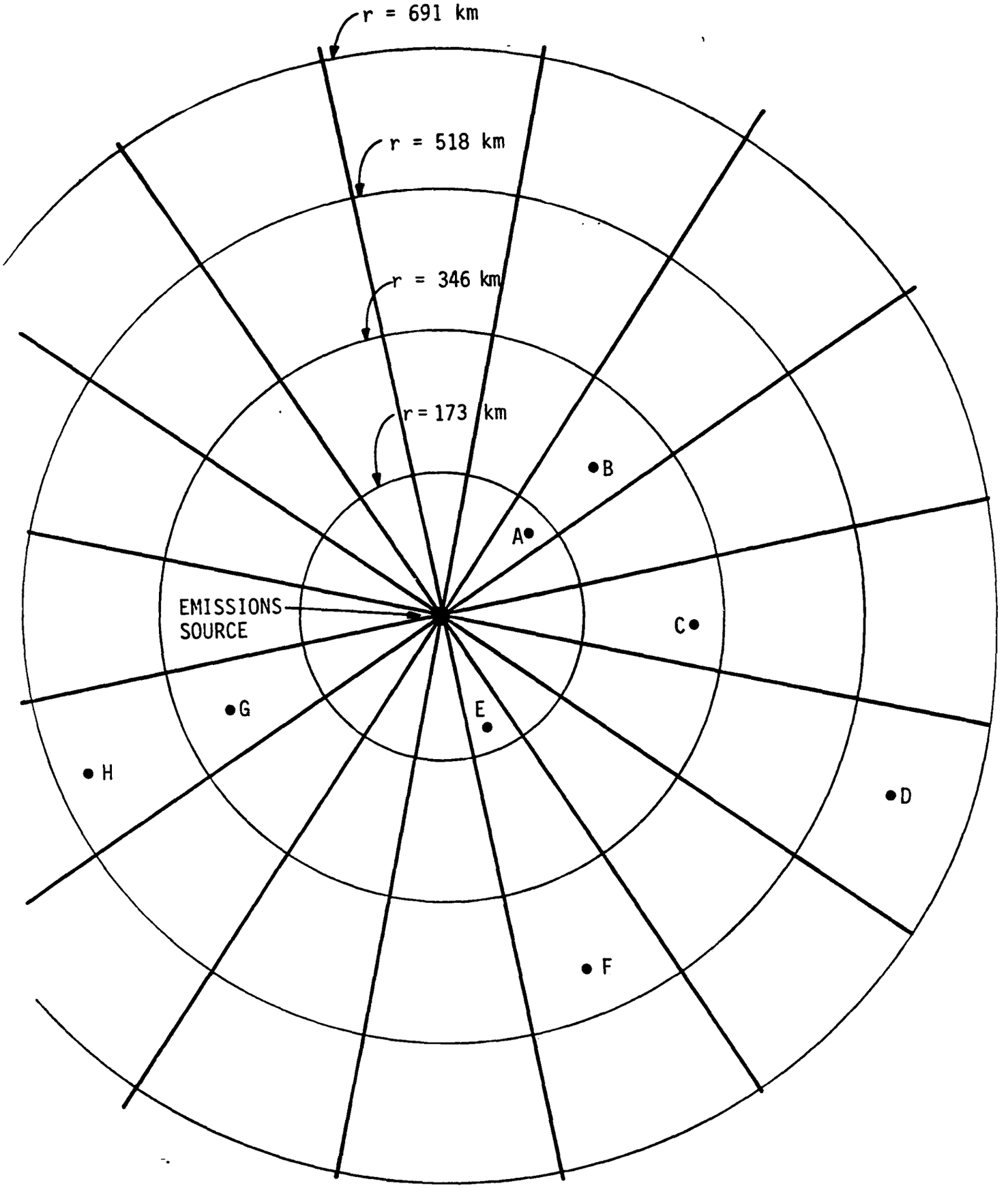

Figure 19. Example map showing class I areas in region around emissions source and wind direction/speed sectors. (Note: Class I area locations are shown at lettered points.)

defined by the wind direction sector boundaries and the wind speed class radii, the occurrence is added to a cumulative frequency total. We proceed until we have identified the worst-case condition with a cumulative frequency of four occurrences in a year. In the example shown in table 2(a), this worst-case condition is a wind speed of 2 m/s and a mixing depth of 1500 m.

The second approach should be used if site mixing depth data are not available or if analytic resources and time are limited. This approach uses information from Holzworth (1972), which shows, among other things, the number of episodes and episode-days without significant precipitation in a five-year period, with mixing depths and wind speeds less than given values persisting for at least two days.

Using this second, simpler approach, we tabulate the number of episodes in five years with given conditions as shown in table 2(b). Holzworth (1972) gives cumulative frequencies (number of episodes and episode-days) of $u < u'$ and $H_m < H_m'$. For our purposes we need to convert these to frequencies in a given u and H_m category, as shown in table 2(b). The number of episode-days in a five-year period within a given limited mixing category is determined from Holzworth (1972) in the manner illustrated in table 3. First, the number of episodes (cf_e) and the number of episode-days (cf_d) in five years is tabulated for each mixing depth and wind speed category. The number of days in five years that were preceded by the given limited mixing condition persisting at least 48 hours is calculated from the difference, $cf_d - cf_e$. To convert these cumulative frequencies to frequencies within each mixing depth/wind speed category, one must subtract the frequencies of the appropriate categories as shown in table 3. We convert these frequencies to episode-days per year within a given wind direction sector and wind speed class radii in which class I areas are located as shown in the footnote in table 2(b). We determine an episode-day cumulative frequency equivalent to four days per year. For the example shown in table 2(b), this worst-case limited mixing condition is u = 4 m/s and H_m = 1000 m. If the cumulative frequency of occurrence of these extreme limited mixing conditions is less

TABLE 3. EXAMPLE TABLES SHOWING COMPUTATION OF DAYS IN A FIVE-YEAR PERIOD WITH THE GIVEN LIMITED MIXING CONDITION

Upper Limits of Limited Mixing Category		Number of Occurrences in a Five-Year Period (from Holzworth, 1972)		Number of Days in Five Years Preceded by at Least 48 Hours of a Given Limited Mixing Condition
u (m/s)	H_m (m)	Episodes cf_e	Episode-days cf_d	$cf_{2+} = cf_d - cf_e$
2	500	2	4	2
4	500	13	48	35
6	500	13	49	36
2	1000	13	37	24
4	1000	37	174	137
6	1000	42	197	155
2	1500	17	43	26
4	1500	52	245	193
6	1500	62	294	232
2	2000	17	43	26
4	2000	59	263	204
6	2000	75	348	273

Wind Speed (m/s)	Mixing Depth (m) 0-500	500-1000	1000-1500	1500-2000
0-2	2 2 1	24 22 (24-2) 4	26 2 (26-24) 7	26 0 (26-26) 10
2-4	35 33 (35-2) 2	137 80 (137-35-22) 5	193 54 (193-137-2) 8	204 11 (204-193-0) 11
4-6	36 1 (36-35) 3	155 17 (155-36-22-80) 6	232 21 (232-155-2-54) 9	273 30 (273-232-11-0) 12

Note: Examples are based on data for Winslow, Arizona, from Holzworth (1972).

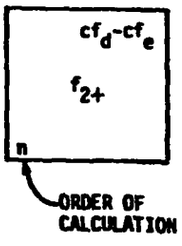

than four days per year for the given region, we use the annual median mixing depths and wind speeds for the region (also given in Holzworth [1972]).

Finally, regardless of which method is used, the seasonal average afternoon wind speeds and mixing depths for the region should be tabulated on the basis of Holzworth (1972) for later use.

4.1.3 Background Ozone Concentration

As noted in chapter 2, an important input parameter to the visibility model is the background ozone concentration, that is, the concentration of ozone outside the plume.

Since we are concerned with background ozone concentrations at the effective stack height, which may be several hundred meters above ground, we must interpret ground-level ozone concentration data with care. In their analysis of long-term ozone concentration data at remote U.S. sites, Singh, Ludwig, and Johnson (1978) reported that there is a significant diurnal variation in ozone concentrations at the surface because of the surface depletion of ozone. They reported a significant reservoir of ozone in the free troposphere varying in concentration from about 30 ppb in the winter to about 60 ppb in the summer. The tropospheric ozone is rapidly mixed to the ground during the daytime; this causes surface concentrations near the free tropospheric value. However, at night and in early morning, ozone is no longer mixed to the ground because of the development of a ground-based stable layer. During this period, ground-level ozone concentrations gradually decrease as a result of a surface depletion mechanism. In relatively remote, unpolluted regions, one would not expect a significant anthropogenic source of ozone. In figure 20, the vertical ozone structure and diurnal and seasonal variations in ozone concentration are shown schematically.

Since we are concerned with ozone concentrations at plume altitude in visibility calculations, it is appropriate to use the daily maximum value

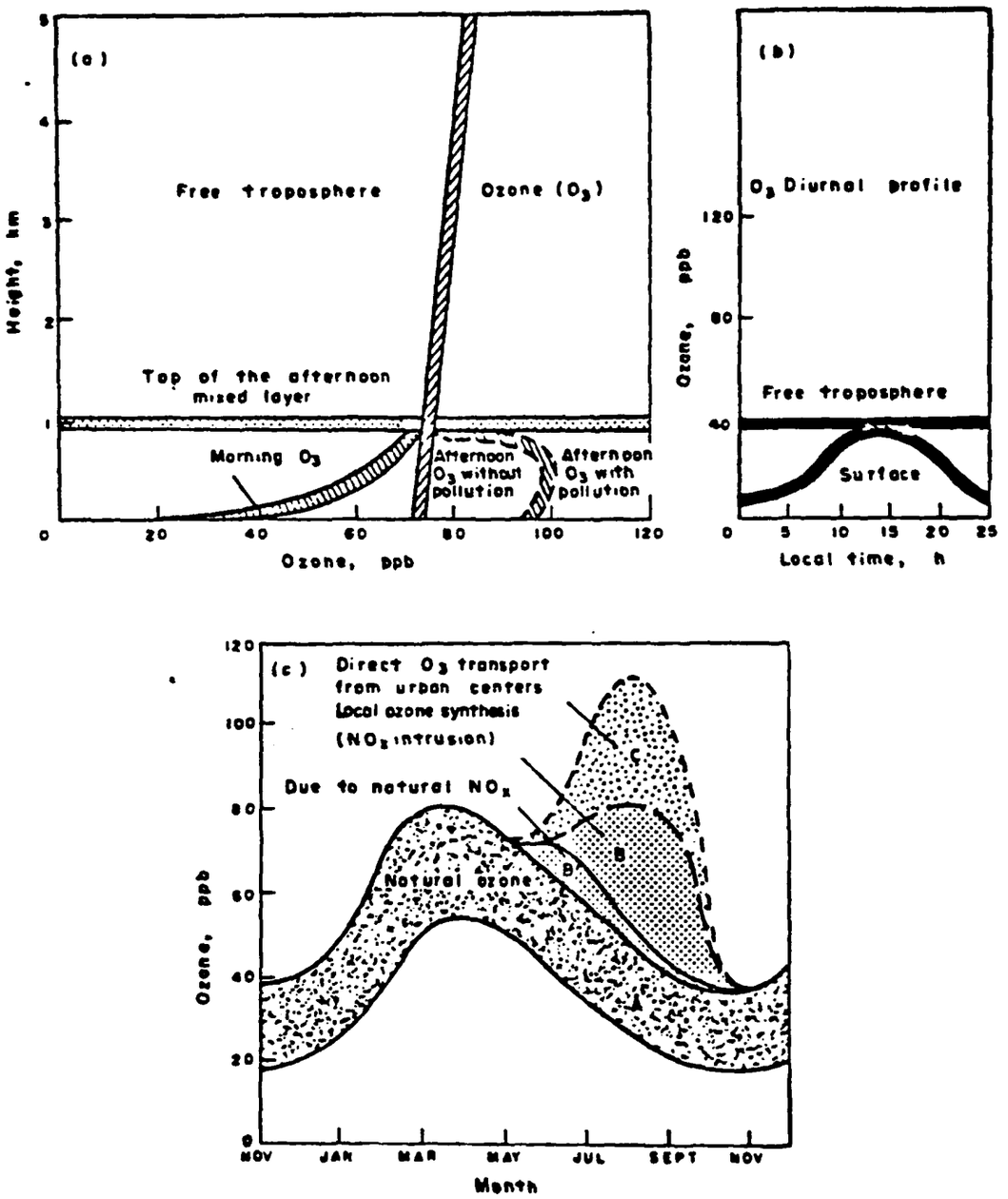

Source: Singh, Ludwig, and Johnson (1978).

Figure 20. A schematic of the vertical O_3 structure and its diurnal and seasonal variations at remote sites.

of the surface concentration to represent the daily average concentration at plume altitude, as shown in figure 20(a).

We select a median background ozone concentration for the assessment of worst-case visual impacts, so, by definition, the frequency of occurrence of ozone concentrations higher than that assumed is 50 percent. This is done so that when the cumulative frequencies of occurrence of meteorological conditions worse than the assumed worst-case meteorological conditions are multiplied by the corresponding frequencies of high background ozone concentration and visual range, the resulting cumulative frequency is the equivalent of one day per year. Thus, we have

(cumulative frequency of assumed worst-case meteorological conditions)
x (cumulative frequency of assumed background ozone concentration)
x (cumulative frequency of assumed background visual range)
= 0.01 x 0.50 x 0.50 x 365 days/year ≅ 1 day/year.

4.1.4 Background Visual Range

As noted previously, we want to select the median background visual range to analyze worst-case visual impact conditions. The impact-magnitude calculations described in the next section are based on the assumption that visual range is calculated at a wavelength λ of 0.55 μm:

$$r_{v0} = \frac{3.912}{b_{ext}\ (\lambda = 0.55\ \mu m)} \quad .$$

Since there can be a significant wavelength dependence of b_{ext}, it is important that the median background visual range for the site and region is based on spectral measurements at 0.55 μm. Such measurements can be made with telephotometers or nephelometers equipped with narrow band-pass filters. If such data are not available, use the estimates of median regional visual range shown in figure 13.

4.2 HAND CALCULATION OF WORST-CASE VISUAL IMPACTS

From the procedures discussed previously, the analyst will have identified the following conditions for calculation of worst-case impacts:

- Worst-case (1-percentile) plume dispersion condition.
  - Worst-case wind direction (one of sixteen 22.5° sectors).
  - Wind speed.
  - Pasquill-Gifford stability class.
- Worst-case (1-percentile) and seasonal average limited mixing condition.
  - Wind speed.
  - Mixing depth.
- Median (50-percentile) background ozone concentration.
- Median (50-percentile) background visual range.
- Distances to terrain objects for various line-of-sight azimuths.
- Downwind distance x along plume trajectory.

In this section we discuss the calculation of visual impact parameters on the basis of those worst-case conditions appropriate for a level-2 visibility screening analysis. We suggest four different alternatives for calculating magnitudes of worst-case visual impacts:

- Hand calculations of plume contrast and sky/terrain contrast reduction using equations (10) and (14) from chapter 2, and procedures presented in this section.
- Reference tables of plume discoloration parameters corresponding to various NO_2 line-of-sight integrals.
- Reference figures of visual range reduction caused by emissions sources of different sizes for various meteorological conditions.
- Computer model calculations using PLUVUE or some other equivalent visibility model.

The analyst can choose which of these methods to use for a level-2 screening analysis, depending on personal preference. However, more accurate estimates (with less conservatism) are possible with the use of computer model calculations. Assessments using different alternative methods can be cross-checked.

We can compute the magnitude of visibility impact corresponding to the worst-case conditions identified earlier in this section by a series of formulas presented here. Some of these calculations are needed to use the reference tables and to set up input for the computer model.

4.2.1 Determining the Geometry of Plume, Observer, Viewing Background, and Sun

In the previous section we discussed the procedure for identifying the worst-case meteorological conditions used in the calculation of visibility impacts. This condition was selected so that on only one day per year (on the average) would conditions be worse than those selected for analysis. As the basis for the selection of this condition, we considered the frequency of occurrence of wind directions that would carry emissions within the 22.5° sector centered on the observer, as shown schematically in figure 21.

Thus, we have identified the cumulative frequency (i.e., the frequency of occurrence of conditions worse than the given value) of wind directions within the worst-case wind direction sector associated with (1) wind speeds less than, (2) stabilities greater than, (3) background ozone concentrations greater than, and (4) background visual ranges greater than, the given values selected for the worst-case impact evaluation.

Because we wish to compute the magnitude of plume visual impact, it is appropriate to consider the plume orientation resulting in the smallest impact associated with the worst-case wind direction sector. Thus, we consider a plume centerline at the edge of the 22.5° sector centered on

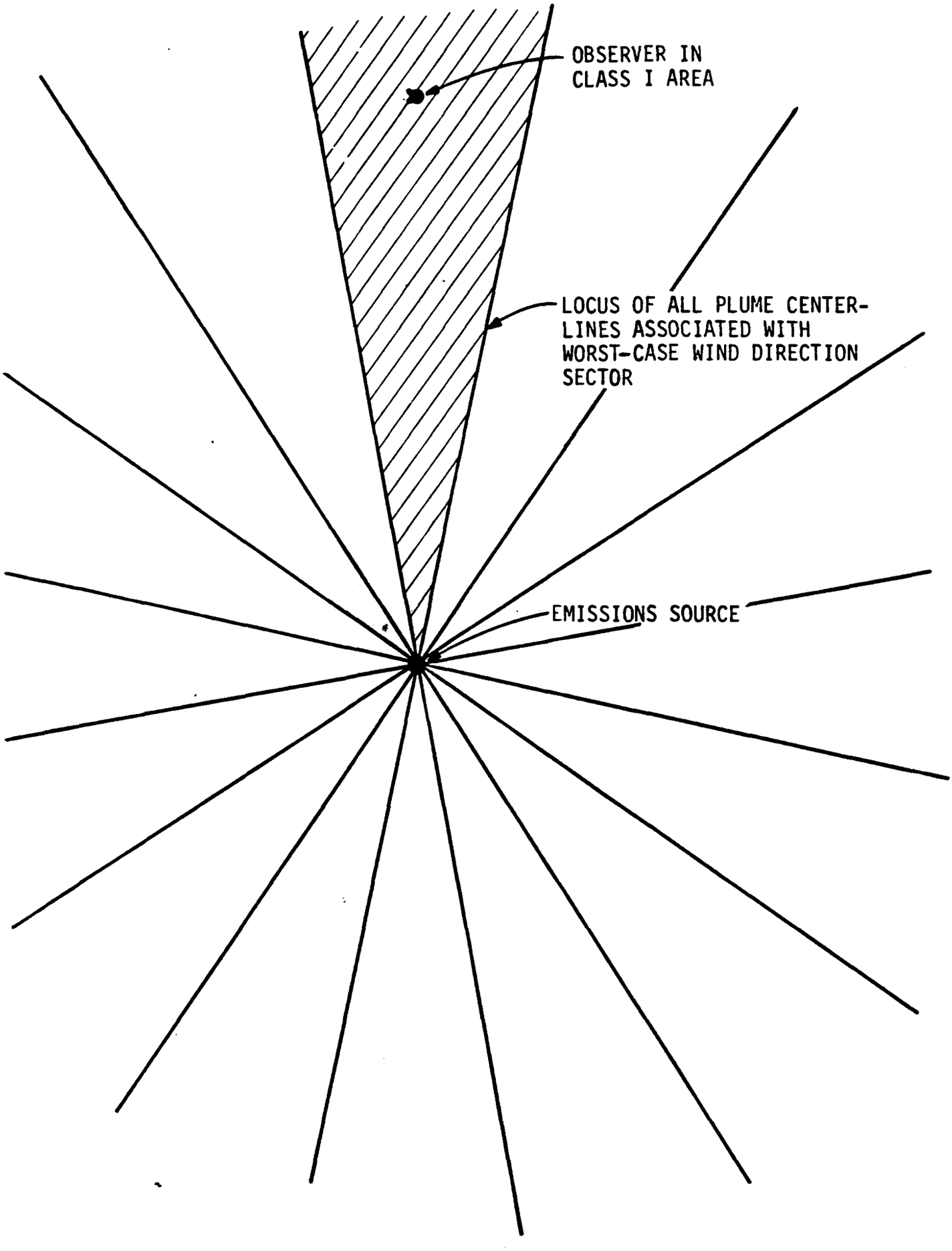

Figure 21. Locus of plume centerlines within worst-case wind direction sector.

the observer, as shown in figure 22. Thus, the minimum distance between the observer and the plume centerline is

$$r_{p\text{-}min} = x \tan\left(\frac{22.5^\circ}{2}\right) = 0.199\ x \quad ,$$

where x is the downwind distance along the plume centerline from the emissions source to the parcel that is observed, as shown in figure 22.

For the worst-case plume discoloration condition, the plume is assumed to have a Gaussian distribution in the vertical direction, with vertical dimensions as a function of the σ_z corresponding to the given worst-case stability class and downwind distance x. For level-2 screening performed on the basis of hand calculations, we further assume that the plume material is uniformly mixed in the horizontal direction within the 22.5° sector. Thus the plume width at a given downwind distance is twice $r_{p\text{-}min}$, or 0.398 x.

For the worst-case general haze conditions one must remember the assumption that plume material has been transported for two days. Therefore, for the evaluation of increases in haze resulting from SO_2 and particle emissions during worst-case 48-hour episodes of limited mixing, we assume that the plume width is 100 km. Several studies suggest that plume spread is a function of travel time and that this 100 km width is a reasonable representation for a 48-hour travel time (see, for example, model calculations of Liu and Durran, 1977, and field data of Randerson, 1972).

For the level-2 analysis (based on hand calculations), we also assume that the plume width is constant within the field of view, as shown in figure 23. This plume width equals $2r_{p\text{-}min}$ (0.398 x, or 100 km). Both the plume optical thickness, τ_{plume}, and the distance to the plume centerline are inversely proportional to the size of the angle α shown in figure

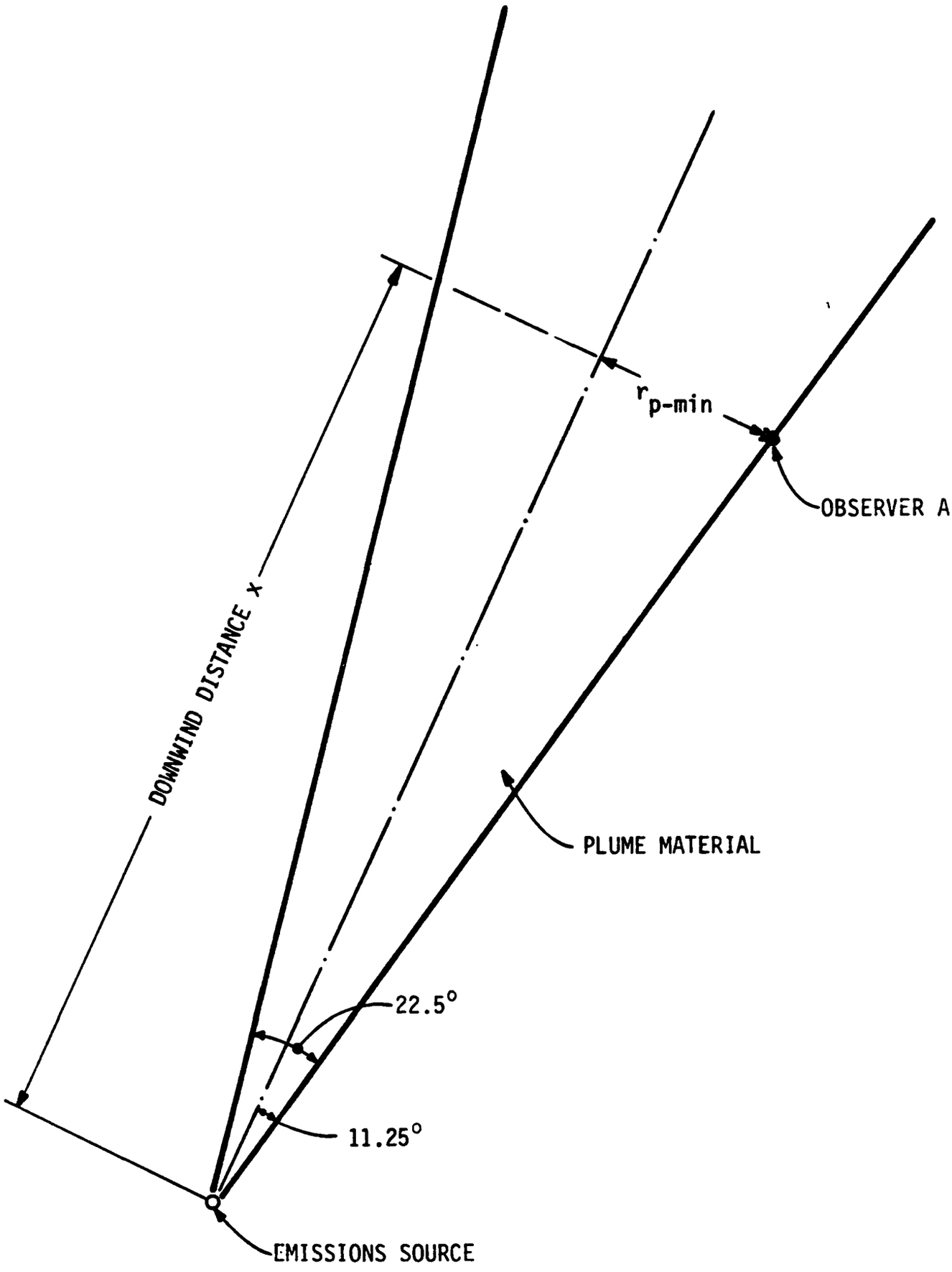

Figure 22. Observer-plume orientation for level-2 visibility screening analysis.

23. Thus,

$$\tau_{plume}(\alpha) = \frac{\tau_{plume}\ (\alpha = 90°)}{\sin\ \alpha} \quad ,$$

$$r_p(\alpha) = \frac{r_{p\text{-}min}}{\sin\ \alpha} \quad .$$

Also, the plume optical thickness between the observer and a given viewed object is a function of the object-observer distance r_o:

$$\tau_{plume}(r_o,\ \alpha) = \begin{cases} \tau_{plume}(\alpha) & , \quad \text{if } r_o > 2r_p(\alpha) \\ \tau_{plume}(\alpha)\left(\dfrac{r_o}{r_p(\alpha)}\right) & , \quad \text{if } r_o < 2r_p(\alpha) \end{cases} \quad .$$

The distances r_o and the azimuths for various terrain viewing objects identified using the procedure discussed previously in this section (see figure 15) should be tabulated. The corresponding values of α and scattering angle Θ should be identified in this table also. The scattering angle Θ for horizontal lines of sight can be determined as follows (Duffie and Beckman, 1974):

$$\cos\ \Theta = \cos\ \delta \sin A \sin H + \sin\ \delta \cos\ \phi \cos A$$

$$- \cos\ \delta \sin\ \phi \cos A \cos H \quad , \qquad \text{(p-11)}$$

where

$A \equiv$ azimuth of the line of sight from observer to viewed object (e.g., $A = 0°$ for the line of sight directly to the north),

$\delta \equiv$ declination,

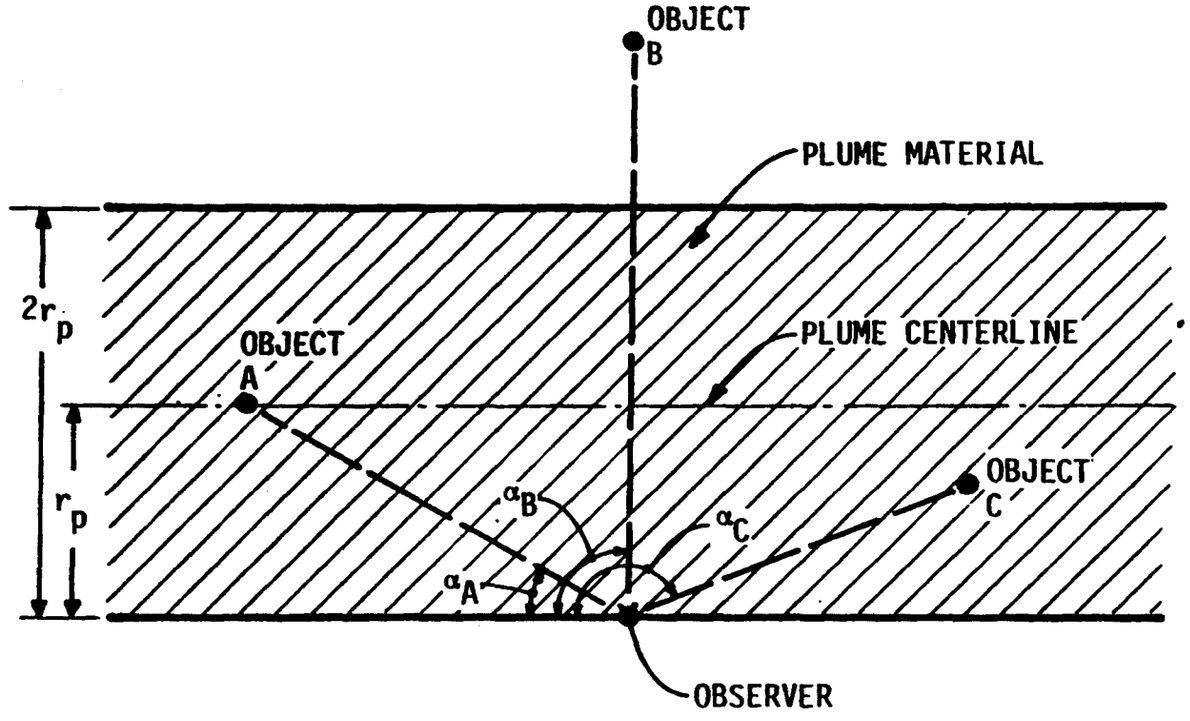

Figure 23. Plan view of assumed plume-observer geometry for level-2 visibility screening calculations.

$$\equiv 23.45 \sin\left(360 \frac{284 + n}{365} \text{ degrees}\right),$$

$n \equiv$ number of the day of the year (e.g., 1 January is $n = 1$),

$\phi \equiv$ latitude of the observer,

$H \equiv$ hour angle, solar noon being zero, each hour equivalent to a 15° displacement, mornings positive and afternoons negative.

Note that stable plumes are usually viewed in the morning at, or shortly after, sunrise. The scattering angle Θ at sunrise at a spring or autumnal equinox is determined for $\delta = 0°$ and $H = 90°$ as follows:

$$\cos \Theta = \sin A \quad .$$

Thus, for these dates and this time

$$\Theta = \begin{cases} |A - 90°| \ , & \text{if } 90° < A < 270° \\ 450° - A \ , & \text{if } A > 270° \end{cases} .$$

The value of the scattering angle and the appropriate line-of-sight azimuth A should also be evaluated for the following values of α: 30°, 45°, 60°, 90°, 120°, 135°, and 150°. Note that both A and α are azimuthal angles descriptive of the line of sight. A is referenced to north and α is referenced to the plume centerline.

4.2.2 Calculating Plume Optical Depth

We start with known emission rates of primary particulate matter, NO_x, and SO_2 from the source. To convert these quantities to plume optical depth (τ), we must know

- Size distribution and density of emitted particles.
- Size distribution and density of secondary sulfate aero-

sol.

- > Fraction of NO_x and SO_2 emissions converted to NO_2 or sulfate ($SO_4^=$) aerosol at a given downwind distance (or transport time).
- > Vertical distribution of plume material.
- > Wind speed.

4.2.2.1 Effects of Primary Particulate Emissions on Optical Depth

If the size and density of primary particle emissions are known, we can compute the plume flux of the scattering coefficient from the following formula:

$$Q_{scat\text{-}part} = \frac{1160\ Q_{part}(b_{scat}/V)}{\rho} \quad , \qquad (p\text{-}12)$$

where

$Q_{scat\text{-}part}$ ≡ plume flux of scattering coefficient at λ = 0.55 μm ($m^2 s^{-1}$),

Q_{part} ≡ primary particle mass emissions rate (metric tons/day),

(b_{scat}/V) ≡ scattering coefficient (at λ = 0.55 μm) per unit volume concentration of aerosol [$10^{-4} m^{-1}/(\mu m^3/cm^3)$] from figure 24,

ρ ≡ density of primary particles (g/cm^3).

Note that the conversion factor in this equation derives from the use of the units given above:

$$\frac{(\text{metric tons/day})\ (10^6 \text{g/metric ton})\ [(10^{-4} m^{-1})/(\mu m^3/cm^3)]}{(24 \text{ hr/day})\ (3600 \text{ s/hr})\ (g/cm^3)\ (100 \text{ cm/m})^3\ (10^{-4} \text{cm}/\mu m)^3}$$

$$= 1.16 \times 10^3\ m^2 s^{-1} \quad .$$

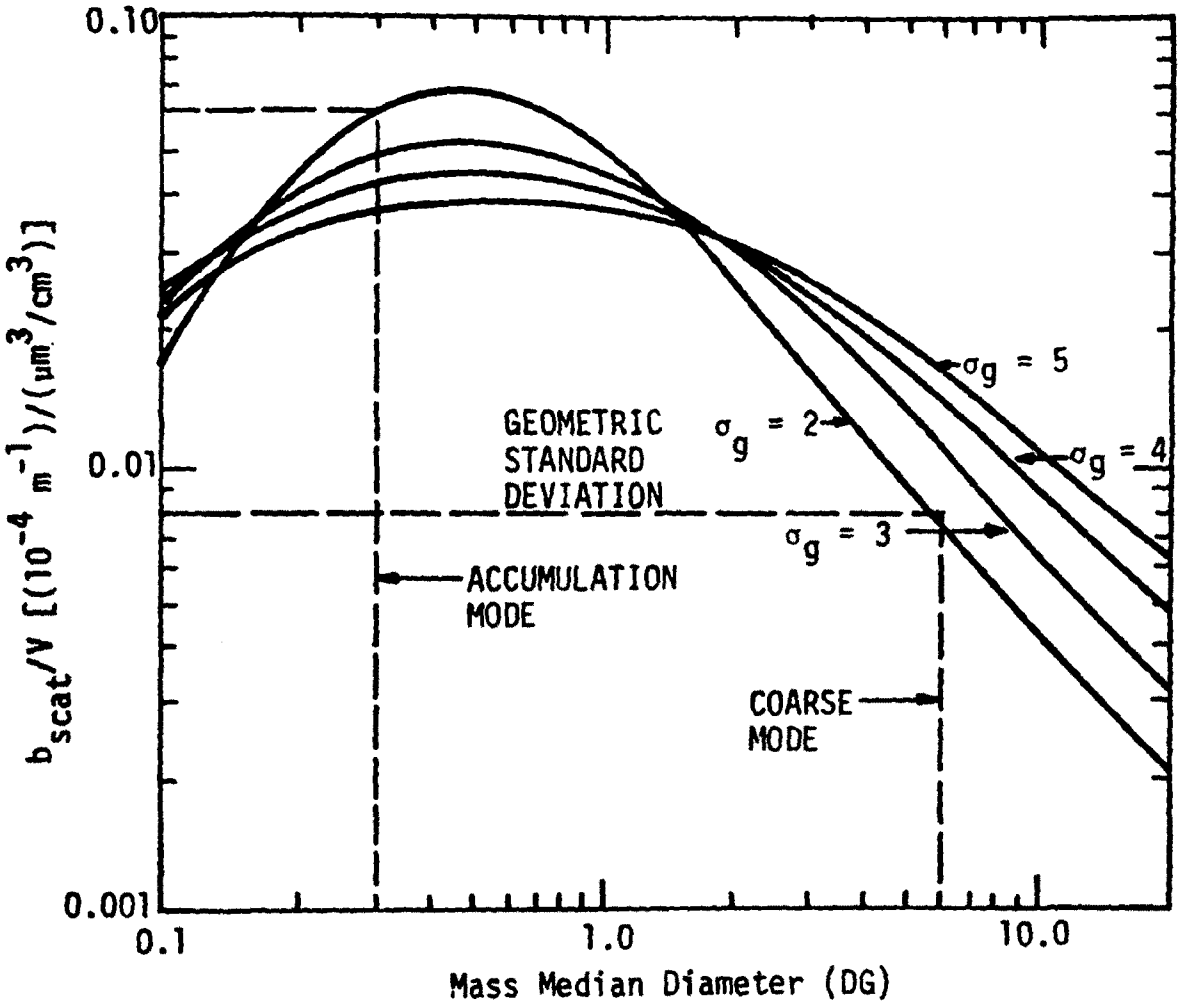

Source: Latimer et al. (1978).

Figure 24. Scattering-to-volume ratios for various size distributions.

If one does not know the primary particle size distribution and density, one can assume the values used for the level-1 analysis--a mass median diameter DG of 2 μm, a geometric standard deviation σ_g of 2, and a density of 2.5 g/cm^3 (Schulz, Engdahl, and Frankenberg, 1975). For this distribution we have $(b_{scat}/V) = 0.025$, and therefore

$$Q_{scat\text{-}part} = 11.6\ Q_{part} \quad . \qquad \text{(p-13)}$$

Another alternative is to use the known stack opacity to calculate the plume scattering coefficient.* Sometimes the stack opacity is known with more precision than is the mass emission rate for primary particles. If both the stack opacity and the particle mass emission rate are known, we can compute the appropriate size distribution that will provide a match. The stack opacity is defined as follows:

$$\text{Opacity} = 1 - e^{-\tau_{stack}} \quad , \qquad \text{(p-14)}$$

where $\tau_{stack} = \frac{Q_{scat\text{-}part}}{D\ v}$, D ≡ inside stack diameter, and v ≡ flue gas stack exit velocity.

We can solve for the scattering coefficient flux per stack as follows:

$$Q_{scat\text{-}part} = -D\ v\ \ell n(1 - \text{Opacity}) \quad . \qquad \text{(p-15)}$$

For many facilities, emissions regulations limit stack opacity to 20 percent. For such facilities

---

* A caution is in order here. If wet scrubbers are used or if hygroscopic material or condensable gases are emitted from the source, it may not be appropriate to calculate the plume flux of scattering coefficient from stack opacity because particles may quickly grow and form as flue gas temperature drops.

$$Q_{scat\text{-}part} = -D\ v\ \ln(1 - 0.20) = 0.22\ D\ v \quad . \quad \text{(p-16)}$$

The total plume scattering coefficient flux is the sum of the contributions from all stacks in the facility. Note, however, that as a result of differences in stack height or plume rise for different stack emissions, stable plumes from different elevations in the facility may be at different elevations, without overlap. In such cases, for the calculation of stable conditions, one would use the maximum single-stack scattering coefficient flux only, not the sum over all stacks. This would be true for NO_2 fluxes also. For the calculations of increases in haze caused by SO_2 and particle emissions during limited mixing conditions, however, one should use the emissions over all stacks because all emissions are assumed to be uniformly mixed within the mixed layer.

If one has both the mass emissions rate and the stack opacity, one can solve these equations for (b_{scat}/V), assuming a particle density of 2.5 or some other appropriate value, and one can use figure 24 to determine the corresponding size distribution.

The scattering coefficient flux is calculated on the basis of a wavelength λ of 0.55 μm. The scattering coefficient (resulting from particles only) at any wavelength can be calculated from the following equation:

$$b_{scat}(\lambda) = b_{scat}(\lambda = 0.55)\left(\frac{\lambda}{0.55}\right)^{-n} \quad , \quad \text{(p-17)}$$

where n is given in table 4 as a function of mass median diameter for a size distribution whose geometric standard deviation is $\sigma_g = 2$.

Note from table 4 that for particle size distributions with mass median diameters larger than about 1.5 μm, the scattering coefficient is independent of wavelength over the visible spectrum. However, for a typical submicron aerosol with a mass median diameter of 0.3 μm, the scattering coefficient at $\lambda = 0.4$ μm (the blue end of the spectrum) is 2.5 times larger than that at $\lambda = 0.7$ μm (the red end).

TABLE 4. WAVELENGTH DEPENDENCE OF SCATTERING COEFFICIENT AS A FUNCTION OF PARTICLE SIZE DISTRIBUTION

Mass Median Diameter DG* (μm)	n†
0.1	2.8
0.2	2.1
0.3	1.6
0.4	1.2
0.5	1.0
0.6	0.7
0.8	0.5
1.0	0.2
> 1.5	0

* Geometric standard deviation $\sigma_g = 2$.

† n is defined as follows: $b_{scat}(\lambda_1) = b_{scat}(\lambda_2)\left(\frac{\lambda_1}{\lambda_2}\right)^{-n}$

(appropriate for $0.4 < \lambda < 0.7$ μm).

The corresponding plume fluxes of scattering coefficients resulting from sulfate aerosol, and absorption coefficients resulting from NO_2, are more difficult to calculate since one has to consider the rate of formation of sulfate or NO_2 from SO_2 and NO_x emissions.*

4.2.2.2 Effects of Nitrogen Dioxide on Optical Depth

We first consider the NO_2 absorption coefficient plume flux. We assume that, for the two-day limited mixing stagnation case, all NO_2 is scavenged by reactions with the hydroxyl radical (OH•), forming nitric acid vapor (HNO_3), or from surface deposition. However, for the stable plume transport case used to calculate worst-case plume discoloration, nitric oxide (NO) emissions will react with background ozone and oxygen to form NO_2.

The fraction of NO_x emissions that is converted to NO_2 can be calculated with formulations used in the visibility computer model (see Latimer et al., 1978). This fraction is dependent on the spatial and temporal variation in ultraviolet radiation, background ozone, and plume SO_2 and NO_x concentrations. However, for stable, nighttime transport cases, a reasonable, somewhat conservative estimate of this fraction can be made as follows: first, we assume that NO_x emissions are uniformly distributed horizontally over a 22.5° sector. Thus, NO_x concentrations can be calculated as follows:

$$[NO_x] = \frac{Q_{NO_x}}{(2\pi)^{1/2}\sigma_z u\left[2\tan\left(\frac{22.5}{2}\right)x\right]} .$$

* For those who will use the computer model or the reference figures based on the computer model runs, these calculations of NO_2 and $SO_4^=$ formation can be omitted.

This can be simplified, using appropriate conversion factors for the units indicated, as follows:

$$[NO_x] = \frac{6.17\ Q_{NO_x}}{\sigma_z u x} \quad , \qquad \text{(p-18)}$$

where

$[NO_x]$ ≡ plume centerline NO_x concentration (ppm),
Q_{NO_x} ≡ mass emissions rate of NO_x, expressed as NO_2 (metric tons per day),
σ_z ≡ Pasquill-Gifford dispersion coefficient at downwind distance x,
u ≡ wind speed (m/s),
x ≡ downwind distance.

For example, this formula yields an NO_x concentration of 0.034 ppm 100 km downwind from a 100 metric ton/day source during F stability and 2 m/s wind conditions. Using a simplified formulation from Latimer et al. (1978), appropriate for stable nighttime transport and early morning situations, we can calculate NO_2 concentrations in the plume as follows:

$$[NO_2] = \begin{cases} h \quad , & \text{if } [NO_x] > h \\ [NO_x] \quad , & \text{if } [NO_x] < h \end{cases} \quad , \qquad \text{(p-19)}$$

where

$[NO_2]$ = plume centerline NO_2 concentration (ppm),
$h = 0.1\ [NO_x] + [O_3]$,
$[NO_x]$ ≡ as defined above,
$[O_3]$ ≡ background ozone concentration (ppm).

For the example shown above, if the background ozone concentration is a typical value of 0.04 ppm, we calculate an NO_2 concentration of 0.034 ppm, indicating that complete conversion of NO to NO_2 occurred.

For viewing situations in which the sun is high above the horizon, this formula overestimates NO_2 concentrations. For such applications, either the visibility model or the following formulation should be used to obtain more accurate determinations (Latimer et al., 1978):

$$[NO_2] = 0.5\left[[NO_x] + h + j - \left\{\left([NO_x] + h + j\right)^2 - 4[NO_x]h\right\}^{1/2}\right] \quad , \qquad \text{(p-20)}$$

where

$j = 2.3 \times 10^{-2} \exp(-0.38/\cos Z_s)$;

$Z_s \equiv$ solar zenith angle, the angle between direct solar rays and the normal to the earth's surface (e.g., $Z_s = 90°$ for sunrise or sunset; $Z_s = 0°$ for sun directly overhead);

$[NO_2]$, $[O_3]$, $[NO_x]$, h are defined as above.

The optical depth resulting from NO_2 is simply

$$\tau_{NO_2} = 0.398\,[NO_2](x)(b_{abs}/ppm) \quad , \qquad \text{(p-21)}$$

where x ≡ downwind distance (km), and $(b_{abs}/ppm) \equiv$ light absorption per ppm NO_2 ($km^{-1}ppm^{-1}$).

The value of (b_{abs}/ppm) for NO_2 as a function of wavelength is plotted in figure 25. Note the extreme variation with wavelength (the plot is on logarithmic paper). Light absorption by NO_2 is more than two orders of magnitude larger at the blue end of the visible spectrum ($\lambda = 0.4$ μm) than at the red end ($\lambda = 0.7$ μm). The values at the three wavelengths that we will use later to calculate contrasts are as follows:

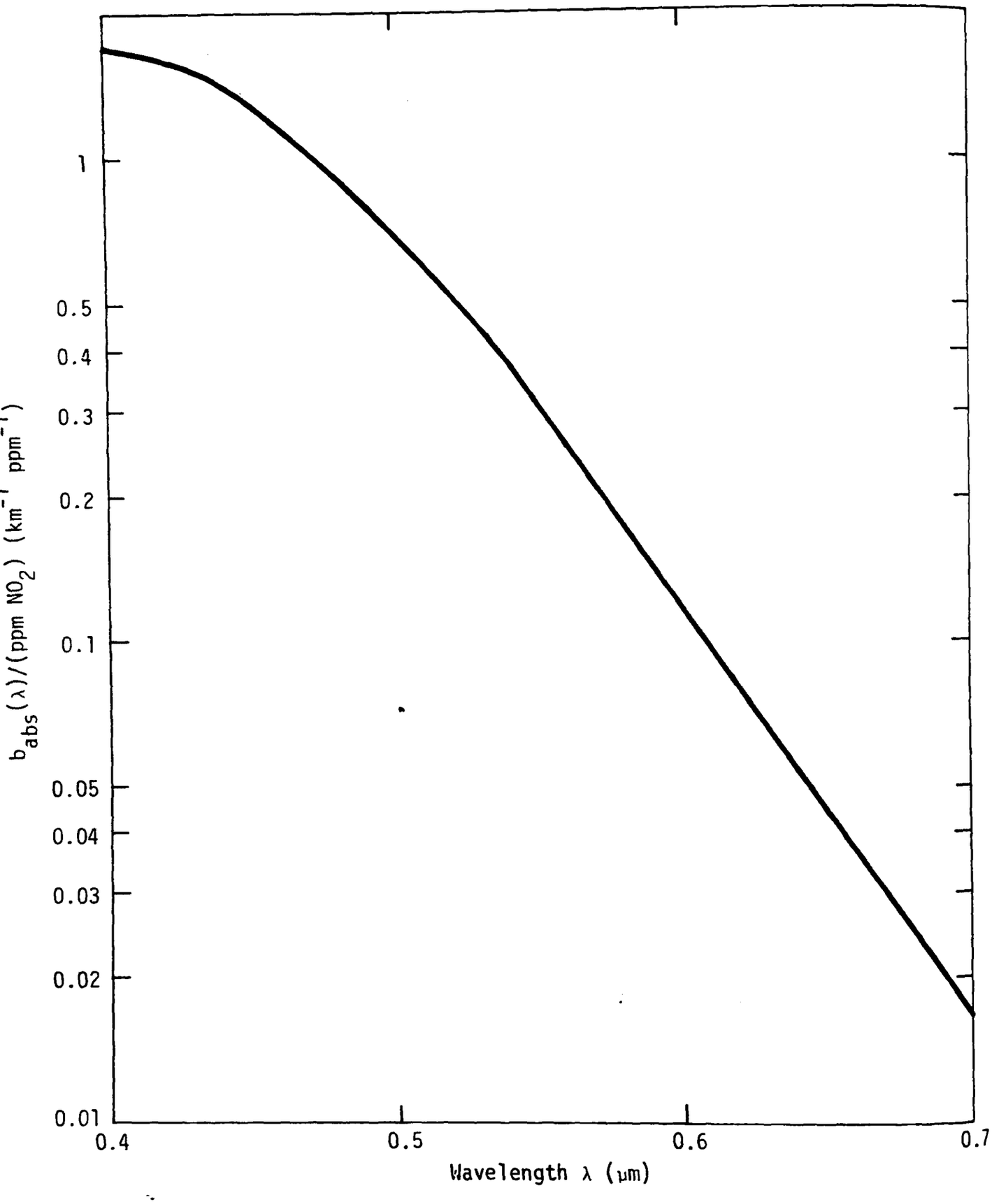

Note: Based on data from Nixon (1940).

Figure 25. Wavelength dependence of light absorption of nitrogen dioxide (NO_2).

λ (μm)	b_{abs}/ppm ($km^{-1}ppm^{-1}$)
0.40	1.71
0.55	0.31
0.70	0.017

4.2.2.3 Effects of Secondary Sulfate Aerosol on Optical Depth

The scattering coefficient for sulfate aerosol is determined from an empirical formula (Latimer et al., 1978):

$$b_{scat}/(\mu g/m^3)\Big|_{\lambda = 0.55\ \mu m} = \frac{2.5 \times 10^{-6}\ m^{-1}(\mu g/m^3)}{1 - (RH/100)} \quad ,$$

where RH is the average relative humidity (in percent) for the area. If this relative humidity is not known for the given area, assume 40 percent and 70 percent for the western and eastern United States, respectively. This sulfate aerosol is assumed to have a size distribution with a mass median diameter of 0.3 μm and a geometric standard deviation of 2.

The sulfate aerosol mass flux in the plume at a given distance downwind is calculated from the emission rate of SO_2 as follows:

$$Q_{SO_4} = \frac{f_{MW}\, k_f\, Q_{SO_2}}{(k_f + k_d)} \left\{ 1 - \exp[-(k_f + k_d)\ t] \right\} \quad ,$$

where

Q_{SO_4} ≡ plume mass flux of sulfate aerosol,

f_{MW} ≡ ratio of molecular weights of $SO_4^=$ and SO_2

= 96/64 = 1.5,

k_f ≡ 24-hour average pseudo-first-order rate constant for SO_2 conversion to $SO_4^=$ in the atmosphere,

k_d ≡ 24-hour average pseudo-first-order rate constant for surface deposition = v_d/H_m,

t ≡ plume parcel transport time (for the level-2 analysis we assume t = 48 hours),

v_d ≡ 24-hour average SO_2 deposition velocity (we suggest using v_d = 0.5 cm/s).

H_m ≡ mixing depth.

On the basis of calculations of homogeneous oxidation rates by Atlshuller (1979), we suggest that the following values be used for the 24-hour average SO_2-to-$SO_4^=$ pseudo-first-order rate constant k_f.

Season	k_f (%/hr)
Winter	0.1
Spring, autumn	0.2
Summer	0.4

The analyst should use the appropriate values of the mixing depth, H_m, for the limited mixing worst-case and for the seasonal-average conditions that were identified by the procedure described previously.

We may combine equations for $SO_4^=$ mass flux and scattering coefficient per mass concentration to obtain a formula for the $SO_4^=$ scattering coefficient plume flux. This formula, with appropriate conversion factors for the units shown, is as follows:

$$Q_{scat\text{-}SO_4} = \frac{43.4\ k_f\ Q_{SO_2}}{k'\ (1 - RH/100)} \left[1 - \exp(-0.48\ k')\right] \quad , \qquad \text{(p-22)}$$

where $k' = k_f + 1800/H_m$, and k_f is taken from the tabulation shown above, Q_{SO_2} is in metric tons per day, RH is in percent, and H_m is in meters.

The plume scattering coefficient flux values for primary particle emissions and for sulfate aerosol formed from SO_2 emissions can be converted to plume optical thickness through division by the appropriate factor.

$$\tau_{part} = \frac{Q_{scat\text{-}part}}{(2\pi)^{1/2}\sigma_z u} \qquad \text{(p-23)}$$

for Gaussian vertical profiles (e.g., the worst-case stable plume condition), and

$$\tau_{aerosol} = \frac{Q_{scat\text{-}part} + Q_{scat\text{-}SO_4}}{uH_m} \qquad \text{(p-24)}$$

for vertically uniformly mixed plumes in the mixed layer $0 < Z < H_m$ (e.g., the worst-case and seasonal-average limited mixing conditions).

From the equations presented thus far, the analyst will be able to calculate the following optical thickness (τ) values for any wavelength λ:

- τ_{NO_2} and τ_{part} for the worst-case plume dispersion conditions (assume no sulfate formation for these worst-case, light-wind, stable conditions).
- $\tau_{aerosol}$ for worst-case limited mixing conditions and each of the seasonal-average limited mixing conditions.

4.2.3 Calculating Phase Functions

The phase function, defined in equation (1) of chapter 2, describes the fraction of total light scattered by a given plume or background

atmosphere parcel in the direction defined by the scattering angle Θ. A scattering angle Θ of 0° means no change in radiation direction, while 180° means that radiation is scattered backward. Much more light is scattered in the forward direction ($\Theta < 90°$) than in the backward direction ($\Theta > 90°$). We need to calculate phase functions to determine the amount of light that is scattered into an observer's line of sight.

Phase functions $p(\lambda,\Theta)$ for the plume and the background atmosphere are determined from the tables in appendix B. These tables show phase functions as a function of scattering angle [i.e., the angle between the direct solar radiation and the line of sight as shown in figure 2(a), chapter 2] for various particle size distributions and wavelengths λ (0.4, 0.55, and 0.7 μm). Figure 26 summarizes the phase functions at $\lambda = 0.55$ μm. Note that $p(\Theta)$ is largest for small scattering angles (i.e., more light is scattered in the forward direction).

To calculate average phase functions for the background atmosphere, we must calculate the fraction of the total extinction coefficient resulting from:

- Light absorption by aerosols.
- Rayleigh light scatter due to air.
- Light scatter caused by submicron (accumulation mode) aerosol.
- Light scatter caused by coarse aerosol.

First, we must calculate the background extinction coefficient from the median visual range for the area:

$$b_{ext}(\lambda = 0.55\ \mu m) = \frac{3.912}{r_{v0}} \quad . \qquad \text{(p-25)}$$

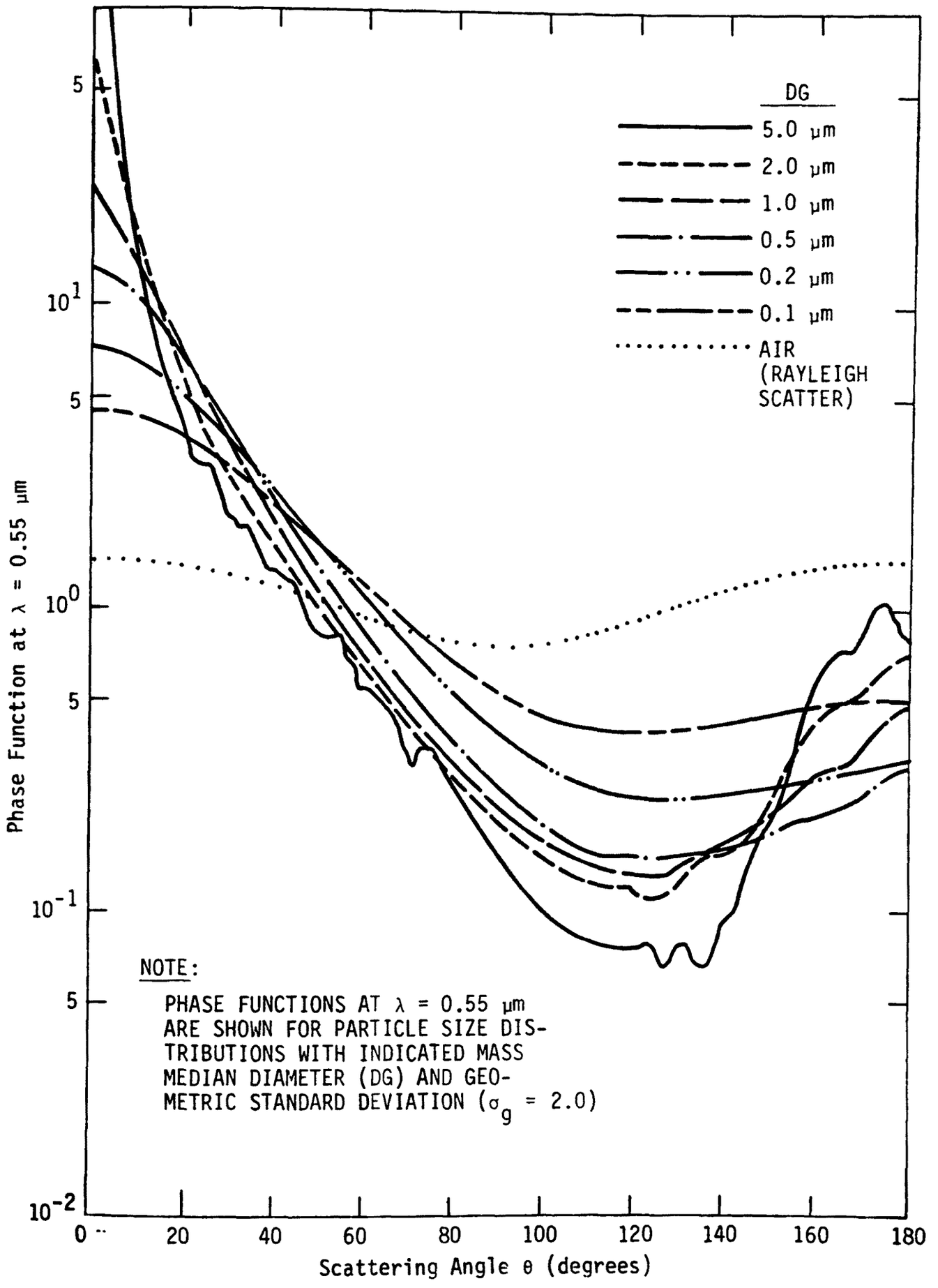

Figure 26. Phase functions for various particle size distributions.

We assume that 5 percent of the background extinction coefficient is caused by light absorption resulting from aerosols such as soot.* Thus,

$$b_{scat}(\lambda = 0.55\ \mu m) = 0.95\ b_{ext} \quad . \qquad \text{(p-26)}$$

The scattering coefficient caused by particles is determined by subtracting the Rayleigh scattering coefficient:

$$b_{sp}(\lambda = 0.55\ \mu m) = b_{scat}(\lambda = 0.55) - b_R(\lambda = 0.55) \quad , \qquad \text{(p-27)}$$

where $b_R(\lambda = 0.55\ \mu m) = (11.62 \times 10^{-6} m^{-1}) \exp\left(-\frac{Z + 500}{9800}\right)$, and Z ≡ elevation of site (m MSL).

Based on data of Whitby and Sverdrup (1978) and calculations of Latimer et al. (1978), the fraction of b_{sp} caused by coarse particles is assumed to be 0.33.† Thus, we have

$$b_{sp\text{-submicron}} = 0.67\ b_{sp} \quad , \qquad \text{(p-28)}$$

$$b_{sp\text{-coarse}} = 0.33\ b_{sp} \quad . \qquad \text{(p-29)}$$

The phase function for each of the scattering components can now be determined. Phase functions for the submicron and coarse background aero-

---

* Charlson and Waggoner, personal communication.

† For marine background atmospheres (coastal locations unaffected by urban plumes), assume this fraction is 95 percent. For urban areas, assume this fraction is 10 percent.

sol modes can be determined from appendix B. We assume that the background submicron aerosol has a mass median diameter of 0.3 μm and the background coarse aerosol has a mass median diameter of 6 μm. Both of these aerosol modes are assumed to have a geometric standard deviation of 2.0. These size distributions are typical of those measured by Whitby and Sverdrup (1978) in a variety of environments, including clean and average rural and urban atmospheres. Phase functions for these two size distributions are given in appendix B.

The Rayleigh scattering phase function (for air) is a function of the scattering angle Θ, but it is independent of wavelength λ and can be approximated quite well by the following relationship:

$$p(\Theta) = 0.75\ [1 + (\cos\ \Theta)^2] \quad . \qquad \text{(p-30)}$$

At this point the analyst should fill in a table similar to table 5 for the scattering angles (Θ) shown or for those identified for specific lines of sight, as portrayed schematically in figure 23. The scattering coefficients at different wavelengths can be determined from the relationship:

$$b_{sp}(\lambda) = b_{sp}(\lambda = 0.55\ \mu m)\left(\frac{\lambda}{0.55\ \mu m}\right)^{-n} \quad , \qquad \text{(p-31)}$$

where values of n are given in table 4 for various particle size distributions and n = 4.1 for Rayleigh scatter.

The average background atmosphere phase functions are calculated for each wavelength λ and scattering angle Θ as follows:

$$p(\lambda,\Theta)\big|_{background} = \frac{\sum b_{sp}(\lambda)\ p(\lambda,\Theta)}{\sum b_{sp}(\lambda)} \quad , \qquad \text{(p-32)}$$

TABLE 5. EXAMPLE TABLE SHOWING BACKGROUND ATMOSPHERE PHASE FUNCTIONS AND SCATTERING COEFFICIENTS

Background Atmosphere Scattering Component	λ(μm)	$b_{sp}(m^{-1})$	Phase Function $p(\lambda,\theta)$ for Indicated θ				
			22°	45°	90°	135°	180°
Rayleigh Scattering	0.40						
Due to air molecules	0.55						
at site elevation	0.70						
Mie Scattering							
Submicron aerosol	0.40						
DG = 0.3 μm	0.55						
σ_g = 2.0	0.70						
Mie Scattering							
Coarse aerosol	0.40						
DG = 6 μm	0.55						
σ_g = 2.0	0.70						
Total (average)	0.40						
	0.55						
	0.70						

where the summation is over Rayleigh, submicron, and coarse mode scattering categories.

The phase functions for the plume can be obtained from the tables in appendix B corresponding to the size distribution of the primary particle emissions. If this size distribution is not known, assume it has a 2.0 μm mass median diameter (Schulz, Engdahl, and Frankenberg, 1975).

4.2.4 Calculating Plume Contrast and Contrast Reduction

With the procedure discussed thus far, the analyst can calculate the magnitude of plume visual impact using equations (10) and (14) from chapter 2. These equations are repeated here for convenience.

Plume Contrast

$$C_{plume} = \left[\frac{(\bar{p}\bar{\omega})_{plume}}{(\bar{p}\bar{\omega})_{background}} - 1\right]\left[1 - \exp(-\tau_{plume})\right]\left[\exp(-b_{ext} r_p)\right] \quad . \qquad \text{(p-33)}$$

Reduction in Sky/Terrain Contrast Caused by Plume

$$\Delta C_r = -C_0 \exp(-b_{ext} r_o)\left[1 - \left(\frac{1}{C_{plume} + 1}\right)\exp(-f_{obj}\tau_{plume})\right] \quad , \qquad \text{(p-34)}$$

where

$\bar{p}_{plume}$, $\bar{p}_{background}$ ≡ average phase functions for plume and back-

ground atmosphere, respectively. $\bar{p}$ is a function of λ and Θ,

$\tau_{plume} = \dfrac{\tau_{NO_2} + \tau_{part} + \tau_{SO_4}}{\sin \alpha}$ *, τ is a function of λ and α,

$\bar{\omega}_{plume} = 1 - \dfrac{\tau_{NO_2}}{\tau_{plume}}$, $\bar{\omega}$ is a function of λ,

$\bar{\omega}_{background} = 0.95$ (by assumption that 5 percent of total estimation is due to light absorption by aerosol and that there is no background NO_2),

$b_{ext} \equiv$ background extinction coefficient

$= b_R(\lambda) + b_{sp\text{-}submicron}(\lambda) + b_{sp\text{-}coarse}(\lambda) + b_{ap}(\lambda)$,

(b_{ext} is a function of λ),

$r_p \equiv$ plume-observer distance

$$= \begin{cases} \dfrac{0.199x}{\sin \alpha} & \text{for stable plume} \\ \dfrac{50 \text{ km}}{\sin \alpha} & \text{for 2-day-old plume during limited mixing conditions} \end{cases},$$

$r_o \equiv$ object-observer distance,

$C_0 \equiv$ intrinsic sky/terrain contrast of viewed object (-0.7 to -0.9 for most terrain),

$f_{obj} \equiv$ fraction of total plume optical thickness between observer and viewed object.

The analyst should calculate values of contrast for the following permutations:

---

* It should be noted again that, for the stable plume case, there is no sulfate ($SO_4^=$), and for the two-day old plume during limited mixing conditions, there is no NO_2.

- Meteorological conditions: the identified worst-case stable and limited mixing conditions and the seasonal-average limited mixing conditions.
- Class I areas: all potentially affected class I areas as identified by level-1 analysis.
- Line-of-sight azimuths: for all terrain features identified for each class I area observer at various r_0 and α and also at standard values of α.
- Wavelength: Certainly at $\lambda = 0.55$ μm. Calculations at $\lambda = 0.40$ and 0.70 μm are recommended, especially for plume contrast (C_{plume}) calculations.

If the absolute value of any plume contrast or contrast reduction value (at any wavelength) is greater than 0.10, one cannot rule out the possibility of adverse or significant visibility impairment. In such a case, one may choose (1) to modify source emissions or siting, or (2) to submit the results of the level-2 analysis or a more detailed (level-3) analysis to the appropriate government official for review and case-specific determination of the significance or adversity of the visual impact in the potentially affected class I area(s).

4.3 USE OF REFERENCE TABLES FOR NO_2 IMPACTS

As an adjunct to the hand calculations or as a replacement for some of the C_{plume} calculations, one may wish to use the reference tables in appendix C. These tables are appropriate only for emissions sources such as power plants, boilers, and other combustion sources that emit NO_x, from which the principal plume colorant is NO_2. One should not use these tables for a source with NO_x mass emissions rates less than 5 times the particulate emissions rate. These tables provide values of the following parameters that describe the contrast of a plume against the horizon sky:

- Blue-red ratio R:

$$R = \frac{1 + C_{plume}(\lambda = 0.4\ \mu m)}{1 + C_{plume}(\lambda = 0.7\ \mu m)}$$

> Plume contrast C_{plume} (λ = 0.55 μm)
> Plume perceptibility parameter $\Delta E(L^*a^*b^*)$.

To use these tables, calculate τ_{part} (for the worst-case stable plume condition only) on the basis of the procedures given earlier in this chapter, using the given particle mass emissions rate and size distribution, σ_z, u, and α. Compute the approximate visual range:

$$r_v = r_{v0} (1 - \tau_{part}/3.912) \quad . \qquad \text{(p-35)}$$

Calculate the line-of-sight integral of plume NO_2, in units of $\mu g/m^2$, from the following formula:

$$\int_{plume} [NO_2]\, dr = \frac{(7.49 \cdot 10^5)(x)[NO_2]}{\sin \alpha} \quad , \qquad \text{(p-36)}$$

where

x ≡ downwind distance in km,
$[NO_2]$ ≡ NO_2 concentration as calculated using procedures in the previous section,
α ≡ angle between the plume centerline and the line of sight.

The analyst should use the appropriate table in appendix C for the given (reduced) visual range, NO_2 line-of-sight integral, and plume-observer distance r_p and determine the visual impact parameters from this table. If the blue-red ratio is less than 0.90, if plume contrast is less than -0.10, or if $\Delta E(L^*a^*b^*)$ is greater than 4.0, the probability of adverse or significant plume discoloration cannot be ruled out.

4.4 USE OF REFERENCE FIGURES FOR POWER PLANTS

If the emissions source is a power plant, one of the figures in appendix D may apply to the case being evaluated. Note that the percentage visual range reduction is for a line of sight perpendicular to the plume centerline. The reduction in sky/terrain contrast at $\lambda = 0.55$ μm can be calculated from this percentage visual range reduction as follows:

$$\Delta C_r = -C_0 \exp\left(-3.912\, r_o/r_{vO}\right)\left[1 - \exp\left(-\frac{3.912}{100} f_{obj} \frac{\Delta V}{\sin \alpha}\right)\right], \quad \text{(p-37)}$$

where

f_{obj} = fraction of plume between observer and object,

ΔV = percentage reduction in visual range or line of sight perpendicular to plume centerline

$$= -\left(\frac{\Delta r_v}{r_{vO}}\right) \cdot 100\%,$$

C_0, r_o, r_{vO}, and α are as defined previously.

4.5 USE OF THE COMPUTER MODEL

Probably the easiest and most accurate method for determining levels of impact is to use the plume visibility computer model (PLUVUE) initialized to the given worst-case conditions and geometry identified using the procedures presented in sections 4.1 and 4.2. The reader should refer to the separate document entitled, "User's Manual for the Plume Visibility Model (PLUVUE)", EPA-450/4-80-032, before using this model.

4.6 EXAMPLE CALCULATIONS

The reader may refer to appendix E for two sets of example calculations using the level-1 and level-2 analysis procedures. These examples

are hypothetical power and cement plants.

4.7 SUMMARY OF LEVEL-1 AND LEVEL-2 PROCEDURES

Figures 27 and 28 (a through f) present a series of schematic, logic, flow diagrams that summarize the major steps of the level-1 and level-2 screening procedures. Once the reader has become familiar with the actual steps necessary to carry out analyses through level-2, these flowcharts can be used as a checklist.

Several conventions in the flowcharts should facilitate their use. The specific section numbers in the workbook describing the individual steps are identified within each flowchart. The reader may, therefore, use the flowcharts to identify the location of various equations and procedures presented in the text. A list of the variables for which numerical values have been determined in that step is presented at the end of each flowchart. This list can be used to locate the calculations leading to each variable. In general, aside from the oval start-and-stop blocks in the flowcharts, three different shapes of blocks are used. Rectangular blocks indicate a straightforward procedure or calculation; diamond-shaped blocks indicate decision points with regard to whether further analysis is needed; and computer-card-shaped blocks (with clipped corners) indicate a data collection or interpretation task.

The presentation of a hand calculation procedure (section 4.2) is not intended to imply that some level of automation is not appropriate. Those users with access to a computer or programmable calculator can benefit from setting up segmented programs for the steps presented in the flowcharts, since the complexity of the calculations contributes to the likelihood of undetected computational errors in results. These flowcharts can be used as the preliminary basis for developing the necessary computer language codes or calculator step sequences, and the accuracy of the results from such programs can be tested using the numerical values contained in the examples in the text and in appendix E.

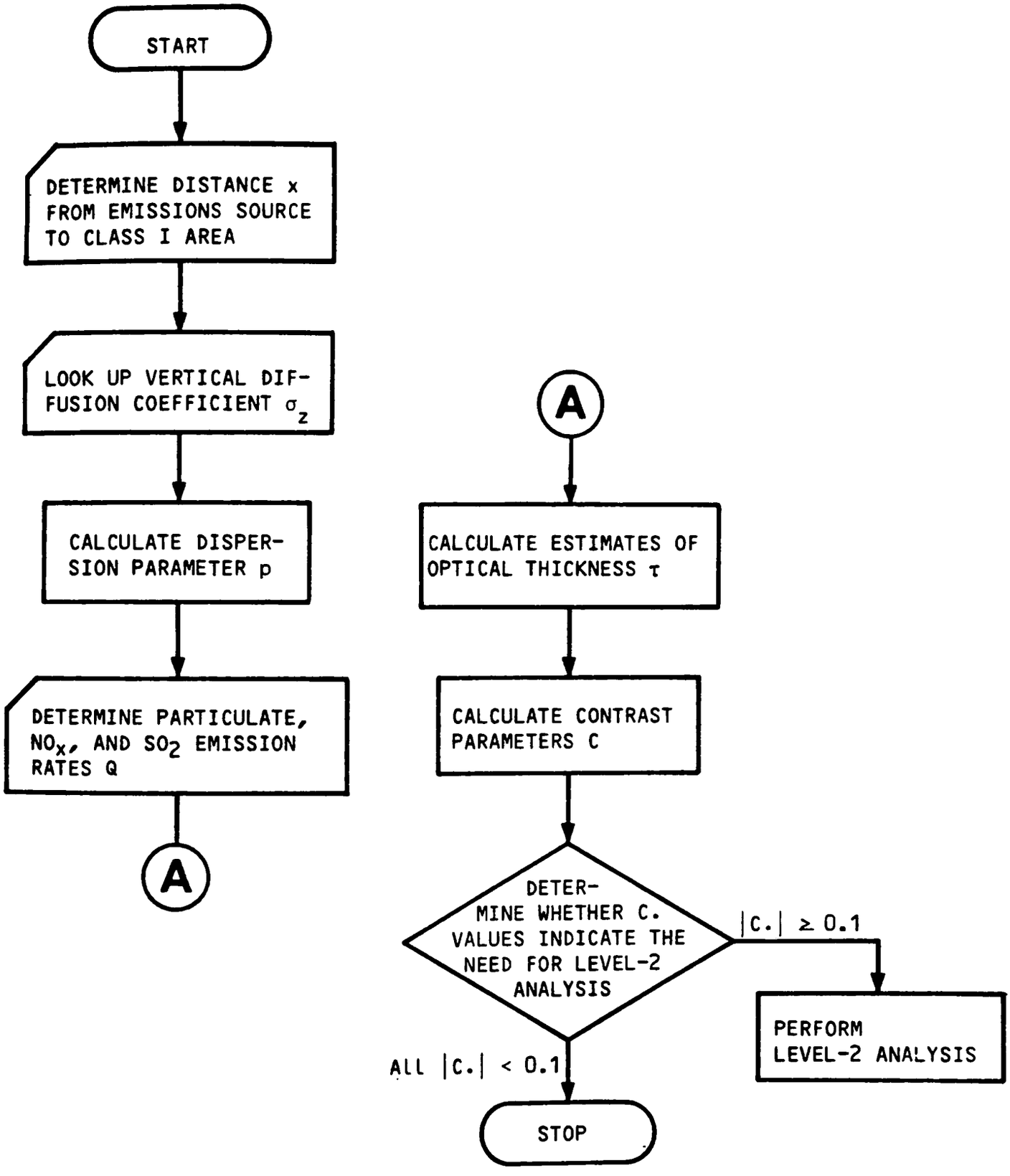

Figure 27. Logic flow diagram for level-1 analysis (see section 3.2)

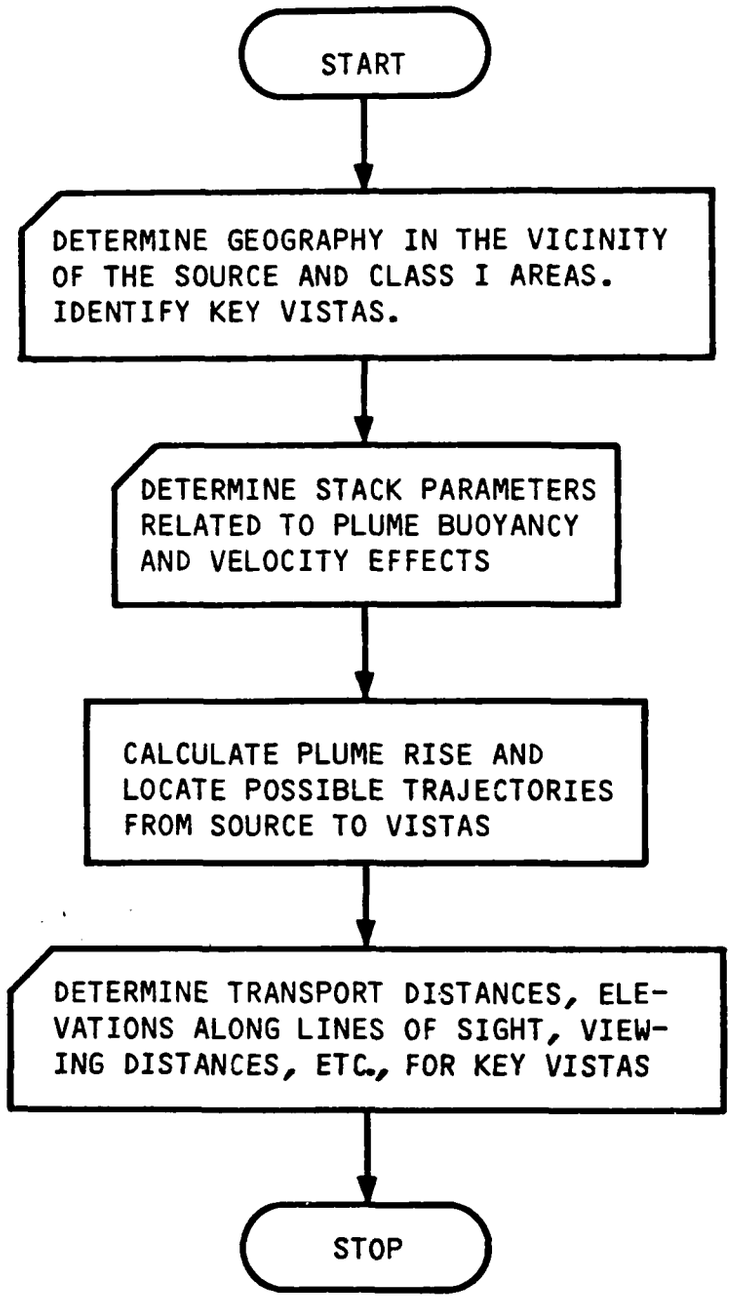

Variables known at the end of Step 1:
$Q.^{*}$, Z, Z_{block}, $x^{\dagger}$

---

* From Level 1.

† Different values can be determined for different trajectories and vistas.

(a) Step 1: Description of the area and possible trajectories

Figure 28. Logic flow diagram for level-2 analysis (see section 4.1.1)

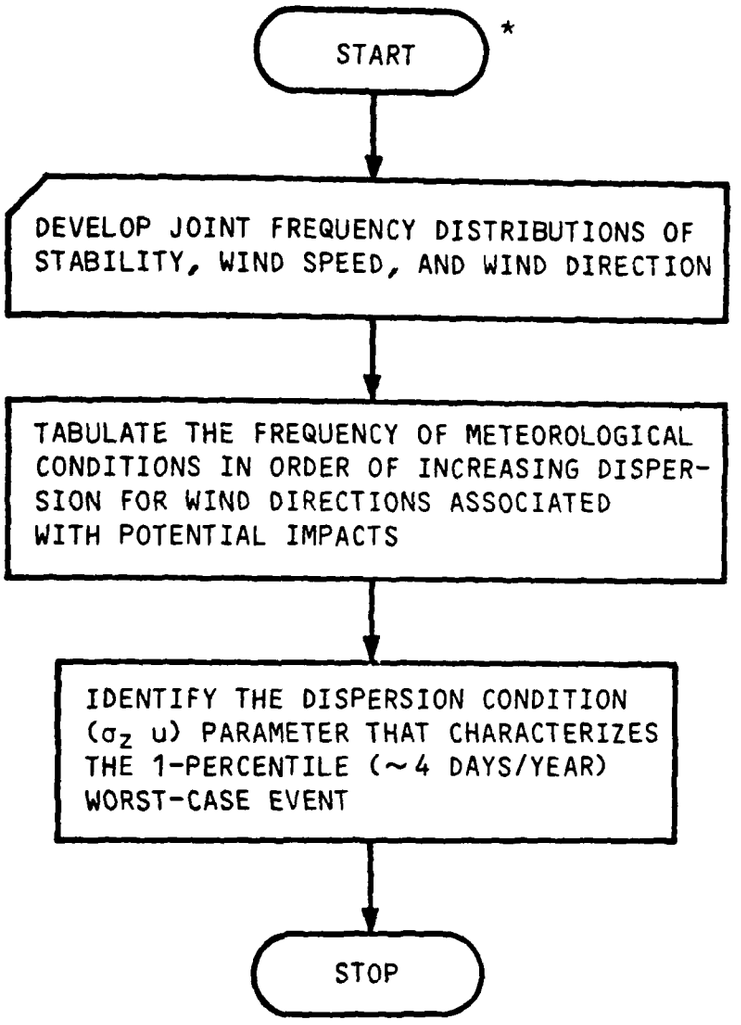

Variables known at the end of step 2: σ_z †, u†

---

* This step is not necessary if the level-1 analysis shows C_1 and C_2 between -0.1 and +0.1.

† Values can be determined for different trajectories and vistas.

(b) Step 2: Specification of worst-case stable transport meteorological conditions (section 4.1.2.1)

Figure 28 (Continued)

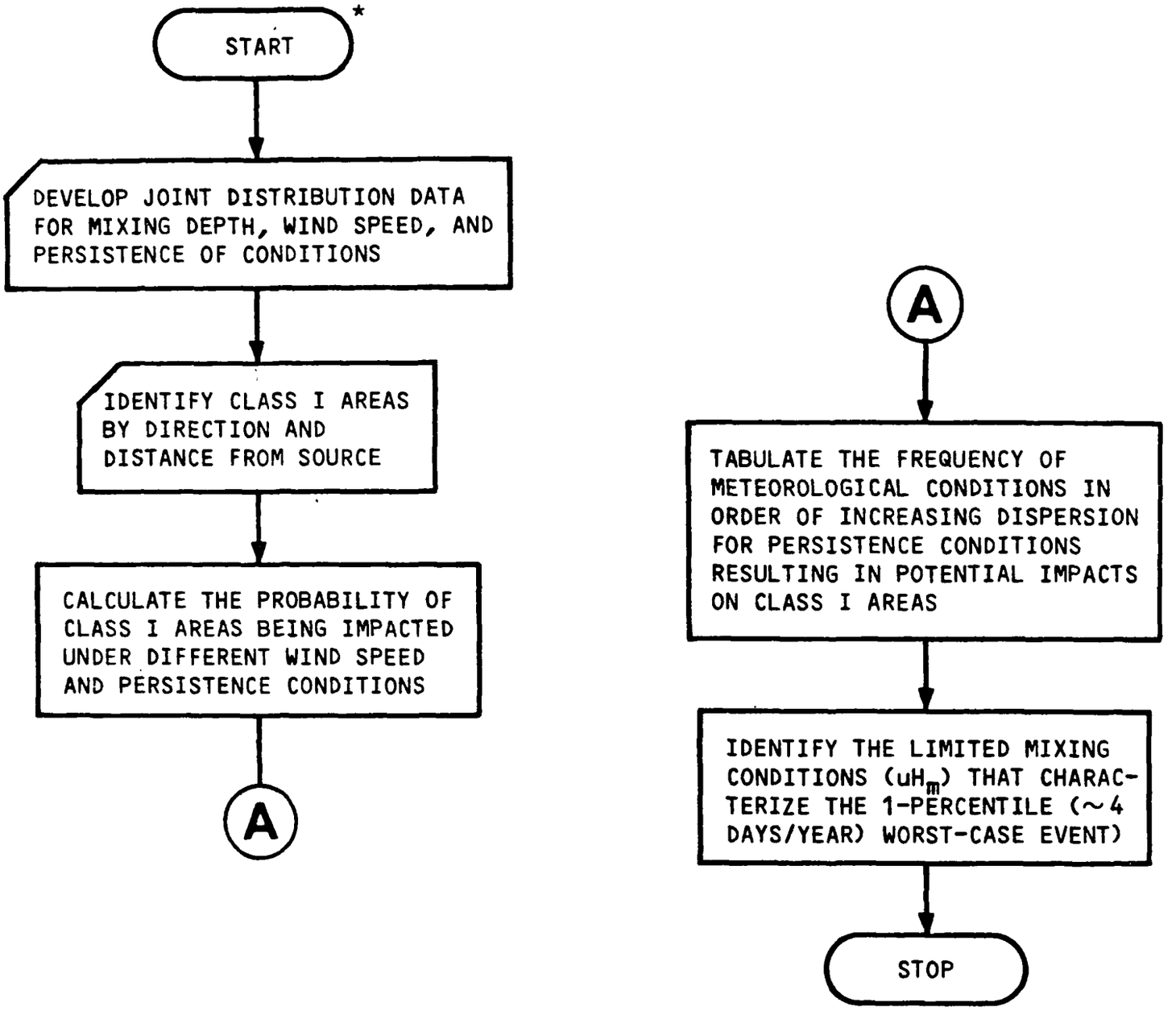

Values known at the end of step 3: $u^{\dagger}H_m{}^{\dagger}$

---

* This step is necessary only if the level-1 analysis shows C_3 to be greater than 0.1.

† Although a single dispersion parameter u•Hm should be determined, multiple pairs of values can be determined at this step. For example, (2 m/s, 1000 m, and 4 m/s, 500 m) give the same value for u•Hm of 2000 m^2/s.

§ Because of the dramatic variability in the type and level of detail of available meteorological data, this flowchart indicates only the general intent of steps necessary to specify the limiting diffusion parameter u•Hm.

(c) Step 3: Specification of worst-case meteorological conditions for general haze§ (see section 4.1.2.2)

Figure 28 (Continued)

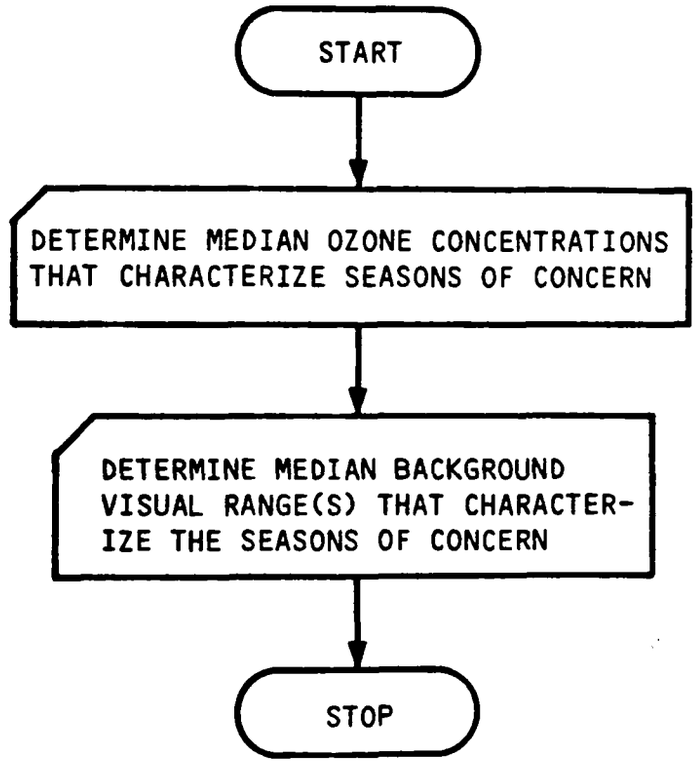

Values known at the end of step 4: $[O_3]$, r_{vO}

(d) Step 4: Background atmosphere description (sections 4.1.3 and 4.1.4)

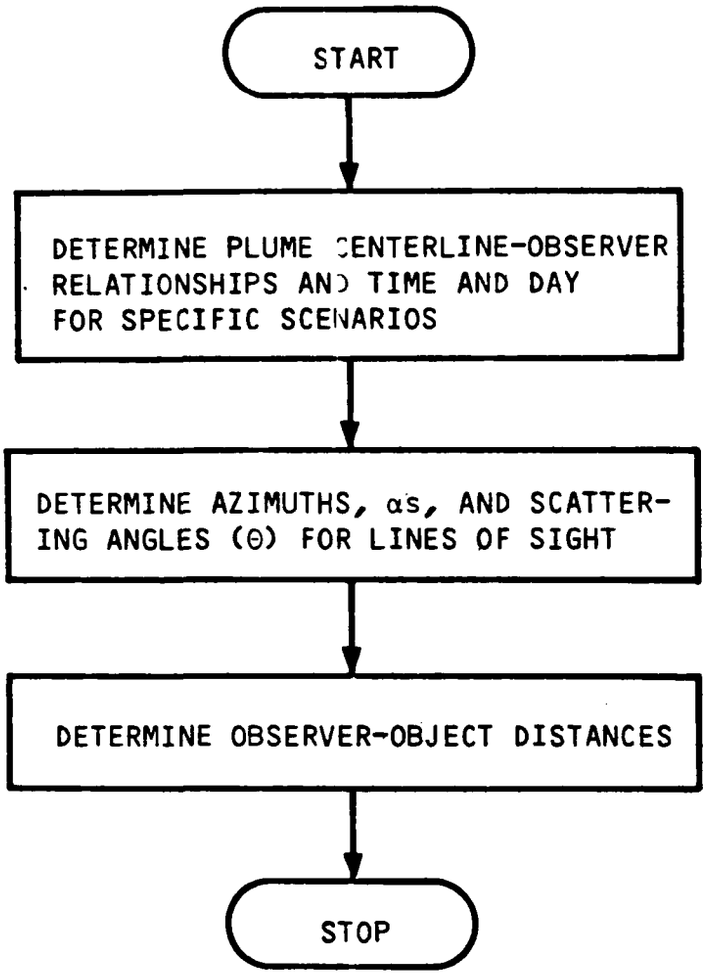

Values known at the end of step 5*:
α, Θ, r_o, r_p

---

* There will be a number of values for each of the lines of sight on data and times considered.

(e) Step 5: Determination of plume-observer geometries and specification of scenarios (section 4.2.1)

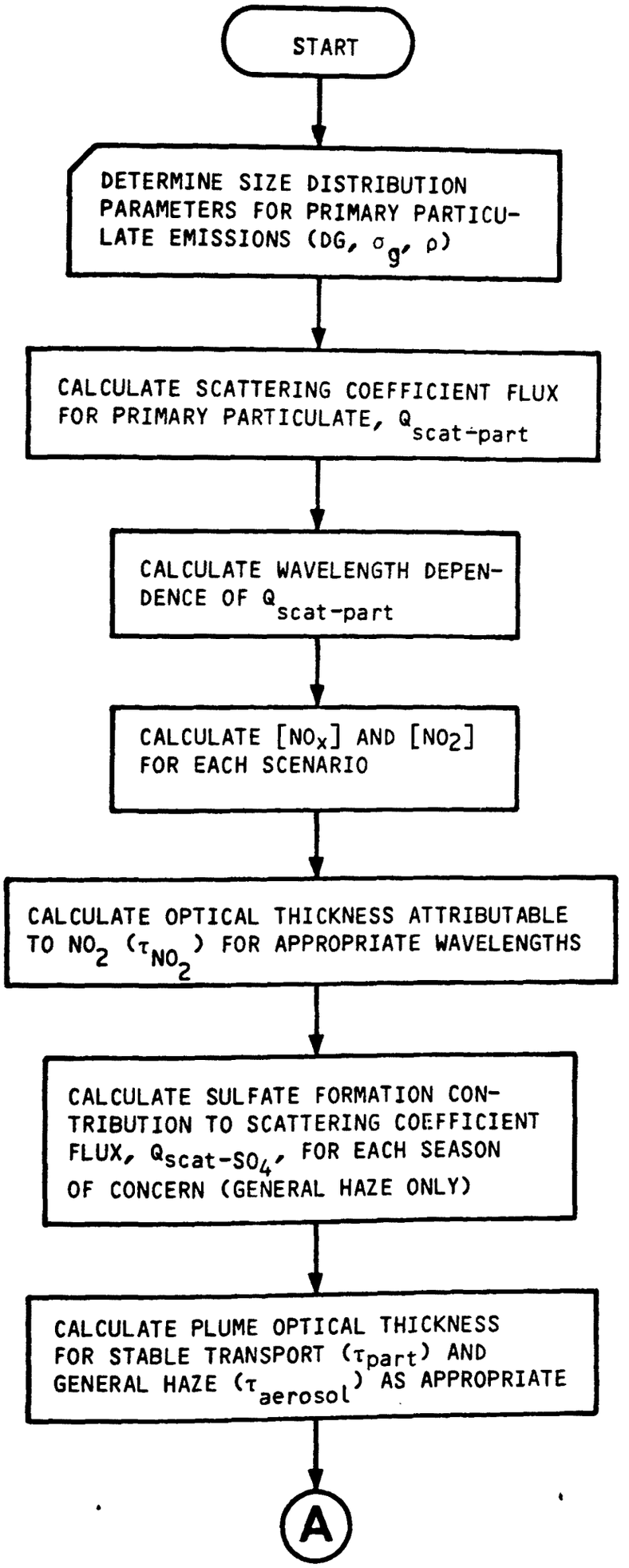

(f) Step 6: Calculation of worst-case impacts (Sections 4.2.2, 4.2.3, and 4.2.4)

Figure 28 (Continued)

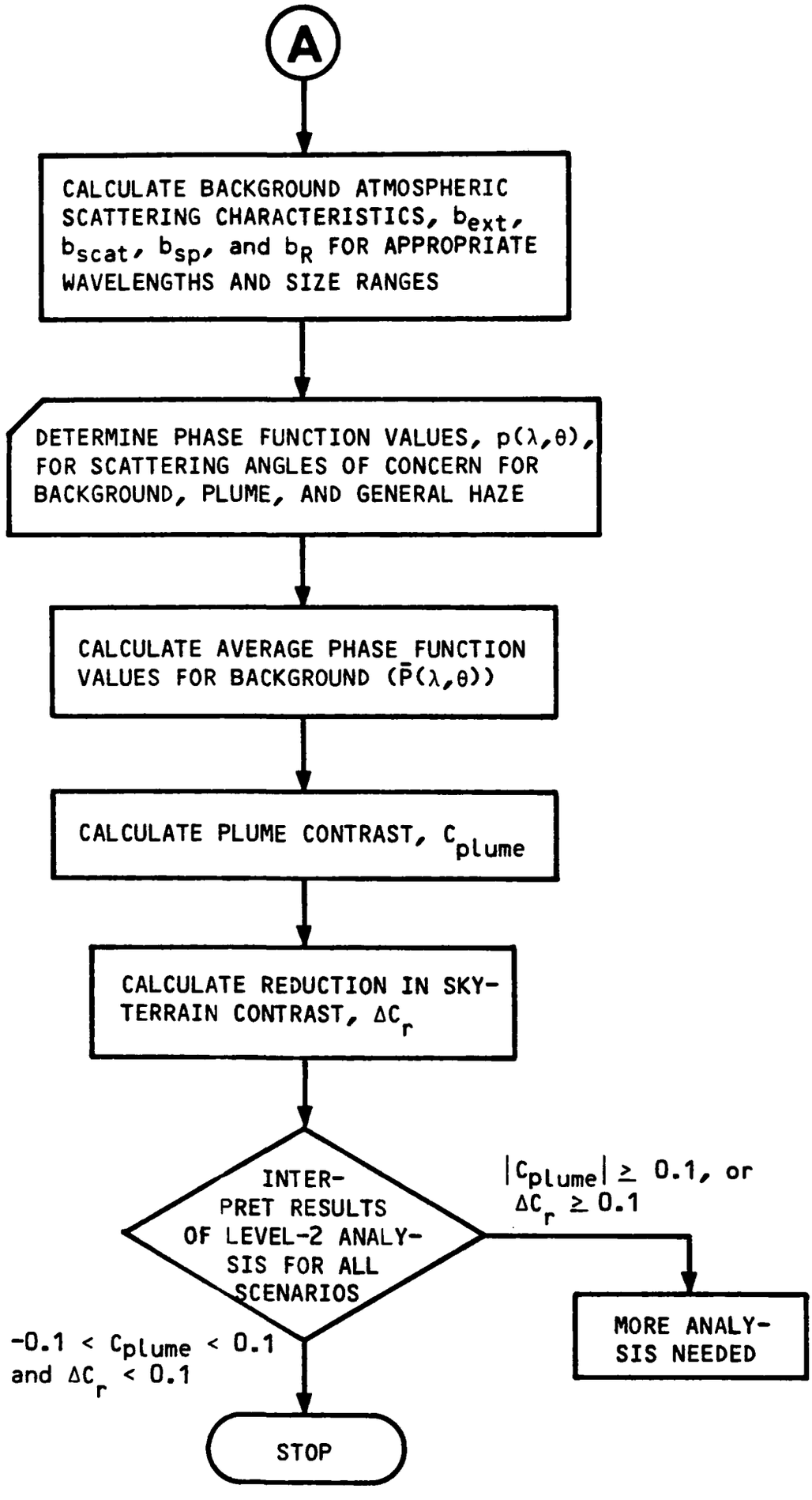

(f) (Concluded)

Figure 28 (Concluded)

5 SUGGESTIONS FOR DETAILED VISIBILITY IMPACT ANALYSES (LEVEL-3)

If the level-1 and -2 visibility screening analyses indicate the possibility of adverse or significant visibility impairment, one may wish to undertake a more detailed analysis (level-3). Even if a source passes the level-1 and -2 screening tests, it may be advisable to analyze potential impacts in greater detail.

More detailed visibility analyses may be needed in the following circumstances:

- When level-1 and -2 screening analyses indicate the possibility of adverse or significant visibility impairment.
- When the potential costs and delays incurred in emissions source siting, emissions control design, and regulatory approvals indicate that more detailed studies would be beneficial, regardless of the outcome of the level-1 and -2 screening tests.
- If greater accuracy and definition are necessary, for example, to define the frequency of occurrence and the time of year of worst-case impacts.
- If emissions are of a special nature, such as reactive hydrocarbons. In such cases one should use models that account for photochemistry (e.g., a reactive plume model with a complete photochemical mechanism).
- When the appearance of the visual impact is a concern (that is, when considering what the worst-case discolored plume or haze will look like).
- When the effect of visibility impairment on perceived scenic beauty in a class I area requires quantification, as when a cost-benefit study is performed.

- When area topography is complex, so that the assumptions made in the level-1 and -2 screening analyses are no longer appropriate, as when plumes are blocked, channeled, or trapped by terrain features.
- When an emissions source that is being analyzed, or is similar to the one being analyzed, is currently operating. Under these circumstances, it would be desirable, especially if level-1 and level-2 tests indicate a potentially adverse or significant impairment, to supplement screening analyses with detailed impact analyses and with intensive and long-term monitoring of meteorological and ambient conditions; plume transport, diffusion, and chemistry; and visual impacts in the potentially affected class I areas.
- When the concern is with the cumulative impacts of several emissions sources within a region.

It is not the purpose of this chapter to provide step-by-step instructions for carrying out these more detailed analyses. Each separate analysis will vary with the specific circumstances. Instead, we briefly outline some important elements in such detailed analyses that the analyst may wish to consider. Indeed, further visibility model development may be needed for some problems.

5.1 FREQUENCY OF OCCURRENCE OF IMPACT

As discussed in chapter 2, the frequency of occurrence of visibility impairment is as critical to the assessment of adversity or significance of impact as is the magnitude of visibility impairment. We can assess the frequency of impact occurrence by applying a computer model to all potential combinations of the following factors:

- Emission rates.
- Wind speed.
- Wind direction.
- Stability.
- Mixing depth.
- Plume dispersion, given a specific meteorological condition.
- Background ozone concentration.
- Background visual range.
- Precipitation.

One might require 100 or more model runs to characterize adequately the magnitude and frequency of impact occurrence in some situations. Impact can then be summarized in figures or graphs, as shown in figures 29, 30, and 31 and tables 6 and 7. Note that these examples were stratified by season to illustrate the seasonal dependence of impact and the fact that for this example the maximum frequency of impact occurrence is predicted in the winter season when class I area visitor use may be minimal.

5.2 APPEARANCE OF IMPACTS

A further specification of the appearance of visual impacts may be necessary to supplement estimates of magnitude and frequency of occurrence. The adversity or significance of an impact is dependent on the size of the area affected by a plume, as well as by the magnitude of discoloration or contrast reduction. A plume viewed from a distant location has a smaller visual impact than it would if viewed from a nearby location, even if the magnitude of discoloration is the same in both instances, because in the former situation, the plume affects fewer lines of sight (i.e., appears smaller). A 200-m-thick plume will subtend an angle of 1.2° when the observer is 10 km away, 0.5° (which is the angle subtended by the moon) when the observer is 25 km away, and 0.1° when the observer is 100 km away from the plume centerline.

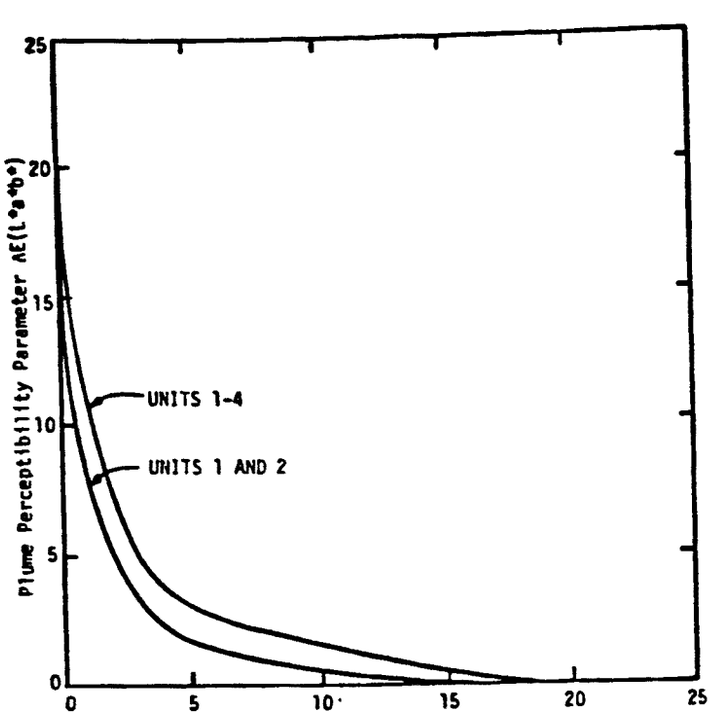

days

(a) Winter

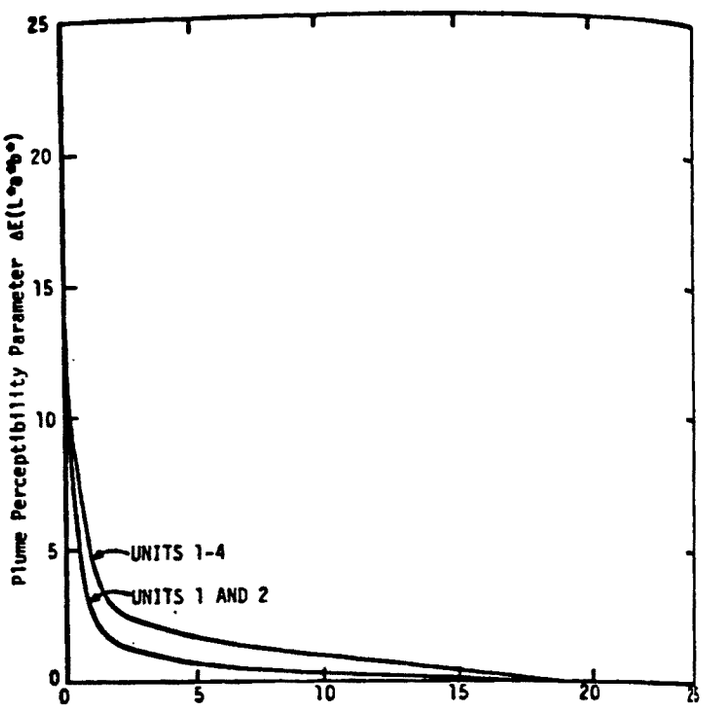

days

(b) Spring

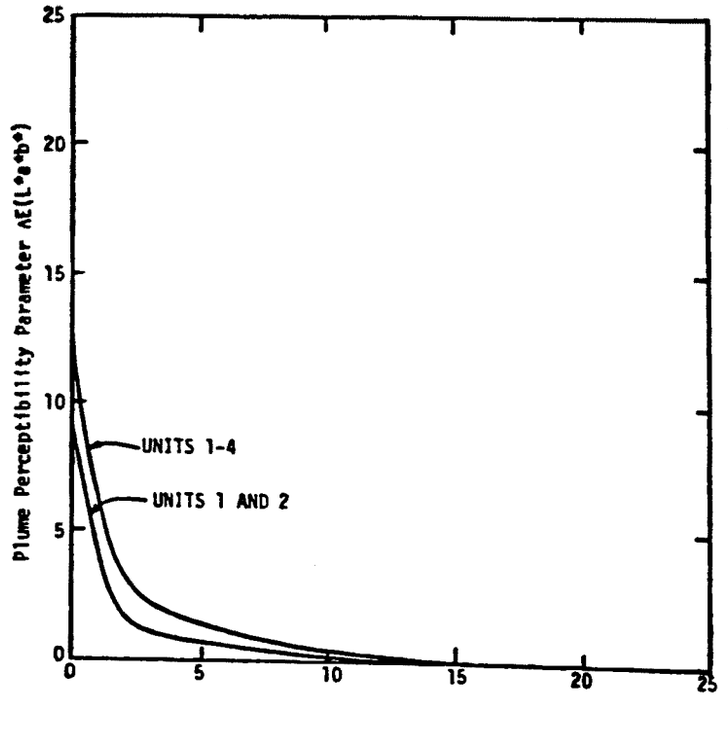

days

(c) Summer

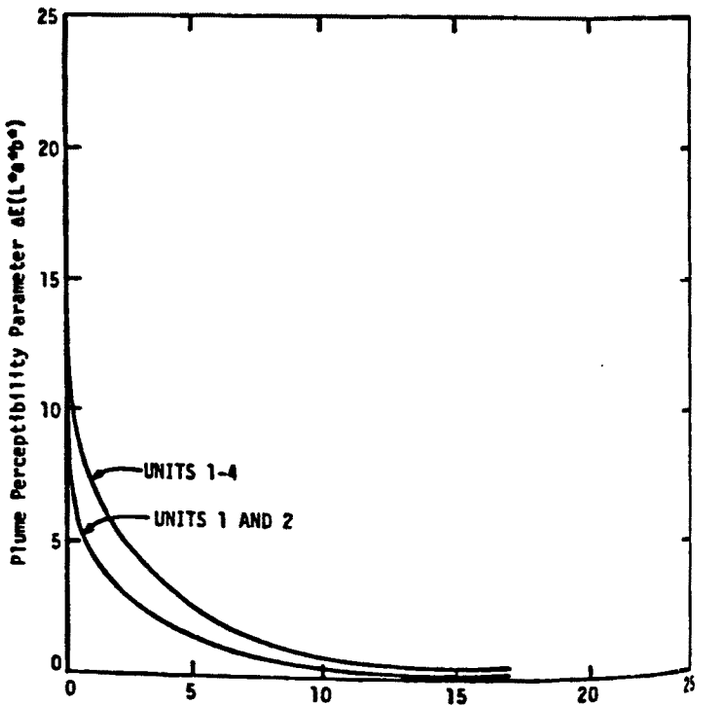

days

(d) Autumn

Figure 29. Examples of predicted frequency of occurrence of plume discoloration perceptible from a class I area: number of mornings in the designated season with an impact greater than the indicated value.

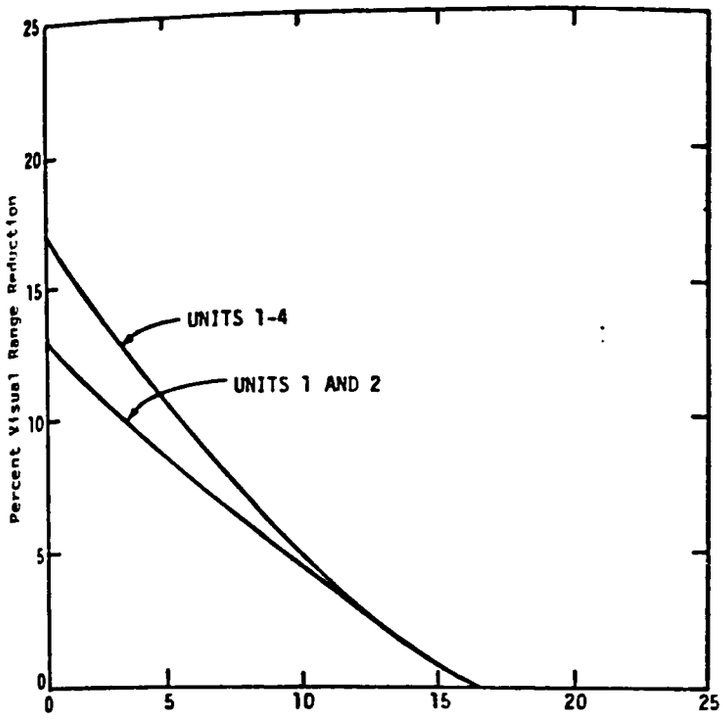

days

(a) Winter

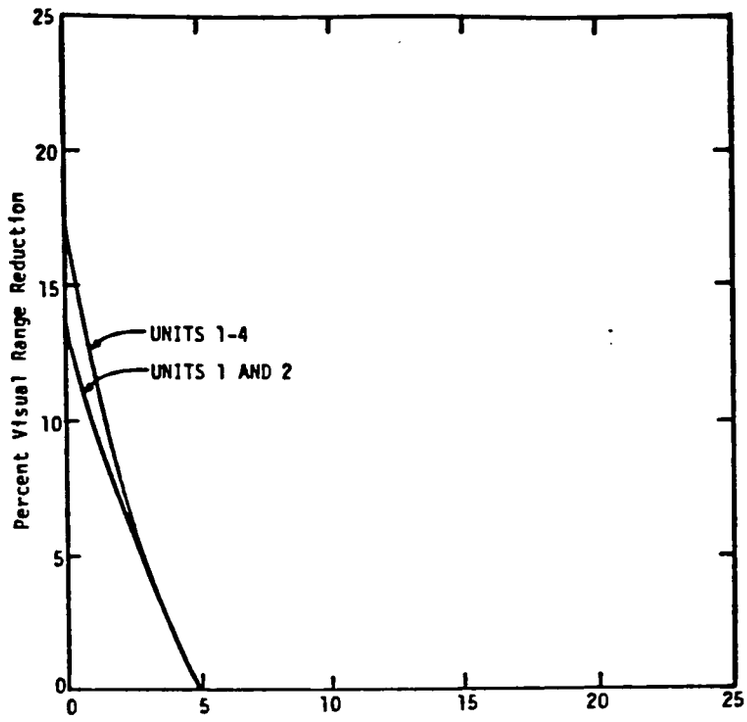

days

(b) Spring

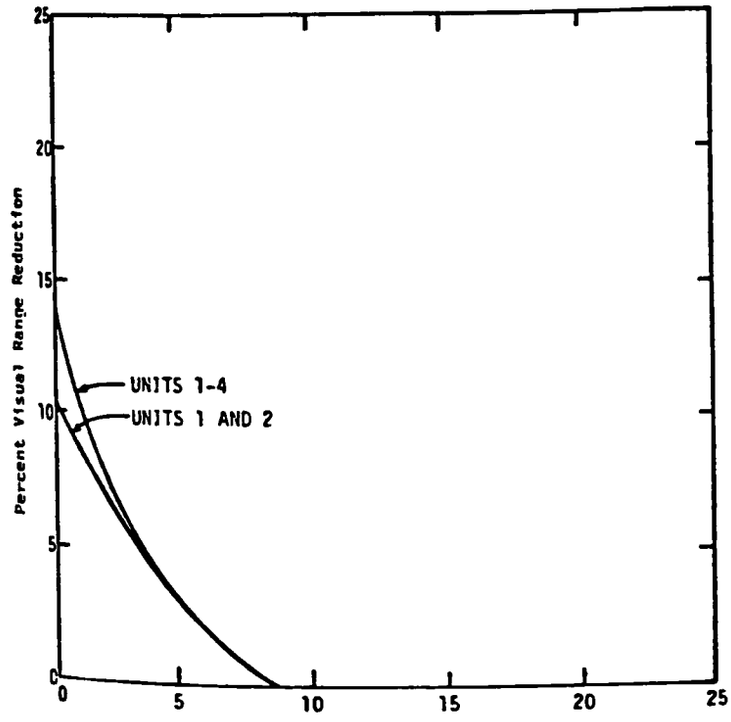

days

(c) Summer

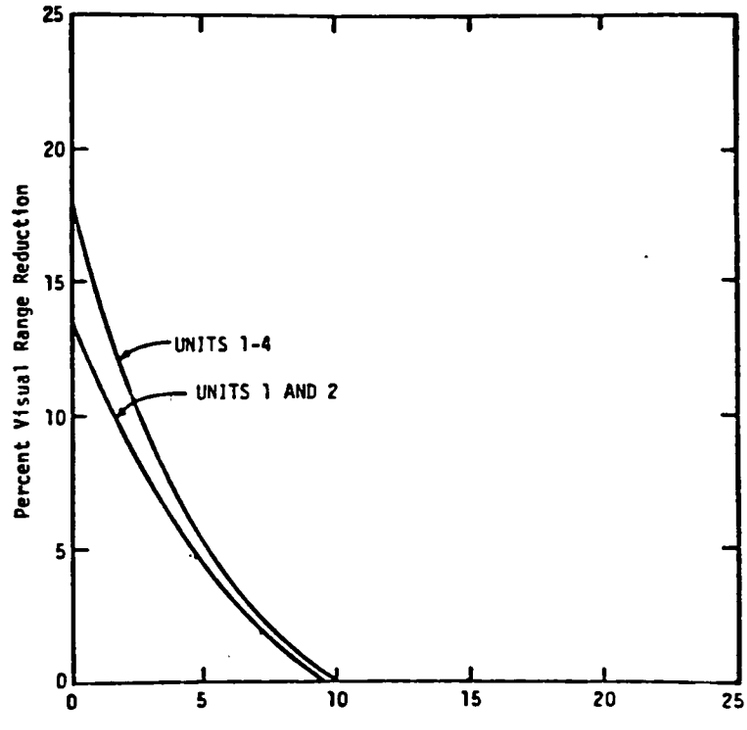

days

(d) Autumn

Figure 30. Examples of predicted frequency of occurrence of haze (visual range reduction) in a class I area: number of afternoons in the designated season with an impact greater than the indicated value.

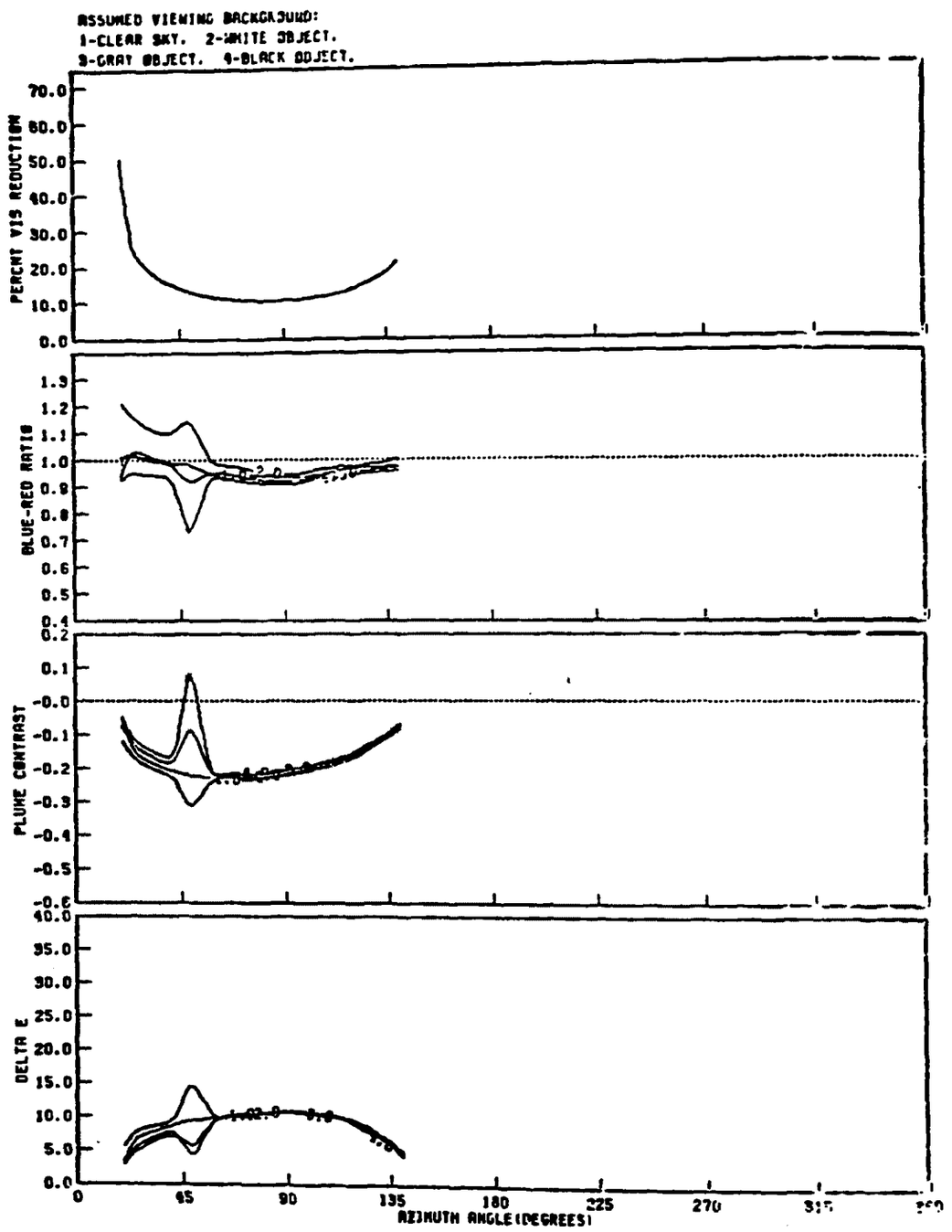

(a) 1 m/s wind speed, stable condition, 348.8 degree wind direction

Figure 31. Examples of calculated plume visibility impairment dependent on wind direction, azimuth of line of sight, and viewing background.

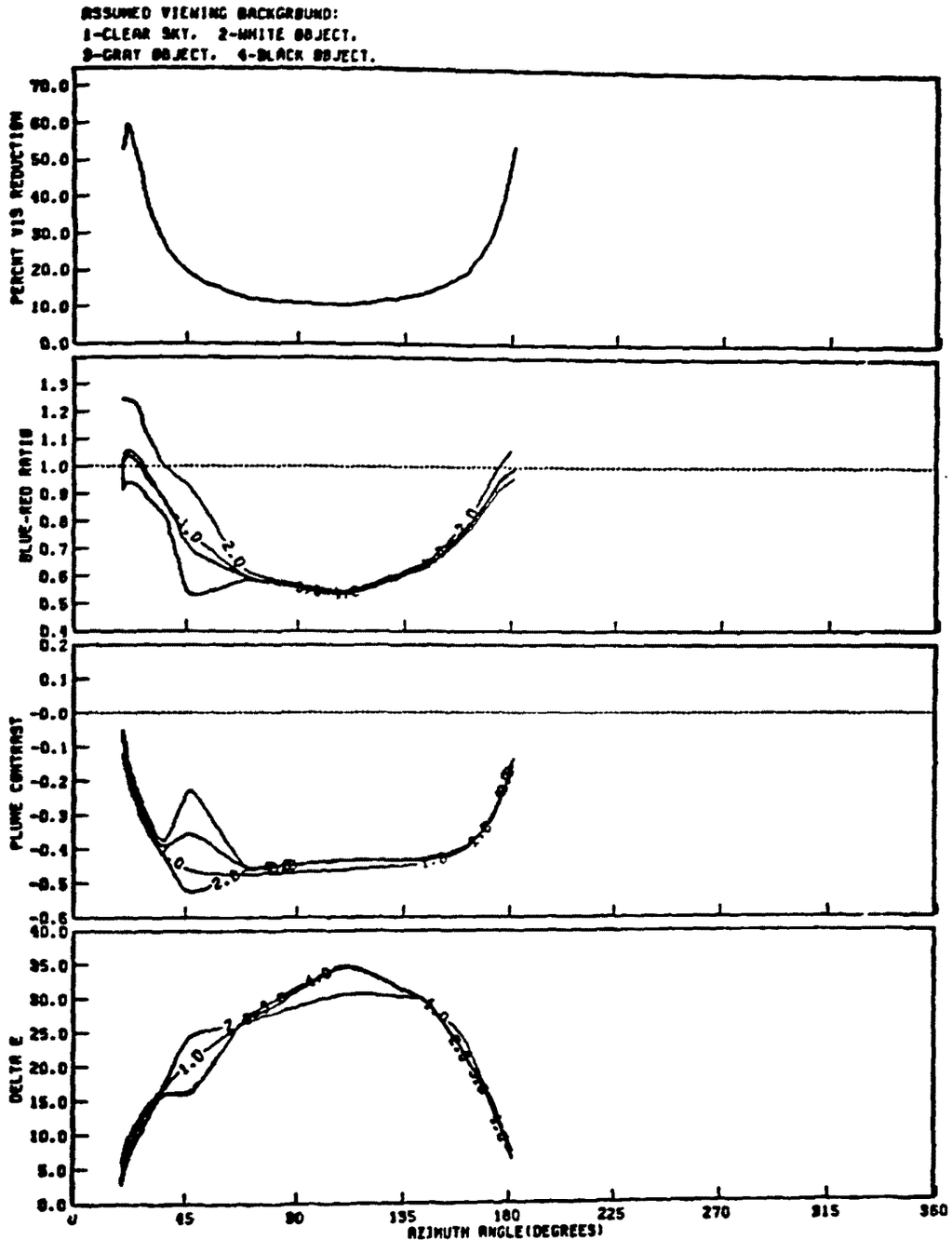

(b) 1 m/s wind speed, stable condition, 11.3 degree wind direction

Figure 31 (Continued)

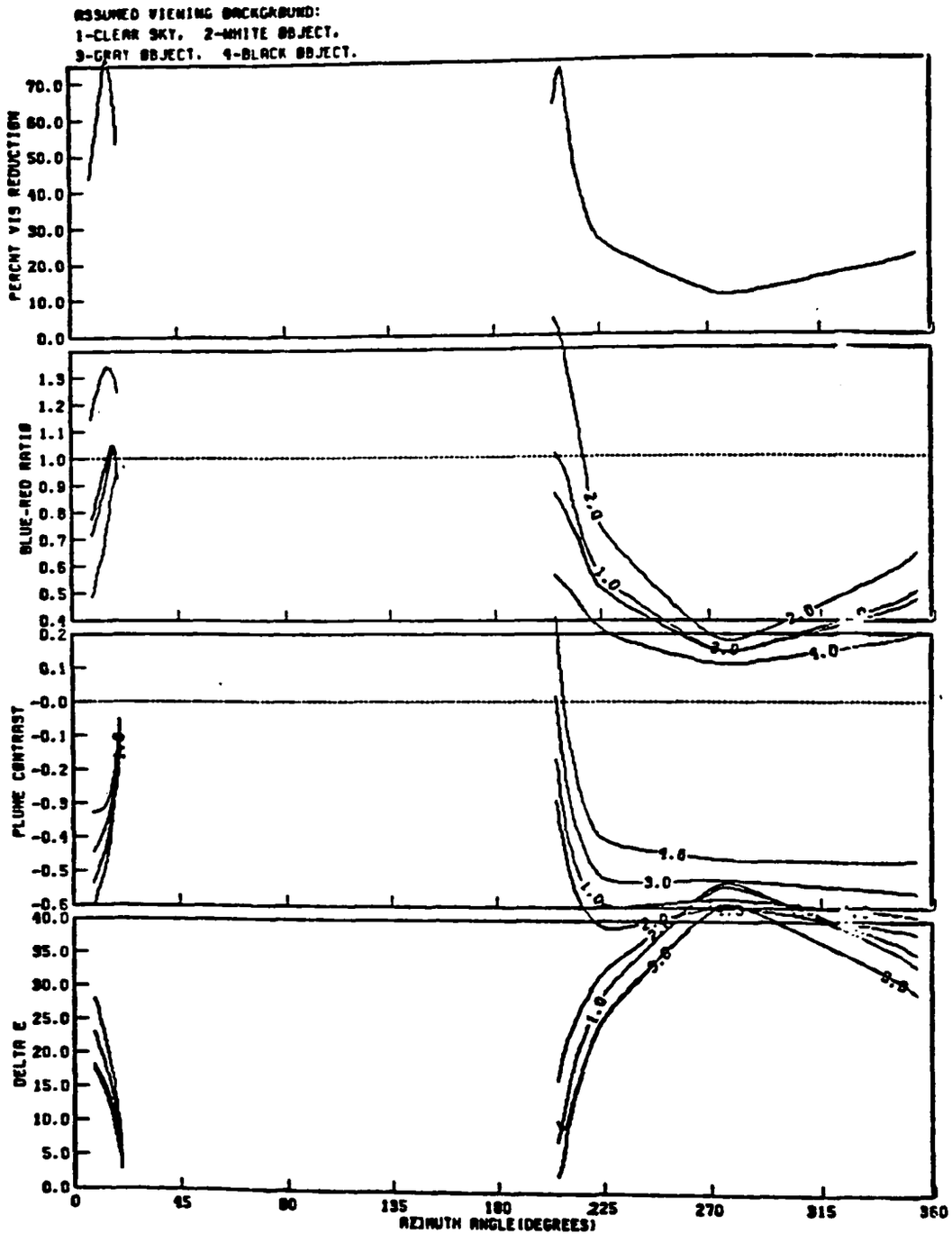

(c) 1 m/s wind speed, stable condition, 22.5 degree wind direction

Figure 31 (Concluded)

TABLE 6. EXAMPLE SUMMARY OF THE FREQUENCY OF OCCURRENCE OF POWER PLANT PLUME DISCOLORATION PERCEPTIBLE FROM A CLASS I AREA

	Number of Mornings with ΔE(L*a*b) Greater than Indicated Value					
	2.5		5		10	
Season	Units 1 and 2	Units 1 through 4	Units 1 and 2	Units 1 through 4	Units 1 and 2	Units 1 through 4
Winter	4	6	2	3	< 1	1
Spring	1	2	< 1	1	0	0
Summer	2	3	1	1	0	0
Fall	3	5	1	2	< 1	< 1
Annual total	10	16	4	7	1	< 2

TABLE 7. EXAMPLE SUMMARY OF FREQUENCY OF OCCURRENCE OF INCREASED HAZE (VISUAL RANGE REDUCTION) IN A CLASS I AREA DUE TO POWER PLANT EMISSIONS

	Number of Days with Visual Range Reduction Greater than Indicated Value					
	5%		10%		15%	
Season	Units 1 and 2	Units 1 through 4	Units 1 and 2	Units 1 through 4	Units 1 and 2	Units 1 through 4
Winter	9	10	3	5	0	1
Spring	3	3	1	2	0	< 1
Summer	4	4	0	1	0	0
Fall	5	5	2	3	0	1
Annual total	21	22	6	11	< 1	2

Also, the appearances of the plume will change depending on the wind direction and the viewing background distance and coloration. Thus, one has to know the viewing background and the vertical and horizontal (azimuthal) extent of the plume to characterize the visual impact completely.

The appearance of plume discoloration and contrast reduction can be quantified using calculations of the magnitude of impact as a function of vertical and horizontal orientation of the line of sight, or by specifying the angle subtended by a plume. Alternatively, one can display impact using

- Black-and-white plume-terrain perspectives (see example in figure 32).
- Color graphic displays, such as those developed by the Los Alamos Scientific Laboratory (Williams, Treiman, and Wecksung, 1980).
- Color photographs of plumes or haze similar to the conditions being analyzed.

5.3 IMPACTS ON SCENIC BEAUTY

There is some recent evidence (Latimer, Daniel, and Hogo, 1980) that the scenic beauty of some areas may not be adversely affected by reductions in visual range, though the scenic beauty of other areas may be very sensitive to visual range. There have been no studies to determine the scenic beauty sensitivities of class I areas to plume visibility impairment (i.e., discoloration and contrast reduction).

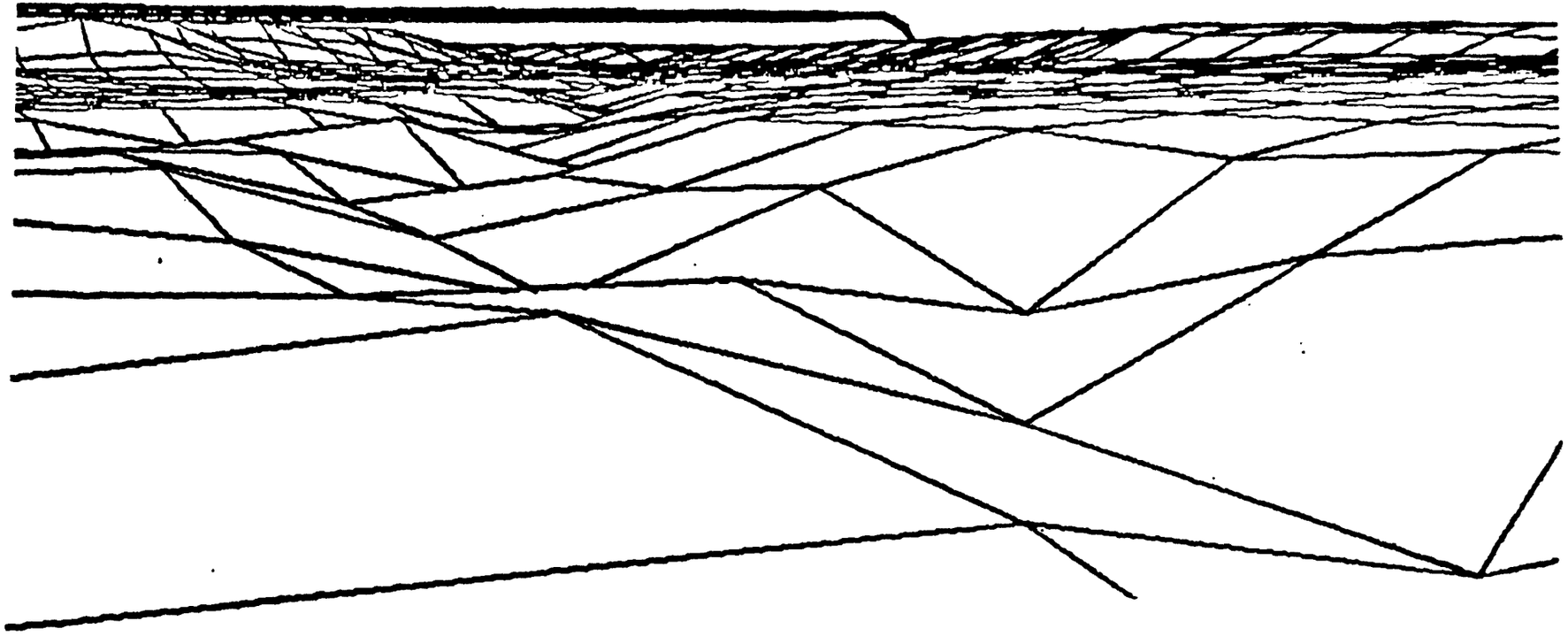

Figure 32. Example of black and white plume-terrain perspective.

In certain detailed visibility impact assessments, it may be desirable to quantify the sensitivity of potentially affected areas. For example, days of visual impact of a given magnitude might be translated into days of a given decrease in class I area scenic beauty (as perceived by an observer). This would be an essential first step in establishing the aesthetic benefits of a given emissions control action.

5.4 IMPACTS OF EXISTING EMISSIONS SOURCES

Although the primary purpose of visibility computer modeling and the screening analysis techniques presented in this workbook is the prediction of future impacts of proposed new sources, these analytic tools can also be used to evaluate the impact of existing sources. However, because these techniques are not required to be routinely exercised in any regulatory program applicable to either new or existing sources, monitoring techniques, especially visual observations (either ground based or with aircraft), are likely to be the first step in identifying the origin of visibility impairment caused by a single source or small group of sources.

EPA has published the document "Interim Guidance for Visibility Monitoring," EPA-450/2-80-082, which contains technical considerations involving the design of visibility monitoring programs, selection of instrumentation, quality assurance and data processing. Instrumental monitoring methods for visibility are not yet routinely required in regulatory programs for visibility protection but the guidance does provide substantial information regarding available visibility monitoring methods presently in use. It is recommended that a minimum of one full

year of monitoring be conducted for visibility impact analyses of major point sources.

In addition to this long-term (one year or longer) measurement/analysis program, it may be desirable to design and implement several short-term, intensive measurement programs to compare measurements and model predictions of plume transport, diffusion, chemistry, aerosol formation, and the resulting optical effects.

5.5 REGIONAL IMPACTS

In many cases, the visibility impairment caused by a single emission source may be small compared to the cumulative impacts of many natural and man-made sources in a region. However, the visibility impairment of that single source may contribute to a significant regional haze.

It is beyond the scope of the first phase of visibility regulations and of this workbook to address such cumulative, regional impacts. Regional visibility models and measurement/analysis programs will be required to assess the extent of existing regional visibility impairment, to determine the relative contributions of various emissions sources to that impairment, and to design and implement effective emissions control

on a regional scale (if possible) to restore and protect class I area visibility.

APPENDIX A

CHARACTERIZING GENERAL HAZE

One of three parameters is customarily used to characterize general atmospheric haze:

- Visual range
- Extinction coefficient
- Sky/terrain contrast.

Each of these is an equally valid means of quantifying atmospheric haze. Since the eye/brain system perceives the environment through color and brightness contrasts in various objects such as landscape features, the sky/terrain contrast is the most fundamental of these three parameters in terms of visual perception. However, contrast may not be the most appropriate means of describing haze, because one can have a large number of contrast values for different landscape features if such features are at various distances from the observer and have different intrinsic contrasts. Thus, in many situations extinction coefficient and visual range are simpler and more useful measures of atmospheric haze than is contrast. The relationships among these physical measures of atmospheric haze are discussed in more detail in the following subsections.

A.1 WAVELENGTH DEPENDENCE

It is important to note that each of these three parameters depends on the wavelength of light (λ) to be considered. Since the light-scattering properties of the atmosphere are a function of wavelength, each of these three atmospheric haze parameters is likewise a function of wave-

length. For example, Rayleigh scattering by air molecules is proportional to λ^{-4}, and Mie scattering for a typical aerosol is proportional to λ^{-n}, where generally $0 < n < 2$. The spectral reflectance of a landscape feature will also be a function of wavelength if the landscape feature is not white, gray, or black.

Because of this wavelength dependence, we must be specific when we define visual range, extinction coefficient, or contrast. Many optical instruments and the human eye respond to a broad wavelength band; others are narrow-band instruments. Indeed, some of the discrepancies among various measurements of atmospheric haze (in which such techniques as nephelometry, telephotometry, photographic photometry, and human observation are used) are due to the different spectral sensitivities of each instrument.

Throughout this discussion we will assume that contrast, visual range, and extinction coefficient are defined in equivalent ways with respect to wavelength. For example, we can define these parameters for a narrow wavelength band at 0.55 μm, the center of the visible spectrum, or a broader band with some characteristic wavelength. This discussion does not depend on which wavelength band is considered, but the three parameters must be defined for similar spectral bands.

A.2 THE CONTRAST FORMULA

For a homogeneous atmosphere, contrast and extinction coefficient are mathematically related by the Lambert-Beer law for contrast, as follows:

$$C_r/C_o = e^{-b_{ext} r_o} \quad , \qquad \text{(A-1)}$$

where C_o is the intrinsic contrast of a landscape feature against the sky (as observed near the feature), C_r is the apparent contrast of the landscape feature observed from a distance r_o, and b_{ext} is the extinction coefficient of the atmosphere through which the terrain is observed.

Using Middleton's (1952) definition of visual range, we can also relate visual range to contrast and extinction coefficient. Visual range is defined as the distance r_v such that

$$C_r/C_o = 0.02 = e^{-b_{ext} r_v} \quad . \tag{A-2}$$

Note that by solving for r_v we have the well-known Koschmieder relationship,

$$r_v = - \frac{\ell n(0.02)}{b_{ext}} = \frac{3.912}{b_{ext}} \quad . \tag{A-3}$$

These relationships can be extended to nonhomogeneous atmospheres if we define an appropriate average extinction coefficient over the line of sight of interest.

A.3 QUANTIFYING INCREASES IN ATMOSPHERIC HAZE

When the impact of a proposed source or combination of sources on atmospheric haze is of concern, the relevant question is: what is the resulting change in atmospheric haze conditions compared with that which would occur otherwise? For example, one might be concerned with the increase in haze that results from certain emissions on a particular day, on the worst day in a year, or on an average day in a year. Alternatively, one's concern might be the shift in the seasonal or annual frequency distributions of haze conditions.

We can quantify increased atmospheric haze by one of four parameters:

- Increased extinction coefficient (Δb_{ext}) or fractional increase relative to a given background ($\Delta b_{ext}/b_{ext0}$).
- Decreased visual range ($-\Delta r_v$) or fractional decrease in visual range relative to a given background ($-\Delta r_v/r_{v0}$).
- Decreased sky/terrain contrast ($-\Delta C_r$) or fractional decrease in contrast relative to the contrast that would occur for a given background ($-\Delta C_r/C_{r0}$).

> Plume optical thickness (τ_{plume}), the integral of extra extinction (Δb_{ext}) along the line of sight through the plume.

The remainder of this discussion describes these four parameters and the relationships among them.

There are two general classifications of spatial distributions of increased extinction (see figure A-1):

> Nonuniform distributions over a portion of the line of sight (e.g., a plume).
> Uniform increase over the entire line of sight (e.g., regional haze or situations in which the plume width is large compared to the visual range or to the line of sight).

The impact of a plume is best described by the plume optical thickness (τ_{plume}), whereas the regional impact is better described by extra extinction (Δb_{ext}).

A.3.1 Plume Impacts

Plume optical thickness is defined as the integral of the extinction coefficient over the line of sight:

$$\tau_{plume} = \int_{plume} b_{ext} dr \quad . \qquad \text{(A-4)}$$

This optical depth can be converted to an average extinction coefficient over some line of sight at distance R:

$$\overline{\Delta b}_{ext} = \tau_{plume}/R \quad . \qquad \text{(A-5)}$$

The distance R may be the distance between the observer and a particular landscape feature (r_o) or the visual range distance (r_v), depending on the

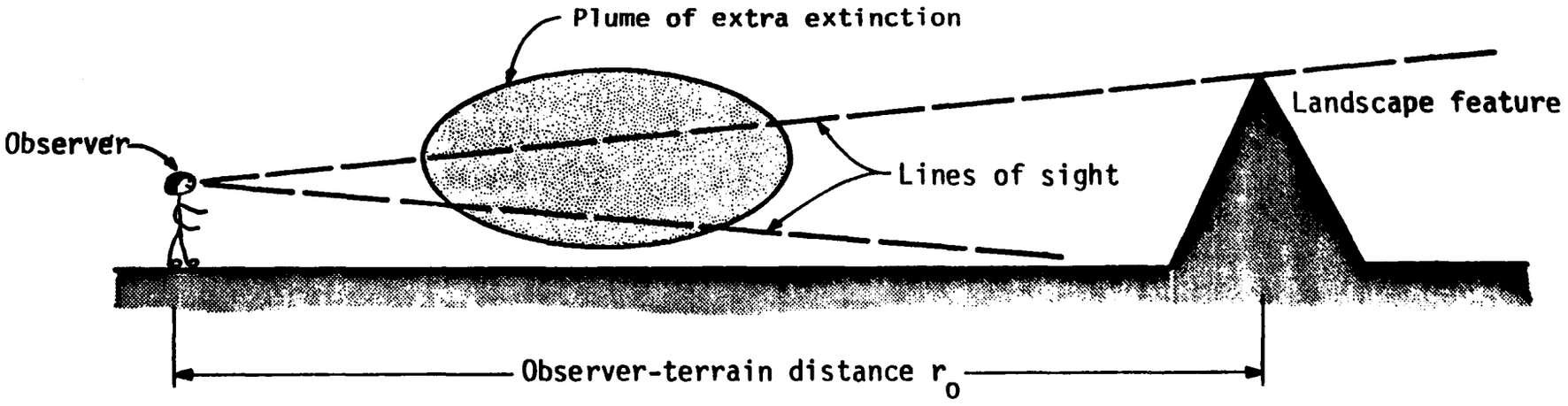

(a) Nonuniform distribution of extra extinction (plume impacts).

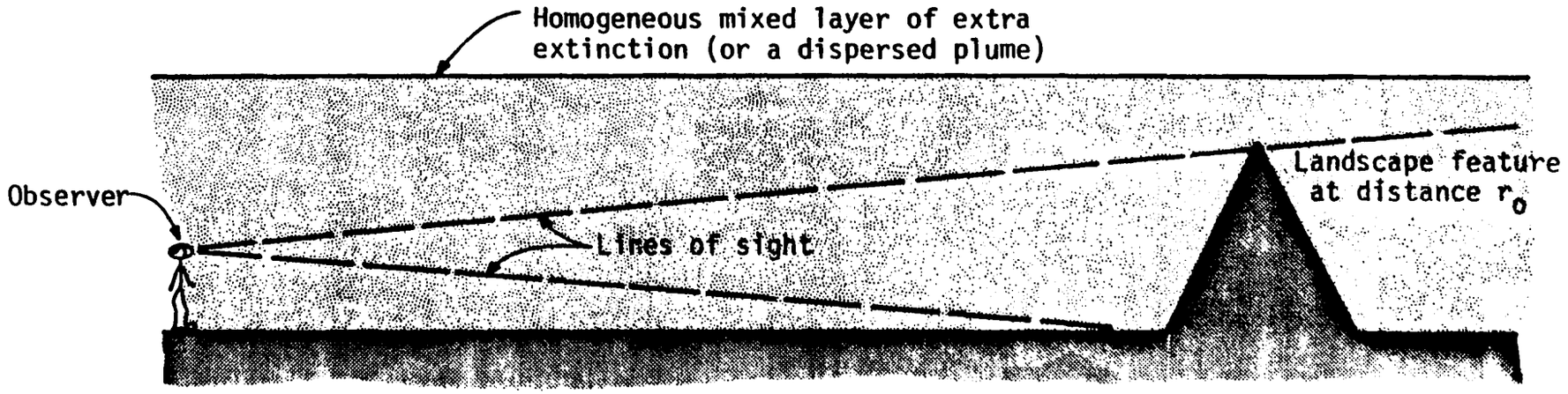

(b) Uniform distribution of extra extinction (regional haze or dispersed plumes)

Figure A-1. Two types of spatial distributions of extra extinction.

problem being addressed. For example, if one is concerned about the contrast loss in a landscape feature at a given distance from an observer, it is appropriate to use the distance to that feature as the value for R. However, if several landscape features at different distances are involved, or if one does not know the distance to a landscape feature, it is appropriate to use the visual range distance r_v as the value of R.

If we do the latter, we obtain a rather simple and elegant formula for the visual range reduction caused by a plume. The total average extinction coefficient of the background atmosphere and the plume together is

$$b_{ext} = b_{ext0} + \frac{\tau_{plume}}{r_v} \quad , \tag{A-6}$$

where b_{ext0} is the extinction coefficient of the background atmosphere with visual range r_{v0}, τ_{plume} is the plume optical thickness, and r_v is the reduced visual range as a result of plume impact.

The reduced visual range caused by plume material can be determined by substituting equation (A-6) into the Koschmieder relationship, equation (A-3), and solving for r_v. The result is

$$r_v = r_{v0} \, (1 - \tau_{plume}/3.912) \quad . \tag{A-7}$$

The fractional reduction in visual range is simply

$$\frac{r_{v0} - r_v}{r_{v0}} = \frac{\tau_{plume}}{3.912} \quad . \tag{A-8}$$

Note that equations (A-7) and (A-8) are not valid for cases in which the plume is opaque (e.g., one cannot see beyond the plume) or is significantly discolored. For such cases a more detailed visibility model or the formulas provided in the text should be employed.

Note that the fractional reduction in visual range for this plume situation is independent of the background visual range (r_{v0}).

A.3.2 Regional Haze Impacts

For the second case, in which there is a uniform increase in extinction coefficient (Δb_{ext}), the fractional decrease in visual range is not independent of the background visual range:

$$r_v = \frac{3.912}{b_{ext0} + \Delta b_{ext}} = \frac{3.912}{3.912/r_{v0} + \Delta b_{ext}} \quad , \tag{A-9}$$

$$r_v = (1/r_{v0} + \Delta b_{ext}/3.912)^{-1} \quad , \tag{A-10}$$

$$\frac{r_{v0} - r_v}{r_{v0}} = 1 - \left[1 + \frac{(r_{v0})\ (\Delta b_{ext})}{3.912}\right]^{-1}$$

$$= 1 - \left[1 + \frac{\Delta b_{ext}}{b_{ext0}}\right]^{-1} \quad . \tag{A-11}$$

A.4 THE EFFECT OF INCREASED HAZE ON THE CONTRAST OF LANDSCAPE FEATURES

The sensitivity to increased haze of the sky/terrain contrast of a landscape feature observed from a distance r_0 can be evaluated by differentiating equation (A-1):

$$\frac{\partial C_r}{\partial b_{ext}} = -rC_o e^{-b_{ext} r_o} \quad . \tag{A-12}$$

The observer-terrain distance r_0 at which the greatest change in contrast per unit change in extinction coefficient occurs can be determined by differentiating equation (A-12) again with respect to r, setting this derivative to zero, and solving for r. This distance is found to be

$$r_o = b_{ext}^{-1} = 0.26\ r_{v0} \quad . \tag{A-13}$$

On the other hand, the greatest fractional change in contrast per unit change in extinction coefficient occurs with the most distant visible landscape features. This can be shown by rearranging equation (12):

$$\frac{1}{C_r}\frac{\partial C_r}{\partial b_{ext}} = -r_o \quad . \tag{A-14}$$

Thus, depending on whether the human observer detects changes in haze conditions as a result of fractional or absolute changes in contrast, landscape features at distances of the full visual range or about one-fourth the visual range will be the most sensitive perceptual cues, respectively.

The change in contrast (ΔC_r) of a landscape feature resulting from a given change in extinction coefficient (Δb_{ext}) can be evaluated by integrating equation (A-12):

$$\Delta C_r = -C_0 e^{-b_{exto} r_o}\left[1 - e^{-\Delta b_{ext} r_o}\right]$$

$$= -C_r\left[1 - e^{-\Delta b_{ext} r_o}\right] \quad . \tag{A-15}$$

If the change in extinction coefficient (Δb_{ext}) is due to a plume between the observer and the landscape feature, then the change in contrast can be calculated as follows, assuming that the plume does not significantly discolor the horizon sky:

$$\Delta C_r = -C_r\left[1 - e^{-\tau_{plume}}\right] \quad . \tag{A-16}$$

With the following transformation of variables, we can relate the change in sky/terrain contrast to extinction coefficient, plume optical thickness, and visual range reduction in a more lucid manner:

$f_r \equiv$ ratio of observer-terrain distance r_o to background visual range

$$= r_o/r_{vo} \quad , \tag{A-17}$$

$f_b \equiv$ fractional increase in extinction coefficient

$$= \frac{\Delta b_{ext}}{b_{ext0}} \quad , \tag{A-18}$$

$f_v \equiv$ fractional decrease in visual range

$$= \frac{r_{v0} - r_v}{r_{v0}} \quad . \tag{A-19}$$

With these transformations we can write the equations for the relationships between contrast change and other visibility parameters as follows:

Extra extinction: $$\Delta C_r = -C_r \left[1 - \exp(-3.912\ f_r f_b)\right] \quad , \tag{A-20}$$

Visual range reduction: $$\Delta C_r = -C_r \left[1 - \exp\left(-3.912\ f_r \frac{f_v}{1 - f_v}\right)\right] \quad , \tag{A-21}$$

Plume optical thickness: $$\Delta C_r = -C_r \left[1 - \exp\left(-\tau_{plume}\right)\right] \quad . \tag{A-22}$$

The value of C_r is a function of the intrinsic contrast (C_0) of the landscape feature and the distance to the feature relative to the background visual range (f_r):

$$C_r = C_0 \exp\left(-3.912\ f_r\right) \quad . \tag{A-23}$$

The change in sky terrain contrast (ΔC_r) as a function of increased extinction, reduced visual range, and plume optical thickness is plotted in figures A-2, A-3, and A-4, respectively. Sky/terrain intrinsic contrast (C_0) was assumed to be -1.0, which is appropriate for a black object. The effect of observer-terrain distance on these relationships is shown by plotting curves for r/r_{v0} = 0.1, 0.26, 0.5, and 0.75. The maximum decrease in contrast for a given increase in extinction or decrease in visual range occurs for landscape features at 26 percent of the visual range, as we noted earlier, while the maximum contrast decrease due to a plume occurs for the closest landscape features.

A.5 SUMMARY

The relationships among the parameters used to characterize increased atmospheric haze are summarized in table A-1.

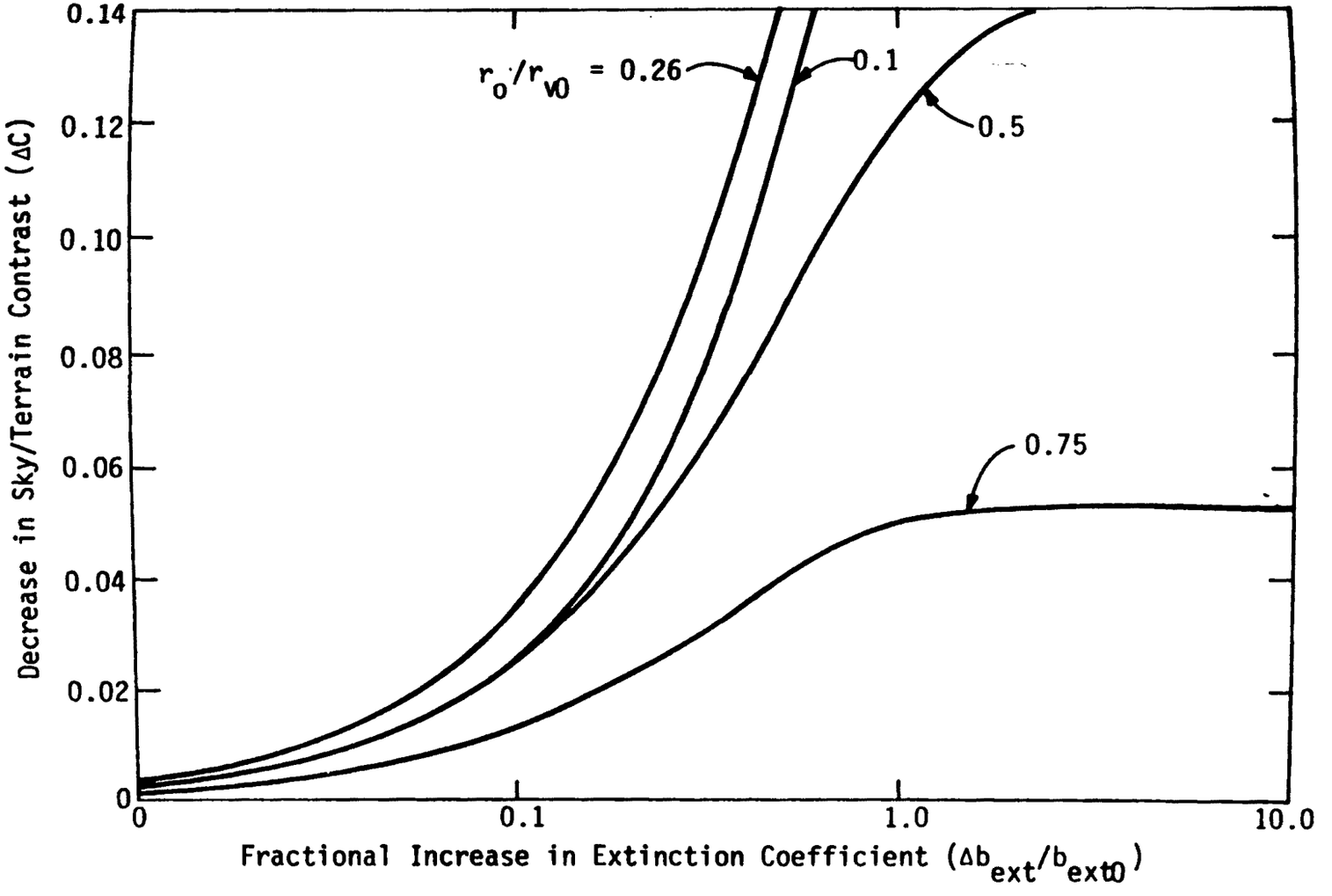

Figure A-2. Change in sky/terrain contrast as a function of fractional increase in extinction coefficient for various observer-terrain distances.

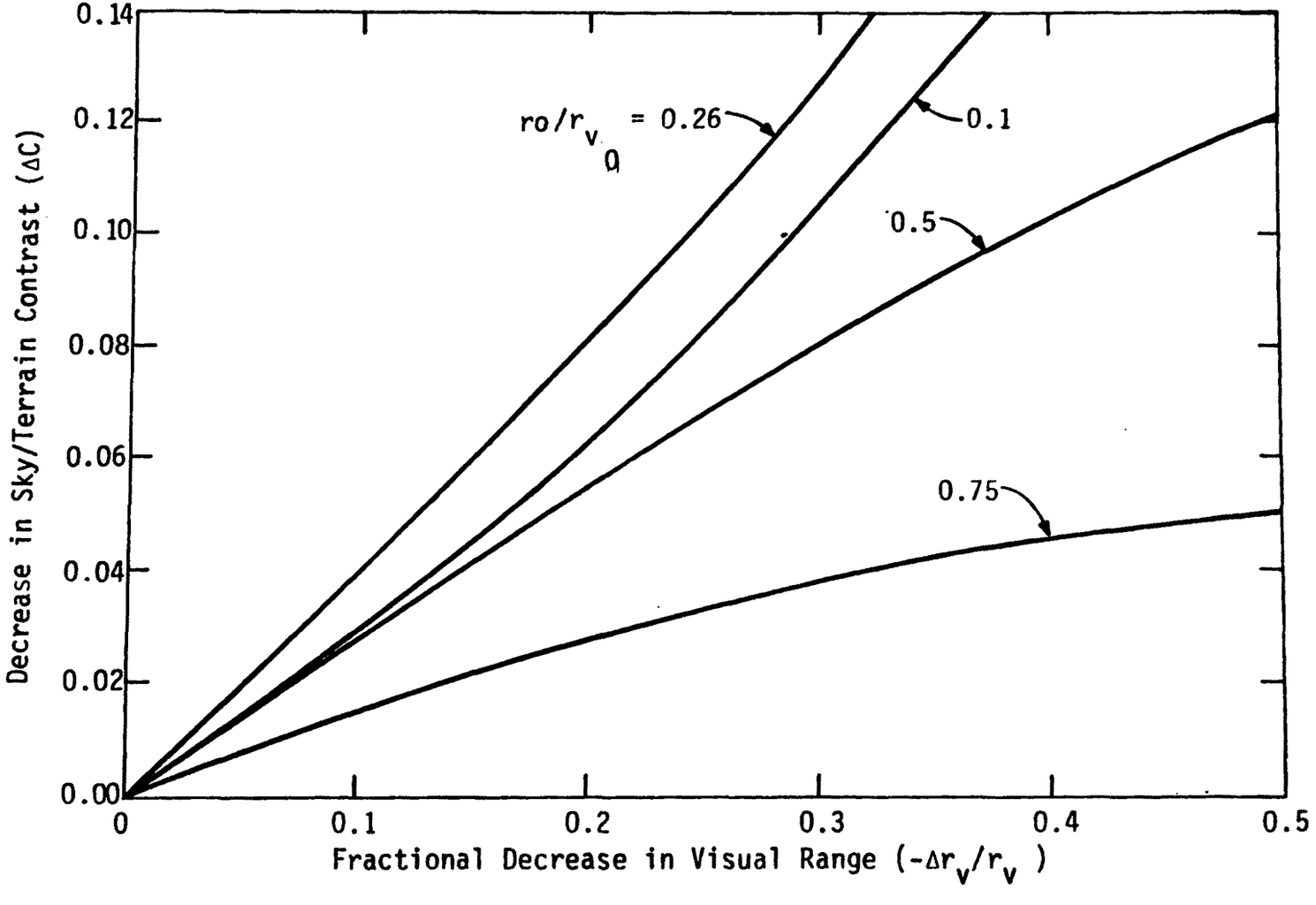

Figure A-3. Change in sky/terrain contrast as a function of fractional decrease in visual range for various observer-terrain distances.

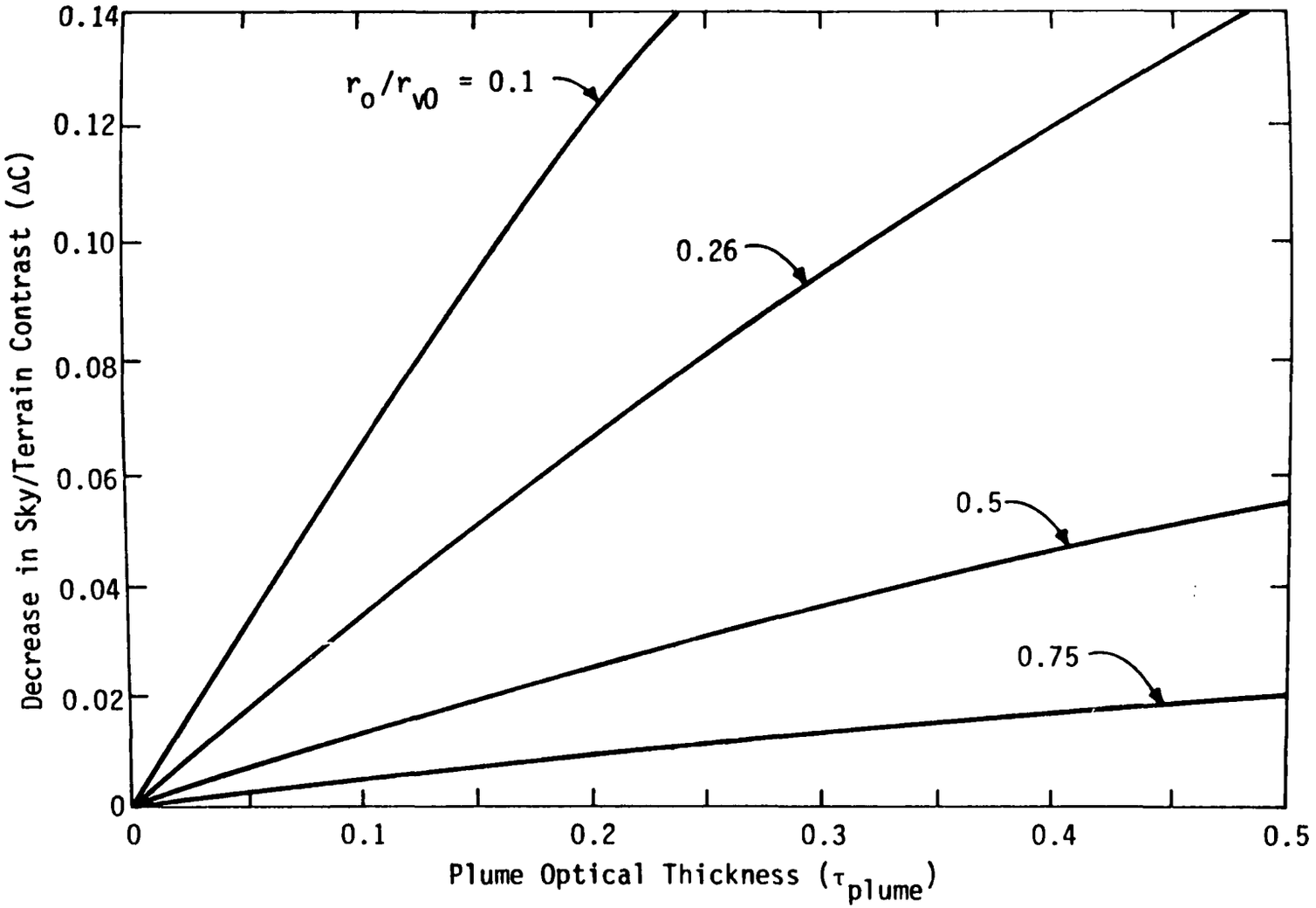

Figure A-4. Change in sky/terrain contrast as a function of plume optical thickness for various observer-terrain distances

TABLE A-1. SUMMARY OF RELATIONSHIPS AMONG PARAMETERS USED FOR QUANTIFYING INCREASED ATMOSPHERIC HAZE*

To:	To Convert From τ_{plume}	f_b	f_v	f_c
τ_{plume}	--	$f_b R b_{ext0}$	$3.912 f_v$	$-\ln(1 - f_c)$
f_b	$\frac{\tau_{plume}}{R b_{ext0}}$	--	$\frac{f_v}{1 - f_v}$	$-\frac{\ln(1 - f_c)}{3.912 f_r}$
f_v	$\frac{\tau_{plume}}{3.912}$	$\frac{f_b}{1 + f_b}$	--	$\frac{-\ln(1 - f_c)}{3.912 f_r - \ln(1 - f_c)}$
f_c	$1 - \exp(-\tau_{plume})$	$1 - \exp(-3.912 f_r f_b)$	$1 - \exp\left[-3.912 f_r \left(\frac{f_v}{1 - f_v}\right)\right]$	--

Nomenclature

$\tau_{plume} \equiv$ optical thickness of plume $= \int^{plume} b_{ext}\, dr$

$f_r \equiv$ ration of observer terrain distance r_o to background visual range r_{v0}

$f_b \equiv$ fractional increase in extinction coefficient $= \frac{\Delta b_{ext}}{b_{ext0}}$

$f_v \equiv$ fractional decrease in visual range $= -\Delta r_v / r_{v0}$

$f_c \equiv$ fractional decrease in sky/terrain contrast $= -\Delta C_r / C_{r0}$

$R \equiv$ line of sight averaging distance

$b_{ext0}, r_{v0}, C_{r0} \equiv$ extinction, visual range, and contrast used as reference baseline for increases in haze.

* These formulas are valid only for cases in which the plume material does not significantly discolor the horizon sky (see section 2 of the text).

APPENDIX B

PHASE FUNCTIONS

Data for the aerosol phase function [$p(\lambda,\theta)$] are provided in this appendix as a function of these factors:

- Aerosol size distribution with different mass median diameters (DG), all with a geometric standard deviation σ_g of 2.0.
- Wavelength λ = 0.40, 0.55, and 0.70 μm.
- Scattering angle θ ($0° < \theta < 180°$).

DG = 0.1 μm

λ = 0.4 μm

Θ	p(λ,Θ)
0.0	5.5738E+00
2.0	5.5565E+00
4.0	5.5052E+00
6.0	5.4219E+00
8.0	5.3094E+00
10.0	5.1714E+00
12.0	5.0121E+00
14.0	4.8357E+00
16.0	4.6462E+00
18.0	4.4474E+00
20.0	4.2428E+00
22.0	4.0355E+00
24.0	3.8278E+00
26.0	3.6221E+00
28.0	3.4199E+00
30.0	3.2227E+00
32.0	3.0316E+00
34.0	2.8472E+00
36.0	2.6702E+00
38.0	2.5011E+00
40.0	2.3401E+00
42.0	2.1873E+00
44.0	2.0429E+00
46.0	1.9068E+00
48.0	1.7788E+00
50.0	1.6589E+00
52.0	1.5467E+00
54.0	1.4419E+00
56.0	1.3442E+00
58.0	1.2533E+00
60.0	1.1687E+00
62.0	1.0902E+00
64.0	1.0175E+00
66.0	9.5022E-01
68.0	8.8806E-01
70.0	8.3073E-01
72.0	7.7791E-01
74.0	7.2930E-01
76.0	6.8463E-01
78.0	6.4363E-01
80.0	6.0607E-01
82.0	5.7172E-01
84.0	5.4039E-01
86.0	5.1189E-01
88.0	4.8603E-01
90.0	4.6264E-01
92.0	4.4155E-01
94.0	4.2261E-01
96.0	4.0568E-01
98.0	3.9061E-01
100.0	3.7729E-01
102.0	3.6558E-01
104.0	3.5536E-01
106.0	3.4653E-01
108.0	3.3899E-01
110.0	3.3264E-01
112.0	3.2741E-01
114.0	3.2319E-01
116.0	3.1992E-01
118.0	3.1752E-01
120.0	3.1589E-01
122.0	3.1499E-01
124.0	3.1473E-01
126.0	3.1508E-01
128.0	3.1598E-01
130.0	3.1738E-01
132.0	3.1925E-01
134.0	3.2154E-01
136.0	3.2420E-01
138.0	3.2719E-01
140.0	3.3043E-01
142.0	3.3390E-01
144.0	3.3753E-01
146.0	3.4130E-01
148.0	3.4516E-01
150.0	3.4909E-01
152.0	3.5307E-01
154.0	3.5709E-01
156.0	3.6113E-01
158.0	3.6518E-01
160.0	3.6922E-01
162.0	3.7323E-01
164.0	3.7719E-01
166.0	3.8110E-01
168.0	3.8490E-01
170.0	3.8854E-01
172.0	3.9189E-01
174.0	3.9481E-01
176.0	3.9710E-01
178.0	3.9856E-01
180.0	3.9906E-01

DG = 0.1 μm

λ = 0.55 μm

Θ	P(λ,Θ)
0.0	4.4905E+00
2.0	4.4799E+00
4.0	4.4483E+00
6.0	4.3967E+00
8.0	4.3263E+00
10.0	4.2389E+00
12.0	4.1367E+00
14.0	4.0217E+00
16.0	3.8963E+00
18.0	3.7627E+00
20.0	3.6228E+00
22.0	3.4787E+00
24.0	3.3319E+00
26.0	3.1840E+00
28.0	3.0363E+00
30.0	2.8898E+00
32.0	2.7455E+00
34.0	2.6042E+00
36.0	2.4666E+00
38.0	2.3331E+00
40.0	2.2043E+00
42.0	2.0804E+00
44.0	1.9617E+00
46.0	1.8482E+00
48.0	1.7401E+00
50.0	1.6373E+00
52.0	1.5398E+00
54.0	1.4476E+00
56.0	1.3606E+00
58.0	1.2786E+00
60.0	1.2016E+00
62.0	1.1294E+00
64.0	1.0619E+00
66.0	9.9882E-01
68.0	9.4009E-01
70.0	8.8549E-01
72.0	8.3485E-01
74.0	7.8799E-01
76.0	7.4473E-01
78.0	7.0490E-01
80.0	6.6833E-01
82.0	6.3485E-01
84.0	6.0429E-01
86.0	5.7650E-01
88.0	5.5130E-01
90.0	5.2857E-01
92.0	5.0814E-01
94.0	4.8986E-01
96.0	4.7367E-01
98.0	4.5938E-01
100.0	4.4689E-01
102.0	4.3609E-01
104.0	4.2685E-01
106.0	4.1908E-01
108.0	4.1267E-01
110.0	4.0754E-01
112.0	4.0357E-01
114.0	4.0070E-01
116.0	3.9884E-01
118.0	3.9791E-01
120.0	3.9784E-01
122.0	3.9854E-01
124.0	3.9996E-01
126.0	4.0202E-01
128.0	4.0466E-01
130.0	4.0781E-01
132.0	4.1142E-01
134.0	4.1544E-01
136.0	4.1981E-01
138.0	4.2447E-01
140.0	4.2938E-01
142.0	4.3447E-01
144.0	4.3970E-01
146.0	4.4501E-01
148.0	4.5035E-01
150.0	4.5568E-01
152.0	4.6095E-01
154.0	4.6612E-01
156.0	4.7117E-01
158.0	4.7608E-01
160.0	4.8083E-01
162.0	4.8539E-01
164.0	4.8975E-01
166.0	4.9388E-01
168.0	4.9772E-01
170.0	5.0120E-01
172.0	5.0424E-01
174.0	5.0675E-01
176.0	5.0862E-01
178.0	5.0979E-01
180.0	5.1018E-01

DG = 0.1 μm

λ 0.7 μm

Θ	p(λ,Θ)
0.0	3.8176E+00
2.0	3.8103E+00
4.0	3.7886E+00
6.0	3.7529E+00
8.0	3.7039E+00
10.0	3.6427E+00
12.0	3.5703E+00
14.0	3.4881E+00
16.0	3.3974E+00
18.0	3.2995E+00
20.0	3.1959E+00
22.0	3.0878E+00
24.0	2.9764E+00
26.0	2.8629E+00
28.0	2.7481E+00
30.0	2.6330E+00
32.0	2.5184E+00
34.0	2.4049E+00
36.0	2.2931E+00
38.0	2.1835E+00
40.0	2.0766E+00
42.0	1.9726E+00
44.0	1.8720E+00
46.0	1.7749E+00
48.0	1.6815E+00
50.0	1.5919E+00
52.0	1.5063E+00
54.0	1.4247E+00
56.0	1.3471E+00
58.0	1.2735E+00
60.0	1.2039E+00
62.0	1.1382E+00
64.0	1.0763E+00
66.0	1.0182E+00
68.0	9.6382E-01
70.0	9.1298E-01
72.0	8.6561E-01
74.0	8.2159E-01
76.0	7.8082E-01
78.0	7.4317E-01
80.0	7.0852E-01
82.0	6.7676E-01
84.0	6.4776E-01
86.0	6.2139E-01
88.0	5.9754E-01
90.0	5.7610E-01
92.0	5.5694E-01
94.0	5.3994E-01
96.0	5.2501E-01
98.0	5.1202E-01
100.0	5.0087E-01
102.0	4.9145E-01
104.0	4.8365E-01
106.0	4.7736E-01
108.0	4.7250E-01
110.0	4.6896E-01
112.0	4.6665E-01
114.0	4.6547E-01
116.0	4.6534E-01
118.0	4.6618E-01
120.0	4.6789E-01
122.0	4.7040E-01
124.0	4.7363E-01
126.0	4.7750E-01
128.0	4.8194E-01
130.0	4.8689E-01
132.0	4.9227E-01
134.0	4.9802E-01
136.0	5.0409E-01
138.0	5.1040E-01
140.0	5.1689E-01
142.0	5.2352E-01
144.0	5.3022E-01
146.0	5.3693E-01
148.0	5.4361E-01
150.0	5.5021E-01
152.0	5.5668E-01
154.0	5.6298E-01
156.0	5.6907E-01
158.0	5.7492E-01
160.0	5.8049E-01
162.0	5.8575E-01
164.0	5.9065E-01
166.0	5.9516E-01
168.0	5.9922E-01
170.0	6.0277E-01
172.0	6.0578E-01
174.0	6.0818E-01
176.0	6.0993E-01
178.0	6.1100E-01
180.0	6.1136E-01

DG = 0.2 μm

λ = 0.4 μm

Θ	p(λ,Θ)
0.0	8.8988E+00
2.0	8.8449E+00
4.0	8.6886E+00
6.0	8.4439E+00
8.0	8.1287E+00
10.0	7.7611E+00
12.0	7.3576E+00
14.0	6.9323E+00
16.0	6.4970E+00
18.0	6.0617E+00
20.0	5.6342E+00
22.0	5.2205E+00
24.0	4.8250E+00
26.0	4.4501E+00
28.0	4.0972E+00
30.0	3.7667E+00
32.0	3.4582E+00
34.0	3.1710E+00
36.0	2.9046E+00
38.0	2.6581E+00
40.0	2.4307E+00
42.0	2.2217E+00
44.0	2.0301E+00
46.0	1.8551E+00
48.0	1.6957E+00
50.0	1.5509E+00
52.0	1.4195E+00
54.0	1.3001E+00
56.0	1.1915E+00
58.0	1.0927E+00
60.0	1.0029E+00
62.0	9.2119E-01
64.0	8.4711E-01
66.0	7.8003E-01
68.0	7.1940E-01
70.0	6.6464E-01
72.0	6.1514E-01
74.0	5.7028E-01
76.0	5.2950E-01
78.0	4.9235E-01
80.0	4.5851E-01
82.0	4.2775E-01
84.0	3.9988E-01
86.0	3.7470E-01
88.0	3.5198E-01
90.0	3.3147E-01
92.0	3.1297E-01
94.0	2.9629E-01
96.0	2.8134E-01
98.0	2.6801E-01
100.0	2.5617E-01
102.0	2.4565E-01
104.0	2.3631E-01
106.0	2.2801E-01
108.0	2.2070E-01
110.0	2.1436E-01
112.0	2.0896E-01
114.0	2.0444E-01
116.0	2.0073E-01
118.0	1.9775E-01
120.0	1.9538E-01
122.0	1.9355E-01
124.0	1.9219E-01
126.0	1.9130E-01
128.0	1.9091E-01
130.0	1.9105E-01
132.0	1.9176E-01
134.0	1.9300E-01
136.0	1.9473E-01
138.0	1.9687E-01
140.0	1.9933E-01
142.0	2.0198E-01
144.0	2.0469E-01
146.0	2.0741E-01
148.0	2.1010E-01
150.0	2.1280E-01
152.0	2.1556E-01
154.0	2.1842E-01
156.0	2.2138E-01
158.0	2.2446E-01
160.0	2.2767E-01
162.0	2.3111E-01
164.0	2.3492E-01
166.0	2.3933E-01
168.0	2.4458E-01
170.0	2.5079E-01
172.0	2.5777E-01
174.0	2.6495E-01
176.0	2.7139E-01
178.0	2.7592E-01
180.0	2.7757E-01

DG = 0.2 μm

λ = 0.55 μm

Θ	p(λ,Θ)
0.0	7.2070E+00
2.0	7.1747E+00
4.0	7.0798E+00
6.0	6.9281E+00
8.0	6.7280E+00
10.0	6.4889E+00
12.0	6.2203E+00
14.0	5.9309E+00
16.0	5.6282E+00
18.0	5.3189E+00
20.0	5.0084E+00
22.0	4.7009E+00
24.0	4.4001E+00
26.0	4.1084E+00
28.0	3.8278E+00
30.0	3.5597E+00
32.0	3.3048E+00
34.0	3.0638E+00
36.0	2.8370E+00
38.0	2.6245E+00
40.0	2.4261E+00
42.0	2.2415E+00
44.0	2.0703E+00
46.0	1.9117E+00
48.0	1.7650E+00
50.0	1.6294E+00
52.0	1.5042E+00
54.0	1.3885E+00
56.0	1.2819E+00
58.0	1.1837E+00
60.0	1.0935E+00
62.0	1.0108E+00
64.0	9.3515E-01
66.0	8.6599E-01
68.0	8.0278E-01
70.0	7.4500E-01
72.0	6.9220E-01
74.0	6.4401E-01
76.0	6.0011E-01
78.0	5.6019E-01
80.0	5.2396E-01
82.0	4.9110E-01
84.0	4.6131E-01
86.0	4.3433E-01
88.0	4.0988E-01
90.0	3.8777E-01
92.0	3.6780E-01
94.0	3.4984E-01
96.0	3.3372E-01
98.0	3.1930E-01
100.0	3.0644E-01
102.0	2.9500E-01
104.0	2.8489E-01
106.0	2.7601E-01
108.0	2.6825E-01
110.0	2.6153E-01
112.0	2.5576E-01
114.0	2.5088E-01
116.0	2.4684E-01
118.0	2.4361E-01
120.0	2.4114E-01
122.0	2.3935E-01
124.0	2.3818E-01
126.0	2.3759E-01
128.0	2.3750E-01
130.0	2.3790E-01
132.0	2.3876E-01
134.0	2.4008E-01
136.0	2.4186E-01
138.0	2.4407E-01
140.0	2.4666E-01
142.0	2.4959E-01
144.0	2.5276E-01
146.0	2.5609E-01
148.0	2.5947E-01
150.0	2.6280E-01
152.0	2.6605E-01
154.0	2.6920E-01
156.0	2.7232E-01
158.0	2.7546E-01
160.0	2.7874E-01
162.0	2.8226E-01
164.0	2.8612E-01
166.0	2.9037E-01
168.0	2.9502E-01
170.0	2.9994E-01
172.0	3.0491E-01
174.0	3.0957E-01
176.0	3.1347E-01
178.0	3.1608E-01
180.0	3.1700E-01

DG = 0.2 μm

λ = 0.7 μm

Θ	P(λ,Θ)
0.0	6.1113E+00
2.0	6.0896E+00
4.0	6.0257E+00
6.0	5.9223E+00
8.0	5.7839E+00
10.0	5.6156E+00
12.0	5.4230E+00
14.0	5.2116E+00
16.0	4.9866E+00
18.0	4.7525E+00
20.0	4.5137E+00
22.0	4.2736E+00
24.0	4.0352E+00
26.0	3.8008E+00
28.0	3.5724E+00
30.0	3.3513E+00
32.0	3.1384E+00
34.0	2.9346E+00
36.0	2.7402E+00
38.0	2.5556E+00
40.0	2.3809E+00
42.0	2.2163E+00
44.0	2.0615E+00
46.0	1.9164E+00
48.0	1.7809E+00
50.0	1.6546E+00
52.0	1.5370E+00
54.0	1.4277E+00
56.0	1.3264E+00
58.0	1.2325E+00
60.0	1.1456E+00
62.0	1.0652E+00
64.0	9.9108E-01
66.0	9.2277E-01
68.0	8.5991E-01
70.0	8.0215E-01
72.0	7.4910E-01
74.0	7.0043E-01
76.0	6.5580E-01
78.0	6.1491E-01
80.0	5.7751E-01
82.0	5.4335E-01
84.0	5.1224E-01
86.0	4.8397E-01
88.0	4.5834E-01
90.0	4.3514E-01

Θ	P(λ,Θ)
92.0	4.1421E-01
94.0	3.9538E-01
96.0	3.7851E-01
98.0	3.6348E-01
100.0	3.5014E-01
102.0	3.3838E-01
104.0	3.2806E-01
106.0	3.1907E-01
108.0	3.1132E-01
110.0	3.0471E-01
112.0	2.9917E-01
114.0	2.9463E-01
116.0	2.9099E-01
118.0	2.8820E-01
120.0	2.8616E-01
122.0	2.8481E-01
124.0	2.8409E-01
126.0	2.8395E-01
128.0	2.8436E-01
130.0	2.8528E-01
132.0	2.8669E-01
134.0	2.8852E-01
136.0	2.9075E-01
138.0	2.9331E-01
140.0	2.9615E-01
142.0	2.9922E-01
144.0	3.0247E-01
146.0	3.0585E-01
148.0	3.0931E-01
150.0	3.1283E-01
152.0	3.1642E-01
154.0	3.2006E-01
156.0	3.2375E-01
158.0	3.2751E-01
160.0	3.3132E-01
162.0	3.3519E-01
164.0	3.3911E-01
166.0	3.4309E-01
168.0	3.4708E-01
170.0	3.5104E-01
172.0	3.5483E-01
174.0	3.5826E-01
176.0	3.6103E-01
178.0	3.6286E-01
180.0	3.6349E-01

DG = 0.3 μm

λ = 0.4 μm

Θ	p(λ,Θ)
0.0	1.1835E+01
2.0	1.1714E+01
4.0	1.1377E+01
6.0	1.0878E+01
8.0	1.0274E+01
10.0	9.6110E+00
12.0	8.9228E+00
14.0	8.2342E+00
16.0	7.5621E+00
18.0	6.9175E+00
20.0	6.3078E+00
22.0	5.7376E+00
24.0	5.2096E+00
26.0	4.7243E+00
28.0	4.2806E+00
30.0	3.8764E+00
32.0	3.5088E+00
34.0	3.1747E+00
36.0	2.8708E+00
38.0	2.5944E+00
40.0	2.3434E+00
42.0	2.1162E+00
44.0	1.9112E+00
46.0	1.7273E+00
48.0	1.5631E+00
50.0	1.4167E+00
52.0	1.2859E+00
54.0	1.1685E+00
56.0	1.0628E+00
58.0	9.6739E-01
60.0	8.8139E-01
62.0	8.0385E-01
64.0	7.3398E-01
66.0	6.7132E-01
68.0	6.1562E-01
70.0	5.6656E-01
72.0	5.2328E-01
74.0	4.8451E-01
76.0	4.4898E-01
78.0	4.1598E-01
80.0	3.8549E-01
82.0	3.5785E-01
84.0	3.3339E-01
86.0	3.1202E-01
88.0	2.9315E-01
90.0	2.7601E-01
92.0	2.6002E-01
94.0	2.4515E-01
96.0	2.3172E-01
98.0	2.2005E-01
100.0	2.1009E-01
102.0	2.0149E-01
104.0	1.9381E-01
106.0	1.8676E-01
108.0	1.8030E-01
110.0	1.7459E-01
112.0	1.6979E-01
114.0	1.6594E-01
116.0	1.6294E-01
118.0	1.6066E-01
120.0	1.5893E-01
122.0	1.5764E-01
124.0	1.5674E-01
126.0	1.5626E-01
128.0	1.5631E-01
130.0	1.5701E-01
132.0	1.5850E-01
134.0	1.6084E-01
136.0	1.6402E-01
138.0	1.6786E-01
140.0	1.7211E-01
142.0	1.7658E-01
144.0	1.8115E-01
146.0	1.8569E-01
148.0	1.9003E-01
150.0	1.9398E-01
152.0	1.9739E-01
154.0	2.0027E-01
156.0	2.0289E-01
158.0	2.0560E-01
160.0	2.0864E-01
162.0	2.1207E-01
164.0	2.1589E-01
166.0	2.2051E-01
168.0	2.2687E-01
170.0	2.3613E-01
172.0	2.4884E-01
174.0	2.6418E-01
176.0	2.7965E-01
178.0	2.9148E-01
180.0	2.9596E-01

DG = 0.3 μm

λ = 0.55 μm

Θ	P(λ,Θ)
0.0	9.4013E+00
2.0	9.3389E+00
4.0	9.1589E+00
6.0	8.8794E+00
8.0	8.5233E+00
10.0	8.1127E+00
12.0	7.6671E+00
14.0	7.2023E+00
16.0	6.7311E+00
18.0	6.2631E+00
20.0	5.8056E+00
22.0	5.3639E+00
24.0	4.9418E+00
26.0	4.5419E+00
28.0	4.1655E+00
30.0	3.8135E+00
32.0	3.4862E+00
34.0	3.1834E+00
36.0	2.9047E+00
38.0	2.6496E+00
40.0	2.4169E+00
42.0	2.2054E+00
44.0	2.0134E+00
46.0	1.8390E+00
48.0	1.6801E+00
50.0	1.5352E+00
52.0	1.4027E+00
54.0	1.2818E+00
56.0	1.1716E+00
58.0	1.0715E+00
60.0	9.8091E-01
62.0	8.9913E-01
64.0	8.2540E-01
66.0	7.5884E-01
68.0	6.9856E-01
70.0	6.4385E-01
72.0	5.9422E-01
74.0	5.4931E-01
76.0	5.0880E-01
78.0	4.7234E-01
80.0	4.3955E-01
82.0	4.1002E-01
84.0	3.8340E-01
86.0	3.5938E-01
88.0	3.3773E-01
90.0	3.1830E-01
92.0	3.0092E-01
94.0	2.8540E-01
96.0	2.7148E-01
98.0	2.5893E-01
100.0	2.4762E-01
102.0	2.3746E-01
104.0	2.2840E-01
106.0	2.2039E-01
108.0	2.1335E-01
110.0	2.0716E-01
112.0	2.0176E-01
114.0	1.9711E-01
116.0	1.9326E-01
118.0	1.9023E-01
120.0	1.8801E-01
122.0	1.8651E-01
124.0	1.8565E-01
126.0	1.8527E-01
128.0	1.8527E-01
130.0	1.8557E-01
132.0	1.8617E-01
134.0	1.8715E-01
136.0	1.8860E-01
138.0	1.9060E-01
140.0	1.9319E-01
142.0	1.9635E-01
144.0	1.9995E-01
146.0	2.0384E-01
148.0	2.0779E-01
150.0	2.1162E-01
152.0	2.1520E-01
154.0	2.1845E-01
156.0	2.2141E-01
158.0	2.2418E-01
160.0	2.2694E-01
162.0	2.2992E-01
164.0	2.3341E-01
166.0	2.3779E-01
168.0	2.4341E-01
170.0	2.5041E-01
172.0	2.5855E-01
174.0	2.6707E-01
176.0	2.7477E-01
178.0	2.8022E-01
180.0	2.8220E-01

DG = 0.3 μm

λ = 0.7 μm

Θ	p(λ,Θ)
0.0	8.0648E+00
2.0	8.0225E+00
4.0	7.8988E+00
6.0	7.7027E+00
8.0	7.4467E+00
10.0	7.1441E+00
12.0	6.8079E+00
14.0	6.4499E+00
16.0	6.0800E+00
18.0	5.7068E+00
20.0	5.3369E+00
22.0	4.9754E+00
24.0	4.6263E+00
26.0	4.2920E+00
28.0	3.9744E+00
30.0	3.6742E+00
32.0	3.3919E+00
34.0	3.1274E+00
36.0	2.8803E+00
38.0	2.6501E+00
40.0	2.4364E+00
42.0	2.2385E+00
44.0	2.0560E+00
46.0	1.8880E+00
48.0	1.7338E+00
50.0	1.5926E+00
52.0	1.4634E+00
54.0	1.3451E+00
56.0	1.2370E+00
58.0	1.1380E+00
60.0	1.0476E+00
62.0	9.6513E-01
64.0	8.8994E-01
66.0	8.2155E-01
68.0	7.5945E-01
70.0	7.0312E-01
72.0	6.5198E-01
74.0	6.0548E-01
76.0	5.6309E-01
78.0	5.2441E-01
80.0	4.8919E-01
82.0	4.5722E-01
84.0	4.2829E-01
86.0	4.0218E-01
88.0	3.7859E-01
90.0	3.5726E-01
92.0	3.3795E-01
94.0	3.2051E-01
96.0	3.0484E-01
98.0	2.9085E-01
100.0	2.7843E-01
102.0	2.6743E-01
104.0	2.5770E-01
106.0	2.4911E-01
108.0	2.4157E-01
110.0	2.3501E-01
112.0	2.2937E-01
114.0	2.2461E-01
116.0	2.2066E-01
118.0	2.1745E-01
120.0	2.1492E-01
122.0	2.1300E-01
124.0	2.1164E-01
126.0	2.1082E-01
128.0	2.1053E-01
130.0	2.1078E-01
132.0	2.1156E-01
134.0	2.1287E-01
136.0	2.1468E-01
138.0	2.1692E-01
140.0	2.1949E-01
142.0	2.2229E-01
144.0	2.2523E-01
146.0	2.2823E-01
148.0	2.3125E-01
150.0	2.3423E-01
152.0	2.3716E-01
154.0	2.4005E-01
156.0	2.4293E-01
158.0	2.4586E-01
160.0	2.4895E-01
162.0	2.5231E-01
164.0	2.5612E-01
166.0	2.6053E-01
168.0	2.6567E-01
170.0	2.7150E-01
172.0	2.7777E-01
174.0	2.8395E-01
176.0	2.8931E-01
178.0	2.9298E-01
180.0	2.9430E-01

DG = 0.5 μm

λ = 0.4 μm

Θ	p(λ,Θ)
0.0	1.7106E+01
2.0	1.6732E+01
4.0	1.5787E+01
6.0	1.4559E+01
8.0	1.3241E+01
10.0	1.1945E+01
12.0	1.0727E+01
14.0	9.6042E+00
16.0	8.5814E+00
18.0	7.6568E+00
20.0	6.8245E+00
22.0	6.0769E+00
24.0	5.4081E+00
26.0	4.8123E+00
28.0	4.2810E+00
30.0	3.8049E+00
32.0	3.3785E+00
34.0	2.9995E+00
36.0	2.6655E+00
38.0	2.3728E+00
40.0	2.1189E+00
42.0	1.9016E+00
44.0	1.7153E+00
46.0	1.5513E+00
48.0	1.4025E+00
50.0	1.2655E+00
52.0	1.1399E+00
54.0	1.0262E+00
56.0	9.2408E-01
58.0	8.3305E-01
60.0	7.5319E-01
62.0	6.8447E-01
64.0	6.2557E-01
66.0	5.7426E-01
68.0	5.2775E-01
70.0	4.8423E-01
72.0	4.4371E-01
74.0	4.0706E-01
76.0	3.7474E-01
78.0	3.4651E-01
80.0	3.2195E-01
82.0	3.0037E-01
84.0	2.8084E-01
86.0	2.6268E-01
88.0	2.4600E-01
90.0	2.3157E-01
92.0	2.1981E-01
94.0	2.1015E-01
96.0	2.0149E-01
98.0	1.9299E-01
100.0	1.8455E-01
102.0	1.7665E-01
104.0	1.6997E-01
106.0	1.6467E-01
108.0	1.6026E-01
110.0	1.5610E-01
112.0	1.5192E-01
114.0	1.4814E-01
116.0	1.4542E-01
118.0	1.4410E-01
120.0	1.4419E-01
122.0	1.4549E-01
124.0	1.4769E-01
126.0	1.5040E-01
128.0	1.5297E-01
130.0	1.5494E-01
132.0	1.5634E-01
134.0	1.5773E-01
136.0	1.5995E-01
138.0	1.6369E-01
140.0	1.6947E-01
142.0	1.7739E-01
144.0	1.8707E-01
146.0	1.9810E-01
148.0	2.1010E-01
150.0	2.2251E-01
152.0	2.3453E-01
154.0	2.4513E-01
156.0	2.5343E-01
158.0	2.5907E-01
160.0	2.6221E-01
162.0	2.6337E-01
164.0	2.6363E-01
166.0	2.6504E-01
168.0	2.7041E-01
170.0	2.8245E-01
172.0	3.0246E-01
174.0	3.2931E-01
176.0	3.5824E-01
178.0	3.8154E-01
180.0	3.9081E-01

DG = 0.5 μm

λ = 0.55 μm

Θ	p(λ,Θ)
0.0	1.3089E+01
2.0	1.2926E+01
4.0	1.2486E+01
6.0	1.1858E+01
8.0	1.1121E+01
10.0	1.0331E+01
12.0	9.5278E+00
14.0	8.7372E+00
16.0	7.9760E+00
18.0	7.2537E+00
20.0	6.5759E+00
22.0	5.9447E+00
24.0	5.3607E+00
26.0	4.8241E+00
28.0	4.3352E+00
30.0	3.8930E+00
32.0	3.4952E+00
34.0	3.1391E+00
36.0	2.8215E+00
38.0	2.5383E+00
40.0	2.2849E+00
42.0	2.0570E+00
44.0	1.8518E+00
46.0	1.6669E+00
48.0	1.5003E+00
50.0	1.3505E+00
52.0	1.2172E+00
54.0	1.1001E+00
56.0	9.9841E-01
58.0	9.0982E-01
60.0	8.3159E-01
62.0	7.6105E-01
64.0	6.9649E-01
66.0	6.3719E-01
68.0	5.8301E-01
70.0	5.3385E-01
72.0	4.8963E-01
74.0	4.5034E-01
76.0	4.1591E-01
78.0	3.8590E-01
80.0	3.5940E-01
82.0	3.3537E-01
84.0	3.1315E-01
86.0	2.9265E-01
88.0	2.7404E-01
90.0	2.5740E-01
92.0	2.4270E-01
94.0	2.2967E-01
96.0	2.1794E-01
98.0	2.0729E-01
100.0	1.9771E-01
102.0	1.8930E-01
104.0	1.8209E-01
106.0	1.7598E-01
108.0	1.7084E-01
110.0	1.6654E-01
112.0	1.6295E-01
114.0	1.5988E-01
116.0	1.5714E-01
118.0	1.5466E-01
120.0	1.5256E-01
122.0	1.5109E-01
124.0	1.5043E-01
126.0	1.5066E-01
128.0	1.5175E-01
130.0	1.5355E-01
132.0	1.5581E-01
134.0	1.5819E-01
136.0	1.6046E-01
138.0	1.6256E-01
140.0	1.6465E-01
142.0	1.6702E-01
144.0	1.6996E-01
146.0	1.7373E-01
148.0	1.7840E-01
150.0	1.8382E-01
152.0	1.8969E-01
154.0	1.9554E-01
156.0	2.0088E-01
158.0	2.0541E-01
160.0	2.0917E-01
162.0	2.1255E-01
164.0	2.1627E-01
166.0	2.2137E-01
168.0	2.2894E-01
170.0	2.3973E-01
172.0	2.5363E-01
174.0	2.6937E-01
176.0	2.8453E-01
178.0	2.9585E-01
180.0	3.0013E-01

DG = 0.5 μm

λ = 0.7 μm

Θ	p(λ,Θ)
0.0	1.1202E+01
2.0	1.1099E+01
4.0	1.0811E+01
6.0	1.0381E+01
8.0	9.8557E+00
10.0	9.2733E+00
12.0	8.6621E+00
14.0	8.0426E+00
16.0	7.4294E+00
18.0	6.8313E+00
20.0	6.2622E+00
22.0	5.7212E+00
24.0	5.2134E+00
26.0	4.7400E+00
28.0	4.3010E+00
30.0	3.8977E+00
32.0	3.5237E+00
34.0	3.1847E+00
36.0	2.8779E+00
38.0	2.6018E+00
40.0	2.3546E+00
42.0	2.1336E+00
44.0	1.9357E+00
46.0	1.7574E+00
48.0	1.5960E+00
50.0	1.4492E+00
52.0	1.3159E+00
54.0	1.1952E+00
56.0	1.0862E+00
58.0	9.8812E-01
60.0	9.0019E-01
62.0	8.2163E-01
64.0	7.5155E-01
66.0	6.8886E-01
68.0	6.3245E-01
70.0	5.8135E-01
72.0	5.3496E-01
74.0	4.9298E-01
76.0	4.5522E-01
78.0	4.2145E-01
80.0	3.9136E-01
82.0	3.6446E-01
84.0	3.4026E-01
86.0	3.1843E-01
88.0	2.9884E-01
90.0	2.8150E-01

Θ	p(λ,Θ)
92.0	2.6627E-01
94.0	2.5280E-01
96.0	2.4068E-01
98.0	2.2960E-01
100.0	2.1947E-01
102.0	2.1037E-01
104.0	2.0235E-01
106.0	1.9531E-01
108.0	1.8904E-01
110.0	1.8339E-01
112.0	1.7833E-01
114.0	1.7400E-01
116.0	1.7054E-01
118.0	1.6797E-01
120.0	1.6629E-01
122.0	1.6531E-01
124.0	1.6504E-01
126.0	1.6538E-01
128.0	1.6610E-01
130.0	1.6701E-01
132.0	1.6800E-01
134.0	1.6912E-01
136.0	1.7059E-01
138.0	1.7264E-01
140.0	1.7542E-01
142.0	1.7895E-01
144.0	1.8311E-01
146.0	1.8779E-01
148.0	1.9284E-01
150.0	1.9808E-01
152.0	2.0322E-01
154.0	2.0789E-01
156.0	2.1180E-01
158.0	2.1492E-01
160.0	2.1749E-01
162.0	2.1999E-01
164.0	2.2301E-01
166.0	2.2724E-01
168.0	2.3339E-01
170.0	2.4207E-01
172.0	2.5332E-01
174.0	2.6625E-01
176.0	2.7879E-01
178.0	2.8813E-01
180.0	2.9162E-01

DG = 1.0 μm

λ = 0.4 μm

Θ	p(λ,Θ)
0.0	3.7205E+01
2.0	3.4113E+01
4.0	2.8447E+01
6.0	2.3027E+01
8.0	1.8552E+01
10.0	1.5086E+01
12.0	1.2456E+01
14.0	1.0416E+01
16.0	8.7882E+00
18.0	7.4851E+00
20.0	6.4288E+00
22.0	5.5419E+00
24.0	4.7979E+00
26.0	4.1993E+00
28.0	3.7081E+00
30.0	3.2660E+00
32.0	2.8612E+00
34.0	2.5124E+00
36.0	2.2196E+00
38.0	1.9634E+00
40.0	1.7391E+00
42.0	1.5705E+00
44.0	1.4500E+00
46.0	1.3443E+00
48.0	1.2268E+00
50.0	1.1004E+00
52.0	9.8318E-01
54.0	8.8292E-01
56.0	7.9617E-01
58.0	7.1528E-01
60.0	6.4210E-01
62.0	5.8359E-01
64.0	5.4073E-01
66.0	5.0907E-01
68.0	4.7807E-01
70.0	4.4058E-01
72.0	3.9912E-01
74.0	3.6252E-01
76.0	3.3251E-01
78.0	3.0725E-01
80.0	2.8732E-01
82.0	2.7168E-01
84.0	2.5657E-01
86.0	2.3863E-01
88.0	2.1891E-01
90.0	2.0319E-01
92.0	1.9514E-01
94.0	1.9146E-01
96.0	1.8733E-01
98.0	1.7999E-01
100.0	1.6978E-01
102.0	1.5977E-01
104.0	1.5360E-01
106.0	1.5159E-01
108.0	1.5093E-01
110.0	1.4805E-01
112.0	1.4231E-01
114.0	1.3635E-01
116.0	1.3327E-01
118.0	1.3347E-01
120.0	1.3591E-01
122.0	1.3950E-01
124.0	1.4431E-01
126.0	1.5042E-01
128.0	1.5607E-01
130.0	1.5912E-01
132.0	1.5923E-01
134.0	1.5853E-01
136.0	1.5959E-01
138.0	1.6424E-01
140.0	1.7375E-01
142.0	1.8850E-01
144.0	2.0651E-01
146.0	2.2781E-01
148.0	2.5428E-01
150.0	2.8571E-01
152.0	3.2061E-01
154.0	3.5496E-01
156.0	3.8431E-01
158.0	4.0679E-01
160.0	4.2248E-01
162.0	4.3079E-01
164.0	4.3140E-01
166.0	4.2702E-01
168.0	4.2428E-01
170.0	4.3121E-01
172.0	4.5529E-01
174.0	5.0015E-01
176.0	5.6003E-01
178.0	6.1772E-01
180.0	6.4553E-01

DG = 1.0 μm

λ = 0.55 μm

Θ	P(λ,Θ)
0.0	2.4235E+01
2.0	2.3146E+01
4.0	2.0795E+01
6.0	1.8208E+01
8.0	1.5786E+01
10.0	1.3636E+01
12.0	1.1779E+01
14.0	1.0203E+01
16.0	8.8673E+00
18.0	7.7290E+00
20.0	6.7585E+00
22.0	5.9240E+00
24.0	5.1935E+00
26.0	4.5507E+00
28.0	3.9946E+00
30.0	3.5183E+00
32.0	3.1068E+00
34.0	2.7513E+00
36.0	2.4504E+00
38.0	2.1951E+00
40.0	1.9696E+00
42.0	1.7631E+00
44.0	1.5765E+00
46.0	1.4104E+00
48.0	1.2595E+00
50.0	1.1198E+00
52.0	9.9389E-01
54.0	8.8980E-01
56.0	8.0944E-01
58.0	7.4742E-01
60.0	6.9539E-01
62.0	6.4388E-01
64.0	5.9033E-01
66.0	5.3788E-01
68.0	4.8982E-01
70.0	4.4628E-01
72.0	4.0673E-01
74.0	3.7175E-01
76.0	3.4301E-01
78.0	3.2123E-01
80.0	3.0410E-01
82.0	2.8696E-01
84.0	2.6833E-01
86.0	2.5010E-01
88.0	2.3343E-01
90.0	2.1865E-01
92.0	2.0635E-01
94.0	1.9597E-01
96.0	1.8628E-01
98.0	1.7669E-01
100.0	1.6786E-01
102.0	1.6063E-01
104.0	1.5509E-01
106.0	1.5061E-01
108.0	1.4693E-01
110.0	1.4417E-01
112.0	1.4233E-01
114.0	1.4092E-01
116.0	1.3922E-01
118.0	1.3674E-01
120.0	1.3401E-01
122.0	1.3226E-01
124.0	1.3214E-01
126.0	1.3368E-01
128.0	1.3701E-01
130.0	1.4218E-01
132.0	1.4846E-01
134.0	1.5445E-01
136.0	1.5912E-01
138.0	1.6260E-01
140.0	1.6589E-01
142.0	1.6988E-01
144.0	1.7573E-01
146.0	1.8464E-01
148.0	1.9687E-01
150.0	2.1183E-01
152.0	2.2878E-01
154.0	2.4649E-01
156.0	2.6267E-01
158.0	2.7614E-01
160.0	2.8677E-01
162.0	2.9473E-01
164.0	3.0065E-01
166.0	3.0683E-01
168.0	3.1718E-01
170.0	3.3542E-01
172.0	3.6308E-01
174.0	3.9732E-01
176.0	4.3312E-01
178.0	4.6321E-01
180.0	4.7624E-01

DG = 1.0 μm

λ = 0.7 μm

Θ	p(λ,Θ)
0.0	1.9198E+01
2.0	1.8651E+01
4.0	1.7338E+01
6.0	1.5727E+01
8.0	1.4086E+01
10.0	1.2541E+01
12.0	1.1137E+01
14.0	9.8766E+00
16.0	8.7478E+00
18.0	7.7425E+00
20.0	6.8525E+00
22.0	6.0661E+00
24.0	5.3728E+00
26.0	4.7626E+00
28.0	4.2212E+00
30.0	3.7355E+00
32.0	3.3004E+00
34.0	2.9168E+00
36.0	2.5837E+00
38.0	2.2963E+00
40.0	2.0502E+00
42.0	1.8421E+00
44.0	1.6640E+00
46.0	1.5056E+00
48.0	1.3590E+00
50.0	1.2224E+00
52.0	1.0982E+00
54.0	9.8769E-01
56.0	8.8944E-01
58.0	8.0176E-01
60.0	7.2439E-01
62.0	6.5781E-01
64.0	6.0167E-01
66.0	5.5381E-01
68.0	5.1072E-01
70.0	4.6956E-01
72.0	4.3004E-01
74.0	3.9377E-01
76.0	3.6171E-01
78.0	3.3418E-01
80.0	3.1103E-01
82.0	2.9089E-01
84.0	2.7206E-01
86.0	2.5385E-01
88.0	2.3718E-01
90.0	2.2367E-01
92.0	2.1356E-01
94.0	2.0541E-01
96.0	1.9747E-01
98.0	1.8897E-01
100.0	1.8033E-01
102.0	1.7274E-01
104.0	1.6708E-01
106.0	1.6294E-01
108.0	1.5902E-01
110.0	1.5450E-01
112.0	1.4965E-01
114.0	1.4549E-01
116.0	1.4286E-01
118.0	1.4183E-01
120.0	1.4203E-01
122.0	1.4321E-01
124.0	1.4548E-01
126.0	1.4878E-01
128.0	1.5254E-01
130.0	1.5583E-01
132.0	1.5804E-01
134.0	1.5952E-01
136.0	1.6128E-01
138.0	1.6458E-01
140.0	1.7023E-01
142.0	1.7822E-01
144.0	1.8804E-01
146.0	1.9950E-01
148.0	2.1274E-01
150.0	2.2758E-01
152.0	2.4328E-01
154.0	2.5818E-01
156.0	2.7048E-01
158.0	2.7930E-01
160.0	2.8452E-01
162.0	2.8662E-01
164.0	2.8696E-01
166.0	2.8728E-01
168.0	2.9067E-01
170.0	3.0172E-01
172.0	3.2426E-01
174.0	3.5778E-01
176.0	3.9630E-01
178.0	4.2906E-01
180.0	4.4254E-01

DG = 2.0 μm

λ = 0.4 μm

Θ	p(λ,Θ)
0.0	1.2297E+02
2.0	9.0406E+01
4.0	5.6397E+01
6.0	3.5683E+01
8.0	2.3137E+01
10.0	1.5843E+01
12.0	1.1765E+01
14.0	9.1684E+00
16.0	7.2031E+00
18.0	5.8805E+00
20.0	5.0181E+00
22.0	4.2417E+00
24.0	3.5217E+00
26.0	3.1323E+00
28.0	2.9327E+00
30.0	2.6408E+00
32.0	2.2583E+00
34.0	1.9883E+00
36.0	1.8312E+00
38.0	1.6625E+00
40.0	1.4057E+00
42.0	1.2811E+00
44.0	1.2644E+00
46.0	1.2519E+00
48.0	1.1435E+00
50.0	9.7606E-01
52.0	8.5096E-01
54.0	7.7963E-01
56.0	7.3736E-01
58.0	6.6932E-01
60.0	5.8159E-01
62.0	5.1537E-01
64.0	4.8134E-01
66.0	4.7532E-01
68.0	4.6708E-01
70.0	4.3169E-01
72.0	3.7085E-01
74.0	3.3237E-01
76.0	3.0714E-01
78.0	2.7878E-01
80.0	2.6212E-01
82.0	2.5514E-01
84.0	2.4739E-01
86.0	2.2709E-01
88.0	1.9407E-01
90.0	1.7104E-01
92.0	1.7022E-01
94.0	1.7507E-01
96.0	1.7484E-01
98.0	1.6581E-01
100.0	1.4965E-01
102.0	1.3445E-01
104.0	1.2977E-01
106.0	1.3477E-01
108.0	1.4077E-01
110.0	1.3724E-01
112.0	1.2555E-01
114.0	1.1416E-01
116.0	1.1111E-01
118.0	1.1353E-01
120.0	1.1792E-01
122.0	1.1906E-01
124.0	1.2031E-01
126.0	1.2567E-01
128.0	1.3301E-01
130.0	1.3644E-01
132.0	1.3293E-01
134.0	1.2889E-01
136.0	1.2761E-01
138.0	1.3219E-01
140.0	1.4298E-01
142.0	1.6307E-01
144.0	1.8212E-01
146.0	2.0175E-01
148.0	2.3615E-01
150.0	2.8372E-01
152.0	3.4637E-01
154.0	4.1651E-01
156.0	4.8343E-01
158.0	5.4464E-01
160.0	6.0069E-01
162.0	6.4171E-01
164.0	6.6431E-01
166.0	6.6373E-01
168.0	6.5967E-01
170.0	6.5348E-01
172.0	6.6260E-01
174.0	6.9356E-01
176.0	7.4148E-01
178.0	7.9484E-01
180.0	8.4408E-01

DG = 2.0 μm

λ = 0.55 μm

Θ	P(λ,Θ)
0.0	6.7621E+01
2.0	5.6399E+01
4.0	4.0690E+01
6.0	2.9172E+01
8.0	2.1412E+01
10.0	1.6065E+01
12.0	1.2359E+01
14.0	9.8339E+00
16.0	8.0182E+00
18.0	6.6206E+00
20.0	5.6044E+00
22.0	4.8621E+00
24.0	4.2125E+00
26.0	3.6039E+00
28.0	3.1331E+00
30.0	2.7882E+00
32.0	2.4822E+00
34.0	2.1839E+00
36.0	1.9654E+00
38.0	1.8186E+00
40.0	1.6826E+00
42.0	1.5013E+00
44.0	1.3322E+00
46.0	1.2131E+00
48.0	1.1073E+00
50.0	9.8480E-01
52.0	8.4368E-01
54.0	7.4411E-01
56.0	6.9060E-01
58.0	6.6276E-01
60.0	6.5327E-01
62.0	6.1788E-01
64.0	5.5483E-01
66.0	4.9251E-01
68.0	4.5052E-01
70.0	4.1562E-01
72.0	3.7931E-01
74.0	3.4123E-01
76.0	3.0951E-01
78.0	2.9285E-01
80.0	2.8928E-01
82.0	2.7623E-01
84.0	2.5372E-01
86.0	2.3570E-01
88.0	2.2013E-01
90.0	2.0316E-01
92.0	1.9138E-01
94.0	1.8175E-01
96.0	1.7148E-01
98.0	1.5967E-01
100.0	1.4927E-01
102.0	1.4230E-01
104.0	1.3846E-01
106.0	1.3435E-01
108.0	1.2933E-01
110.0	1.2580E-01
112.0	1.2472E-01
114.0	1.2443E-01
116.0	1.2388E-01
118.0	1.2052E-01
120.0	1.1516E-01
122.0	1.1200E-01
124.0	1.1194E-01
126.0	1.1315E-01
128.0	1.1670E-01
130.0	1.2490E-01
132.0	1.3651E-01
134.0	1.4585E-01
136.0	1.5063E-01
138.0	1.5267E-01
140.0	1.5578E-01
142.0	1.5959E-01
144.0	1.6762E-01
146.0	1.8413E-01
148.0	2.0772E-01
150.0	2.3652E-01
152.0	2.7321E-01
154.0	3.1725E-01
156.0	3.5580E-01
158.0	3.9039E-01
160.0	4.2586E-01
162.0	4.6030E-01
164.0	4.8391E-01
166.0	4.9765E-01
168.0	5.1283E-01
170.0	5.3801E-01
172.0	5.7908E-01
174.0	6.1972E-01
176.0	6.5144E-01
178.0	6.7966E-01
180.0	7.0395E-01

DG = 2.0 μm

λ = 0.7 μm

Θ	p(λ,Θ)
0.0	4.5647E+01
2.0	4.0621E+01
4.0	3.2228E+01
6.0	2.5005E+01
8.0	1.9507E+01
10.0	1.5472E+01
12.0	1.2536E+01
14.0	1.0334E+01
16.0	8.5974E+00
18.0	7.2296E+00
20.0	6.1638E+00
22.0	5.3024E+00
24.0	4.5942E+00
26.0	4.0348E+00
28.0	3.5710E+00
30.0	3.1378E+00
32.0	2.7278E+00
34.0	2.3841E+00
36.0	2.1104E+00
38.0	1.8789E+00
40.0	1.6754E+00
42.0	1.5240E+00
44.0	1.4141E+00
46.0	1.3128E+00
48.0	1.1939E+00
50.0	1.0590E+00
52.0	9.4174E-01
54.0	8.5224E-01
56.0	7.7446E-01
58.0	6.9755E-01
60.0	6.2394E-01
62.0	5.6372E-01
64.0	5.2230E-01
66.0	4.9648E-01
68.0	4.7247E-01
70.0	4.3594E-01
72.0	3.9121E-01
74.0	3.5383E-01
76.0	3.2291E-01
78.0	2.9782E-01
80.0	2.8195E-01
82.0	2.6897E-01
84.0	2.5342E-01
86.0	2.3255E-01
88.0	2.1110E-01
90.0	1.9799E-01
92.0	1.9512E-01
94.0	1.9361E-01
96.0	1.8789E-01
98.0	1.7863E-01
100.0	1.6747E-01
102.0	1.5755E-01
104.0	1.5435E-01
106.0	1.5562E-01
108.0	1.5473E-01
110.0	1.4926E-01
112.0	1.4125E-01
114.0	1.3480E-01
116.0	1.3203E-01
118.0	1.3203E-01
120.0	1.3293E-01
122.0	1.3475E-01
124.0	1.3902E-01
126.0	1.4513E-01
128.0	1.5237E-01
130.0	1.5851E-01
132.0	1.6041E-01
134.0	1.5990E-01
136.0	1.5924E-01
138.0	1.6146E-01
140.0	1.7017E-01
142.0	1.8513E-01
144.0	2.0244E-01
146.0	2.2249E-01
148.0	2.4791E-01
150.0	2.7898E-01
152.0	3.1741E-01
154.0	3.5993E-01
156.0	4.0126E-01
158.0	4.3886E-01
160.0	4.6656E-01
162.0	4.7993E-01
164.0	4.8531E-01
166.0	4.7950E-01
168.0	4.6447E-01
170.0	4.6328E-01
172.0	4.9794E-01
174.0	5.5906E-01
176.0	6.3299E-01
178.0	7.1435E-01
180.0	7.5961E-01

DG = 5.0 μm

λ = 0.4 μm

Θ	p(λ,Θ)
0.0	7.9565E+02
2.0	2.6889E+02
4.0	8.4314E+01
6.0	3.4376E+01
8.0	1.8114E+01
10.0	1.0982E+01
12.0	6.8298E+00
14.0	5.4713E+00
16.0	5.1956E+00
18.0	4.0134E+00
20.0	3.1310E+00
22.0	2.9371E+00
24.0	3.2867E+00
26.0	2.6165E+00
28.0	2.1797E+00
30.0	1.9894E+00
32.0	2.1999E+00
34.0	1.7970E+00
36.0	1.4804E+00
38.0	1.4041E+00
40.0	1.4186E+00
42.0	1.3284E+00
44.0	1.0442E+00
46.0	9.6599E-01
48.0	8.9514E-01
50.0	8.7358E-01
52.0	8.5406E-01
54.0	6.8448E-01
56.0	5.9507E-01
58.0	6.3776E-01
60.0	5.5437E-01
62.0	5.8233E-01
64.0	4.3533E-01
66.0	3.9400E-01
68.0	3.7307E-01
70.0	3.4408E-01
72.0	3.0768E-01
74.0	3.0094E-01
76.0	2.5665E-01
78.0	2.7041E-01
80.0	2.3869E-01
82.0	1.9631E-01
84.0	1.6655E-01
86.0	1.8343E-01
88.0	1.6451E-01
90.0	1.4554E-01
92.0	1.2908E-01
94.0	1.2259E-01
96.0	1.1205E-01
98.0	9.7706E-02
100.0	9.8068E-02
102.0	9.6403E-02
104.0	9.2371E-02
106.0	8.7764E-02
108.0	7.3019E-02
110.0	6.9935E-02
112.0	7.4079E-02
114.0	7.4495E-02
116.0	7.3793E-02
118.0	7.6182E-02
120.0	6.4509E-02
122.0	6.9198E-02
124.0	6.7755E-02
126.0	6.8843E-02
128.0	5.2239E-02
130.0	4.5340E-02
132.0	5.9780E-02
134.0	7.0037E-02
136.0	6.6038E-02
138.0	7.1004E-02
140.0	8.2036E-02
142.0	8.0308E-02
144.0	7.9962E-02
146.0	1.1021E-01
148.0	1.2230E-01
150.0	1.4994E-01
152.0	2.1790E-01
154.0	3.0461E-01
156.0	3.9510E-01
158.0	5.1616E-01
160.0	6.7709E-01
162.0	7.8635E-01
164.0	7.7468E-01
166.0	7.0390E-01
168.0	7.6104E-01
170.0	8.3835E-01
172.0	8.5001E-01
174.0	9.6368E-01
176.0	1.1466E+00
178.0	1.0917E+00
180.0	9.9826E-01

DG = 5.0 μm

λ = 0.55 μm

Θ	p(λ,Θ)
0.0	4.1757E+02
2.0	2.0231E+02
4.0	8.2805E+01
6.0	3.7331E+01
8.0	2.0382E+01
10.0	1.3639E+01
12.0	9.5098E+00
14.0	6.3674E+00
16.0	5.1845E+00
18.0	4.8925E+00
20.0	4.0161E+00
22.0	3.1430E+00
24.0	2.9589E+00
26.0	2.9736E+00
28.0	2.4711E+00
30.0	2.0062E+00
32.0	1.8844E+00
34.0	1.8918E+00
36.0	1.7197E+00
38.0	1.3958E+00
40.0	1.3041E+00
42.0	1.2193E+00
44.0	1.2382E+00
46.0	1.0343E+00
48.0	8.6689E-01
50.0	8.2807E-01
52.0	8.1049E-01
54.0	8.2681E-01
56.0	6.9598E-01
58.0	5.5694E-01
60.0	5.5088E-01
62.0	5.3200E-01
64.0	5.0124E-01
66.0	4.6319E-01
68.0	3.6985E-01
70.0	3.0699E-01
72.0	3.4453E-01
74.0	3.5201E-01
76.0	3.2578E-01
78.0	2.8199E-01
80.0	2.6041E-01
82.0	2.2883E-01
84.0	1.9175E-01
86.0	1.9043E-01
88.0	1.7620E-01
90.0	1.8360E-01
92.0	1.6240E-01
94.0	1.3971E-01
96.0	1.2113E-01
98.0	1.0863E-01
100.0	1.0096E-01
102.0	1.0004E-01
104.0	1.0204E-01
106.0	9.0620E-02
108.0	8.2523E-02
110.0	8.2967E-02
112.0	8.6000E-02
114.0	8.0458E-02
116.0	7.1856E-02
118.0	7.5816E-02
120.0	7.5982E-02
122.0	8.0725E-02
124.0	7.5396E-02
126.0	6.7658E-02
128.0	7.1720E-02
130.0	7.8774E-02
132.0	7.7014E-02
134.0	6.7032E-02
136.0	6.5703E-02
138.0	8.1393E-02
140.0	9.4488E-02
142.0	9.7912E-02
144.0	1.2569E-01
146.0	1.5335E-01
148.0	1.7296E-01
150.0	2.0108E-01
152.0	2.3190E-01
154.0	2.8534E-01
156.0	3.9740E-01
158.0	4.8310E-01
160.0	5.8629E-01
162.0	6.5817E-01
164.0	7.1868E-01
166.0	7.1876E-01
168.0	7.3058E-01
170.0	8.2375E-01
172.0	9.7124E-01
174.0	1.0614E+00
176.0	1.0610E+00
178.0	8.9788E-01
180.0	8.3257E-01

DG = 5.0 μm

λ = 0.7 μm

Θ	P(λ,Θ)	Θ	P(λ,Θ)
0.0	2.6480E+02	92.0	1.7580E-01
2.0	1.5749E+02	94.0	1.6683E-01
4.0	7.7035E+01	96.0	1.5698E-01
6.0	4.0296E+01	98.0	1.4065E-01
8.0	2.3568E+01	100.0	1.4109E-01
10.0	1.4828E+01	102.0	1.5139E-01
12.0	9.8602E+00	104.0	1.4722E-01
14.0	7.5849E+00	106.0	1.3075E-01
16.0	6.3676E+00	108.0	1.1202E-01
18.0	5.0234E+00	110.0	1.0241E-01
20.0	3.9793E+00	112.0	1.0893E-01
22.0	3.5115E+00	114.0	1.2510E-01
24.0	3.3596E+00	116.0	1.3644E-01
26.0	2.8113E+00	118.0	1.2553E-01
28.0	2.3001E+00	120.0	1.0533E-01
30.0	2.1436E+00	122.0	9.2263E-02
32.0	2.1586E+00	124.0	9.1035E-02
34.0	1.9176E+00	126.0	8.9195E-02
36.0	1.6658E+00	128.0	8.3564E-02
38.0	1.5810E+00	130.0	8.6422E-02
40.0	1.5058E+00	132.0	9.5672E-02
42.0	1.3993E+00	134.0	1.0699E-01
44.0	1.1188E+00	136.0	1.1237E-01
46.0	9.7098E-01	138.0	1.2433E-01
48.0	9.2299E-01	140.0	1.3612E-01
50.0	9.4042E-01	142.0	1.3832E-01
52.0	8.9965E-01	144.0	1.4608E-01
54.0	7.3557E-01	146.0	1.6626E-01
56.0	6.6473E-01	148.0	1.9556E-01
58.0	6.4689E-01	150.0	2.3148E-01
60.0	6.4426E-01	152.0	2.7975E-01
62.0	6.6536E-01	154.0	3.5564E-01
64.0	5.5700E-01	156.0	4.3107E-01
66.0	4.6199E-01	158.0	5.1053E-01
68.0	4.0291E-01	160.0	6.1903E-01
70.0	3.6564E-01	162.0	7.5079E-01
72.0	3.5903E-01	164.0	8.0816E-01
74.0	3.6784E-01	166.0	8.9124E-01
76.0	3.6199E-01	168.0	9.4776E-01
78.0	3.3127E-01	170.0	8.8497E-01
80.0	2.7367E-01	172.0	8.2381E-01
82.0	2.2102E-01	174.0	8.3002E-01
84.0	2.1747E-01	176.0	9.1128E-01
86.0	2.2305E-01	178.0	1.0573E+00
88.0	2.1526E-01	180.0	1.1981E+00
90.0	2.0554E-01		

DG = 6.0 μm

λ = 0.4 μm

Θ	p(λ,Θ)
0.0	1.1126E+03
2.0	2.8064E+02
4.0	7.9413E+01
6.0	3.4158E+01
8.0	1.6399E+01
10.0	8.3863E+00
12.0	6.2203E+00
14.0	6.4324E+00
16.0	4.4826E+00
18.0	3.4664E+00
20.0	3.3067E+00
22.0	3.6043E+00
24.0	2.7225E+00
26.0	2.5249E+00
28.0	2.3341E+00
30.0	2.5885E+00
32.0	1.8914E+00
34.0	1.7029E+00
36.0	1.5552E+00
38.0	1.7358E+00
40.0	1.3523E+00
42.0	1.1528E+00
44.0	1.1949E+00
46.0	1.0661E+00
48.0	1.1049E+00
50.0	8.1922E-01
52.0	7.0991E-01
54.0	7.2970E-01
56.0	6.0113E-01
58.0	6.1991E-01
60.0	5.1920E-01
62.0	4.1039E-01
64.0	4.0253E-01
66.0	4.2403E-01
68.0	3.2681E-01
70.0	3.1107E-01
72.0	2.9351E-01
74.0	2.7378E-01
76.0	2.1644E-01
78.0	2.2893E-01
80.0	2.0834E-01
82.0	1.8139E-01
84.0	2.0606E-01
86.0	1.7027E-01
88.0	1.3813E-01
90.0	1.4674E-01
92.0	1.2963E-01
94.0	1.1839E-01
96.0	1.2426E-01
98.0	1.0064E-01
100.0	9.5558E-02
102.0	8.5544E-02
104.0	7.8424E-02
106.0	7.9941E-02
108.0	7.4618E-02
110.0	6.6036E-02
112.0	6.1884E-02
114.0	6.3875E-02
116.0	5.6318E-02
118.0	6.2281E-02
120.0	5.8581E-02
122.0	3.8323E-02
124.0	4.3659E-02
126.0	6.1722E-02
128.0	6.1479E-02
130.0	5.5222E-02
132.0	4.1597E-02
134.0	5.3466E-02
136.0	6.2306E-02
138.0	5.5411E-02
140.0	6.3714E-02
142.0	8.0479E-02
144.0	8.5606E-02
146.0	9.7589E-02
148.0	1.2500E-01
150.0	1.3792E-01
152.0	1.7834E-01
154.0	2.6000E-01
156.0	3.4989E-01
158.0	5.1256E-01
160.0	6.3263E-01
162.0	7.4068E-01
164.0	7.8683E-01
166.0	7.7357E-01
168.0	7.3928E-01
170.0	7.9157E-01
172.0	8.6179E-01
174.0	1.0965E+00
176.0	1.3260E+00
178.0	1.2144E+00
180.0	8.7101E-01

DG = 6.0 μm

λ = 0.55 μm

Θ	p(λ,Θ)
0.0	5.9837E+02
2.0	2.3864E+02
4.0	8.4333E+01
6.0	3.6464E+01
8.0	1.9598E+01
10.0	1.1672E+01
12.0	7.3511E+00
14.0	5.6980E+00
16.0	5.3109E+00
18.0	4.1334E+00
20.0	3.3929E+00
22.0	3.2012E+00
24.0	3.2902E+00
26.0	2.5045E+00
28.0	2.1333E+00
30.0	2.0002E+00
32.0	2.1568E+00
34.0	1.7476E+00
36.0	1.4438E+00
38.0	1.3488E+00
40.0	1.4409E+00
42.0	1.3234E+00
44.0	1.0819E+00
46.0	9.6575E-01
48.0	8.6523E-01
50.0	8.9038E-01
52.0	8.4175E-01
54.0	6.8993E-01
56.0	5.9678E-01
58.0	6.0795E-01
60.0	5.8605E-01
62.0	5.8777E-01
64.0	4.6363E-01
66.0	4.0276E-01
68.0	3.7129E-01
70.0	3.4780E-01
72.0	3.3912E-01
74.0	3.4018E-01
76.0	2.5823E-01
78.0	2.7114E-01
80.0	2.5480E-01
82.0	2.2744E-01
84.0	1.8408E-01
86.0	1.8516E-01
88.0	1.7551E-01
90.0	1.6071E-01
92.0	1.5174E-01
94.0	1.2810E-01
96.0	1.1275E-01
98.0	1.0254E-01
100.0	1.0532E-01
102.0	9.7556E-02
104.0	8.7953E-02
106.0	9.8605E-02
108.0	8.9522E-02
110.0	8.5131E-02
112.0	7.8283E-02
114.0	6.8889E-02
116.0	7.8401E-02
118.0	8.0501E-02
120.0	7.3009E-02
122.0	7.0228E-02
124.0	6.9672E-02
126.0	6.9512E-02
128.0	5.0821E-02
130.0	5.2856E-02
132.0	7.8969E-02
134.0	8.5595E-02
136.0	7.4026E-02
138.0	7.7631E-02
140.0	8.4944E-02
142.0	7.7718E-02
144.0	7.8121E-02
146.0	1.1487E-01
148.0	1.3688E-01
150.0	1.7801E-01
152.0	2.2154E-01
154.0	2.8313E-01
156.0	3.7795E-01
158.0	5.6904E-01
160.0	7.2422E-01
162.0	7.3746E-01
164.0	7.5574E-01
166.0	7.2057E-01
168.0	7.8312E-01
170.0	9.0357E-01
172.0	9.2176E-01
174.0	9.1178E-01
176.0	9.9483E-01
178.0	1.1056E+00
180.0	1.1667E+00

DG = 6.0 μm

λ = 0.7 μm

Θ	p(λ,Θ)
0.0	3.5921E+02
2.0	1.8132E+02
4.0	7.9809E+01
6.0	4.0735E+01
8.0	2.2247E+01
10.0	1.2830E+01
12.0	8.8730E+00
14.0	7.2267E+00
16.0	5.3723E+00
18.0	4.1778E+00
20.0	3.7811E+00
22.0	3.6245E+00
24.0	2.9216E+00
26.0	2.5204E+00
28.0	2.4463E+00
30.0	2.4644E+00
32.0	1.9509E+00
34.0	1.6958E+00
36.0	1.6065E+00
38.0	1.6441E+00
40.0	1.4773E+00
42.0	1.2424E+00
44.0	1.1644E+00
46.0	1.1110E+00
48.0	1.0606E+00
50.0	8.8863E-01
52.0	7.7652E-01
54.0	7.5106E-01
56.0	6.5813E-01
58.0	6.5287E-01
60.0	5.5942E-01
62.0	4.5480E-01
64.0	4.6734E-01
66.0	4.6117E-01
68.0	4.0685E-01
70.0	3.7656E-01
72.0	3.6795E-01
74.0	3.0608E-01
76.0	2.4464E-01
78.0	2.5892E-01
80.0	2.3868E-01
82.0	2.4390E-01
84.0	2.5612E-01
86.0	2.2227E-01
88.0	1.6931E-01
90.0	1.6677E-01
92.0	1.5807E-01
94.0	1.5960E-01
96.0	1.6582E-01
98.0	1.5529E-01
100.0	1.3948E-01
102.0	1.1957E-01
104.0	1.0682E-01
106.0	1.0517E-01
108.0	1.0623E-01
110.0	9.8925E-02
112.0	9.5926E-02
114.0	9.6554E-02
116.0	9.2290E-02
118.0	8.5100E-02
120.0	7.8155E-02
122.0	6.3083E-02
124.0	6.6224E-02
126.0	7.6304E-02
128.0	8.3037E-02
130.0	8.2523E-02
132.0	8.9650E-02
134.0	9.3877E-02
136.0	9.9709E-02
138.0	9.9421E-02
140.0	1.0578E-01
142.0	1.1701E-01
144.0	1.3316E-01
146.0	1.5252E-01
148.0	1.7965E-01
150.0	2.0123E-01
152.0	2.3833E-01
154.0	3.1284E-01
156.0	4.0959E-01
158.0	5.3554E-01
160.0	6.7165E-01
162.0	7.9780E-01
164.0	8.5063E-01
166.0	8.6800E-01
168.0	8.2406E-01
170.0	8.3210E-01
172.0	9.0794E-01
174.0	1.0623E+00
176.0	1.1837E+00
178.0	1.1326E+00
180.0	1.1702E+00

DG = 10.0 μm

λ = 0.4 μm

θ	p(λ,θ)
0.0	3.1416E+03
2.0	3.3448E+02
4.0	6.0017E+01
6.0	2.0556E+01
8.0	1.0354E+01
10.0	7.2783E+00
12.0	4.9905E+00
14.0	4.4552E+00
16.0	4.6422E+00
18.0	3.3900E+00
20.0	2.9238E+00
22.0	2.5360E+00
24.0	3.3278E+00
26.0	2.5297E+00
28.0	2.1617E+00
30.0	1.8642E+00
32.0	2.2933E+00
34.0	1.7068E+00
36.0	1.4710E+00
38.0	1.4628E+00
40.0	1.2687E+00
42.0	1.3003E+00
44.0	1.0522E+00
46.0	9.4500E-01
48.0	8.6352E-01
50.0	7.7440E-01
52.0	8.4416E-01
54.0	6.9212E-01
56.0	5.9936E-01
58.0	6.3026E-01
60.0	5.0728E-01
62.0	5.5583E-01
64.0	3.5909E-01
66.0	3.9871E-01
68.0	3.3947E-01
70.0	3.1150E-01
72.0	2.6914E-01
74.0	2.3358E-01
76.0	2.0913E-01
78.0	1.9751E-01
80.0	1.7160E-01
82.0	1.7361E-01
84.0	1.5345E-01
86.0	1.3907E-01
88.0	1.2262E-01
90.0	1.1299E-01
92.0	8.7944E-02
94.0	1.0204E-01
96.0	8.8620E-02
98.0	8.2212E-02
100.0	7.1707E-02
102.0	6.8097E-02
104.0	6.6905E-02
106.0	5.4047E-02
108.0	4.8558E-02
110.0	4.6377E-02
112.0	4.5968E-02
114.0	4.8803E-02
116.0	4.5828E-02
118.0	4.5963E-02
120.0	3.8626E-02
122.0	4.5970E-02
124.0	3.9541E-02
126.0	4.2393E-02
128.0	3.3869E-02
130.0	3.1168E-02
132.0	3.3250E-02
134.0	4.8081E-02
136.0	4.1103E-02
138.0	3.9023E-02
140.0	4.5845E-02
142.0	4.3432E-02
144.0	4.7809E-02
146.0	6.1372E-02
148.0	6.5830E-02
150.0	8.2346E-02
152.0	1.2595E-01
154.0	2.2242E-01
156.0	3.4421E-01
158.0	5.1661E-01
160.0	7.6899E-01
162.0	8.3350E-01
164.0	6.6505E-01
166.0	5.7081E-01
168.0	6.2542E-01
170.0	7.2376E-01
172.0	7.5246E-01
174.0	1.0194E+00
176.0	1.4827E+00
178.0	1.7329E+00
180.0	9.1932E-01

DG = 10.0 μm

λ = 0.55μm

Θ	P(λ,Θ)
0.0	1.6527E+03
2.0	3.2431E+02
4.0	7.8859E+01
6.0	2.4380E+01
8.0	1.2268E+01
10.0	9.2333E+00
12.0	7.0872E+00
14.0	4.0919E+00
16.0	3.9799E+00
18.0	4.4184E+00
20.0	3.5455E+00
22.0	2.7037E+00
24.0	2.6000E+00
26.0	2.9295E+00
28.0	2.3530E+00
30.0	1.9059E+00
32.0	1.8434E+00
34.0	1.8286E+00
36.0	1.6454E+00
38.0	1.3106E+00
40.0	1.3277E+00
42.0	1.1131E+00
44.0	1.2802E+00
46.0	9.7435E-01
48.0	8.2255E-01
50.0	8.2317E-01
52.0	7.5121E-01
54.0	7.7305E-01
56.0	6.3669E-01
58.0	5.1430E-01
60.0	5.1914E-01
62.0	4.6138E-01
64.0	4.2715E-01
66.0	4.3592E-01
68.0	3.2580E-01
70.0	2.6874E-01
72.0	3.1122E-01
74.0	2.8495E-01
76.0	2.6069E-01
78.0	2.0971E-01
80.0	2.1870E-01
82.0	1.8566E-01
84.0	1.5468E-01
86.0	1.7003E-01
88.0	1.2922E-01
90.0	1.3860E-01
92.0	1.1120E-01
94.0	1.0371E-01
96.0	9.3618E-02
98.0	7.8050E-02
100.0	7.1817E-02
102.0	6.3150E-02
104.0	6.6977E-02
106.0	5.7462E-02
108.0	5.1555E-02
110.0	5.3868E-02
112.0	5.5367E-02
114.0	5.5315E-02
116.0	4.7693E-02
118.0	4.8507E-02
120.0	4.5075E-02
122.0	5.1935E-02
124.0	4.2683E-02
126.0	3.5343E-02
128.0	4.2719E-02
130.0	4.5446E-02
132.0	4.1629E-02
134.0	3.5040E-02
136.0	3.4405E-02
138.0	4.4392E-02
140.0	5.5252E-02
142.0	4.8550E-02
144.0	6.5509E-02
146.0	7.8154E-02
148.0	9.3585E-02
150.0	1.1857E-01
152.0	1.4233E-01
154.0	2.0208E-01
156.0	3.9002E-01
158.0	5.1219E-01
160.0	6.8064E-01
162.0	6.9125E-01
164.0	6.7259E-01
166.0	6.4324E-01
168.0	6.5291E-01
170.0	7.7627E-01
172.0	9.2989E-01
174.0	1.1345E+00
176.0	1.3415E+00
178.0	1.1624E+00
180.0	6.0788E-01

DG = 10.0 μm

λ = 0.7 μm

Θ	p(λ,Θ)
0.0	1.0363E+03
2.0	2.9556E+02
4.0	8.4219E+01
6.0	3.0616E+01
8.0	1.5879E+01
10.0	1.0547E+01
12.0	6.2757E+00
14.0	5.1969E+00
16.0	5.1354E+00
18.0	4.0094E+00
20.0	3.0535E+00
22.0	2.8477E+00
24.0	3.1410E+00
26.0	2.5329E+00
28.0	2.0336E+00
30.0	1.9797E+00
32.0	2.2379E+00
34.0	1.9207E+00
36.0	1.5092E+00
38.0	1.5033E+00
40.0	1.4204E+00
42.0	1.4677E+00
44.0	1.0822E+00
46.0	9.5145E-01
48.0	8.9091E-01
50.0	8.6757E-01
52.0	8.6788E-01
54.0	6.3056E-01
56.0	5.7304E-01
58.0	5.6387E-01
60.0	5.0441E-01
62.0	5.3660E-01
64.0	4.3073E-01
66.0	3.8706E-01
68.0	3.2562E-01
70.0	3.0359E-01
72.0	2.9542E-01
74.0	2.6654E-01
76.0	2.6294E-01
78.0	2.5834E-01
80.0	2.1122E-01
82.0	1.5734E-01
84.0	1.8043E-01
86.0	1.7165E-01
88.0	1.6065E-01
90.0	1.7134E-01
92.0	1.2614E-01
94.0	1.2479E-01
96.0	1.1375E-01
98.0	9.8057E-02
100.0	9.7283E-02
102.0	1.0176E-01
104.0	9.4704E-02
106.0	8.6427E-02
108.0	7.0802E-02
110.0	6.8655E-02
112.0	7.6000E-02
114.0	7.6921E-02
116.0	8.2341E-02
118.0	6.2353E-02
120.0	5.5198E-02
122.0	5.3670E-02
124.0	5.4156E-02
126.0	4.7891E-02
128.0	5.3351E-02
130.0	5.5562E-02
132.0	5.5605E-02
134.0	6.9402E-02
136.0	6.3578E-02
138.0	6.3616E-02
140.0	7.4934E-02
142.0	7.9538E-02
144.0	8.3610E-02
146.0	1.0838E-01
148.0	1.2155E-01
150.0	1.4688E-01
152.0	1.8696E-01
154.0	2.6538E-01
156.0	3.3697E-01
158.0	4.8033E-01
160.0	6.2154E-01
162.0	7.3836E-01
164.0	7.6687E-01
166.0	7.6803E-01
168.0	8.0254E-01
170.0	7.8523E-01
172.0	8.8127E-01
174.0	1.0879E+00
176.0	1.1791E+00
178.0	1.2030E+00
180.0	9.9160E-01

APPENDIX C

PLUME DISCOLORATION PARAMETERS FOR VARIOUS NO_2 LINE-OF-SIGHT INTEGRALS AND BACKGROUND CONDITIONS

This appendix contains the following plume-discoloration parameters:

- Blue-red ratio
- Plume contrast (λ = 0.55 μm)
- Plume perceptibility ΔE (L*a*b*).

These parameters were calculated using PLUVUE, the plume visibility model, for a scattering angle of 90°,* an assumed horizon-sky viewing background, and the following input conditions:

- NO_2 line-of-sight integrals from 1×10^2 to 5×10^7 $\mu g/m^2$.
- Plume-observer distances r_p, and background visual ranges r_{v_0} of 5, 10, 20, 50, 100, 150, 200, and 250 km.

---

* For plumes that are predominantly NO_2 (e.g., plumes from well-controlled power plants), the values of these parameters do not vary significantly with scattering angle.

BACKGROUND VISUAL RANGE (KM) 10.00
PLUME-OBSERVER DISTANCE (KM) 5.00

(NO2) INTEGRAL (UG/M**2)	BLUE-RED RATIO	CONTRAST	DELTA E
1.0E+02	1.000	-.000	.000
2.0E+02	1.000	-.000	.001
5.0E+02	1.000	-.000	.002
1.0E+03	1.000	-.000	.004
2.0E+03	1.000	-.000	.007
5.0E+03	1.000	-.000	.018
1.0E+04	1.000	-.000	.037
2.0E+04	.999	-.000	.073
5.0E+04	.998	-.001	.181
1.0E+05	.996	-.002	.355
2.0E+05	.992	-.005	.684
5.0E+05	.982	-.011	1.533
1.0E+06	.971	-.021	2.587
2.0E+06	.961	-.040	3.863
5.0E+06	.960	-.079	5.761
1.0E+07	.970	-.114	7.422
2.0E+07	.992	-.136	8.625
5.0E+07	1.049	-.141	9.727

BACKGROUND VISUAL RANGE (KM) 10.00
PLUME-OBSERVER DISTANCE (KM) 10.00

(NO2) INTEGRAL (UG/M**2)	BLUE-RED RATIO	CONTRAST	DELTA E
1.0E+02	1.000	-.000	.000
2.0E+02	1.000	-.000	.000
5.0E+02	1.000	-.000	.000
1.0E+03	1.000	-.000	.000
2.0E+03	1.000	-.000	.001
5.0E+03	1.000	-.000	.001
1.0E+04	1.000	-.000	.003
2.0E+04	1.000	-.000	.005
5.0E+04	1.000	-.000	.013
1.0E+05	1.000	-.000	.026
2.0E+05	1.000	-.001	.050
5.0E+05	.999	-.002	.118
1.0E+06	.999	-.003	.218
2.0E+06	.999	-.006	.387
5.0E+06	1.000	-.011	.776
1.0E+07	1.003	-.016	1.151
2.0E+07	1.009	-.019	1.497
5.0E+07	1.023	-.020	1.901

BACKGROUND VISUAL RANGE (KM) 20.00
PLUME-OBSERVER DISTANCE (KM) 3.00

(NO2) INTEGRAL (UG/M**2)	BLUE-RED RATIO	CONTRAST	DELTA E
1.0E+02	1.000	-.000	.001
2.0E+02	1.000	-.000	.002
5.0E+02	1.000	-.000	.005
1.0E+03	1.000	-.000	.011
2.0E+03	1.000	-.000	.021
5.0E+03	.999	-.000	.053
1.0E+04	.998	-.001	.105
2.0E+04	.996	-.001	.209
5.0E+04	.991	-.003	.517
1.0E+05	.981	-.006	1.017
2.0E+05	.965	-.012	1.965
5.0E+05	.922	-.030	4.437
1.0E+06	.874	-.057	7.531
2.0E+06	.824	-.106	11.153
5.0E+06	.802	-.211	14.719
1.0E+07	.818	-.304	17.127
2.0E+07	.854	-.362	18.728
5.0E+07	.962	-.376	19.729

BACKGROUND VISUAL RANGE (KM) 20.00
PLUME-OBSERVER DISTANCE (KM) 10.00

(NO2) INTEGRAL (UG/M**2)	BLUE-RED RATIO	CONTRAST	DELTA E
1.0E+02	1.000	-.000	.000
2.0E+02	1.000	-.000	.001
5.0E+02	1.000	-.000	.001
1.0E+03	1.000	-.000	.003
2.0E+03	1.000	-.000	.005
5.0E+03	1.000	-.000	.013
1.0E+04	1.000	-.000	.026
2.0E+04	.999	-.000	.051
5.0E+04	.998	-.001	.126
1.0E+05	.996	-.002	.248
2.0E+05	.993	-.005	.477
5.0E+05	.984	-.011	1.071
1.0E+06	.974	-.021	1.816
2.0E+06	.965	-.040	2.770
5.0E+06	.964	-.079	4.380
1.0E+07	.975	-.114	5.894
2.0E+07	.996	-.136	6.989
5.0E+07	1.054	-.141	7.951

BACKGROUND VISUAL RANGE (KM) 20.00
PLUME-OBSERVER DISTANCE (KM) 15.00

(NO2) INTEGRAL (UG/M**2)	BLUE-RED RATIO	CONTRAST	DELTA E
1.0E+02	1.000	-.000	.000
2.0E+02	1.000	-.000	.000
5.0E+02	1.000	-.000	.000
1.0E+03	1.000	-.000	.001
2.0E+03	1.000	-.000	.001
5.0E+03	1.000	-.000	.003
1.0E+04	1.000	-.000	.007
2.0E+04	1.000	-.000	.013
5.0E+04	1.000	-.000	.032
1.0E+05	.999	-.001	.064
2.0E+05	.999	-.002	.124
5.0E+05	.997	-.004	.233
1.0E+06	.995	-.008	.502
2.0E+06	.994	-.015	.845
5.0E+06	.996	-.039	1.601
1.0E+07	1.001	-.043	2.313
2.0E+07	1.013	-.051	2.836
5.0E+07	1.042	-.053	3.475

BACKGROUND VISUAL RANGE (KM) 20.00
PLUME-OBSERVER DISTANCE (KM) 20.00

(NO2) INTEGRAL (UC/M**2)	BLUE-RED RATIO	CONTRAST	DELTA E
1.0E+02	1.000	-.000	.000
2.0E+02	1.000	-.000	.000
5.0E+02	1.000	-.000	.000
1.0E+03	1.000	-.000	.000
2.0E+03	1.000	-.000	.000
5.0E+03	1.000	-.000	.001
1.0E+04	1.000	-.000	.002
2.0E+04	1.000	-.000	.004
5.0E+04	1.000	-.000	.010
1.0E+05	1.000	-.000	.019
2.0E+05	1.000	-.001	.037
5.0E+05	.999	-.002	.088
1.0E+06	.999	-.003	.166
2.0E+06	.999	-.006	.305
5.0E+06	1.001	-.011	.629
1.0E+07	1.004	-.016	.936
2.0E+07	1.010	-.019	1.217
5.0E+07	1.024	-.020	1.541

BACKGROUND VISUAL RANGE (KM) 50.00
PLUME-OBSERVER DISTANCE (KM) 5.00

(NO2) INTEGRAL (UG/M**2)	BLUE-RED RATIO	CONTRAST	DELTA E
1.0E+02	1.000	-.000	.002
2.0E+02	1.000	-.000	.004
5.0E+02	1.000	-.000	.010
1.0E+03	1.000	-.000	.019
2.0E+03	.999	-.000	.039
5.0E+03	.998	-.001	.096
1.0E+04	.995	-.001	.193
2.0E+04	.991	-.002	.384
5.0E+04	.977	-.006	.953
1.0E+05	.956	-.011	1.880
2.0E+05	.915	-.022	3.661
5.0E+05	.813	-.053	8.449
1.0E+06	.693	-.103	14.795
2.0E+06	.574	-.190	22.827
5.0E+06	.504	-.389	29.043
1.0E+07	.515	-.546	32.047
2.0E+07	.552	-.651	33.594
5.0E+07	.669	-.676	33.737

BACKGROUND VISUAL RANGE (KM) 50.00
PLUME-OBSERVER DISTANCE (KM) 10.00

(NO2) INTEGRAL (UG/M**2)	BLUE-RED RATIO	CONTRAST	DELTA E
1.0E+02	1.000	-.000	.001
2.0E+02	1.000	-.000	.002
5.0E+02	1.000	-.000	.005
1.0E+03	1.000	-.000	.011
2.0E+03	1.000	-.000	.021
5.0E+03	.999	-.000	.053
1.0E+04	.998	-.001	.106
2.0E+04	.995	-.002	.212
5.0E+04	.988	-.004	.524
1.0E+05	.977	-.007	1.032
2.0E+05	.956	-.015	1.996
5.0E+05	.904	-.036	4.524
1.0E+06	.844	-.069	7.718
2.0E+06	.783	-.128	11.499
5.0E+06	.754	-.257	15.267
1.0E+07	.771	-.369	17.968
2.0E+07	.811	-.440	19.870
5.0E+07	.932	-.457	20.912

BACKGROUND VISUAL RANGE (KM) 50.00
PLUME-OBSERVER DISTANCE (KM) 15.00

(NO2) INTEGRAL (UG/M**2)	BLUE-RED RATIO	CONTRAST	DELTA E
1.0E+02	1.000	-.000	.001
2.0E+02	1.000	-.000	.001
5.0E+02	1.000	-.000	.003
1.0E+03	1.000	-.000	.006
2.0E+03	1.000	-.000	.012
5.0E+03	.999	-.000	.029
1.0E+04	.999	-.001	.059
2.0E+04	.998	-.001	.117
5.0E+04	.994	-.003	.289
1.0E+05	.988	-.005	.568
2.0E+05	.978	-.010	1.095
5.0E+05	.951	-.024	2.462.
1.0E+06	.921	-.047	4.162
2.0E+06	.890	-.087	6.198
5.0E+06	.830	-.174	8.868
1.0E+07	.896	-.250	11.295
2.0E+07	.931	-.298	12.971
5.0E+07	1.032	-.309	14.111

BACKGROUND VISUAL RANGE (KM)
PLUME-OBSERVER DISTANCE (KM) 20.00

(NO2) INTEGRAL (UG/M**2)	BLUE-RED RATIO	CONTRAST	DELTA E
1.0E+02	1.000	-.000	.000
2.0E+02	1.000	-.000	.001
5.0E+02	1.000	-.000	.002
1.0E+03	1.000	-.000	.003
2.0E+03	1.000	-.000	.007
5.0E+03	1.000	-.000	.016
1.0E+04	.999	-.000	.033
2.0E+04	.999	-.001	.065
5.0E+04	.997	-.002	.160
1.0E+05	.994	-.003	.314
2.0E+05	.989	-.007	.606
5.0E+05	.975	-.017	1.361
1.0E+06	.960	-.032	2.308
2.0E+06	.945	-.059	3.515
5.0E+06	.943	-.117	5.545
1.0E+07	.957	-.169	7.484
2.0E+07	.985	-.201	8.833
5.0E+07	1.064	-.209	9.872

BACKGROUND VISUAL RANGE (KM) 50.00
PLUME-OBSERVER DISTANCE (KM) 30.00

(NO2) INTEGRAL (UG/M**2)	BLUE-RED RATIO	CONTRAST	DELTA E
1.0E+02	1.000	-.000	.000
2.0E+02	1.000	-.000	.000
5.0E+02	1.000	-.000	.001
1.0E+03	1.000	-.000	.001
2.0E+03	1.000	-.000	.002
5.0E+03	1.000	-.000	.005
1.0E+04	1.000	-.000	.010
2.0E+04	1.000	-.000	.021
5.0E+04	.999	-.001	.051
1.0E+05	.998	-.002	.101
2.0E+05	.997	-.003	.195
5.0E+05	.994	-.008	.445
1.0E+06	.990	-.015	.764
2.0E+06	.987	-.027	1.306
5.0E+06	.990	-.054	2.449
1.0E+07	.999	-.077	3.515
2.0E+07	1.016	-.092	4.309
5.0E+07	1.061	-.096	5.036

BACKGROUND VISUAL RANGE (KM) 50.00
PLUME-OBSERVER DISTANCE (KM) 40.00

(NO2) INTEGRAL (UG/M**2)	BLUE-RED RATIO	CONTRAST	DELTA E
1.0E+02	1.000	-.000	.000
2.0E+02	1.000	-.000	.000
5.0E+02	1.000	-.000	.000
1.0E+03	1.000	-.000	.000
2.0E+03	1.000	-.000	.001
5.0E+03	1.000	-.000	.002
1.0E+04	1.000	-.000	.004
2.0E+04	1.000	-.000	.007
5.0E+04	1.000	-.000	.018
1.0E+05	1.000	-.001	.036
2.0E+05	.999	-.001	.071
5.0E+05	.999	-.003	.168
1.0E+06	.998	-.007	.313
2.0E+06	.998	-.012	.567
5.0E+06	1.000	-.025	1.158
1.0E+07	1.006	-.035	1.699
2.0E+07	1.016	-.042	2.147
5.0E+07	1.042	-.044	2.614

BACKGROUND VISUAL RANGE (KM) 50.00
PLUME-OBSERVER DISTANCE (KM) 50.00

(NO2) INTEGRAL (UG/M**2)	BLUE-RED RATIO	CONTRAST	DELTA E
1.0E+02	1.000	-.000	.000
2.0E+02	1.000	-.000	.000
5.0E+02	1.000	-.000	.000
1.0E+03	1.000	-.000	.000
2.0E+03	1.000	-.000	.000
5.0E+03	1.000	-.000	.001
1.0E+04	1.000	-.000	.002
2.0E+04	1.000	-.000	.003
5.0E+04	1.000	-.000	.008
1.0E+05	1.000	-.000	.015
2.0E+05	1.000	-.001	.030
5.0E+05	1.000	-.002	.073
1.0E+06	1.000	-.003	.141
2.0E+06	1.000	-.006	.266
5.0E+06	1.002	-.011	.556
1.0E+07	1.005	-.016	.826
2.0E+07	1.011	-.019	1.076
5.0E+07	1.026	-.020	1.364

BACKGROUND VISUAL RANGE (KM) 100.0
PLUME-OBSERVER DISTANCE (KM) 5.00

(NO2) INTEGRAL (UG/M**2)	BLUE-RED RATIO	CONTRAST	DELTA E
1.0E+02	1.000	-.000	.002
2.0E+02	1.000	-.000	.005
5.0E+02	1.000	-.000	.012
1.0E+03	.999	-.000	.024
2.0E+03	.999	-.000	.047
5.0E+03	.997	-.001	.118
1.0E+04	.994	-.001	.235
2.0E+04	.988	-.003	.470
5.0E+04	.970	-.007	1.167
1.0E+05	.941	-.013	2.308
2.0E+05	.886	-.027	4.514
5.0E+05	.750	-.063	10.556
1.0E+06	.592	-.125	18.892
2.0E+06	.427	-.231	30.283
5.0E+06	.329	-.462	41.397
1.0E+07	.334	-.664	43.263
2.0E+07	.361	-.792	44.532
5.0E+07	.453	-.822	43.992

BACKGROUND VISUAL RANGE (KM) 100.0
PLUME-OBSERVER DISTANCE (KM) 10.00

(NO2) INTEGRAL (UG/M**2)	BLUE-RED RATIO	CONTRAST	DELTA E
1.0E+02	1.000	-.000	.002
2.0E+02	1.000	-.000	.003
5.0E+02	1.000	-.000	.009
1.0E+03	1.000	-.000	.017
2.0E+03	.999	-.000	.034
5.0E+03	.998	-.001	.086
1.0E+04	.996	-.001	.171
2.0E+04	.992	-.002	.341
5.0E+04	.979	-.006	.845
1.0E+05	.959	-.011	1.668
2.0E+05	.922	-.022	3.246
5.0E+05	.828	-.054	7.478
1.0E+06	.719	-.103	13.060
2.0E+06	.608	-.190	20.081
5.0E+06	.545	-.389	26.427
1.0E+07	.559	-.546	29.246
2.0E+07	.598	-.651	31.489
5.0E+07	.726	-.676	32.139

BACKGROUND VISUAL RANGE (KM) 100.0
PLUME-OBSERVER DISTANCE (KM) 15.00

(NO2) INTEGRAL (UG/M**2)	BLUE-RED RATIO	CONTRAST	DELTA E
1.0E+02	1.000	-.000	.001
2.0E+02	1.000	-.000	.002
5.0E+02	1.000	-.000	.006
1.0E+03	1.000	-.000	.012
2.0E+03	.999	-.000	.025
5.0E+03	.999	-.000	.062
1.0E+04	.997	-.001	.124
2.0E+04	.994	-.002	.247
5.0E+04	.986	-.005	.613
1.0E+05	.972	-.009	1.207
2.0E+05	.946	-.018	2.340
5.0E+05	.882	-.044	5.335
1.0E+06	.807	-.085	9.177
2.0E+06	.732	-.156	13.825
5.0E+06	.694	-.312	18.429
1.0E+07	.711	-.449	21.663
2.0E+07	.754	-.336	24.065
5.0E+07	.889	-.356	25.152

BACKGROUND VISUAL RANGE (KM) 100.0
PLUME-OBSERVER DISTANCE (KM) 20.00

(NO2) INTEGRAL (UG/M**2)	BLUE-RED RATIO	CONTRAST	DELTA E
1.0E+02	1.000	-.000	.001
2.0E+02	1.000	-.000	.002
5.0E+02	1.000	-.000	.005
1.0E+03	1.000	-.000	.009
2.0E+03	1.000	-.000	.018
5.0E+03	.999	-.000	.045
1.0E+04	.998	-.001	.090
2.0E+04	.996	-.002	.180
5.0E+04	.990	-.004	.445
1.0E+05	.981	-.007	.874
2.0E+05	.963	-.015	1.691
5.0E+05	.919	-.036	3.829
1.0E+06	.868	-.070	6.528
2.0E+06	.817	-.128	9.768
5.0E+06	.795	-.257	13.532
1.0E+07	.813	-.370	16.789
2.0E+07	.856	-.441	19.091
5.0E+07	.986	-.457	20.332

BACKGROUND VISUAL RANGE (KM) 100.0
PLUME-OBSERVER DISTANCE (KM) 30.00

(NO2) INTEGRAL (UG/M**2)	BLUE-RED RATIO	CONTRAST	DELTA E
1.0E+02	1.000	-.000	.000
2.0E+02	1.000	-.000	.001
5.0E+02	1.000	-.000	.002
1.0E+03	1.000	-.000	.005
2.0E+03	1.000	-.000	.010
5.0E+03	1.000	-.000	.024
1.0E+04	.999	-.001	.048
2.0E+04	.998	-.001	.095
5.0E+04	.995	-.003	.235
1.0E+05	.991	-.005	.462
2.0E+05	.983	-.010	.891
5.0E+05	.962	-.024	2.007
1.0E+06	.939	-.047	3.413
2.0E+06	.916	-.087	5.190
5.0E+06	.910	-.174	8.056
1.0E+07	.928	-.259	10.828
2.0E+07	.964	-.293	12.710
5.0E+07	1.071	-.310	13.942

BACKGROUND VISUAL RANGE (KM) 100.0
PLUME-OBSERVER DISTANCE (KM) 40.00

(NO2) INTEGRAL (UG/M**2)	BLUE-RED RATIO	CONTRAST	DELTA E
1.0E+02	1.000	-.000	.000
2.0E+02	1.000	-.000	.001
5.0E+02	1.000	-.000	.001
1.0E+03	1.000	-.000	.003
2.0E+03	1.000	-.000	.005
5.0E+03	1.000	-.000	.013
1.0E+04	1.000	-.000	.026
2.0E+04	.999	-.001	.051
5.0E+04	.998	-.002	.126
1.0E+05	.996	-.003	.248
2.0E+05	.992	-.007	.479
5.0E+05	.982	-.017	1.035
1.0E+06	.972	-.032	1.872
2.0E+06	.962	-.059	2.981
5.0E+06	.963	-.118	5.205
1.0E+07	.978	-.169	7.321
2.0E+07	1.007	-.202	8.770
5.0E+07	1.089	-.209	9.852

BACKGROUND VISUAL RANGE (KM) 100.0
PLUME-OBSERVER DISTANCE (KM) 50.00

(NO2) INTEGRAL (UG/M**2)	BLUE-RED RATIO	CONTRAST	DELTA E
1.0E+02	1.000	-.000	.000
2.0E+02	1.000	-.000	.000
5.0E+02	1.000	-.000	.001
1.0E+03	1.000	-.000	.001
2.0E+03	1.000	-.000	.003
5.0E+03	1.000	-.000	.007
1.0E+04	1.000	-.000	.014
2.0E+04	1.000	-.000	.028
5.0E+04	.999	-.001	.070
1.0E+05	.998	-.002	.138
2.0E+05	.996	-.005	.267
5.0E+05	.992	-.011	.613
1.0E+06	.988	-.022	1.090
2.0E+06	.984	-.040	1.842
5.0E+06	.987	-.089	3.512
1.0E+07	.999	-.115	5.051
2.0E+07	1.022	-.137	6.144
5.0E+07	1.084	-.142	7.051

BACKGROUND VISUAL RANGE (KM) 100.9
PLUME-OBSERVER DISTANCE (KM) 100.0

(NO2) INTEGRAL (UG/M**2)	BLUE-RED RATIO	CONTRAST	DELTA E
1.0E+02	1.000	-.000	.000
2.0E+02	1.000	-.000	.000
5.0E+02	1.000	-.000	.000
1.0E+03	1.000	-.000	.000
2.0E+03	1.000	-.000	.000
5.0E+03	1.000	-.000	.001
1.0E+04	1.000	-.000	.002
2.0E+04	1.000	-.000	.003
5.0E+04	1.000	-.000	.008
1.0E+05	1.000	-.000	.015
2.0E+05	1.000	-.001	.030
5.0E+05	1.000	-.002	.075
1.0E+06	1.000	-.003	.146
2.0E+06	1.001	-.006	.276
5.0E+06	1.003	-.012	.569
1.0E+07	1.006	-.017	.841
2.0E+07	1.012	-.029	1.098
5.0E+07	1.027	-.020	1.392

BACKGROUND VISUAL RANGE (KM) 150.0
PLUME-OBSERVER DISTANCE (KM) 5.00

(NO2) INTEGRAL (UG/M**2)	BLUE-RED RATIO	CONTRAST	DELTA E
1.0E+02	1.000	-.000	.003
2.0E+02	1.000	-.000	.005
5.0E+02	1.000	-.000	.013
1.0E+03	.999	-.000	.025
2.0E+03	.999	-.000	.051
5.0E+03	.997	-.001	.127
1.0E+04	.993	-.001	.253
2.0E+04	.986	-.003	.506
5.0E+04	.967	-.007	1.256
1.0E+05	.935	-.014	2.487
2.0E+05	.875	-.028	4.873
5.0E+05	.725	-.069	11.460
1.0E+06	.550	-.133	20.705
2.0E+06	.368	-.247	33.622
5.0E+06	.257	-.493	47.793
1.0E+07	.259	-.709	49.714
2.0E+07	.281	-.845	50.786
5.0E+07	.358	-.878	49.940

BACKGROUND VISUAL RANGE (KM) 150.0
PLUME-OBSERVER DISTANCE (KM) 10.00

(NO2) INTEGRAL (UG/M**2)	BLUE-RED RATIO	CONTRAST	DELTA E
1.0E+02	1.000	-.000	.002
2.0E+02	1.000	-.000	.004
5.0E+02	1.000	-.000	.010
1.0E+03	.999	-.000	.020
2.0E+03	.999	-.000	.040
5.0E+03	.997	-.001	.101
1.0E+04	.995	-.001	.202
2.0E+04	.990	-.003	.402
5.0E+04	.975	-.006	.998
1.0E+05	.950	-.013	1.972
2.0E+05	.905	-.025	3.848
5.0E+05	.791	-.061	8.937
1.0E+06	.659	-.117	15.814
2.0E+06	.522	-.216	24.844
5.0E+06	.443	-.433	33.292
1.0E+07	.454	-.622	36.091
2.0E+07	.489	-.742	38.543
5.0E+07	.606	-.771	38.918

BACKGROUND VISUAL RANGE (KM) 150.0
PLUME-OBSERVER DISTANCE (KM) 15.00

(NO2) INTEGRAL (UG/M**2)	BLUE-RED RATIO	CONTRAST	DELTA E
1.0E+02	1.000	-.000	.002
2.0E+02	1.000	-.000	.003
5.0E+02	1.000	-.000	.008
1.0E+03	1.000	-.000	.016
2.0E+03	.999	-.000	.032
5.0E+03	.998	-.001	.080
1.0E+04	.996	-.001	.160
2.0E+04	.992	-.002	.320
5.0E+04	.981	-.005	.793
1.0E+05	.962	-.011	1.564
2.0E+05	.928	-.022	3.043
5.0E+05	.842	-.054	7.001
1.0E+06	.742	-.103	12.205
2.0E+06	.669	-.190	18.732
5.0E+06	.593	-.389	24.921
1.0E+07	.599	-.547	28.416
2.0E+07	.641	-.652	31.265
5.0E+07	.773	-.677	32.190

BACKGROUND VISUAL RANGE (KM) 150.0
PLUME-OBSERVER DISTANCE (KM) 20.00

(NO2) INTEGRAL (UG/M**2)	BLUE-RED RATIO	CONTRAST	DELTA E
1.0E+02	1.000	-.000	.001
2.0E+02	1.000	-.000	.003
5.0E+02	1.000	-.000	.006
1.0E+03	1.000	-.000	.013
2.0E+03	.999	-.000	.026
5.0E+03	.999	-.000	.064
1.0E+04	.997	-.001	.128
2.0E+04	.994	-.002	.255
5.0E+04	.985	-.005	.631
1.0E+05	.971	-.010	1.242
2.0E+05	.945	-.019	2.419
5.0E+05	.880	-.047	5.505
1.0E+06	.865	-.090	9.493
2.0E+06	.728	-.167	14.383
5.0E+06	.609	-.334	19.464
1.0E+07	.708	-.439	23.298
2.0E+07	.753	-.572	26.202
5.0E+07	.896	-.594	27.393

BACKGROUND VISUAL RANGE (KM) 150.0
PLUME-OBSERVER DISTANCE (KM) 30.00

(NO2) INTEGRAL (UG/M**2)	BLUE-RED RATIO	CONTRAST	DELTA E
1.0E+02	1.000	-.000	.001
2.0E+02	1.000	-.000	.002
5.0E+02	1.000	-.000	.004
1.0E+03	1.000	-.000	.008
2.0E+03	1.000	-.000	.016
5.0E+03	.999	-.000	.041
1.0E+04	.998	-.001	.081
2.0E+04	.997	-.002	.161
5.0E+04	.992	-.004	.400
1.0E+05	.984	-.007	.786
2.0E+05	.969	-.015	1.520
5.0E+05	.931	-.036	3.441
1.0E+06	.889	-.070	5.875
2.0E+06	.846	-.129	8.867
5.0E+06	.829	-.257	12.904
1.0E+07	.849	-.370	16.727
2.0E+07	.894	-.441	19.372
5.0E+07	1.029	-.458	20.728

BACKGROUND VISUAL RANGE (KM) 150.0
PLUME-OBSERVER DISTANCE (KM) 40.00

(NO2) INTEGRAL (UG/M**2)	BLUE-RED RATIO	CONTRAST	DELTA E
1.0E+02	1.000	-.000	.001
2.0E+02	1.000	-.000	.001
5.0E+02	1.000	-.000	.003
1.0E+03	1.000	-.000	.005
2.0E+03	1.000	-.000	.010
5.0E+03	1.000	-.000	.026
1.0E+04	.999	-.001	.052
2.0E+04	.998	-.001	.103
5.0E+04	.995	-.003	.255
1.0E+05	.991	-.006	.501
2.0E+05	.982	-.011	.967
5.0E+05	.961	-.028	2.186
1.0E+06	.937	-.054	3.738
2.0E+06	.914	-.099	5.754
5.0E+06	.909	-.193	9.209
1.0E+07	.928	-.285	12.537
2.0E+07	.968	-.340	14.849
5.0E+07	1.086	-.353	16.165

BACKGROUND VISUAL RANGE (KM) 150.0
PLUME-OBSERVER DISTANCE (KM) 50.00

(NO2) INTEGRAL (UG/M**2)	BLUE-RED RATIO	CONTRAST	DELTA E
1.0E+02	1.000	-.000	.000
2.0E+02	1.000	-.000	.001
5.0E+02	1.000	-.000	.002
1.0E+03	1.000	-.000	.003
2.0E+03	1.000	-.000	.007
5.0E+03	1.000	-.000	.017
1.0E+04	.999	-.000	.033
2.0E+04	.999	-.001	.067
5.0E+04	.997	-.002	.165
1.0E+05	.995	-.004	.323
2.0E+05	.990	-.009	.625
5.0E+05	.978	-.022	1.419
1.0E+06	.965	-.041	2.457
2.0E+06	.952	-.077	3.926
5.0E+06	.953	-.153	6.877
1.0E+07	.970	-.220	9.696
2.0E+07	1.005	-.262	11.566
5.0E+07	1.104	-.272	12.739

BACKGROUND VISUAL RANGE (KM) 150.0
PLUME-OBSERVER DISTANCE (KM) 100.0

(NO2) INTEGRAL (UG/M**2)	BLUE-RED RATIO	CONTRAST	DELTA E
1.0E+02	1.000	-.000	.000
2.0E+02	1.000	-.000	.000
5.0E+02	1.000	-.000	.000
1.0E+03	1.000	-.000	.001
2.0E+03	1.000	-.000	.001
5.0E+03	1.000	-.000	.003
1.0E+04	1.000	-.000	.006
2.0E+04	1.000	-.000	.011
5.0E+04	1.000	-.001	.028
1.0E+05	1.000	-.001	.056
2.0E+05	1.000	-.002	.111
5.0E+05	.999	-.006	.271
1.0E+06	.999	-.011	.520
2.0E+06	.999	-.021	.971
5.0E+06	1.003	-.042	1.994
1.0E+07	1.011	-.061	2.833
2.0E+07	1.025	-.072	3.571
5.0E+07	1.062	-.075	4.198

BACKGROUND VISUAL RANGE (KM) 150.0
PLUME-OBSERVER DISTANCE (KM) 150.0

(NO2) INTEGRAL (UG/M**2)	BLUE-RED RATIO	CONTRAST	DELTA E
1.0E+02	1.000	-.000	.000
2.0E+02	1.000	-.000	.000
5.0E+02	1.000	-.000	.000
1.0E+03	1.000	-.000	.000
2.0E+03	1.000	-.000	.000
5.0E+03	1.000	-.000	.001
1.0E+04	1.000	-.000	.002
2.0E+04	1.000	-.000	.003
5.0E+04	1.000	-.000	.008
1.0E+05	1.000	-.000	.017
2.0E+05	1.000	-.001	.034
5.0E+05	1.000	-.002	.083
1.0E+06	1.000	-.003	.160
2.0E+06	1.001	-.006	.300
5.0E+06	1.002	-.012	.600
1.0E+07	1.005	-.017	.882
2.0E+07	1.010	-.021	1.122
5.0E+07	1.023	-.021	1.377

BACKGROUND VISUAL RANGE (KM) 200.0
PLUME-OBSERVER DISTANCE (KM) 5.00

(NO2) INTEGRAL (UG/M**2)	BLUE-RED RATIO	CONTRAST	DELTA E
1.0E+02	1.000	-.000	.003
2.0E+02	1.000	-.000	.005
5.0E+02	1.000	-.000	.013
1.0E+03	.999	-.000	.026
2.0E+03	.999	-.000	.053
5.0E+03	.996	-.001	.132
1.0E+04	.993	-.001	.264
2.0E+04	.986	-.003	.527
5.0E+04	.965	-.007	1.310
1.0E+05	.931	-.015	2.594
2.0E+05	.869	-.029	5.037
5.0E+05	.711	-.072	11.999
1.0E+06	.520	-.133	21.794
2.0E+06	.337	-.255	36.003
5.0E+06	.219	-.509	52.093
1.0E+07	.219	-.732	54.237
2.0E+07	.238	-.873	55.169
5.0E+07	.305	-.907	54.193

BACKGROUND VISUAL RANGE (KM) 200.0
PLUME-OBSERVER DISTANCE (KM) 10.00

(NO2) INTEGRAL (UG/M**2)	BLUE-RED RATIO	CONTRAST	DELTA E
1.0E+02	1.000	-.000	.002
2.0E+02	1.000	-.000	.004
5.0E+02	1.000	-.000	.011
1.0E+03	.999	-.000	.022
2.0E+03	.999	-.000	.044
5.0E+03	.997	-.001	.110
1.0E+04	.994	-.001	.220
2.0E+04	.989	-.003	.439
5.0E+04	.972	-.007	1.090
1.0E+05	.945	-.013	2.154
2.0E+05	.895	-.027	4.211
5.0E+05	.770	-.065	9.828
1.0E+06	.624	-.125	17.529
2.0E+06	.473	-.231	27.936
5.0E+06	.384	-.462	38.112
1.0E+07	.392	-.664	40.945
2.0E+07	.424	-.792	43.563
5.0E+07	.532	-.822	43.771

BACKGROUND VISUAL RANGE (KM) 200.0
PLUME-OBSERVER DISTANCE (KM) 15.00

(NO2) INTEGRAL (UG/M**2)	BLUE-RED RATIO	CONTRAST	DELTA E
1.0E+02	1.000	-.000	.002
2.0E+02	1.000	-.000	.004
5.0E+02	1.000	-.000	.009
1.0E+03	1.000	-.000	.018
2.0E+03	.999	-.000	.037
5.0E+03	.998	-.001	.092
1.0E+04	.995	-.001	.183
2.0E+04	.991	-.002	.366
5.0E+04	.978	-.006	.907
1.0E+05	.956	-.012	1.790
2.0E+05	.917	-.024	3.490
5.0E+05	.817	-.059	8.076
1.0E+06	.701	-.113	14.296
2.0E+06	.582	-.209	22.114
5.0E+06	.515	-.419	29.669
1.0E+07	.528	-.602	33.313
2.0E+07	.568	-.718	36.516
5.0E+07	.700	-.746	37.301

BACKGROUND VISUAL RANGE (KM) 200.0
PLUME-OBSERVER DISTANCE (KM) 29.00

(NO2) INTEGRAL (UG/M**2)	BLUE-RED RATIO	CONTRAST	DELTA E
1.0E+02	1.000	-.000	.002
2.0E+02	1.000	-.000	.003
5.0E+02	1.000	-.000	.008
1.0E+03	1.000	-.000	.015
2.0E+03	.999	-.000	.031
5.0E+03	.998	-.001	.076
1.0E+04	.996	-.001	.153
2.0E+04	.993	-.002	.305
5.0E+04	.982	-.006	.755
1.0E+05	.965	-.011	1.489
2.0E+05	.934	-.022	2.895
5.0E+05	.854	-.053	6.654
1.0E+06	.762	-.103	11.585
2.0E+06	.668	-.190	17.765
5.0E+06	.618	-.380	23.969
1.0E+07	.635	-.546	28.141
2.0E+07	.680	-.651	31.518
5.0E+07	.824	-.676	32.613

BACKGROUND VISUAL RANGE (KM) 200.0
PLUME-OBSERVER DISTANCE (KM) 30.00

(NO2) INTEGRAL (UG/M**2)	BLUE-RED RATIO	CONTRAST	DELTA E
1.0E+02	1.000	-.000	.091
2.0E+02	1.000	-.000	.002
5.0E+02	1.000	-.000	.005
1.0E+03	1.000	-.000	.011
2.0E+03	1.000	-.000	.021
5.0E+03	.999	-.000	.053
1.0E+04	.998	-.001	.106
2.0E+04	.995	-.002	.212
5.0E+04	.989	-.005	.524
1.0E+05	.978	-.009	1.032
2.0E+05	.958	-.018	2.001
5.0E+05	.908	-.044	4.555
1.0E+06	.850	-.085	7.830
2.0E+06	.792	-.156	11.869
5.0E+06	.766	-.312	16.636
1.0E+07	.786	-.449	21.355
2.0E+07	.833	-.536	24.601
5.0E+07	.982	-.556	25.951

BACKGROUND VISUAL RANGE (KM) 200.0
PLUME-OBSERVER DISTANCE (KM) 40.00

(NO2) INTEGRAL (UG/M**2)	BLUE-RED RATIO	CONTRAST	DELTA E
1.0E+02	1.000	-.000	.001
2.0E+02	1.000	-.000	.001
5.0E+02	1.000	-.000	.004
1.0E+03	1.000	-.000	.007
2.0E+03	1.000	-.000	.015
5.0E+03	.999	-.000	.037
1.0E+04	.999	-.001	.074
2.0E+04	.997	-.002	.148
5.0E+04	.993	-.004	.366
1.0E+05	.986	-.007	.720
2.0E+05	.973	-.015	1.392
5.0E+05	.942	-.036	3.154
1.0E+06	.906	-.070	5.403
2.0E+06	.870	-.128	8.255
5.0E+06	.858	-.257	12.639
1.0E+07	.879	-.369	16.949
2.0E+07	.925	-.441	19.849
5.0E+07	1.063	-.457	21.241

BACKGROUND VISUAL RANGE (KM) 200.0
PLUME-OBSERVER DISTANCE (KM) 50.00

(NO2) INTEGRAL (UG/M**2)	BLUE-RED RATIO	CONTRAST	DELTA E
1.0E+02	1.000	-.000	.001
2.0E+02	1.000	-.000	.001
5.0E+02	1.000	-.000	.003
1.0E+03	1.000	-.000	.005
2.0E+03	1.000	-.000	.010
5.0E+03	1.000	-.000	.026
1.0E+04	.999	-.001	.052
2.0E+04	.998	-.001	.104
5.0E+04	.996	-.003	.257
1.0E+05	.991	-.006	.506
2.0E+05	.983	-.012	.978
5.0E+05	.964	-.030	2.216
1.0E+06	.941	-.057	3.815
2.0E+06	.920	-.106	5.965
5.0E+06	.916	-.211	9.909
1.0E+07	.936	-.304	13.769
2.0E+07	.973	-.362	16.288
5.0E+07	1.102	-.376	17.633

BACKGROUND VISUAL RANGE (KM) 200.0
PLUME-OBSERVER DISTANCE (KM) 100.0

(NO2) INTEGRAL (UG/M**2)	BLUE-RED RATIO	CONTRAST	DELTA E
1.0E+02	1.000	-.000	.000
2.0E+02	1.000	-.000	.000
5.0E+02	1.000	-.000	.001
1.0E+03	1.000	-.000	.001
2.0E+03	1.000	-.000	.002
5.0E+03	1.000	-.000	.006
1.0E+04	1.000	-.000	.012
2.0E+04	1.000	-.000	.023
5.0E+04	1.000	-.001	.058
1.0E+05	.999	-.002	.114
2.0E+05	.999	-.005	.225
5.0E+05	.997	-.011	.537
1.0E+06	.995	-.022	1.010
2.0E+06	.995	-.040	1.845
5.0E+06	1.000	-.080	3.746
1.0E+07	1.011	-.114	5.398
2.0E+07	1.032	-.136	6.528
5.0E+07	1.090	-.142	7.378

BACKGROUND VISUAL RANGE (KM) 200.0
PLUME-OBSERVER DISTANCE (KM) 150.0

(NO2) INTEGRAL (UG/M**2)	BLUE-RED RATIO	CONTRAST	DELTA E
1.0E+02	1.000	-.000	.000
2.0E+02	1.000	-.000	.000
5.0E+02	1.000	-.000	.000
1.0E+03	1.000	-.000	.000
2.0E+03	1.000	-.000	.001
5.0E+03	1.000	-.000	.002
1.0E+04	1.000	-.000	.004
2.0E+04	1.000	-.000	.008
5.0E+04	1.000	-.000	.021
1.0E+05	1.000	-.001	.042
2.0E+05	1.000	-.002	.083
5.0E+05	1.000	-.004	.203
1.0E+06	1.000	-.008	.393
2.0E+06	1.001	-.015	.736
5.0E+06	1.004	-.030	1.491
1.0E+07	1.008	-.043	2.134
2.0E+07	1.018	-.051	2.618
5.0E+07	1.042	-.053	3.045

BACKGROUND VISUAL RANGE (KM) 200.0
PLUME-OBSERVER DISTANCE (KM) 200.0

(NO2) INTEGRAL (UG/M**2)	BLUE-RED RATIO	CONTRAST	DELTA E
1.0E+02	1.000	-.000	.000
2.0E+02	1.000	-.000	.000
5.0E+02	1.000	-.000	.000
1.0E+03	1.000	-.000	.000
2.0E+03	1.000	-.000	.000
5.0E+03	1.000	-.000	.001
1.0E+04	1.000	-.000	.002
2.0E+04	1.000	-.000	.003
5.0E+04	1.000	-.000	.008
1.0E+05	1.000	-.000	.016
2.0E+05	1.000	-.001	.032
5.0E+05	1.000	-.002	.079
1.0E+06	1.000	-.003	.154
2.0E+06	1.000	-.006	.287
5.0E+06	1.001	-.011	.575
1.0E+07	1.003	-.016	.816
2.0E+07	1.006	-.020	.995
5.0E+07	1.013	-.020	1.146

BACKGROUND VISUAL RANGE (KM) 250.0
PLUME-OBSERVER DISTANCE (KM) 5.00

(NO2) INTEGRAL (UG/M**2)	BLUE-RED RATIO	CONTRAST	DELTA E
1.0E+02	1.000	-.000	.003
2.0E+02	1.000	-.000	.005
5.0E+02	1.000	-.000	.014
1.0E+03	.999	-.000	.027
2.0E+03	.999	-.000	.054
5.0E+03	.996	-.001	.136
1.0E+04	.993	-.002	.271
2.0E+04	.985	-.003	.542
5.0E+04	.964	-.008	1.347
1.0E+05	.929	-.015	2.668
2.0E+05	.865	-.030	5.236
5.0E+05	.703	-.073	12.372
1.0E+06	.514	-.140	22.548
2.0E+06	.317	-.260	37.523
5.0E+06	.195	-.519	55.254
1.0E+07	.194	-.747	57.677
2.0E+07	.211	-.890	58.499
5.0E+07	.272	-.924	57.484

BACKGROUND VISUAL RANGE (KM) 259.0
PLUME-OBSERVER DISTANCE (KM) 10.00

(NO2) INTEGRAL (UG/M**2)	BLUE-RED RATIO	CONTRAST	DELTA E
1.0E+02	1.000	-.000	.002
2.0E+02	1.000	-.000	.005
5.0E+02	1.000	-.000	.012
1.0E+03	.999	-.000	.023
2.0E+03	.999	-.000	.047
5.0E+03	.997	-.001	.116
1.0E+04	.994	-.001	.232
2.0E+04	.988	-.003	.464
5.0E+04	.970	-.007	1.152
1.0E+05	.942	-.014	2.279
2.0E+05	.889	-.028	4.460
5.0E+05	.756	-.063	10.441
1.0E+06	.601	-.130	18.721
2.0E+06	.441	-.240	30.137
5.0E+06	.345	-.480	41.743
1.0E+07	.352	-.690	44.645
2.0E+07	.381	-.823	47.390
5.0E+07	.482	-.854	47.501

BACKGROUND VISUAL RANGE (KM) 250.0
PLUME-OBSERVER DISTANCE (KM) 15.00

(NO2) INTEGRAL (UG/M**2)	BLUE-RED RATIO	CONTRAST	DELTA E
1.0E+02	1.000	-.000	.002
2.0E+02	1.000	-.000	.004
5.0E+02	1.000	-.000	.010
1.0E+03	1.000	-.000	.020
2.0E+03	.999	-.000	.040
5.0E+03	.998	-.001	.100
1.0E+04	.995	-.001	.199
2.0E+04	.990	-.003	.397
5.0E+04	.976	-.006	.986
1.0E+05	.952	-.013	1.948
2.0E+05	.909	-.026	3.802
5.0E+05	.800	-.062	8.832
1.0E+06	.673	-.120	15.636
2.0E+06	.543	-.222	24.601
5.0E+06	.468	-.443	33.327
1.0E+07	.480	-.638	37.078
2.0E+07	.517	-.761	40.565
5.0E+07	.644	-.790	41.248

BACKGROUND VISUAL RANGE (KM) 250.0
PLUME-OBSERVER DISTANCE (KM) 20.00

(NO2) INTEGRAL (UG/M**2)	BLUE-RED RATIO	CONTRAST	DELTA E
1.0E+02	1.000	-.000	.002
2.0E+02	1.000	-.000	.003
5.0E+02	1.000	-.000	.009
1.0E+03	1.000	-.000	.017
2.0E+03	.999	-.000	.034
5.0E+03	.998	-.001	.085
1.0E+04	.996	-.001	.171
2.0E+04	.992	-.002	.340
5.0E+04	.980	-.005	.844
1.0E+05	.961	-.012	1.666
2.0E+05	.925	-.024	3.244
5.0E+05	.836	-.058	7.489
1.0E+06	.733	-.111	13.124
2.0E+06	.626	-.205	20.329
5.0E+06	.568	-.410	27.512
1.0E+07	.534	-.590	31.906
2.0E+07	.627	-.703	35.668
5.0E+07	.769	-.739	36.675

BACKGROUND VISUAL RANGE (KM) 250.0
PLUME-OBSERVER DISTANCE (KM) 30.00

(NO2) INTEGRAL (UG/M**2)	BLUE-RED RATIO	CONTRAST	DELTA E
1.0E+02	1.000	-.000	.001
2.0E+02	1.000	-.000	.003
5.0E+02	1.000	-.000	.006
1.0E+03	1.000	-.000	.013
2.0E+03	.999	-.000	.025
5.0E+03	.999	-.001	.063
1.0E+04	.997	-.001	.125
2.0E+04	.995	-.002	.250
5.0E+04	.987	-.005	.620
1.0E+05	.974	-.010	1.221
2.0E+05	.950	-.020	2.370
5.0E+05	.890	-.049	5.419
1.0E+06	.821	-.095	9.370
2.0E+06	.751	-.175	14.292
5.0E+06	.717	-.350	20.039
1.0E+07	.737	-.504	25.044
2.0E+07	.785	-.601	28.787
5.0E+07	.939	-.623	30.091

BACKGROUND VISUAL RANGE (KM) 250.0
PLUME-OBSERVER DISTANCE (KM) 40.00

(NO2) INTEGRAL (UG/M**2)	BLUE-RED RATIO	CONTRAST	DELTA E
1.0E+02	1.000	-.000	.001
2.0E+02	1.000	-.000	.002
5.0E+02	1.000	-.000	.005
1.0E+03	1.000	-.000	.009
2.0E+03	1.000	-.000	.019
5.0E+03	.999	-.000	.046
1.0E+04	.998	-.001	.093
2.0E+04	.996	-.002	.184
5.0E+04	.991	-.004	.457
1.0E+05	.982	-.009	.899
2.0E+05	.966	-.017	1.740
5.0E+05	.926	-.042	3.958
1.0E+06	.880	-.081	6.803
2.0E+06	.835	-.150	10.390
5.0E+06	.817	-.299	15.515
1.0E+07	.838	-.430	20.520
2.0E+07	.887	-.513	23.960
5.0E+07	1.036	-.532	25.348

BACKGROUND VISUAL RANGE (KM) 250.0
PLUME-OBSERVER DISTANCE (KM) 50.00

(NO2) INTEGRAL (UG/M**2)	BLUE-RED RATIO	CONTRAST	DELTA E
1.0E+02	1.000	-.000	.001
2.0E+02	1.000	-.000	.001
5.0E+02	1.000	-.000	.003
1.0E+03	1.000	-.000	.007
2.0E+03	1.000	-.000	.014
5.0E+03	.999	-.000	.034
1.0E+04	.999	-.001	.069
2.0E+04	.998	-.001	.137
5.0E+04	.994	-.004	.338
1.0E+05	.988	-.007	.665
2.0E+05	.978	-.015	1.287
5.0E+05	.951	-.036	2.922
1.0E+06	.920	-.069	5.028
2.0E+06	.891	-.128	7.793
5.0E+06	.883	-.255	12.514
1.0E+07	.904	-.367	17.197
2.0E+07	.950	-.438	20.265
5.0E+07	1.090	-.455	21.643

BACKGROUND VISUAL RANGE (KM) 250.0
PLUME-OBSERVER DISTANCE (KM) 100.0

(NO2) INTEGRAL (UG/M**2)	BLUE-RED RATIO	CONTRAST	DELTA E
1.0E+02	1.000	-.000	.000
2.0E+02	1.000	-.000	.000
5.0E+02	1.000	-.000	.001
1.0E+03	1.000	-.000	.002
2.0E+03	1.000	-.000	.004
5.0E+03	1.000	-.000	.009
1.0E+04	1.000	-.000	.018
2.0E+04	1.000	-.001	.037
5.0E+04	.999	-.002	.091
1.0E+05	.999	-.003	.180
2.0E+05	.997	-.007	.352
5.0E+05	.994	-.016	.830
1.0E+06	.991	-.031	1.533
2.0E+06	.989	-.058	2.740
5.0E+06	.994	-.115	5.434
1.0E+07	1.008	-.166	7.868
2.0E+07	1.035	-.198	9.439
5.0E+07	1.110	-.205	10.420

BACKGROUND VISUAL RANGE (KM) 250.0
PLUME-OBSERVER DISTANCE (KM) 150.0

(NO2) INTEGRAL (UG/M**2)	BLUE-RED RATIO	CONTRAST	DELTA E
1.0E+02	1.000	-.000	.000
2.0E+02	1.000	-.000	.000
5.0E+02	1.000	-.000	.000
1.0E+03	1.000	-.000	.001
2.0E+03	1.000	-.000	.001
5.0E+03	1.000	-.000	.004
1.0E+04	1.000	-.000	.007
2.0E+04	1.000	-.000	.015
5.0E+04	1.000	-.001	.036
1.0E+05	1.000	-.001	.072
2.0E+05	1.000	-.003	.143
5.0E+05	.999	-.007	.349
1.0E+06	.999	-.014	.673
2.0E+06	1.000	-.026	1.256
5.0E+06	1.004	-.051	2.549
1.0E+07	1.011	-.074	3.633
2.0E+07	1.024	-.088	4.381
5.0E+07	1.060	-.091	4.943

BACKGROUND VISUAL RANGE (KM) 250.0
PLUME-OBSERVER DISTANCE (KM) 200.0

(NO2) INTEGRAL (UG/M**2)	BLUE-RED RATIO	CONTRAST	DELTA E
1.0E+02	1.000	-.000	.000
2.0E+02	1.000	-.000	.000
5.0E+02	1.000	-.000	.000
1.0E+03	1.000	-.000	.000
2.0E+03	1.000	-.000	.001
5.0E+03	1.000	-.000	.002
1.0E+04	1.000	-.000	.003
2.0E+04	1.000	-.000	.006
5.0E+04	1.000	-.000	.016
1.0E+05	1.000	-.001	.032
2.0E+05	1.000	-.001	.063
5.0E+05	1.000	-.003	.154
1.0E+06	1.000	-.006	.298
2.0E+06	1.000	-.011	.556
5.0E+06	1.002	-.022	1.115
1.0E+07	1.005	-.032	1.576
2.0E+07	1.010	-.038	1.095
5.0E+07	1.023	-.039	2.136

BACKGROUND VISUAL RANGE (KM) 250.0
PLUME-OBSERVER DISTANCE (KM) 250.0

(NO2) INTEGRAL (UG/M**2)	BLUE-RED RATIO	CONTRAST	DELTA E
1.0E+02	1.000	-.000	.000
2.0E+02	1.000	-.000	.000
5.0E+02	1.000	-.000	.000
1.0E+03	1.000	-.000	.000
2.0E+03	1.000	-.000	.000
5.0E+03	1.000	-.000	.001
1.0E+04	1.000	-.000	.001
2.0E+04	1.000	-.000	.003
5.0E+04	1.000	-.000	.007
1.0E+05	1.000	-.000	.014
2.0E+05	1.000	-.001	.027
5.0E+05	1.000	-.001	.066
1.0E+06	1.000	-.002	.125
2.0E+06	.999	-.004	.228
5.0E+06	.999	-.009	.449
1.0E+07	1.000	-.012	.621
2.0E+07	1.000	-.015	.714
5.0E+07	1.000	-.015	.746

APPENDIX D

REFERENCE FIGURES AND TABLES FOR POWER PLANT VISUAL IMPACTS

This appendix presents figures and tables that show the calculated visual impacts of emissions from power plants of various sizes under different meteorological and ambient conditions. These reference data are based on calculations made using the plume visibility model (PLUVUE).

If one is evaluating a power plant (or another emissions source with similar particulate, SO_2, and NO_x emission rates), one can identify the emission, meteorological, and background conditions shown here closest to the given case under evaluation. Alternatively, one can interpolate the values in the reference tables in this appendix to obtain a best estimate of a source's impact. These reference tables and figures would be used in a level-2 visibility screening analyses.

The tables and figures are based on 96 PLUVUE runs for the permutations of the following input parameters:

- Power plant size: 500, 1000, and 2000 Mwe
- Pasquill-Gifford stability category: C, D, E, F
- Wind speed: 2.5 and 5.0 m/s
- Background visual range: 20, 50, 100, and 200 km.

The emissions used in this appendix are based on emission rates of controlled power plants meeting the EPA's New Source Performance Standards. Emission rates of 0.03, 0.3, and 0.6 pound per million Btu heat input--for particulates, SO_2, and NO_x, respectively--were assumed. The emission rates for the 1000 Mwe and 2000 Mwe plants are simple multiples of those for the 500 Mwe case: The mass emission rates for a 500 Mwe power plant are as follows:

> Particles: 1.6 tons/day
= 1.5 metric tons/day
= 17 g/s

> SO_2: = 16 tons/day
= 14.5 metric tons/day
= 168 g/s

> NO_x: 32 tons/day
= 29 metric tons/day
= 336 g/s.

Other important input parameters for the PLUVUE runs used to generate the tables and figures in this appendix are summarized below:

> Flue gas flow rate (per stack): 1,270,000 ft^3/min
= 599 m^3/s

> Flue gas temperature: 175°F
= 353°K

> Ambient relative humidity: 40%

> Background ozone concentration: 40 ppb

> Mixing depth: 1000 m

> Simulation date/time: 23 September/10:00 a.m.

> Plume-observer distance: Maximum of 5 km or a half-sector width (r_p = 0.2 x)

> Scattering angle: 90°

> Line-of-sight orientation: Horizontal, perpendicular to the plume centerline.

As noted, if the user has a situation in which conditions are between those used in this appendix, interpolation will yield a reasonable estimate of impacts. However, if one has to extrapolate the results of this appendix, one should exercise extreme caution: Many visual impacts do not have a linear relationship with input conditions.

500MW COAL-FIRED PLANT
PASQUILL-GIFFORD C
WIND SPEED = 2.5 M/S
BACKGROUND VISUAL RANGE = 20. KM

DOWNWIND DISTANCE (KM)	PLUME-OBSERVER DISTANCE (KM)	VISUAL RANGE REDUCTION (%)	BLUE-RED RATIO	PLUME CONTRAST AT 0.55 MICRON	PLUME PERCEPT-IBILITY E(L*A*B*)
1.	5.0	1.3	0.992	-.004	0.52
2.	5.0	0.8	0.988	-.005	0.72
5.	5.0	0.5	0.987	-.005	0.77
10.	5.0	0.4	0.987	-.005	0.78
15.	5.0	0.4	0.986	-.005	0.81
20.	5.0	0.4	0.986	-.006	0.83
30.	6.0	0.4	0.990	-.004	0.61
40.	8.0	0.5	0.995	-.003	0.33
50.	9.9	0.5	0.998	-.002	0.18
75.	14.9	0.5	1.000	-.001	0.04
100.	19.9	0.3	1.000	-.000	0.01
150.	29.8	0.1	1.000	-.000	0.00
200.	39.8	0.0	1.000	-.000	0.00
250.	49.7	0.0	1.000	-.000	0.00
300.	59.7	0.0	1.000	-.000	0.00
350.	69.6	0.0	1.000	-.000	0.00

500MW COAL-FIRED PLANT
PASQUILL-GIFFORD C
WIND SPEED = 2.5 M/S
BACKGROUND VISUAL RANGE = 50. KM

DOWNWIND DISTANCE (KM)	PLUME-OBSERVER DISTANCE (KM)	VISUAL RANGE REDUCTION (%)	BLUE-RED RATIO	PLUME CONTRAST AT 0.55 MICRON	PLUME PERCEPT-IBILITY E(L*A*B*)
1.	5.0	1.2	0.978	-.008	1.04
2.	5.0	0.7	0.969	-.010	1.41
5.	5.0	0.4	0.966	-.010	1.51
10.	5.0	0.3	0.965	-.010	1.53
15.	5.0	0.3	0.964	-.010	1.59
20.	5.0	0.3	0.963	-.010	1.62
30.	6.0	0.3	0.968	-.009	1.42
40.	8.0	0.4	0.977	-.008	1.08
50.	9.9	0.4	0.983	-.006	0.81
75.	14.9	0.5	0.993	-.004	0.38
100.	19.9	0.5	0.997	-.002	0.18
150.	29.8	0.7	1.000	-.001	0.04
200.	39.8	0.8	1.000	-.000	0.01
250.	49.7	0.5	1.000	-.000	0.00
300.	59.7	0.3	1.000	-.000	0.00
350.	69.6	0.2	1.000	-.000	0.00

500MW COAL-FIRED PLANT
PASQUILL-GIFFORD C
WIND SPEED - 2.5 M/S
BACKGROUND VISUAL RANGE = 100. KM

DOWNWIND DISTANCE (KM)	PLUME-OBSERVER DISTANCE (KM)	VISUAL RANGE REDUCTION (%)	BLUE-RED RATIO	PLUME CONTRAST AT 0.55 MICRON	PLUME PERCEPT-IBILITY E(L*A*B*)
1.	5.0	1.1	0.963	-.012	1.34
2.	5.0	0.6	0.956	-.013	1.78
5.	5.0	0.3	0.953	-.012	1.90
10.	5.0	0.2	0.952	-.012	1.93
15.	5.0	0.2	0.950	-.012	1.99
20.	5.0	0.2	0.949	-.013	2.04
30.	6.0	0.3	0.954	-.012	1.88
40.	8.0	0.3	0.961	-.011	1.60
50.	9.9	0.3	0.968	-.010	1.35
75.	14.9	0.4	0.981	-.007	0.85
100.	19.9	0.4	0.989	-.005	0.54
150.	29.8	0.7	0.996	-.003	0.22
200.	39.8	0.9	0.999	-.002	0.08
250.	49.7	1.1	1.000	-.001	0.04
300.	59.7	1.2	1.000	-.001	0.02
350.	69.6	1.4	1.000	-.000	0.02

500MW COAL-FIRED PLANT
PASQUILL-GIFFORD C
WIND SPEED = 2.5 M/S
BACKGROUND VISUAL RANGE = 200. KM

DOWNWIND DISTANCE (KM)	PLUME-OBSERVER DISTANCE (KM)	VISUAL RANGE REDUCTION (%)	BLUE-RED RATIO	PLUME CONTRAST AT 0.55 MICRON	PLUME PERCEPT-IBILITY E(L*A*B*)
1.	5.0	1.0	0.959	-.016	1.58
2.	5.0	0.5	0.947	-.016	2.05
5.	5.0	0.3	0.944	-.014	2.17
10.	5.0	0.2	0.943	-.014	2.20
15.	5.0	0.2	0.941	-.014	2.27
20.	5.0	0.2	0.940	-.014	2.32
30.	6.0	0.2	0.943	-.014	2.21
40.	8.0	0.2	0.950	-.013	1.99
50.	9.9	0.2	0.956	-.012	1.78
75.	14.9	0.3	0.969	-.010	1.30
100.	19.9	0.3	0.979	-.008	0.95
150.	29.8	0.6	0.989	-.006	0.52
200.	39.8	0.8	0.995	-.005	0.25
250.	49.7	1.0	0.997	-.004	0.16
300.	59.7	1.2	0.998	-.003	0.12
350.	69.6	1.4	0.998	-.003	0.11

500MW COAL-FIRED PLANT
PASQUILL-GIFFORD C
WIND SPEED = 5.0 M/S
BACKGROUND VISUAL RANGE = 20. KM

DOWNWIND DISTANCE (KM)	PLUME-OBSERVER DISTANCE (KM)	VISUAL RANGE REDUCTION (%)	BLUE-RED RATIO	PLUME CONTRAST AT 0.55 MICRON	PLUME PERCEPT-IBILITY E(L*A*B*)
1.	5.0	0.7	0.993	-.003	0.42
2.	5.0	0.5	0.991	-.004	0.57
5.	5.0	0.3	0.990	-.004	0.58
10.	5.0	0.2	0.992	-.003	0.47
15.	5.0	0.2	0.992	-.003	0.45
20.	5.0	0.2	0.992	-.003	0.44
30.	6.0	0.2	0.995	-.002	0.33
40.	8.0	0.3	0.997	-.002	0.18
50.	9.9	0.3	0.999	-.001	0.10
75.	14.9	0.3	1.000	-.000	0.02
100.	19.9	0.2	1.000	-.000	0.01
150.	29.8	0.1	1.000	-.000	0.00
200.	39.8	0.0	1.000	-.000	0.00
250.	49.7	0.0	1.000	-.000	0.00
300.	59.7	0.0	1.000	-.000	0.00
350.	69.6	0.0	1.000	-.000	0.00

500MW COAL-FIRED PLANT
PASQUILL-GIFFORD C
WIND SPEED = 5.0 M/S
BACKGROUND VISUAL RANGE = 50. KM

DOWNWIND DISTANCE (KM)	PLUME-OBSERVER DISTANCE (KM)	VISUAL RANGE REDUCTION (%)	BLUE-RED RATIO	PLUME CONTRAST AT 0.55 MICRON	PLUME PERCEPT-IBILITY E(L*A*B*)
1.	5.0	0.6	0.982	-.006	0.83
2.	5.0	0.4	0.975	-.007	1.11
5.	5.0	0.2	0.974	-.007	1.13
10.	5.0	0.2	0.979	-.005	0.92
15.	5.0	0.2	0.980	-.005	0.87
20.	5.0	0.2	0.980	-.005	0.87
30.	6.0	0.2	0.983	-.005	0.76
40.	8.0	0.2	0.988	-.004	0.58
50.	9.9	0.2	0.991	-.003	0.44
75.	14.9	0.3	0.996	-.002	0.21
100.	19.9	0.3	0.998	-.001	0.11
150.	29.8	0.4	1.000	-.000	0.02
200.	39.8	0.3	1.000	-.000	0.01
250.	49.7	0.2	1.000	-.000	0.00
300.	59.7	0.1	1.000	-.000	0.00
350.	69.6	0.0	1.000	-.000	0.00

500MW COAL-FIRED PLANT
PASQUILL-GIFFORD C
WIND SPEED = 5.0 M/S
BACKGROUND VISUAL RANGE = 100. KM

DOWNWIND DISTANCE (KM)	PLUME-OBSERVER DISTANCE (KM)	VISUAL RANGE REDUCTION (%)	BLUE-RED RATIO	PLUME CONTRAST AT 0.55 MICRON	PLUME PERCEPTIBILITY E(L*A*B*)
1.	5.0	0.6	0.974	-.008	1.06
2.	5.0	0.3	0.965	-.009	1.40
5.	5.0	0.2	0.964	-.009	1.42
10.	5.0	0.1	0.971	-.007	1.15
15.	5.0	0.1	0.973	-.007	1.09
20.	5.0	0.1	0.973	-.007	1.09
30.	6.0	0.1	0.975	-.006	1.00
40.	8.0	0.2	0.979	-.006	0.86
50.	9.9	0.2	0.983	-.005	0.73
75.	14.9	0.2	0.990	-.004	0.48
100.	19.9	0.3	0.994	-.003	0.31
150.	29.8	0.4	0.998	-.002	0.11
200.	39.8	0.4	0.999	-.001	0.05
250.	49.7	0.4	1.000	-.001	0.03
300.	59.7	0.3	1.000	-.000	0.01
350.	69.6	0.3	1.000	-.000	0.01

500MW COAL-FIRED PLANT
PASQUILL-GIFFORD C
WIND SPEED = 5.0 M/S
BACKGROUND VISUAL RANGE = 200. KM

DOWNWIND DISTANCE (KM)	PLUME-OBSERVER DISTANCE (KM)	VISUAL RANGE REDUCTION (%)	BLUE-RED RATIO	PLUME CONTRAST AT 0.55 MICRON	PLUME PERCEPTIBILITY E(L*A*B*)
1.	5.0	0.5	0.968	-.011	1.23
2.	5.0	0.3	0.958	-.011	1.61
5.	5.0	0.1	0.958	-.010	1.62
10.	5.0	0.1	0.966	-.008	1.31
15.	5.0	0.1	0.968	-.008	1.24
20.	5.0	0.1	0.968	-.008	1.24
30.	6.0	0.1	0.970	-.007	1.17
40.	8.0	0.1	0.973	-.007	1.07
50.	9.9	0.1	0.976	-.007	0.96
75.	14.9	0.2	0.983	-.006	0.73
100.	19.9	0.2	0.988	-.005	0.55
150.	29.8	0.3	0.994	-.003	0.27
200.	39.8	0.3	0.997	-.002	0.16
250.	49.7	0.3	0.998	-.002	0.10
300.	59.7	0.3	0.999	-.001	0.07
350.	69.6	0.3	0.999	-.001	0.05

500MW COAL-FIRED PLANT
PASQUILL-GIFFORD D
WIND SPEED = 2.5 M/S
BACKGROUND VISUAL RANGE = 20. KM

DOWNWIND DISTANCE (KM)	PLUME-OBSERVER DISTANCE (KM)	VISUAL RANGE REDUCTION (%)	BLUE-RED RATIO	PLUME CONTRAST AT 0.55 MICRON	PLUME PERCEPT-IBILITY E(L*A*B*)
1.	5.0	1.6	0.990	-.005	0.63
2.	5.0	1.3	0.987	-.006	0.78
5.	5.0	1.0	0.982	-.008	1.10
10.	5.0	0.9	0.978	-.009	1.35
15.	5.0	0.8	0.976	-.010	1.41
20.	5.0	0.8	0.977	-.009	1.39
30.	6.0	0.7	0.985	-.007	0.95
40.	8.0	0.7	0.993	-.004	0.48
50.	9.9	0.7	0.997	-.003	0.25
75.	14.9	0.6	1.000	-.001	0.05
100.	19.9	0.3	1.000	-.000	0.02
150.	29.8	0.0	1.000	-.000	0.00
200.	39.8	0.0	1.000	-.000	0.00
250.	49.7	0.0	1.000	-.000	0.00
300.	59.7	0.0	1.000	-.000	0.00
350.	69.6	0.0	1.000	-.000	0.00

500MW COAL-FIRED PLANT
PASQUILL-GIFFORD D
WIND SPEED = 2.5 M/S
BACKGROUND VISUAL RANGE = 50. KM

DOWNWIND DISTANCE (KM)	PLUME-OBSERVER DISTANCE (KM)	VISUAL RANGE REDUCTION (%)	BLUE-RED RATIO	PLUME CONTRAST AT 0.55 MICRON	PLUME PERCEPT-IBILITY E(L*A*B*)
1.	5.0	1.5	0.973	-.010	1.25
2.	5.0	1.2	0.966	-.011	1.55
5.	5.0	0.9	0.952	-.014	2.17
10.	5.0	0.7	0.941	-.017	2.65
15.	5.0	0.6	0.938	-.018	2.78
20.	5.0	0.6	0.939	-.017	2.73
30.	6.0	0.5	0.951	-.014	2.20
40.	8.0	0.5	0.967	-.011	1.57
50.	9.9	0.5	0.977	-.009	1.14
75.	14.9	0.6	0.990	-.005	0.54
100.	19.9	0.6	0.996	-.003	0.26
150.	29.8	0.7	0.999	-.001	0.07
200.	39.8	0.7	1.000	-.001	0.02
250.	49.7	0.5	1.000	-.000	0.01
300.	59.7	0.2	1.000	-.000	0.00
350.	69.6	0.1	1.000	-.000	0.00

500MW COAL-FIRED PLANT
PASQUILL-GIFFORD D
WIND SPEED - 2.5 M/S
BACKGROUND VISUAL RANGE = 100. KM

DOWNWIND DISTANCE (KM)	PLUME-OBSERVER DISTANCE (KM)	VISUAL RANGE REDUCTION (%)	BLUE-RED RATIO	PLUME CONTRAST AT 0.55 MICRON	PLUME PERCEPT-IBILITY E(L*A*B*)
1.	5.0	1.3	0.961	-.014	1.61
2.	5.0	1.1	0.952	-.015	1.97
5.	5.0	0.7	0.932	-.019	2.74
10.	5.0	0.6	0.918	-.021	3.34
15.	5.0	0.5	0.914	-.022	3.51
20.	5.0	0.4	0.915	-.022	3.43
30.	6.0	0.4	0.928	-.019	2.93
40.	8.0	0.4	0.944	-.016	2.35
50.	9.9	0.4	0.956	-.014	1.91
75.	14.9	0.4	0.974	-.010	1.20
100.	19.9	0.5	0.984	-.007	0.77
150.	29.8	0.6	0.994	-.005	0.35
200.	39.8	0.7	0.998	-.003	0.17
250.	49.7	0.9	0.999	-.002	0.08
300.	59.7	1.1	1.000	-.001	0.04
350.	69.6	1.5	1.000	-.001	0.02

500MW COAL-FIRED PLANT
PASQUILL-GIFFORD D
WIND SPEED = 2.5 M/S
BACKGROUND VISUAL RANGE = 200. KM

DOWNWIND DISTANCE (KM)	PLUME-OBSERVER DISTANCE (KM)	VISUAL RANGE REDUCTION (%)	BLUE-RED RATIO	PLUME CONTRAST AT 0.55 MICRON	PLUME PERCEPT-IBILITY E(L*A*B*)
1.	5.0	1.2	0.951	-.020	1.90
2.	5.0	0.9	0.941	-.020	2.29
5.	5.0	0.6	0.919	-.022	3.15
10.	5.0	0.5	0.902	-.025	3.83
15.	5.0	0.4	0.893	-.026	4.01
20.	5.0	0.4	0.900	-.025	3.93
30.	6.0	0.3	0.913	-.022	3.44
40.	8.0	0.3	0.927	-.019	2.92
50.	9.9	0.3	0.938	-.017	2.52
75.	14.9	0.3	0.957	-.014	1.83
100.	19.9	0.4	0.970	-.011	1.36
150.	29.8	0.5	0.983	-.009	0.83
200.	39.8	0.6	0.991	-.007	0.52
250.	49.7	0.8	0.995	-.005	0.33
300.	59.7	1.0	0.997	-.004	0.20
350.	69.6	1.4	0.998	-.003	0.12

500MW COAL-FIRED PLANT
PASQUILL-GIFFORD D
WIND SPEED = 5.0 M/S
BACKGROUND VISUAL RANGE = 20. KM

DOWNWIND DISTANCE (KM)	PLUME-OBSERVER DISTANCE (KM)	VISUAL RANGE REDUCTION (%)	BLUE-RED RATIO	PLUME CONTRAST AT 0.55 MICRON	PLUME PERCEPT-IBILITY E(L*A*B*)
1.	5.0	1.2	0.994	-.003	0.37
2.	5.0	0.9	0.991	-.004	0.53
5.	5.0	0.6	0.987	-.005	0.81
10.	5.0	0.5	0.984	-.006	0.95
15.	5.0	0.5	0.985	-.006	0.91
20.	5.0	0.4	0.986	-.006	0.83
30.	6.0	0.4	0.991	-.004	0.53
40.	8.0	0.4	0.996	-.002	0.26
50.	9.9	0.4	0.998	-.001	0.13
75.	14.9	0.3	1.000	-.000	0.03
100.	19.9	0.2	1.000	-.000	0.01
150.	29.8	0.0	1.000	-.000	0.00
200.	39.8	0.0	1.000	-.000	0.00
250.	49.7	0.0	1.000	-.000	0.00
300.	59.7	0.0	1.000	-.000	0.00
350.	69.6	0.0	1.000	-.000	0.00

500MW COAL-FIRED PLANT
PASQUILL-GIFFORD D
WIND SPEED = 5.0 M/S
BACKGROUND VISUAL RANGE = 50. KM

DOWNWIND DISTANCE (KM)	PLUME-OBSERVER DISTANCE (KM)	VISUAL RANGE REDUCTION (%)	BLUE-RED RATIO	PLUME CONTRAST AT 0.55 MICRON	PLUME PERCEPT-IBILITY E(L*A*B*)
1.	5.0	1.1	0.984	-.006	0.74
2.	5.0	0.8	0.977	-.007	1.04
5.	5.0	0.5	0.964	-.010	1.59
10.	5.0	0.4	0.958	-.012	1.85
15.	5.0	0.3	0.960	-.011	1.78
20.	5.0	0.3	0.963	-.010	1.63
30.	6.0	0.3	0.973	-.008	1.23
40.	8.0	0.3	0.982	-.006	0.84
50.	9.9	0.3	0.988	-.005	0.59
75.	14.9	0.3	0.995	-.003	0.26
100.	19.9	0.3	0.998	-.002	0.12
150.	29.8	0.4	1.000	-.001	0.03
200.	39.8	0.4	1.000	-.000	0.01
250.	49.7	0.2	1.000	-.000	0.00
300.	59.7	0.1	1.000	-.000	0.00
350.	69.6	0.0	1.000	-.000	0.00

500MW COAL-FIRED PLANT
PASQUILL-GIFFORD D
WIND SPEED = 5.0 M/S
BACKGROUND VISUAL RANGE = 100. KM

DOWNWIND DISTANCE (KM)	PLUME-OBSERVER DISTANCE (KM)	VISUAL RANGE REDUCTION (%)	BLUE-RED RATIO	PLUME CONTRAST AT 0.55 MICRON	PLUME PERCEPT-IBILITY E(L*A*B*)
1.	5.0	1.1	0.977	-.010	0.97
2.	5.0	0.7	0.967	-.010	1.33
5.	5.0	0.4	0.950	-.013	2.00
10.	5.0	0.3	0.942	-.015	2.33
15.	5.0	0.3	0.944	-.014	2.23
20.	5.0	0.2	0.949	-.013	2.05
30.	6.0	0.2	0.960	-.010	1.63
40.	8.0	0.2	0.970	-.008	1.25
50.	9.9	0.2	0.977	-.007	0.98
75.	14.9	0.2	0.987	-.005	0.58
100.	19.9	0.3	0.993	-.003	0.36
150.	29.8	0.4	0.998	-.002	0.13
200.	39.8	0.4	0.999	-.001	0.05
250.	49.7	0.4	1.000	-.001	0.03
300.	59.7	0.3	1.000	-.000	0.01
350.	69.6	0.3	1.000	-.000	0.01

500MW COAL-FIRED PLANT
PASQUILL-GIFFORD D
WIND SPEED = 5.0 M/S
BACKGROUND VISUAL RANGE = 200. KM

DOWNWIND DISTANCE (KM)	PLUME-OBSERVER DISTANCE (KM)	VISUAL RANGE REDUCTION (%)	BLUE-RED RATIO	PLUME CONTRAST AT 0.55 MICRON	PLUME PERCEPT-IBILITY E(L*A*B*)
1.	5.0	1.0	0.970	-.014	1.16
2.	5.0	0.6	0.960	-.013	1.54
5.	5.0	0.4	0.941	-.016	2.29
10.	5.0	0.3	0.931	-.017	2.66
15.	5.0	0.2	0.934	-.016	2.55
20.	5.0	0.2	0.939	-.014	2.34
30.	6.0	0.2	0.951	-.012	1.91
40.	8.0	0.2	0.961	-.010	1.55
50.	9.9	0.2	0.968	-.009	1.29
75.	14.9	0.2	0.979	-.007	0.88
100.	19.9	0.2	0.986	-.005	0.63
150.	29.8	0.3	0.993	-.004	0.32
200.	39.8	0.3	0.997	-.003	0.17
250.	49.7	0.3	0.998	-.002	0.11
300.	59.7	0.3	0.999	-.001	0.07
350.	69.6	0.3	0.999	-.001	0.05

500MW COAL-FIRED PLANT
PASQUILL-GIFFORD E
WIND SPEED = 2.5 M/S
BACKGROUND VISUAL RANGE 20. KM

DOWNWIND DISTANCE (KM)	PLUME-OBSERVER DISTANCE (KM)	VISUAL RANGE REDUCTION (%)	BLUE-RED RATIO	PLUME CONTRAST AT 0.55 MICRON	PLUME PERCEPT-IBILITY E(L*A*B*)
1.	5.0	2.9	0.989	-.006	0.74
2.	5.0	2.2	0.987	-.005	0.85
5.	5.0	1.5	0.981	-.003	1.14
10.	5.0	1.3	0.976	-.010	1.47
15.	5.0	1.2	0.972	-.012	1.67
20.	5.0	1.2	0.970	-.012	1.80
30.	6.0	1.2	0.977	-.011	1.45
40.	8.0	1.3	0.983	-.008	0.81
50.	9.9	1.3	0.994	-.005	0.44
75.	14.9	1.2	0.999	-.002	0.10
100.	19.9	0.6	1.000	-.001	0.06
150.	29.8	0.0	1.000	-.000	0.00
200.	39.8	0.0	1.000	-.000	0.00
250.	49.7	0.0	1.000	-.000	0.00
300.	59.7	0.0	1.000	-.000	0.00
350.	69.6	0.0	1.000	-.000	0.00

500MW COAL-FIRED PLANT
PASQUILL-GIFFORD E
WIND SPEED = 2.5 M/S
BACKGROUND VISUAL RANGE = 50. KM

DOWNWIND DISTANCE (KM)	PLUME-OBSERVER DISTANCE (KM)	VISUAL RANGE REDUCTION (%)	BLUE-RED RATIO	PLUME CONTRAST AT 0.55 MICRON	PLUME PERCEPT-IBILITY E(L*A*B*)
1.	5.0	2.7	0.969	-.013	1.50
2.	5.0	2.0	0.964	-.014	1.70
5.	5.0	1.3	0.950	-.016	2.26
10.	5.0	1.1	0.936	-.019	2.90
15.	5.0	1.0	0.927	-.021	3.30
20.	5.0	0.9	0.921	-.023	3.56
30.	6.0	0.9	0.927	-.023	3.38
40.	8.0	0.9	0.945	-.020	2.64
50.	9.9	1.0	0.960	-.016	2.01
75.	14.9	1.1	0.982	-.010	0.98
100.	19.9	1.1	0.993	-.006	0.47
150.	29.8	1.2	0.999	-.002	0.13
200.	39.8	1.3	1.000	-.001	0.04
250.	49.7	0.7	1.000	-.000	0.02
300.	59.7	0.2	1.000	-.000	0.01
350.	69.6	0.0	1.000	-.000	0.00

500MW COAL-FIRED PLANT
PASQUILL-GIFFORD E
WIND SPEED = 2.5 M/S
BACKGROUND VISUAL RANGE = 100. KM

DOWNWIND DISTANCE (KM)	PLUME-OBSERVER DISTANCE (KM)	VISUAL RANGE REDUCTION (%)	BLUE-RED RATIO	PLUME CONTRAST AT 0.55 MICRON	PLUME PERCEPT-IBILITY E(L*A*B*)
1.	5.0	2.5	0.954	-.020	1.97
2.	5.0	1.8	0.943	-.019	2.19
5.	5.0	1.2	0.930	-.021	2.88
10.	5.0	0.9	0.910	-.025	3.68
15.	5.0	0.8	0.898	-.027	4.17
20.	5.0	0.8	0.890	-.029	4.50
30.	6.0	0.7	0.892	-.030	4.52
40.	8.0	0.7	0.907	-.027	3.97
50.	9.9	0.8	0.922	-.025	3.39
75.	14.9	0.8	0.953	-.019	2.20
100.	19.9	0.9	0.972	-.014	1.40
150.	29.8	1.1	0.990	-.008	0.62
200.	39.8	1.2	0.996	-.005	0.29
250.	49.7	1.3	0.999	-.003	0.16
300.	59.7	1.5	1.000	-.002	0.08
350.	69.6	1.8	1.000	-.001	0.05

500MW COAL-FIRED PLANT
PASQUILL-GIFFORD E
WIND SPEED = 2.5 M/S
BACKGROUND VISUAL RANGE = 200. KM

DOWNWIND DISTANCE (KM)	PLUME-OBSERVER DISTANCE (KM)	VISUAL RANGE REDUCTION (%)	BLUE-RED RATIO	PLUME CONTRAST AT 0.55 MICRON	PLUME PERCEPT-IBILITY E(L*A*B*)
1.	5.0	2.2	0.940	-.030	2.38
2.	5.0	1.6	0.933	-.027	2.59
5.	5.0	1.1	0.914	-.027	3.33
10.	5.0	0.8	0.892	-.030	4.23
15.	5.0	0.7	0.879	-.032	4.79
20.	5.0	0.6	0.870	-.034	5.16
30.	6.0	0.6	0.867	-.035	5.32
40.	8.0	0.6	0.879	-.033	4.96
50.	9.9	0.6	0.892	-.031	4.50
75.	14.9	0.6	0.922	-.026	3.37
100.	19.9	0.7	0.946	-.021	2.43
150.	29.8	0.9	0.971	-.016	1.46
200.	39.8	1.0	0.984	-.012	0.90
250.	49.7	1.2	0.990	-.010	0.61
300.	59.7	1.3	0.994	-.008	0.40
350.	69.6	1.7	0.997	-.006	0.26

500MW COAL-FIRED PLANT
PASQUILL-GIFFORD E
WIND SPEED = 5.0 M/S
BACKGROUND VISUAL RANGE = 20. KM

DOWNWIND DISTANCE (KM)	PLUME-OBSERVER DISTANCE (KM)	VISUAL RANGE REDUCTION (%)	BLUE-RED RATIO	PLUME CONTRAST AT 0.55 MICRON	PLUME PERCEPT-IBILITY E(L*A*B*)
1.	5.0	1.7	0.994	-.003	0.42
2.	5.0	1.2	0.992	-.004	0.52
5.	5.0	0.9	0.987	-.006	0.81
10.	5.0	0.7	0.982	-.007	1.06
15.	5.0	0.7	0.980	-.008	1.18
20	5.0	0.7	0.980	-.008	1.23
30.	6.0	0.7	0.986	-.007	0.91
40.	8.0	0.7	0.993	-.004	0.48
50.	9.9	0.7	0.997	-.003	0.25
75.	14.9	0.7	1.000	-.001	0.06
100.	19.9	0.3	1.000	-.000	0.01
150.	29.8	0.0	1.000	-.000	0.00
200.	39.8	0.0	1.000	-.000	0.00
250.	49.7	0.0	1.000	-.000	0.00
300.	59.7	0.0	1.000	-.000	0.00
350.	69.6	0.0	1.000	-.000	0.00

500MW COAL-FIRED PLANT
PASQUILL-GIFFORD E
WIND SPEED = 5.0 M/S
BACKGROUND VISUAL RANGE = 50. KM

DOWNWIND DISTANCE (KM)	PLUME-OBSERVER DISTANCE (KM)	VISUAL RANGE REDUCTION (%)	BLUE-RED RATIO	PLUME CONTRAST AT 0.55 MICRON	PLUME PERCEPT-IBILITY E(L*A*B*)
1.	5.0	1.6	0.982	-.003	0.86
2.	5.0	1.1	0.977	-.005	1.04
5.	5.0	0.7	0.964	-.011	1.59
10.	5.0	0.6	0.953	-.013	2.08
15.	5.0	0.5	0.948	-.015	2.33
20.	5.0	0.5	0.946	-.015	2.41
30.	6.0	0.5	0.954	-.014	2.10
40.	8.0	0.5	0.967	-.011	1.56
50.	9.9	0.5	0.977	-.009	1.15
75.	14.9	0.6	0.990	-.005	0.54
100.	19.9	0.6	0.996	-.003	0.26
150.	29.8	0.6	0.999	-.001	0.06
200.	39.8	0.6	1.000	-.000	0.02
250.	49.7	0.3	1.000	-.000	0.01
300.	59.7	0.1	1.000	-.000	0.00
350.	69.6	0.0	1.000	-.000	0.00

500MW COAL-FIRED PLANT
PASQUILL-GIFFORD E
WIND SPEED = 5.0 M/S
BACKGROUND VISUAL RANGE = 100. KM

DOWNWIND DISTANCE (KM)	PLUME-OBSERVER DISTANCE (KM)	VISUAL RANGE REDUCTION (%)	BLUE-RED RATIO	PLUME CONTRAST AT 0.55 MICRON	PLUME PERCEPT-IBILITY E(L*A*B*)
1.	5.0	1.5	0.974	-.012	1.13
2.	5.0	1.0	0.968	-.012	1.33
5.	5.0	0.6	0.950	-.014	2.01
10.	5.0	0.5	0.935	-.017	2.63
15.	5.0	0.4	0.928	-.019	2.93
20.	5.0	0.4	0.925	-.019	3.04
30.	6.0	0.4	0.932	-.018	2.80
40.	8.0	0.4	0.945	-.016	2.32
50.	9.9	0.4	0.955	-.014	1.92
75.	14.9	0.4	0.974	-.010	1.20
100.	19.9	0.5	0.985	-.007	0.76
150.	29.8	0.5	0.995	-.004	0.30
200.	39.8	0.5	0.998	-.002	0.13
250.	49.7	0.6	1.000	-.001	0.05
300.	59.7	0.5	1.000	-.001	0.03
350.	69.6	0.5	1.000	-.000	0.01

500MW COAL-FIRED PLANT
PASQUILL-GIFFORD E
WIND SPEED = 5.0 M/S
BACKGROUND VISUAL RANGE = 200. KM

DOWNWIND DISTANCE (KM)	PLUME-OBSERVER DISTANCE (KM)	VISUAL RANGE REDUCTION (%)	BLUE-RED RATIO	PLUME CONTRAST AT 0.55 MICRON	PLUME PERCEPT-IBILITY E(L*A*B*)
1.	5.0	1.4	0.965	-.018	1.37
2.	5.0	0.9	0.959	-.016	1.57
5.	5.0	0.6	0.940	-.017	2.31
10.	5.0	0.4	0.922	-.020	3.01
15.	5.0	0.4	0.914	-.021	3.35
20.	5.0	0.3	0.911	-.022	3.47
30.	6.0	0.3	0.916	-.021	3.29
40.	8.0	0.3	0.928	-.019	2.89
50.	9.9	0.3	0.938	-.017	2.53
75.	14.9	0.3	0.957	-.014	1.83
100.	19.9	0.4	0.970	-.011	1.33
150.	29.8	0.4	0.986	-.008	0.71
200.	39.8	0.5	0.993	-.005	0.39
250.	49.7	0.5	0.997	-.003	0.21
300.	59.7	0.5	0.998	-.002	0.12
350.	69.6	0.5	0.999	-.002	0.08

500MW COAL-FIRED PLANT
PASQUILL-GIFFORD F
WIND SPEED = 2.5 M/S
BACKGROUND VISUAL RANGE = 20. KM

DOWNWIND DISTANCE (KM)	PLUME-OBSERVER DISTANCE (KM)	VISUAL RANGE REDUCTION (%)	BLUE-RED RATIO	PLUME CONTRAST AT 0.55 MICRON	PLUME PERCEPT-IBILITY E(L*A*B*)
1.	5.0	3.9	0.986	-.008	0.94
2.	5.0	3.1	0.983	-.009	1.10
5.	5.0	2.4	0.979	-.010	1.35
10.	5.0	2.0	0.974	-.012	1.62
15.	5.0	1.8	0.970	-.013	1.83
20.	5.0	1.8	0.967	-.014	1.99
30.	6.0	1.8	0.974	-.013	1.68
40.	8.0	1.9	0.986	-.010	1.00
50.	9.9	2.0	0.993	-.007	0.59
75.	14.9	2.2	0.999	-.003	0.16
100.	19.9	1.1	1.000	-.001	0.05
150.	29.8	0.0	1.000	-.000	0.01
200.	39.8	0.0	1.000	-.000	0.00
250.	49.7	0.0	1.000	-.000	0.00
300.	59.7	0.0	1.000	-.000	0.00
350.	69.6	0.0	1.000	-.000	0.00

500MW COAL-FIRED PLANT
PASQUILL-GIFFORD F
WIND SPEED = 2.5 M/S
BACKGROUND VISUAL RANGE = 50. KM

DOWNWIND DISTANCE (KM)	PLUME-OBSERVER DISTANCE (KM)	VISUAL RANGE REDUCTION (%)	BLUE-RED RATIO	PLUME CONTRAST AT 0.55 MICRON	PLUME PERCEPT-IBILITY E(L*A*B*)
1.	5.0	3.6	0.961	-.018	1.92
2.	5.0	2.9	0.953	-.018	2.21
5.	5.0	2.1	0.942	-.020	2.68
10.	5.0	1.7	0.930	-.022	3.21
15.	5.0	1.5	0.920	-.025	3.62
20.	5.0	1.5	0.913	-.026	3.96
30.	6.0	1.4	0.915	-.027	3.94
40.	8.0	1.5	0.932	-.025	3.31
50.	9.9	1.6	0.946	-.023	2.71
75.	14.9	1.8	0.973	-.017	1.56
100.	19.9	2.0	0.987	-.012	0.87
150.	29.8	2.2	0.998	-.005	0.28
200.	39.8	2.3	1.000	-.002	0.10
250.	49.7	1.2	1.000	-.001	0.05
300.	59.7	0.1	1.000	-.000	0.02
350.	69.6	0.0	1.000	-.000	0.01

500MW COAL-FIRED PLANT
PASQUILL-GIFFORD F
WIND SPEED = 2.5 M/S
BACKGROUND VISUAL RANGE = 100. KM

DOWNWIND DISTANCE (KM)	PLUME-OBSERVER DISTANCE (KM)	VISUAL RANGE REDUCTION (%)	BLUE-RED RATIO	PLUME CONTRAST AT 0.55 MICRON	PLUME PERCEPT-IBILITY E(L*A*B*)
1.	5.0	3.4	0.942	-.027	2.53
2.	5.0	2.7	0.932	-.026	2.86
5.	5.0	1.9	0.917	-.027	3.43
10.	5.0	1.5	0.901	-.029	4.08
15.	5.0	1.3	0.889	-.032	4.60
20.	5.0	1.3	0.879	-.034	5.02
30.	6.0	1.2	0.874	-.036	5.30
40.	8.0	1.2	0.885	-.036	4.99
50.	9.9	1.3	0.897	-.035	4.59
75.	14.9	1.4	0.926	-.031	3.51
100.	19.9	1.6	0.950	-.026	2.57
150.	29.8	1.9	0.978	-.018	1.32
200.	39.8	2.1	0.991	-.012	0.69
250.	49.7	2.3	0.997	-.008	0.38
300.	59.7	2.5	0.999	-.005	0.22
350.	69.6	2.8	1.000	-.003	0.14

500MW COAL-FIRED PLANT
PASQUILL-GIFFORD F
WIND SPEED = 2.5 M/S
BACKGROUND VISUAL RANGE = 200. KM

DOWNWIND DISTANCE (KM)	PLUME-OBSERVER DISTANCE (KM)	VISUAL RANGE REDUCTION (%)	BLUE-RED RATIO	PLUME CONTRAST AT 0.55 MICRON	PLUME PERCEPT-IBILITY E(L*A*B*)
1.	5.0	3.1	0.923	-.039	3.06
2.	5.0	2.4	0.913	-.036	3.40
5.	5.0	1.7	0.898	-.035	4.00
10.	5.0	1.3	0.880	-.036	4.72
15.	5.0	1.2	0.866	-.039	5.31
20.	5.0	1.1	0.855	-.041	5.78
30.	6.0	1.0	0.845	-.043	6.27
40.	8.0	1.0	0.849	-.044	6.27
50.	9.9	1.0	0.855	-.045	6.12
75.	14.9	1.1	0.873	-.043	5.41
100.	19.9	1.2	0.902	-.040	4.58
150.	29.8	1.5	0.940	-.033	3.12
200.	39.8	1.7	0.964	-.027	2.11
250.	49.7	1.9	0.978	-.022	1.45
300.	59.7	2.1	0.987	-.018	1.01
350.	69.6	2.5	0.992	-.015	0.72

500MW COAL-FIRED PLANT
PASQUILL-GIFFORD F
WIND SPEED = 5.0 M/S
BACKGROUND VISUAL RANGE = 20. KM

DOWNWIND DISTANCE (KM)	PLUME-OBSERVER DISTANCE (KM)	VISUAL RANGE REDUCTION (%)	BLUE-RED RATIO	PLUME CONTRAST AT 0.55 MICRON	PLUME PERCEPT-IBILITY E(L*A*B*)
1.	5.0	2.3	0.993	-.004	0.47
2.	5.0	1.7	0.992	-.004	0.54
5.	5.0	1.2	0.988	-.005	0.76
10.	5.0	1.1	0.983	-.007	1.03
15.	5.0	1.0	0.980	-.008	1.21
20.	5.0	1.0	0.978	-.009	1.35
30.	6.0	1.0	0.982	-.009	1.15
40.	8.0	1.1	0.990	-.006	0.68
50.	9.9	1.1	0.995	-.004	0.39
75.	14.9	1.2	0.999	-.002	0.10
100.	19.9	0.6	1.000	-.001	0.03
150.	29.8	0.0	1.000	-.000	0.00
200.	39.8	0.0	1.000	-.000	0.00
250.	49.7	0.0	1.000	-.000	0.00
300.	59.7	0.0	1.000	-.000	0.00
350.	69.6	0.0	1.000	-.000	0.00

500MW COAL-FIRED PLANT
PASQUILL-GIFFORD F
WIND SPEED = 5.0 M/S
BACKGROUND VISUAL RANGE = 50. KM

DOWNWIND DISTANCE (KM)	PLUME-OBSERVER DISTANCE (KM)	VISUAL RANGE REDUCTION (%)	BLUE-RED RATIO	PLUME CONTRAST AT 0.55 MICRON	PLUME PERCEPT-IBILITY E(L*A*B*)
1.	5.0	2.1	0.981	-.009	0.97
2.	5.0	1.6	0.977	-.009	1.09
5.	5.0	1.1	0.967	-.011	1.50
10.	5.0	0.9	0.955	-.014	2.03
15.	5.0	0.8	0.947	-.016	2.39
20.	5.0	0.8	0.941	-.017	2.66
30.	6.0	0.8	0.942	-.018	2.67
40.	8.0	0.8	0.953	-.016	2.22
50.	9.9	0.9	0.964	-.014	1.78
75.	14.9	1.0	0.983	-.010	0.97
100.	19.9	1.1	0.992	-.007	0.52
150.	29.8	1.2	0.999	-.003	0.15
200.	39.8	1.2	1.000	-.001	0.05
250.	49.7	0.6	1.000	-.001	0.02
300.	59.7	0.0	1.000	-.000	0.01
350.	69.6	0.0	1.000	-.000	0.01

500MW COAL-FIRED PLANT
PASQUILL-GIFFORD F
WIND SPEED = 5.0 M/S
BACKGROUND VISUAL RANGE = 100. KM

DOWNWIND DISTANCE (KM)	PLUME-OBSERVER DISTANCE (KM)	VISUAL RANGE REDUCTION (%)	BLUE-RED RATIO	PLUME CONTRAST AT 0.55 MICRON	PLUME PERCEPT-IBILITY E(L*A*B*)
1.	5.0	2.0	0.971	-.015	1.28
2.	5.0	1.5	0.966	-.014	1.41
5.	5.0	1.0	0.953	-.015	1.91
10.	5.0	0.8	0.937	-.018	2.57
15.	5.0	0.7	0.926	-.020	3.02
20.	5.0	0.7	0.918	-.022	3.35
30.	6.0	0.6	0.914	-.024	3.57
40.	8.0	0.7	0.922	-.023	3.32
50.	9.9	0.7	0.931	-.022	2.99
75.	14.9	0.8	0.953	-.018	2.17
100.	19.9	0.9	0.970	-.015	1.53
150.	29.8	1.0	0.988	-.010	0.75
200.	39.8	1.1	0.995	-.006	0.37
250.	49.7	1.1	0.998	-.004	0.20
300.	59.7	1.2	0.999	-.003	0.11
350.	69.6	1.2	1.000	-.002	0.07

500MW COAL-FIRED PLANT
PASQUILL-GIFFORD F
WIND SPEED = 5.0 M/S
BACKGROUND VISUAL RANGE = 200. KM

DOWNWIND DISTANCE (KM)	PLUME-OBSERVER DISTANCE (KM)	VISUAL RANGE REDUCTION (%)	BLUE-RED RATIO	PLUME CONTRAST AT 0.55 MICRON	PLUME PERCEPT-IBILITY E(L*A*B*)
1.	5.0	1.8	0.960	-.022	1.58
2.	5.0	1.3	0.957	-.019	1.69
5.	5.0	0.9	0.943	-.019	2.21
10.	5.0	0.7	0.924	-.022	2.95
15.	5.0	0.6	0.911	-.024	3.46
20.	5.0	0.6	0.902	-.026	3.84
30.	6.0	0.5	0.894	-.028	4.21
40.	8.0	0.5	0.898	-.028	4.15
50.	9.9	0.5	0.904	-.028	3.96
75.	14.9	0.6	0.924	-.025	3.32
100.	19.9	0.6	0.941	-.023	2.70
150.	29.8	0.8	0.965	-.018	1.75
200.	39.8	0.9	0.980	-.014	1.14
250.	49.7	1.0	0.988	-.011	0.75
300.	59.7	1.0	0.993	-.009	0.51
350.	69.6	1.1	0.996	-.007	0.36

1000MW COAL-FIRED PLANT
PASQUILL-GIFFORD C
WIND SPEED = 2.5 M/S
BACKGROUND VISUAL RANGE = 20. KM

DOWNWIND DISTANCE (KM)	PLUME-OBSERVER DISTANCE (KM)	VISUAL RANGE REDUCTION (%)	BLUE-RED RATIO	PLUME CONTRAST AT 0.55 MICRON	PLUME PERCEPT-IBILITY E(L*A*B*)
1.	5.0	2.4	0.990	-.005	0.66
2.	5.0	1.5	0.986	-.006	0.86
5.	5.0	0.8	0.985	-.006	0.94
10.	5.0	0.7	0.981	-.008	1.12
15.	5.0	0.7	0.978	-.009	1.33
20.	5.0	0.8	0.976	-.010	1.45
30.	6.0	0.8	0.982	-.008	1.12
40.	8.0	0.9	0.991	-.006	0.62
50.	9.9	0.9	0.996	-.004	0.34
75.	14.9	0.8	0.999	-.001	0.08
100.	19.9	0.5	1.000	-.000	0.02
150.	29.8	0.2	1.000	-.000	0.00
200.	39.8	0.1	1.000	-.000	0.00
250.	49.7	0.0	1.000	-.000	0.00
300.	59.7	0.0	1.000	-.000	0.00
350.	69.6	0.0	1.000	-.000	0.00

1000MW COAL-FIRED PLANT
PASQUILL-GIFFORD C
WIND SPEED = 2.5 M/S
BACKGROUND VISUAL RANGE = 50. KM

DOWNWIND DISTANCE (KM)	PLUME-OBSERVER DISTANCE (KM)	VISUAL RANGE REDUCTION (%)	BLUE-RED RATIO	PLUME CONTRAST AT 0.55 MICRON	PLUME PERCEPT-IBILITY E(L*A*B*)
1.	5.0	2.3	0.973	-.012	1.32
2.	5.0	1.3	0.963	-.012	1.71
5.	5.0	0.7	0.959	-.012	1.84
10.	5.0	0.5	0.950	-.014	2.21
15.	5.0	0.5	0.941	-.017	2.61
20.	5.0	0.6	0.936	-.018	2.86
30.	6.0	0.6	0.943	-.017	2.60
40.	8.0	0.7	0.957	-.015	2.03
50.	9.9	0.7	0.969	-.012	1.55
75.	14.9	0.8	0.986	-.008	0.77
100.	19.9	0.9	0.994	-.005	0.38
150.	29.8	1.1	0.999	-.002	0.11
200.	39.8	1.0	1.000	-.001	0.04
250.	49.7	0.7	1.000	-.000	0.02
300.	59.7	0.5	1.000	-.000	0.01
350.	69.6	0.3	1.000	-.000	0.00

1000MW COAL-FIRED PLANT
PASQUILL-GIFFORD C
WIND SPEED = 2.5 M/S
BACKGROUND VISUAL RANGE = 100. KM

DOWNWIND DISTANCE (KM)	PLUME-OBSERVER DISTANCE (KM)	VISUAL RANGE REDUCTION (%)	BLUE-RED RATIO	PLUME CONTRAST AT 0.55 MICRON	PLUME PERCEPT-IBILITY E(L*A*B*)
1.	5.0	2.1	0.960	-.018	1.73
2.	5.0	1.2	0.947	-.017	2.18
5.	5.0	0.6	0.942	-.016	2.32
10.	5.0	0.4	0.931	-.018	2.78
15.	5.0	0.4	0.919	-.021	3.29
20.	5.0	0.4	0.911	-.022	3.60
30.	6.0	0.5	0.916	-.022	3.47
40.	8.0	0.5	0.928	-.021	3.04
50.	9.9	0.6	0.940	-.019	2.61
75.	14.9	0.7	0.963	-.014	1.72
100.	19.9	0.7	0.977	-.011	1.12
150.	29.8	1.0	0.991	-.007	0.53
200.	39.8	1.2	0.997	-.004	0.26
250.	49.7	1.4	0.999	-.003	0.13
300.	59.7	1.7	1.000	-.002	0.07
350.	69.6	2.2	1.000	-.001	0.04

1000MW COAL-FIRED PLANT
PASQUILL-GIFFORD C
WIND SPEED = 2.5 M/S
BACKGROUND VISUAL RANGE = 200. KM

DOWNWIND DISTANCE (KM)	PLUME-OBSERVER DISTANCE (KM)	VISUAL RANGE REDUCTION (%)	BLUE-RED RATIO	PLUME CONTRAST AT 0.55 MICRON	PLUME PERCEPT-IBILITY E(L*A*B*)
1.	5.0	1.9	0.947	-.026	2.09
2.	5.0	1.1	0.934	-.022	2.54
5.	5.0	0.5	0.931	-.019	2.66
10.	5.0	0.4	0.918	-.021	3.18
15.	5.0	0.4	0.904	-.024	3.76
20.	5.0	0.4	0.895	-.026	4.11
30.	6.0	0.4	0.897	-.026	4.08
40.	8.0	0.4	0.906	-.025	3.78
50.	9.9	0.4	0.916	-.024	3.45
75.	14.9	0.5	0.939	-.020	2.63
100.	19.9	0.6	0.956	-.017	1.99
150.	29.8	0.8	0.975	-.014	1.25
200.	39.8	1.0	0.986	-.011	0.80
250.	49.7	1.2	0.992	-.009	0.52
300.	59.7	1.6	0.995	-.007	0.32
350.	69.6	2.2	0.997	-.005	0.21

1000MW COAL-FIRED PLANT
PASQUILL-GIFFORD C
WIND SPEED = 5.0 M/S
BACKGROUND VISUAL RANGE = 20. KM

DOWNWIND DISTANCE (KM)	PLUME-OBSERVER DISTANCE (KM)	VISUAL RANGE REDUCTION (%)	BLUE-RED RATIO	PLUME CONTRAST AT 0.55 MICRON	PLUME PERCEPT-IBILITY E(L*A*B*)
1.	5.0	1.3	0.992	-.004	0.50
2.	5.0	0.8	0.989	-.005	0.70
5.	5.0	0.5	0.985	-.006	0.88
10.	5.0	0.4	0.986	-.006	0.84
15.	5.0	0.4	0.986	-.006	0.83
20.	5.0	0.4	0.986	-.006	0.85
30.	6.0	0.4	0.990	-.005	0.64
40.	8.0	0.5	0.995	-.003	0.35
50.	9.9	0.5	0.998	-.002	0.19
75.	14.9	0.5	1.000	-.001	0.05
100.	19.9	0.3	1.000	-.000	0.01
150.	29.8	0.1	1.000	-.000	0.00
200.	39.8	0.0	1.000	-.000	0.00
250.	49.7	0.0	1.000	-.000	0.00
300.	59.7	0.0	1.000	-.000	0.00
350.	69.6	0.0	1.000	-.000	0.00

1000MW COAL-FIRED PLANT
PASQUILL-GIFFORD C
WIND SPEED = 5.0 M/S
BACKGROUND VISUAL RANGE = 50. KM

DOWNWIND DISTANCE (KM)	PLUME-OBSERVER DISTANCE (KM)	VISUAL RANGE REDUCTION (%)	BLUE-RED RATIO	PLUME CONTRAST AT 0.55 MICRON	PLUME PERCEPT-IBILITY E(L*A*B*)
1.	5.0	1.2	0.979	-.009	0.99
2.	5.0	0.7	0.969	-.009	1.37
5.	5.0	0.4	0.961	-.011	1.73
10.	5.0	0.3	0.963	-.010	1.64
15.	5.0	0.3	0.963	-.010	1.62
20.	5.0	0.3	0.962	-.010	1.66
30.	6.0	0.3	0.967	-.010	1.47
40.	8.0	0.4	0.976	-.008	1.14
50.	9.9	0.4	0.982	-.007	0.88
75.	14.9	0.5	0.992	-.004	0.45
100.	19.9	0.5	0.996	-.003	0.23
150.	29.3	0.6	0.999	-.001	0.06
200.	39.8	0.5	1.000	-.000	0.02
250.	49.7	0.4	1.000	-.000	0.01
300.	59.7	0.2	1.000	-.000	0.00
350.	69.6	0.1	1.000	-.000	0.00

1000MW COAL-FIRED PLANT
PASQUILL-GIFFORD C
WIND SPEED = 5.0 M/S
BACKGROUND VISUAL RANGE = 100. KM

DOWNWIND DISTANCE (KM)	PLUME-OBSERVER DISTANCE (KM)	VISUAL RANGE REDUCTION (%)	BLUE-RED RATIO	PLUME CONTRAST AT 0.55 MICRON	PLUME PERCEPT-IBILITY E(L*A*B*)
1.	5.0	1.1	0.969	-.012	1.28
2.	5.0	0.6	0.957	-.012	1.73
5.	5.0	0.3	0.946	-.014	2.18
10.	5.0	0.2	0.948	-.013	2.06
15.	5.0	0.2	0.949	-.013	2.04
20.	5.0	0.2	0.948	-.013	2.08
30.	6.0	0.2	0.952	-.012	1.95
40.	8.0	0.3	0.959	-.011	1.70
50.	9.9	0.3	0.966	-.010	1.46
75.	14.9	0.4	0.978	-.008	0.99
100.	19.9	0.4	0.987	-.006	0.67
150.	29.8	0.5	0.995	-.004	0.29
200.	39.8	0.6	0.998	-.002	0.12
250.	49.7	0.7	1.000	-.001	0.05
300.	59.7	0.7	1.000	-.001	0.03
350.	69.6	0.6	1.000	-.000	0.02

1000MW COAL-FIRED PLANT
PASQUILL-GIFFORD C
WIND SPEED = 5.0 M/S
BACKGROUND VISUAL RANGE = 200. KM

DOWNWIND DISTANCE (KM)	PLUME-OBSERVER DISTANCE (KM)	VISUAL RANGE REDUCTION (%)	BLUE-RED RATIO	PLUME CONTRAST AT 0.55 MICRON	PLUME PERCEPT-IBILITY E(L*A*B*)
1.	5.0	1.0	0.961	-.016	1.51
2.	5.0	0.6	0.948	-.015	2.00
5.	5.0	0.3	0.935	-.016	2.49
10.	5.0	0.2	0.939	-.015	2.35
15.	5.0	0.2	0.940	-.014	2.32
20.	5.0	0.2	0.939	-.015	2.37
30.	6.0	0.2	0.941	-.014	2.29
40.	8.0	0.2	0.947	-.014	2.11
50.	9.9	0.2	0.952	-.013	1.93
75.	14.9	0.3	0.964	-.011	1.51
100.	19.9	0.3	0.974	-.010	1.18
150.	29.8	0.5	0.986	-.007	0.68
200.	39.8	0.5	0.993	-.005	0.39
250.	49.7	0.6	0.996	-.004	0.22
300.	59.7	0.6	0.998	-.003	0.14
350.	69.6	0.6	0.999	-.002	0.10

1000MW COAL-FIRED PLANT
PASQUILL-GIFFORD D
WIND SPEED = 2.5 M/S
BACKGROUND VISUAL RANGE = 20. KM

DOWNWIND DISTANCE (KM)	PLUME-OBSERVER DISTANCE (KM)	VISUAL RANGE REDUCTION (%)	BLUE-RED RATIO	PLUME CONTRAST AT 0.55 MICRON	PLUME PERCEPT-IBILITY E(L*A*B*)
1.	5.0	3.0	0.983	-.006	0.79
2.	5.0	2.5	0.985	-.007	0.97
5.	5.0	1.8	0.978	-.010	1.38
10.	5.0	1.5	0.971	-.012	1.77
15.	5.0	1.4	0.968	-.014	1.95
20.	5.0	1.3	0.967	-.014	2.03
30.	6.0	1.3	0.976	-.012	1.52
40.	8.0	1.3	0.988	-.008	0.82
50.	9.9	1.3	0.994	-.005	0.44
75.	14.9	1.1	0.999	-.002	0.10
100.	19.9	0.6	1.000	-.001	0.03
150.	29.8	0.1	1.000	-.000	0.00
200.	39.8	0.0	1.000	-.000	0.00
250.	49.7	0.0	1.000	-.000	0.00
300.	59.7	0.0	1.000	-.000	0.00
350.	69.6	0.0	1.000	-.000	0.00

1000MW COAL-FIRED PLANT
PASQUILL-GIFFORD D
WIND SPEED = 2.5 M/S
BACKGROUND VISUAL RANGE = 50. KM

DOWNWIND DISTANCE (KM)	PLUME-OBSERVER DISTANCE (KM)	VISUAL RANGE REDUCTION (%)	BLUE-RED RATIO	PLUME CONTRAST AT 0.55 MICRON	PLUME PERCEPT-IBILITY E(L*A*B*)
1.	5.0	2.8	0.967	-.014	1.59
2.	5.0	2.2	0.959	-.015	1.93
5.	5.0	1.6	0.940	-.019	2.74
10.	5.0	1.2	0.923	-.023	3.51
15.	5.0	1.1	0.915	-.025	3.87
20.	5.0	1.0	0.911	-.026	4.02
30.	6.0	0.9	0.923	-.024	3.56
40.	8.0	0.9	0.944	-.020	2.68
50.	9.9	1.0	0.959	-.016	2.02
75.	14.9	1.0	0.982	-.010	1.00
100.	19.9	1.1	0.992	-.006	0.51
150.	29.8	1.2	0.999	-.003	0.15
200.	39.8	1.1	1.000	-.001	0.05
250.	49.7	0.7	1.000	-.001	0.02
300.	59.7	0.3	1.000	-.000	0.01
350.	69.6	0.1	1.000	-.000	0.00

1000MW COAL-FIRED PLANT
PASQUILL-GIFFORD D
WIND SPEED = 2.5 M/S
BACKGROUND VISUAL RANGE = 100. KM

DOWNWIND DISTANCE (KM)	PLUME-OBSERVER DISTANCE (KM)	VISUAL RANGE REDUCTION (%)	BLUE-RED RATIO	PLUME CONTRAST AT 0.55 MICRON	PLUME PERCEPT-IBILITY E(L*A*B*)
1.	5.0	2.6	0.951	-.022	2.09
2.	5.0	2.1	0.941	-.022	2.49
5.	5.0	1.4	0.915	-.026	3.48
10.	5.0	1.1	0.892	-.030	4.44
15.	5.0	0.9	0.881	-.032	4.90
20.	5.0	0.8	0.877	-.033	5.09
30.	6.0	0.7	0.886	-.031	4.77
40.	8.0	0.7	0.906	-.028	4.03
50.	9.9	0.7	0.922	-.025	3.40
75.	14.9	0.8	0.952	-.019	2.25
100.	19.9	0.8	0.970	-.014	1.49
150.	29.8	1.0	0.988	-.009	0.73
200.	39.8	1.2	0.995	-.006	0.37
250.	49.7	1.3	0.998	-.004	0.20
300.	59.7	1.5	1.000	-.003	0.11
350.	69.6	1.7	1.000	-.002	0.07

1000MW COAL-FIRED PLANT
PASQUILL-GIFFORD D
WIND SPEED = 2.5 M/S
BACKGROUND VISUAL RANGE = 200. KM

DOWNWIND DISTANCE (KM)	PLUME-OBSERVER DISTANCE (KM)	VISUAL RANGE REDUCTION (%)	BLUE-RED RATIO	PLUME CONTRAST AT 0.55 MICRON	PLUME PERCEPT-IBILITY E(L*A*B*)
1.	5.0	2.4	0.936	-.031	2.53
2.	5.0	1.9	0.925	-.030	2.94
5.	5.0	1.3	0.897	-.032	4.03
10.	5.0	0.9	0.871	-.036	5.11
15.	5.0	0.8	0.859	-.038	5.63
20.	5.0	0.7	0.854	-.038	5.84
30.	6.0	0.6	0.860	-.037	5.62
40.	8.0	0.6	0.877	-.034	5.04
50.	9.9	0.6	0.892	-.031	4.50
75.	14.9	0.6	0.921	-.026	3.44
100.	19.9	0.6	0.942	-.022	2.64
150.	29.8	0.8	0.966	-.018	1.71
200.	39.8	1.0	0.980	-.014	1.13
250.	49.7	1.1	0.988	-.012	0.77
300.	59.7	1.3	0.993	-.009	0.52
350.	69.6	1.6	0.996	-.007	0.35

1000MW COAL-FIRED PLANT
PASQUILL-GIFFORD D
WIND SPEED = 5.0 M/S
BACKGROUND VISUAL RANGE = 20. KM

DOWNWIND DISTANCE (KM)	PLUME-OBSERVER DISTANCE (KM)	VISUAL RANGE REDUCTION (%)	BLUE-RED RATIO	PLUME CONTRAST AT 0.55 MICRON	PLUME PERCEPT-IBILITY E(L*A*B*)
1.	5.0	2.4	0.993	-.004	0.49
2.	5.0	1.6	0.990	-.005	0.64
5.	5.0	1.1	0.983	-.007	1.02
10.	5.0	0.9	0.978	-.009	1.32
15.	5.0	0.8	0.976	-.010	1.42
20.	5.0	0.8	0.976	-.010	1.42
30.	6.0	0.7	0.984	-.007	0.98
40.	8.0	0.7	0.993	-.004	0.49
50.	9.9	0.7	0.997	-.003	0.25
75.	14.9	0.6	1.000	-.001	0.05
100.	19.9	0.3	1.000	-.000	0.01
150.	29.8	0.0	1.000	-.000	0.00
200.	39.8	0.0	1.000	-.000	0.00
250.	49.7	0.0	1.000	-.000	0.00
300.	59.7	0.0	1.000	-.000	0.00
350.	69.6	0.0	1.000	-.000	0.00

1000MW COAL-FIRED PLANT
PASQUILL-GIFFORD D
WIND SPEED = 5.0 M/S
BACKGROUND VISUAL RANGE = 50. KM

DOWNWIND DISTANCE (KM)	PLUME-OBSERVER DISTANCE (KM)	VISUAL RANGE REDUCTION (%)	BLUE-RED RATIO	PLUME CONTRAST AT 0.55 MICRON	PLUME PERCEPT-IBILITY E(L*A*B*)
1.	5.0	2.3	0.980	-.010	1.00
2.	5.0	1.5	0.973	-.010	1.28
5.	5.0	0.9	0.955	-.014	2.01
10.	5.0	0.7	0.942	-.017	2.59
15.	5.0	0.6	0.937	-.018	2.80
20.	5.0	0.6	0.937	-.018	2.80
30.	6.0	0.5	0.950	-.015	2.27
40.	8.0	0.5	0.966	-.012	1.60
50.	9.9	0.5	0.977	-.009	1.15
75.	14.9	0.5	0.990	-.005	0.53
100.	19.9	0.6	0.996	-.003	0.26
150.	29.8	0.6	0.999	-.001	0.06
200.	39.8	0.5	1.000	-.000	0.02
250.	49.7	0.3	1.000	-.000	0.01
300.	59.7	0.1	1.000	-.000	0.00
350.	69.6	0.0	1.000	-.000	0.00

1000MW COAL-FIRED PLANT
PASQUILL-GIFFORD D
WIND SPEED = 5.0 M/S
BACKGROUND VISUAL RANGE = 100. KM

DOWNWIND DISTANCE (KM)	PLUME-OBSERVER DISTANCE (KM)	VISUAL RANGE REDUCTION (%)	BLUE-RED RATIO	PLUME CONTRAST AT 0.55 MICRON	PLUME PERCEPT-IBILITY E(L*A*B*)
1.	5.0	2.1	0.970	-.016	1.33
2.	5.0	1.3	0.961	-.015	1.64
5.	5.0	0.8	0.937	-.018	2.54
10.	5.0	0.6	0.919	-.021	3.27
15.	5.0	0.5	0.913	-.022	3.54
20.	5.0	0.5	0.913	-.022	3.52
30.	6.0	0.4	0.926	-.019	3.02
40.	8.0	0.4	0.943	-.016	2.40
50.	9.9	0.4	0.955	-.014	1.93
75.	14.9	0.4	0.974	-.010	1.18
100.	19.9	0.5	0.985	-.007	0.75
150.	29.8	0.5	0.995	-.004	0.31
200.	39.8	0.6	0.998	-.002	0.14
250.	49.7	0.6	0.999	-.001	0.06
300.	59.7	0.6	1.000	-.001	0.03
350.	69.6	0.6	1.000	-.000	0.02

1000MW COAL-FIRED PLANT
PASQUILL-GIFFORD D
WIND SPEED = 5.0 M/S
BACKGROUND VISUAL RANGE = 200. KM

DOWNWIND DISTANCE (KM)	PLUME-OBSERVER DISTANCE (KM)	VISUAL RANGE REDUCTION (%)	BLUE-RED RATIO	PLUME CONTRAST AT 0.55 MICRON	PLUME PERCEPT-IBILITY E(L*A*B*)
1.	5.0	1.9	0.959	-.023	1.64
2.	5.0	1.2	0.950	-.020	1.94
5.	5.0	0.7	0.924	-.022	2.93
10.	5.0	0.5	0.904	-.025	3.75
15.	5.0	0.4	0.897	-.026	4.04
20.	5.0	0.4	0.897	-.025	4.03
30.	6.0	0.3	0.910	-.023	3.55
40.	8.0	0.3	0.926	-.020	2.98
50.	9.9	0.3	0.938	-.017	2.54
75.	14.9	0.3	0.953	-.014	1.79
100.	19.9	0.4	0.970	-.011	1.33
150.	29.8	0.4	0.985	-.008	0.74
200.	39.8	0.5	0.992	-.006	0.43
250.	49.7	0.5	0.996	-.004	0.25
300.	59.7	0.6	0.998	-.003	0.15
350.	69.6	0.6	0.999	-.002	0.10

1000MW COAL-FIRED PLANT
PASQUILL-GIFFORD E
WIND SPEED = 2.5 M/S
BACKGROUND VISUAL RANGE = 20. KM

DOWNWIND DISTANCE (KM)	PLUME-OBSERVER DISTANCE (KM)	VISUAL RANGE REDUCTION (%)	BLUE-RED RATIO	PLUME CONTRAST AT 0.55 MICRON	PLUME PERCEPT-IBILITY E(L*A*B*)
1.	5.0	5.7	0.983	-.010	1.18
2.	5.0	4.3	0.978	-.011	1.43
5.	5.0	3.0	0.972	-.013	1.75
10.	5.0	2.4	0.966	-.015	2.09
15.	5.0	2.2	0.962	-.017	2.35
20.	5.0	2.1	0.959	-.018	2.54
30.	6.0	2.1	0.967	-.017	2.09
40.	8.0	2.2	0.983	-.012	1.22
50.	9.9	2.3	0.991	-.008	0.70
75.	14.9	2.2	0.999	-.003	0.18
100.	19.9	1.1	1.000	-.001	0.05
150.	29.8	0.0	1.000	-.000	0.01
200.	39.8	0.0	1.000	-.000	0.00
250.	49.7	0.0	1.000	-.000	0.00
300.	59.7	0.0	1.000	-.000	0.00
350.	69.6	0.0	1.000	-.000	0.00

1000MW COAL-FIRED PLANT
PASQUILL-GIFFORD E
WIND SPEED = 2.5 M/S
BACKGROUND VISUAL RANGE = 50. KM

DOWNWIND DISTANCE (KM)	PLUME-OBSERVER DISTANCE (KM)	VISUAL RANGE REDUCTION (%)	BLUE-RED RATIO	PLUME CONTRAST AT 0.55 MICRON	PLUME PERCEPT-IBILITY E(L*A*B*)
1.	5.0	5.3	0.952	-.023	2.41
2.	5.0	3.9	0.940	-.024	2.88
5.	5.0	2.6	0.925	-.026	3.48
10.	5.0	2.0	0.909	-.029	4.16
15.	5.0	1.8	0.893	-.032	4.67
20.	5.0	1.7	0.880	-.034	5.05
30.	6.0	1.6	0.895	-.034	4.93
40.	8.0	1.7	0.917	-.031	4.03
50.	9.9	1.8	0.937	-.027	3.20
75.	14.9	1.9	0.970	-.018	1.69
100.	19.9	1.9	0.987	-.011	0.86
150.	29.8	2.1	0.998	-.005	0.25
200.	39.8	2.1	1.000	-.002	0.09
250.	49.7	1.2	1.000	-.001	0.04
300.	59.7	0.3	1.000	-.000	0.02
350.	69.6	0.0	1.000	-.000	0.01

1000MW COAL-FIRED PLANT
PASQUILL-GIFFORD E
WIND SPEED = 2.5 M/S
BACKGROUND VISUAL RANGE = 100. KM

DOWNWIND DISTANCE (KM)	PLUME-OBSERVER DISTANCE (KM)	VISUAL RANGE REDUCTION (%)	BLUE-RED RATIO	PLUME CONTRAST AT 0.55 MICRON	PLUME PERCEPT-IBILITY E(L*A*B*)
1.	5.0	5.0	0.928	-.036	3.20
2.	5.0	3.6	0.912	-.035	3.74
5.	5.0	2.4	0.894	-.035	4.46
10.	5.0	1.8	0.873	-.038	5.30
15.	5.0	1.6	0.858	-.041	5.94
20.	5.0	1.4	0.847	-.043	6.43
30.	6.0	1.3	0.844	-.045	6.64
40.	8.0	1.4	0.860	-.044	6.10
50.	9.9	1.4	0.879	-.041	5.44
75.	14.9	1.5	0.920	-.033	3.81
100.	19.9	1.6	0.950	-.026	2.54
150.	29.8	1.8	0.980	-.016	1.22
200.	39.8	2.0	0.992	-.010	0.60
250.	49.7	2.3	0.997	-.007	0.32
300.	59.7	2.4	0.999	-.004	0.18
350.	69.6	2.7	1.000	-.003	0.11

1000MW COAL-FIRED PLANT
PASQUILL-GIFFORD E
WIND SPEED = 2.5 M/S
BACKGROUND VISUAL RANGE = 200. KM

DOWNWIND DISTANCE (KM)	PLUME-OBSERVER DISTANCE (KM)	VISUAL RANGE REDUCTION (%)	BLUE-RED RATIO	PLUME CONTRAST AT 0.55 MICRON	PLUME PERCEPT-IBILITY E(L*A*B*)
1.	5.0	4.5	0.902	-.053	3.93
2.	5.0	3.3	0.888	-.043	4.46
5.	5.0	2.1	0.869	-.045	5.20
10.	5.0	1.6	0.847	-.046	6.13
15.	5.0	1.4	0.830	-.049	6.86
20.	5.0	1.2	0.817	-.051	7.41
30.	6.0	1.1	0.809	-.054	7.88
40.	8.0	1.1	0.817	-.054	7.68
50.	9.9	1.1	0.830	-.053	7.26
75.	14.9	1.2	0.868	-.047	5.88
100.	19.9	1.2	0.903	-.040	4.53
150.	29.8	1.4	0.944	-.031	2.87
200.	39.8	1.7	0.968	-.024	1.84
250.	49.7	2.0	0.981	-.019	1.23
300.	59.7	2.2	0.989	-.015	0.84
350.	69.6	2.4	0.993	-.012	0.59

1000MW COAL-FIRED PLANT
PASQUILL-GIFFORD E
WIND SPEED = 5.0 M/S
BACKGROUND VISUAL RANGE = 20. KM

DOWNWIND DISTANCE (KM)	PLUME-OBSERVER DISTANCE (KM)	VISUAL RANGE REDUCTION (%)	BLUE-RED RATIO	PLUME CONTRAST AT 0.55 MICRON	PLUME PERCEPT-IBILITY E(L*A*B*)
1.	5.0	3.4	0.991	-.006	0.64
2.	5.0	2.3	0.989	-.006	0.74
5.	5.0	1.6	0.983	-.007	1.03
10.	5.0	1.3	0.977	-.010	1.39
15.	5.0	1.2	0.973	-.011	1.61
20.	5.0	1.2	0.971	-.012	1.76
30.	6.0	1.2	0.977	-.011	1.43
40.	8.0	1.2	0.988	-.008	0.81
50.	9.9	1.3	0.994	-.005	0.45
75.	14.9	1.2	0.999	-.002	0.10
100.	19.9	0.6	1.000	-.001	0.03
150.	29.8	0.0	1.000	-.000	0.00
200.	39.8	0.0	1.000	-.000	0.00
250.	49.7	0.0	1.000	-.000	0.00
300.	59.7	0.0	1.000	-.000	0.00
350.	69.6	0.0	1.000	-.000	0.00

1000MW COAL-FIRED PLANT
PASQUILL-GIFFORD E
WIND SPEED = 5.0 M/S
BACKGROUND VISUAL RANGE = 50. KM

DOWNWIND DISTANCE (KM)	PLUME-OBSERVER DISTANCE (KM)	VISUAL RANGE REDUCTION (%)	BLUE-RED RATIO	PLUME CONTRAST AT 0.55 MICRON	PLUME PERCEPT-IBILITY E(L*A*B*)
1.	5.0	3.2	0.974	-.013	1.32
2.	5.0	2.1	0.969	-.012	1.47
5.	5.0	1.4	0.955	-.015	2.05
10.	5.0	1.1	0.939	-.018	2.75
15.	5.0	1.0	0.929	-.021	3.19
20.	5.0	0.9	0.923	-.023	3.48
30.	6.0	0.9	0.927	-.023	3.35
40.	8.0	0.9	0.945	-.020	2.64
50.	9.9	1.0	0.959	-.016	2.03
75.	14.9	1.0	0.982	-.010	1.01
100.	19.9	1.0	0.992	-.006	0.50
150.	29.8	1.1	0.999	-.002	0.13
200.	39.8	1.0	1.000	-.001	0.04
250.	49.7	0.5	1.000	-.000	0.01
300.	59.7	0.1	1.000	-.000	0.01
350.	69.6	0.0	1.000	-.000	0.00

1000MW COAL-FIRED PLANT
PASQUILL-GIFFORD E
WIND SPEED = 5.0 M/S
BACKGROUND VISUAL RANGE = 100. KM

DOWNWIND DISTANCE (KM)	PLUME-OBSERVER DISTANCE (KM)	VISUAL RANGE REDUCTION (%)	BLUE-RED RATIO	PLUME CONTRAST AT 0.55 MICRON	PLUME PERCEPT-IBILITY E(L*A*B*)
1.	5.0	3.0	0.961	-.021	1.76
2.	5.0	2.0	0.955	-.018	1.92
5.	5.0	1.2	0.937	-.020	2.60
10.	5.0	0.9	0.915	-.024	3.48
15.	5.0	0.8	0.902	-.026	4.03
20.	5.0	0.8	0.893	-.028	4.41
30.	6.0	0.7	0.892	-.029	4.48
40.	8.0	0.7	0.907	-.027	3.97
50.	9.9	0.8	0.922	-.025	3.42
75.	14.9	0.8	0.952	-.019	2.26
100.	19.9	0.8	0.971	-.014	1.47
150.	29.8	0.9	0.990	-.008	0.62
200.	39.8	0.9	0.997	-.004	0.27
250.	49.7	0.9	0.999	-.003	0.12
300.	59.7	0.9	1.000	-.001	0.06
350.	69.6	0.9	1.000	-.001	0.03

1000MW COAL-FIRED PLANT
PASQUILL-GIFFORD E
WIND SPEED = 5.0 M/S
BACKGROUND VISUAL RANGE = 200. KM

DOWNWIND DISTANCE (KM)	PLUME-OBSERVER DISTANCE (KM)	VISUAL RANGE REDUCTION (%)	BLUE-RED RATIO	PLUME CONTRAST AT 0.55 MICRON	PLUME PERCEPT-IBILITY E(L*A*B*)
1.	5.0	2.7	0.945	-.031	2.19
2.	5.0	1.8	0.941	-.026	2.29
5.	5.0	1.1	0.922	-.025	3.02
10.	5.0	0.8	0.893	-.029	4.00
15.	5.0	0.7	0.883	-.031	4.63
20.	5.0	0.6	0.872	-.033	5.05
30.	6.0	0.6	0.868	-.035	5.28
40.	8.0	0.6	0.879	-.033	4.96
50.	9.9	0.6	0.891	-.032	4.53
75.	14.9	0.6	0.920	-.026	3.46
100.	19.9	0.6	0.943	-.022	2.60
150.	29.8	0.7	0.971	-.015	1.46
200.	39.8	0.8	0.985	-.011	0.82
250.	49.7	0.8	0.993	-.007	0.48
300.	59.7	0.8	0.996	-.005	0.28
350.	69.6	0.8	0.998	-.004	0.17

1000MW COAL-FIRED PLANT
PASQUILL-GIFFORD F
WIND SPEED = 2.5 M/S
BACKGROUND VISUAL RANGE = 20. KM

DOWNWIND DISTANCE (KM)	PLUME-OBSERVER DISTANCE (KM)	VISUAL RANGE REDUCTION (%)	BLUE-RED RATIO	PLUME CONTRAST AT 0.55 MICRON	PLUME PERCEPT-IBILITY E(L*A*B*)
1.	5.0	7.7	0.978	-.014	1.57
2.	5.0	6.4	0.968	-.017	2.15
5.	5.0	4.6	0.959	-.020	2.63
10.	5.0	3.9	0.955	-.021	2.84
15.	5.0	3.6	0.952	-.022	3.00
20.	5.0	3.4	0.949	-.023	3.16
30.	6.0	3.3	0.961	-.021	2.57
40.	8.0	3.5	0.979	-.015	1.50
50.	9.9	3.6	0.990	-.011	0.88
75.	14.9	3.8	0.999	-.005	0.25
100.	19.9	1.8	1.000	-.002	0.09
150.	29.8	0.0	1.000	-.000	0.01
200.	39.8	0.0	1.000	-.000	0.00
250.	49.7	0.0	1.000	-.000	0.00
300.	59.7	0.0	1.000	-.000	0.00
350.	69.6	0.0	1.000	-.000	0.00

1000MW COAL-FIRED PLANT
PASQUILL-GIFFORD F
WIND SPEED = 2.5 M/S
BACKGROUND VISUAL RANGE = 50. KM

DOWNWIND DISTANCE (KM)	PLUME-OBSERVER DISTANCE (KM)	VISUAL RANGE REDUCTION (%)	BLUE-RED RATIO	PLUME CONTRAST AT 0.55 MICRON	PLUME PERCEPT-IBILITY E(L*A*B*)
1.	5.0	7.3	0.936	-.031	3.22
2.	5.0	5.9	0.910	-.036	4.34
5.	5.0	4.3	0.883	-.040	5.29
10.	5.0	3.4	0.878	-.041	5.70
15.	5.0	3.0	0.871	-.043	6.02
20.	5.0	2.8	0.865	-.044	6.34
30.	6.0	2.7	0.872	-.044	6.09
40.	8.0	2.8	0.899	-.040	5.00
50.	9.9	2.9	0.922	-.036	4.05
75.	14.9	3.2	0.960	-.027	2.34
100.	19.9	3.5	0.981	-.019	1.33
150.	29.8	3.9	0.996	-.009	0.46
200.	39.8	4.2	1.000	-.004	0.19
250.	49.7	1.9	1.000	-.002	0.09
300.	59.7	0.1	1.000	-.001	0.04
350.	69.6	0.0	1.000	-.000	0.02

1000MW COAL-FIRED PLANT
PASQUILL-GIFFORD F
WIND SPEED = 2.5 M/S
BACKGROUND VISUAL RANGE = 100. KM

DOWNWIND DISTANCE (KM)	PLUME-OBSERVER DISTANCE (KM)	VISUAL RANGE REDUCTION (%)	BLUE-RED RATIO	PLUME CONTRAST AT 0.55 MICRON	PLUME PERCEPT-IBILITY E(L*A*B*)
1.	5.0	6.8	0.904	-.048	4.29
2.	5.0	5.4	0.869	-.052	5.66
5.	5.0	3.9	0.841	-.054	6.81
10.	5.0	3.0	0.829	-.054	7.31
15.	5.0	2.7	0.820	-.056	7.72
20.	5.0	2.5	0.810	-.057	8.12
30.	6.0	2.3	0.810	-.059	8.26
40.	8.0	2.3	0.829	-.058	7.62
50.	9.9	2.4	0.848	-.056	6.94
75.	14.9	2.6	0.891	-.050	5.32
100.	19.9	2.9	0.925	-.043	3.96
150.	29.8	3.4	0.966	-.031	2.14
200.	39.8	3.7	0.986	-.021	1.17
250.	49.7	4.0	0.995	-.015	0.68
300.	59.7	4.2	0.999	-.010	0.42
350.	69.6	4.5	1.000	-.007	0.28

1000MW COAL-FIRED PLANT
PASQUILL-GIFFORD F
WIND SPEED = 2.5 M/S
BACKGROUND VISUAL RANGE = 200. KM

DOWNWIND DISTANCE (KM)	PLUME-OBSERVER DISTANCE (KM)	VISUAL RANGE REDUCTION (%)	BLUE-RED RATIO	PLUME CONTRAST AT 0.55 MICRON	PLUME PERCEPT-IBILITY E(L*A*B*)
1.	5.0	6.2	0.871	-.070	5.27
2.	5.0	4.9	0.833	-.071	6.75
5.	5.0	3.5	0.804	-.069	7.98
10.	5.0	2.7	0.792	-.067	8.51
15.	5.0	2.4	0.782	-.068	8.96
20.	5.0	2.2	0.772	-.069	9.42
30.	6.0	2.0	0.765	-.072	9.85
40.	8.0	2.0	0.775	-.072	9.66
50.	9.9	2.0	0.787	-.072	9.34
75.	14.9	2.1	0.820	-.070	8.30
100.	19.9	2.2	0.852	-.067	7.14
150.	29.8	2.6	0.905	-.058	5.08
200.	39.8	3.0	0.941	-.049	3.56
250.	49.7	3.3	0.964	-.041	2.52
300.	59.7	3.6	0.979	-.034	1.82
350.	69.6	4.0	0.987	-.028	1.35

1000MW COAL-FIRED PLANT
PASQUILL-GIFFORD F
WIND SPEED = 5.0 M/S
BACKGROUND VISUAL RANGE = 20. KM

DOWNWIND DISTANCE (KM)	PLUME-OBSERVER DISTANCE (KM)	VISUAL RANGE REDUCTION (%)	BLUE-RED RATIO	PLUME CONTRAST AT 0.55 MICRON	PLUME PERCEPT-IBILITY E(L*A*B*)
1.	5.0	4.5	0.990	-.007	0.76
2.	5.0	3.4	0.987	-.007	0.90
5.	5.0	2.4	0.982	-.008	1.12
10.	5.0	1.9	0.977	-.010	1.41
15.	5.0	1.8	0.973	-.012	1.65
20.	5.0	1.7	0.970	-.013	1.83
30.	6.0	1.8	0.975	-.012	1.58
40.	8.0	1.9	0.987	-.009	0.96
50.	9.9	2.0	0.993	-.007	0.57
75.	14.9	2.1	0.999	-.003	0.16
100.	19.9	1.1	1.000	-.001	0.05
150.	29.8	0.0	1.000	-.000	0.01
200.	39.8	0.0	1.000	-.000	0.00
250.	49.7	0.0	1.000	-.000	0.00
300.	59.7	0.0	1.000	-.000	0.00
350.	69.6	0.0	1.000	-.000	0.00

1000MW COAL-FIRED PLANT
PASQUILL-GIFFORD F
WIND SPEED = 5.0 M/S
BACKGROUND VISUAL RANGE = 50. KM

DOWNWIND DISTANCE (KM)	PLUME-OBSERVER DISTANCE (KM)	VISUAL RANGE REDUCTION (%)	BLUE-RED RATIO	PLUME CONTRAST AT 0.55 MICRON	PLUME PERCEPT-IBILITY E(L*A*B*)
1.	5.0	4.2	0.970	-.016	1.57
2.	5.0	3.1	0.963	-.016	1.81
5.	5.0	2.1	0.952	-.017	2.23
10.	5.0	1.7	0.939	-.020	2.79
15.	5.0	1.5	0.928	-.022	3.26
20.	5.0	1.4	0.920	-.024	3.63
30.	6.0	1.4	0.920	-.026	3.71
40.	8.0	1.5	0.935	-.024	3.16
50.	9.9	1.6	0.943	-.022	2.62
75.	14.9	1.8	0.973	-.016	1.53
100.	19.9	1.9	0.987	-.012	0.86
150.	29.8	2.1	0.993	-.005	0.28
200.	39.8	2.2	1.000	-.002	0.10
250.	49.7	1.1	1.000	-.001	0.05
300.	59.7	0.1	1.000	-.000	0.02
350.	69.6	0.0	1.000	-.000	0.01

1000MW COAL-FIRED PLANT
PASQUILL-GIFFORD F
WIND SPEED = 5.0 M/S
BACKGROUND VISUAL RANGE = 100. KM

DOWNWIND DISTANCE (KM)	PLUME-OBSERVER DISTANCE (KM)	VISUAL RANGE REDUCTION (%)	BLUE-RED RATIO	PLUME CONTRAST AT 0.55 MICRON	PLUME PERCEPT-IBILITY E(L*A*B*)
1.	5.0	4.0	0.953	-.026	2.12
2.	5.0	2.9	0.945	-.024	2.33
5.	5.0	2.0	0.931	-.024	2.86
10.	5.0	1.5	0.914	-.026	3.56
15.	5.0	1.3	0.900	-.029	4.14
20.	5.0	1.2	0.883	-.032	4.61
30.	6.0	1.2	0.881	-.034	4.98
40.	8.0	1.2	0.890	-.034	4.77
50.	9.9	1.3	0.900	-.034	4.44
75.	14.9	1.4	0.927	-.030	3.45
100.	19.9	1.6	0.950	-.026	2.55
150.	29.8	1.8	0.978	-.018	1.33
200.	39.8	1.9	0.991	-.012	0.69
250.	49.7	2.0	0.997	-.008	0.38
300.	59.7	2.1	0.999	-.005	0.22
350.	69.6	2.1	1.000	-.003	0.14

1000MW COAL-FIRED PLANT
PASQUILL-GIFFORD F
WIND SPEED = 5.0 M/S
BACKGROUND VISUAL RANGE = 200. KM

DOWNWIND DISTANCE (KM)	PLUME-OBSERVER DISTANCE (KM)	VISUAL RANGE REDUCTION (%)	BLUE-RED RATIO	PLUME CONTRAST AT 0.55 MICRON	PLUME PERCEPT-IBILITY E(L*A*B*)
1.	5.0	3.6	0.934	-.040	2.66
2.	5.0	2.6	0.927	-.035	2.87
5.	5.0	1.7	0.914	-.032	3.36
10.	5.0	1.3	0.895	-.033	4.12
15.	5.0	1.2	0.879	-.036	4.78
20.	5.0	1.1	0.866	-.038	5.31
30.	6.0	1.0	0.854	-.041	5.90
40.	8.0	1.0	0.855	-.043	5.99
50.	9.9	1.0	0.860	-.043	5.91
75.	14.9	1.1	0.880	-.042	5.32
100.	19.9	1.2	0.903	-.040	4.54
150.	29.8	1.4	0.940	-.033	3.13
200.	39.8	1.5	0.964	-.027	2.11
250.	49.7	1.7	0.979	-.022	1.43
300.	59.7	1.8	0.988	-.017	0.99
350.	69.6	1.9	0.993	-.014	0.71

2000MW COAL-FIRED PLANT
PASQUILL-GIFFORD C
WIND SPEED = 2.5 M/S
BACKGROUND VISUAL RANGE = 20. KM

DOWNWIND DISTANCE (KM)	PLUME-OBSERVER DISTANCE (KM)	VISUAL RANGE REDUCTION (%)	BLUE-RED RATIO	PLUME CONTRAST AT 0.55 MICRON	PLUME PERCEPT-IBILITY E(L*A*B*)
1.	5.0	4.8	0.988	-.008	0.88
2.	5.0	2.8	0.983	-.008	1.10
5.	5.0	1.4	0.982	-.006	1.12
10.	5.0	1.2	0.977	-.010	1.39
15.	5.0	1.3	0.970	-.012	1.80
20.	5.0	1.4	0.965	-.015	2.14
30.	6.0	1.5	0.972	-.014	1.77
40.	8.0	1.6	0.985	-.010	1.04
50.	9.9	1.7	0.993	-.007	0.59
75.	14.9	1.5	0.999	-.003	0.15
100.	19.9	0.9	1.000	-.001	0.04
150.	29.8	0.3	1.000	-.000	0.01
200.	39.8	0.1	1.000	-.000	0.00
250.	49.7	0.0	1.000	-.000	0.00
300.	59.7	0.0	1.000	-.000	0.00
350.	69.6	0.0	1.000	-.000	0.00

1000MW COAL-FIRED PLANT
PASQUILL-GIFFORD C
WIND SPEED = 2.5 M/S
BACKGROUND VISUAL RANGE = 50. KM

DOWNWIND DISTANCE (KM)	PLUME-OBSERVER DISTANCE (KM)	VISUAL RANGE REDUCTION (%)	BLUE-RED RATIO	PLUME CONTRAST AT 0.55 MICRON	PLUME PERCEPT-IBILITY E(L*A*B*)
1.	5.0	4.5	0.964	-.018	1.81
2.	5.0	2.6	0.953	-.018	2.20
5.	5.0	1.2	0.951	-.015	2.21
10.	5.0	1.0	0.939	-.018	2.73
15.	5.0	1.0	0.921	-.023	3.56
20.	5.0	1.0	0.907	-.027	4.23
30.	6.0	1.1	0.910	-.025	4.16
40.	8.0	1.2	0.929	-.026	3.41
50.	9.9	1.3	0.946	-.022	2.70
75.	14.9	1.5	0.975	-.015	1.41
100.	19.9	1.6	0.989	-.009	0.72
150.	29.8	1.9	0.998	-.004	0.22
200.	39.8	1.7	1.000	-.002	0.08
250.	49.7	1.1	1.000	-.001	0.04
300.	59.7	0.6	1.000	-.000	0.02
350.	69.6	0.4	1.000	-.000	0.01

2000MW COAL-FIRED PLANT
PASQUILL-GIFFORD C
WIND SPEED = 2.5 M/S
BACKGROUND VISUAL RANGE = 100. KM

DOWNWIND DISTANCE (KM)	PLUME-OBSERVER DISTANCE (KM)	VISUAL RANGE REDUCTION (%)	BLUE-RED RATIO	PLUME CONTRAST AT 0.55 MICRON	PLUME PERCEPT-IBILITY E(L*A*B*)
1.	5.0	4.2	0.946	-.029	2.43
2.	5.0	2.4	0.932	-.025	2.84
5.	5.0	1.1	0.931	-.020	2.81
10.	5.0	0.8	0.915	-.023	3.46
15.	5.0	0.8	0.891	-.029	4.50
20.	5.0	0.8	0.871	-.034	5.36
30.	6.0	0.9	0.867	-.037	5.58
40.	8.0	1.0	0.881	-.036	5.14
50.	9.9	1.0	0.897	-.034	4.56
75.	14.9	1.2	0.933	-.027	3.16
100.	19.9	1.3	0.958	-.021	2.12
150.	29.8	1.6	0.982	-.014	1.07
200.	39.8	1.9	0.993	-.010	0.55
250.	49.7	2.1	0.997	-.006	0.31
300.	59.7	2.4	0.999	-.004	0.18
350.	69.6	2.6	1.000	-.003	0.11

2000MW COAL-FIRED PLANT
PASQUILL-GIFFORD C
WIND SPEED = 2.5 M/S
BACKGROUND VISUAL RANGE = 200. KM

DOWNWIND DISTANCE (KM)	PLUME-OBSERVER DISTANCE (KM)	VISUAL RANGE REDUCTION (%)	BLUE-RED RATIO	PLUME CONTRAST AT 0.55 MICRON	PLUME PERCEPT-IBILITY E(L*A*B*)
1.	5.0	3.9	0.925	-.043	3.02
2.	5.0	2.1	0.914	-.034	3.36
5.	5.0	1.0	0.917	-.025	3.24
10.	5.0	0.7	0.899	-.028	3.97
15.	5.0	0.7	0.870	-.034	5.16
20.	5.0	0.7	0.846	-.040	6.15
30.	6.0	0.7	0.833	-.043	6.59
40.	8.0	0.8	0.845	-.044	6.45
50.	9.9	0.8	0.856	-.043	6.07
75.	14.9	0.9	0.890	-.038	4.86
100.	19.9	1.0	0.918	-.033	3.77
150.	29.8	1.3	0.951	-.027	2.52
200.	39.8	1.6	0.970	-.022	1.70
250.	49.7	1.8	0.982	-.018	1.19
300.	59.7	2.1	0.990	-.015	0.80
350.	69.6	2.5	0.994	-.012	0.56

20000MW COAL-FIRED PLAN
PASQUILL-GIFFORD C
WIND SPEED = 5.0 M/S
BACKGROUND VISUAL RANGE = 20. KM

DOWNWIND DISTANCE (KM)	PLUME-OBSERVER DISTANCE (KM)	VISUAL RANGE REDUCTION (%)	BLUE-RED RATIO	PLUME CONTRAST AT 0.55 MICRON	PLUME PERCEPT-IBILITY E(L*A*B*)
1.	5.0	2.6	0.991	-.005	0.61
2.	5.0	1.5	0.987	-.006	0.82
5.	5.0	0.9	0.981	-.008	1.17
10.	5.0	0.8	0.979	-.009	1.27
15.	5.0	0.8	0.977	-.009	1.36
20.	5.0	0.8	0.976	-.010	1.46
30.	6.0	0.8	0.982	-.009	1.14
40.	8.0	0.9	0.991	-.006	0.64
50.	9.9	1.0	0.995	-.004	0.36
75.	14.9	0.9	0.999	-.001	0.09
100.	19.9	0.5	1.000	-.001	0.03
150.	29.8	0.2	1.000	-.000	0.00
200.	39.8	0.0	1.000	-.000	0.00
250.	49.7	0.0	1.000	-.000	0.00
300.	59.7	0.0	1.000	-.000	0.00
350.	69.6	0.0	1.000	-.000	0.00

2000MW COAL-FIRED PLANT
PASQUILL-GIFFORD C
WIND SPEED = 5.0 M/S
BACKGROUND VISUAL RANGE = 50. KM

DOWNWIND DISTANCE (KM)	PLUME-OBSERVER DISTANCE (KM)	VISUAL RANGE REDUCTION (%)	BLUE-RED RATIO	PLUME CONTRAST AT 0.55 MICRON	PLUME PERCEPT-IBILITY E(L*A*B*)
1.	5.0	2.4	0.975	-.012	1.24
2.	5.0	1.3	0.965	-.012	1.62
5.	5.0	0.7	0.949	-.015	2.30
10.	5.0	0.6	0.944	-.016	2.50
15.	5.0	0.6	0.940	-.017	2.69
20.	5.0	0.6	0.936	-.018	2.83
30.	6.0	0.6	0.942	-.018	2.65
40.	8.0	0.7	0.956	-.015	2.10
50.	9.9	0.7	0.967	-.013	1.64
75.	14.9	0.9	0.985	-.009	0.86
100.	19.9	0.9	0.993	-.006	0.45
150.	29.8	1.0	0.999	-.002	0.12
200.	39.8	0.9	1.000	-.001	0.04
250.	49.7	0.5	1.000	-.000	0.02
300.	59.7	0.3	1.000	-.000	0.01
350.	69.6	0.2	1.000	-.000	0.00

2000MW COAL-FIRED PLANT
PASQUILL-GIFFORD C
WIND SPEED = 5.0 M/S
BACKGROUND VISUAL RANGE = 100. KM

DOWNWIND DISTANCE (KM)	PLUME-OBSERVER DISTANCE (KM)	VISUAL RANGE REDUCTION (%)	BLUE-RED RATIO	PLUME CONTRAST AT 0.55 MICRON	PLUME PERCEPT-IBILITY E(L*A*B*)
1.	5.0	2.3	0.962	-.018	1.64
2.	5.0	1.2	0.950	-.017	2.07
5.	5.0	0.6	0.929	-.019	2.90
10.	5.0	0.5	0.922	-.020	3.15
15.	5.0	0.4	0.917	-.021	3.38
20.	5.0	0.4	0.911	-.023	3.63
30.	6.0	0.5	0.914	-.023	3.53
40.	8.0	0.5	0.926	-.021	3.14
50.	9.9	0.6	0.937	-.020	2.75
75.	14.9	0.7	0.959	-.016	1.91
100.	19.9	0.8	0.974	-.013	1.31
150.	29.8	0.9	0.990	-.008	0.60
200.	39.8	1.0	0.996	-.005	0.28
250.	49.7	1.0	0.999	-.003	0.14
300.	59.7	1.1	1.000	-.002	0.07
350.	69.6	1.1	1.000	-.001	0.04

2000MW COAL-FIRED PLANT
PASQUILL-GIFFORD C
WIND SPEED = 5.0 M/S
BACKGROUND VISUAL RANGE = 200. KM

DOWNWIND DISTANCE (KM)	PLUME-OBSERVER DISTANCE (KM)	VISUAL RANGE REDUCTION (%)	BLUE-RED RATIO	PLUME CONTRAST AT 0.55 MICRON	PLUME PERCEPT-IBILITY E(L*A*B*)
1.	5.0	2.0	0.949	-.026	1.99
2.	5.0	1.1	0.938	-.022	2.41
5.	5.0	0.5	0.915	-.022	3.32
10.	5.0	0.4	0.908	-.023	3.60
15.	5.0	0.4	0.901	-.024	3.87
20.	5.0	0.4	0.894	-.026	4.15
30.	6.0	0.4	0.895	-.026	4.15
40.	8.0	0.4	0.903	-.026	3.92
50.	9.9	0.4	0.912	-.025	3.64
75.	14.9	0.5	0.932	-.022	2.93
100.	19.9	0.6	0.949	-.020	2.32
150.	29.8	0.7	0.972	-.015	1.42
200.	39.8	0.8	0.985	-.011	0.87
250.	49.7	0.9	0.992	-.008	0.53
300.	59.7	1.0	0.995	-.006	0.33
350.	69.6	1.0	0.998	-.005	0.21

2000MW COAL-FIRED PLANT
PASQUILL-GIFFORD D
WIND SPEED = 2.5 M/S
BACKGROUND VISUAL RANGE = 20. KM

DOWNWIND DISTANCE (KM)	PLUME-OBSERVER DISTANCE (KM)	VISUAL RANGE REDUCTION (%)	BLUE-RED RATIO	PLUME CONTRAST AT 0.55 MICRON	PLUME PERCEPT-IBILITY E(L*A*B*)
1.	5.0	6.0	0.926	-.009	1.06
2.	5.0	4.8	0.939	-.011	1.35
5.	5.0	3.5	0.971	-.014	1.84
10.	5.0	2.8	0.963	-.017	2.33
15.	5.0	2.4	0.959	-.018	2.54
20.	5.0	2.3	0.957	-.019	2.63
30.	6.0	2.1	0.968	-.016	2.07
40.	8.0	2.2	0.984	-.011	1.17
50.	9.9	2.2	0.992	-.008	0.66
75.	14.9	2.0	0.999	-.003	0.17
100.	19.9	1.1	1.000	-.001	0.05
150.	29.8	0.1	1.000	-.000	0.01
200.	39.8	0.0	1.000	-.000	0.00
250.	49.7	0.0	1.000	-.000	0.00
300.	59.7	0.0	1.000	-.000	0.00
350.	69.6	0.0	1.000	-.000	0.00

2000MW COAL-FIRED PLANT
PASQUILL-GIFFORD D
WIND SPEED = 2.5 M/S
BACKGROUND VISUAL RANGE = 50. KM

DOWNWIND DISTANCE (KM)	PLUME-OBSERVER DISTANCE (KM)	VISUAL RANGE REDUCTION (%)	BLUE-RED RATIO	PLUME CONTRAST AT 0.55 MICRON	PLUME PERCEPT-IBILITY E(L*A*B*)
1.	5.0	5.6	0.958	-.022	2.18
2.	3.0	4.4	0.944	-.024	2.72
5.	5.0	3.1	0.921	-.028	3.69
10.	5.0	2.3	0.899	-.032	4.65
15.	5.0	2.0	0.890	-.034	5.07
20.	5.0	1.8	0.886	-.035	5.25
30.	6.0	1.7	0.896	-.034	4.88
40.	8.0	1.7	0.920	-.030	3.87
50.	9.9	1.7	0.940	-.026	3.04
75.	14.9	1.9	0.971	-.018	1.64
100.	19.9	1.9	0.987	-.012	0.87
150.	29.8	2.2	0.998	-.005	0.28
200.	39.8	2.0	1.000	-.002	0.10
250.	49.7	1.2	1.000	-.001	0.05
300.	59.7	0.4	1.000	-.001	0.02
350.	69.6	0.1	1.000	-.000	0.01

2000MW COAL-FIRED PLANT
PASQUILL-GIFFORD D
WIND SPEED = 2.5 M/S
BACKGROUND VISUAL RANGE = 100. KM

DOWNWIND DISTANCE (KM)	PLUME-OBSERVER DISTANCE (KM)	VISUAL RANGE REDUCTION (%)	BLUE-RED RATIO	PLUME CONTRAST AT 0.55 MICRON	PLUME PERCEPT-IBILITY E(L*A*B*)
1.	5.0	5.3	0.935	-.035	2.93
2.	5.0	4.1	0.917	-.035	3.57
5.	5.0	2.8	0.883	-.038	4.73
10.	5.0	2.1	0.859	-.042	5.93
15.	5.0	1.7	0.847	-.044	6.46
20.	5.0	1.5	0.841	-.045	6.69
30.	6.0	1.4	0.846	-.045	6.57
40.	8.0	1.3	0.866	-.042	5.85
50.	9.9	1.4	0.884	-.039	5.17
75.	14.9	1.5	0.922	-.033	3.70
100.	19.9	1.6	0.949	-.026	2.58
150.	29.8	1.8	0.978	-.018	1.33
200.	39.8	2.0	0.991	-.012	0.70
250.	49.7	2.2	0.997	-.008	0.40
300.	59.7	2.4	0.999	-.005	0.23
350.	69.6	2.6	1.000	-.004	0.15

2000MW COAL-FIRED PLANT
PASQUILL-GIFFORD D
WIND SPEED = 2.5 M/S
BACKGROUND VISUAL RANGE = 200. KM

DOWNWIND DISTANCE (KM)	PLUME-OBSERVER DISTANCE (KM)	VISUAL RANGE REDUCTION (%)	BLUE-RED RATIO	PLUME CONTRAST AT 0.55 MICRON	PLUME PERCEPT-IBILITY E(L*A*B*)
1.	5.0	4.8	0.910	-.053	3.65
2.	5.0	3.7	0.892	-.050	4.29
5.	5.0	2.5	0.861	-.049	5.53
10.	5.0	1.8	0.829	-.052	6.87
15.	5.0	1.5	0.816	-.053	7.45
20.	5.0	1.3	0.810	-.053	7.71
30.	6.0	1.1	0.811	-.053	7.79
40.	8.0	1.1	0.824	-.052	7.36
50.	9.9	1.1	0.838	-.050	6.89
75.	14.9	1.1	0.872	-.045	5.72
100.	19.9	1.2	0.901	-.040	4.61
150.	29.8	1.4	0.939	-.033	3.14
200.	39.8	1.6	0.963	-.027	2.13
250.	49.7	1.9	0.978	-.023	1.50
300.	59.7	2.1	0.987	-.018	1.04
350.	69.6	2.3	0.992	-.015	0.74

2000MW COAL-FIRED PLANT
PASQUILL-GIFFORD D
WIND SPEED = 5.0 M/S
BACKGROUND VISUAL RANGE = 20. KM

DOWNWIND DISTANCE (KM)	PLUME-OBSERVER DISTANCE (KM)	VISUAL RANGE REDUCTION (%)	BLUE-RED RATIO	PLUME CONTRAST AT 0.55 MICRON	PLUME PERCEPT-IBILITY E(L*A*B*)
1.	5.0	4.3	0.991	-.007	0.70
2.	5.0	3.1	0.987	-.007	0.87
5.	5.0	2.0	0.980	-.009	1.27
10.	5.0	1.6	0.972	-.012	1.71
15.	5.0	1.4	0.968	-.014	1.95
20.	5.0	1.3	0.966	-.014	2.08
30.	6.0	1.3	0.975	-.012	1.60
40.	8.0	1.3	0.988	-.003	0.86
50.	9.9	1.3	0.994	-.005	0.45
75.	14.9	1.1	0.999	-.002	0.10
100.	19.9	0.6	1.000	-.001	0.03
150.	29.8	0.1	1.000	-.000	0.00
200.	39.8	0.0	1.000	-.000	0.00
250.	49.7	0.0	1.000	-.000	0.00
300.	59.7	0.0	1.000	-.000	0.00
350.	69.6	0.0	1.000	-.000	0.00

2000MW COAL-FIRED PLANT
PASQUILL-GIFFORD D
WIND SPEED = 5.0 M/S
BACKGROUND VISUAL RANGE = 50. KM

DOWNWIND DISTANCE (KM)	PLUME-OBSERVER DISTANCE (KM)	VISUAL RANGE REDUCTION (%)	BLUE-RED RATIO	PLUME CONTRAST AT 0.55 MICRON	PLUME PERCEPT-IBILITY E(L*A*B*)
1.	5.0	4.5	0.973	-.016	1.45
2.	5.0	2.9	0.964	-.015	1.75
5.	5.0	1.7	0.945	-.018	2.53
10.	5.0	1.3	0.925	-.023	3.38
15.	5.0	1.1	0.915	-.025	3.86
20.	5.0	1.0	0.909	-.027	4.12
30.	6.0	1.0	0.919	-.025	3.74
40.	8.0	1.0	0.941	-.021	2.80
50.	9.9	1.0	0.953	-.017	2.07
75.	14.9	1.0	0.982	-.010	0.99
100.	19.9	1.0	0.992	-.006	0.49
150.	29.8	1.1	0.999	-.002	0.13
200.	39.8	0.9	1.000	-.001	0.04
250.	49.7	0.5	1.000	-.000	0.02
300.	59.7	0.2	1.000	-.000	0.01
350.	69.6	0.1	1.000	-.000	0.00

2000MW COAL-FIRED PLANT
PASQUILL-GIFFORD D
WIND SPEED = 5.0 M/S
BACKGROUND VISUAL RANGE = 100. KM

DOWNWIND DISTANCE (KM)	PLUME-OBSERVER DISTANCE (KM)	VISUAL RANGE REDUCTION (%)	BLUE-RED RATIO	PLUME CONTRAST AT 0.55 MICRON	PLUME PERCEPT-IBILITY E(L*A*B*)
1.	5.0	4.2	0.957	-.026	1.99
2.	5.0	2.7	0.947	-.023	2.29
5.	5.0	1.6	0.922	-.025	3.22
10.	5.0	1.1	0.896	-.029	4.29
15.	5.0	0.9	0.882	-.032	4.83
20.	5.0	0.8	0.874	-.034	5.21
30.	6.0	0.8	0.880	-.033	5.00
40.	8.0	0.7	0.902	-.029	4.21
50.	9.9	0.8	0.920	-.025	3.49
75.	14.9	0.8	0.952	-.019	2.22
100.	19.9	0.8	0.971	-.014	1.45
150.	29.8	0.9	0.989	-.008	0.64
200.	39.8	0.9	0.996	-.005	0.30
250.	49.7	1.0	0.999	-.003	0.14
300.	59.7	1.0	1.000	-.002	0.08
350.	69.6	1.0	1.000	-.001	0.04

2000MW COAL-FIRED PLANT
PASQUILL-GIFFORD D
WIND SPEED = 5.0 M/S
BACKGROUND VISUAL RANGE = 200. KM

DOWNWIND DISTANCE (KM)	PLUME-OBSERVER DISTANCE (KM)	VISUAL RANGE REDUCTION (%)	BLUE-RED RATIO	PLUME CONTRAST AT 0.55 MICRON	PLUME PERCEPT-IBILITY E(L*A*B*)
1.	5.0	3.9	0.939	-.040	2.53
2.	5.0	2.4	0.930	-.038	2.75
5.	5.0	1.4	0.904	-.031	3.74
10.	5.0	1.0	0.875	-.035	4.94
15.	5.0	0.8	0.859	-.038	5.60
20.	5.0	0.7	0.850	-.039	5.98
30.	6.0	0.6	0.854	-.038	5.90
40.	8.0	0.6	0.872	-.035	5.26
50.	9.9	0.6	0.889	-.032	4.63
75.	14.9	0.6	0.922	-.026	3.40
100.	19.9	0.6	0.944	-.022	2.57
150.	29.8	0.7	0.970	-.016	1.51
200.	39.8	0.8	0.984	-.011	0.91
250.	49.7	0.8	0.991	-.008	0.56
300.	59.7	0.9	0.995	-.006	0.35
350.	69.6	0.9	0.997	-.005	0.23

2000MW COAL-FIRED PLANT
PASQUILL-GIFFORD E
WIND SPEED = 2.5 M/S
BACKGROUND VISUAL RANGE = 20. KM

DOWNWIND DISTANCE (KM)	PLUME-OBSERVER DISTANCE (KM)	VISUAL RANGE REDUCTION (%)	BLUE-RED RATIO	PLUME CONTRAST AT 0.55 MICRON	PLUME PERCEPT-IBILITY E(L*A*B*)
1.	5.0	11.4	0.975	-.017	1.85
2.	5.0	8.8	0.959	-.023	2.76
5.	5.0	6.1	0.950	-.025	3.25
10.	5.0	4.8	0.946	-.026	3.44
15.	5.0	4.3	0.943	-.027	3.62
20.	5.0	4.0	0.940	-.029	3.80
30.	6.0	3.9	0.954	-.026	3.05
40.	8.0	3.9	0.976	-.018	1.76
50.	9.9	4.0	0.983	-.013	1.02
75.	14.9	3.9	0.998	-.005	0.28
100.	19.9	1.9	1.000	-.002	0.09
150.	29.8	0.0	1.000	-.000	0.01
200.	39.8	0.0	1.000	-.000	0.00
250.	49.7	0.0	1.000	-.000	0.00
300.	59.7	0.0	1.000	-.000	0.00
350.	69.6	0.0	1.000	-.000	0.00

2000MW COAL-FIRED PLANT
PASQUILL-GIFFORD E
WIND SPEED = 2.5 M/S
BACKGROUND VISUAL RANGE = 50. KM

DOWNWIND DISTANCE (KM)	PLUME-OBSERVER DISTANCE (KM)	VISUAL RANGE REDUCTION (%)	BLUE-RED RATIO	PLUME CONTRAST AT 0.55 MICRON	PLUME PERCEPT-IBILITY E(L*A*B*)
1.	5.0	10.3	0.926	-.039	3.84
2.	5.0	8.1	0.883	-.047	5.61
5.	5.0	5.4	0.862	-.050	6.58
10.	5.0	4.1	0.854	-.050	6.94
15.	5.0	3.6	0.846	-.052	7.32
20.	5.0	3.3	0.838	-.054	7.68
30.	6.0	3.1	0.849	-.054	7.23
40.	8.0	3.2	0.882	-.040	5.88
50.	9.9	3.2	0.910	-.042	4.69
75.	14.9	3.4	0.956	-.030	2.58
100.	19.9	3.5	0.980	-.020	1.33
150.	29.8	3.3	0.996	-.009	0.44
200.	39.8	3.6	1.000	-.004	0.17
250.	49.7	1.9	1.000	-.002	0.08
300.	59.7	0.5	1.000	-.001	0.04
350.	69.6	0.0	1.000	-.000	0.02

2000MW COAL-FIRED PLANT
PASQUILL-GIFFORD E
WIND SPEED = 2.5 M/S
BACKGROUND VISUAL RANGE = 100. KM

DOWNWIND DISTANCE (KM)	PLUME-OBSERVER DISTANCE (KM)	VISUAL RANGE REDUCTION (%)	BLUE-RED RATIO	PLUME CONTRAST AT 0.55 MICRON	PLUME PERCEPT-IBILITY E(L*A*B*)
1.	5.0	10.2	0.837	-.061	5.19
2.	5.0	7.5	0.833	-.068	7.35
5.	5.0	5.0	0.805	-.068	8.51
10.	5.0	3.7	0.794	-.067	8.93
15.	5.0	3.2	0.784	-.068	9.41
20.	5.0	2.9	0.774	-.070	9.87
30.	6.0	2.6	0.776	-.071	9.91
40.	8.0	2.6	0.801	-.068	9.01
50.	9.9	2.6	0.826	-.065	8.07
75.	14.9	2.8	0.881	-.055	5.87
100.	19.9	2.9	0.922	-.044	4.09
150.	29.8	3.3	0.967	-.030	2.08
200.	39.8	3.5	0.987	-.020	1.09
250.	49.7	3.8	0.995	-.013	0.62
300.	59.7	4.0	0.999	-.009	0.36
350.	69.6	4.4	1.000	-.006	0.23

2000MW COAL-FIRED PLANT
PASQUILL-GIFFORD E
WIND SPEED = 2.5 M/S
BACKGROUND VISUAL RANGE = 200. KM

DOWNWIND DISTANCE (KM)	PLUME-OBSERVER DISTANCE (KM)	VISUAL RANGE REDUCTION (%)	BLUE-RED RATIO	PLUME CONTRAST AT 0.55 MICRON	PLUME PERCEPT-IBILITY E(L*A*B*)
1.	5.0	9.4	0.844	-.092	6.48
2.	5.0	6.9	0.787	-.093	8.79
5.	5.0	4.4	0.759	-.087	10.00
10.	5.0	3.2	0.750	-.082	10.42
15.	5.0	2.8	0.739	-.082	10.94
20.	5.0	2.5	0.728	-.084	11.47
30.	6.0	2.2	0.723	-.086	11.86
40.	8.0	2.1	0.738	-.085	11.45
50.	9.9	2.1	0.755	-.083	10.89
75.	14.9	2.2	0.802	-.077	9.18
100.	19.9	2.2	0.847	-.069	7.39
150.	29.8	2.6	0.903	-.056	4.93
200.	39.3	2.9	0.945	-.045	3.30
250.	49.7	3.2	0.967	-.037	2.31
300.	59.7	3.5	0.981	-.030	1.59
350.	69.6	3.9	0.989	-.024	1.14

2000MW COAL-FIRED PLANT
PASQUILL-GIFFORD E
WIND SPEED = 5.0 M/S
BACKGROUND VISUAL RANGE = 20. KM

DOWNWIND DISTANCE (KM)	PLUME-OBSERVER DISTANCE (KM)	VISUAL RANGE REDUCTION (%)	BLUE-RED RATIO	PLUME CONTRAST AT 0.55 MICRON	PLUME PERCEPT-IBILITY E(L*A*B*)
1.	5.0	6.8	0.987	-.009	1.02
2.	5.0	4.6	0.982	-.010	1.22
5.	5.0	3.0	0.977	-.011	1.49
10.	5.0	2.4	0.970	-.013	1.87
15.	5.0	2.2	0.965	-.015	2.16
20.	5.0	2.1	0.961	-.017	2.38
30.	6.0	2.1	0.969	-.016	2.00
40.	8.0	2.2	0.983	-.011	1.18
50.	9.9	2.2	0.992	-.008	0.68
75.	14.9	2.2	0.999	-.003	0.18
100.	19.9	1.1	1.000	-.001	0.05
150.	29.8	0.0	1.000	-.000	0.01
200.	39.8	0.0	1.000	-.000	0.00
250.	49.7	0.0	1.000	-.000	0.00
300.	59.7	0.0	1.000	-.000	0.00
350.	69.6	0.0	1.000	-.000	0.00

2000MW COAL-FIRED PLANT
PASQUILL-GIFFORD E
WIND SPEED = 5.0 M/S
BACKGROUND VISUAL RANGE = 50. KM

DOWNWIND DISTANCE (KM)	PLUME-OBSERVER DISTANCE (KM)	VISUAL RANGE REDUCTION (%)	BLUE-RED RATIO	PLUME CONTRAST AT 0.55 MICRON	PLUME PERCEPT-IBILITY E(L*A*B*)
1.	5.0	6.5	0.960	-.023	2.11
2.	5.0	4.3	0.949	-.022	2.47
5.	5.0	2.7	0.936	-.022	2.97
10.	5.0	2.1	0.919	-.025	3.72
15.	5.0	1.8	0.906	-.029	4.30
20.	5.0	1.7	0.897	-.032	4.73
30.	6.0	1.6	0.899	-.033	4.72
40.	8.0	1.7	0.920	-.030	3.91
50.	9.9	1.8	0.938	-.027	3.13
75.	14.9	1.9	0.970	-.018	1.69
100.	19.9	1.9	0.987	-.012	0.87
150.	29.8	1.9	0.998	-.005	0.24
200.	39.8	1.7	1.000	-.002	0.03
250.	49.7	0.9	1.000	-.001	0.03
300.	59.7	0.2	1.000	-.000	0.01
350.	69.6	0.0	1.000	-.000	0.01

2000MW COAL-FIRED PLANT
PASQUILL-GIFFORD E
WIND SPEED = 5.0 M/S
BACKGROUND VISUAL RANGE = 100. KM

DOWNWIND DISTANCE (KM)	PLUME-OBSERVER DISTANCE (KM)	VISUAL RANGE REDUCTION (%)	BLUE-RED RATIO	PLUME CONTRAST AT 0.55 MICRON	PLUME PERCEPT-IBILITY E(L*A*B*)
1.	5.0	6.1	0.938	-.037	2.88
2.	5.0	4.0	0.925	-.033	3.24
5.	5.0	2.5	0.909	-.031	3.81
10.	5.0	1.8	0.886	-.034	4.74
15.	5.0	1.6	0.869	-.038	5.47
20.	5.0	1.4	0.856	-.041	6.02
30.	6.0	1.3	0.851	-.043	6.35
40.	8.0	1.4	0.865	-.042	5.91
50.	9.9	1.4	0.881	-.040	5.32
75.	14.9	1.5	0.920	-.033	3.80
100.	19.9	1.6	0.949	-.026	2.59
150.	29.8	1.6	0.981	-.016	1.17
200.	39.8	1.6	0.993	-.009	0.53
250.	49.7	1.6	0.998	-.005	0.25
300.	59.7	1.6	1.000	-.003	0.13
350.	69.6	1.5	1.000	-.002	0.07

2000MW COAL-FIRED PLANT
PASQUILL-GIFFORD E
WIND SPEED = 5.0 M/S
BACKGROUND VISUAL RANGE = 200. KM

DOWNWIND DISTANCE (KM)	PLUME-OBSERVER DISTANCE (KM)	VISUAL RANGE REDUCTION (%)	BLUE-RED RATIO	PLUME CONTRAST AT 0.55 MICRON	PLUME PERCEPT-IBILITY E(L*A*B*)
1.	5.0	5.6	0.912	-.057	3.65
2.	5.0	3.7	0.902	-.047	3.91
5.	5.0	2.2	0.887	-.041	4.47
10.	5.0	1.6	0.862	-.043	5.43
15.	5.0	1.4	0.842	-.046	6.31
20.	5.0	1.2	0.828	-.048	6.94
30.	6.0	1.1	0.816	-.052	7.52
40.	8.0	1.1	0.823	-.052	7.43
50.	9.9	1.1	0.834	-.051	7.10
75.	14.9	1.1	0.869	-.047	5.87
100.	19.9	1.2	0.901	-.040	4.62
150.	29.8	1.3	0.947	-.029	2.75
200.	39.8	1.3	0.972	-.021	1.62
250.	49.7	1.4	0.986	-.015	0.95
300.	59.7	1.4	0.992	-.010	0.58
350.	69.6	1.3	0.996	-.007	0.36

2000MW COAL-FIRED PLANT
PASQUILL-GIFFORD F
WIND SPEED = 2.5 M/S
BACKGROUND VISUAL RANGE = 20. KM

DOWNWIND DISTANCE (KM)	PLUME-OBSERVER DISTANCE (KM)	VISUAL RANGE REDUCTION (%)	BLUE-RED RATIO	PLUME CONTRAST AT 0.55 MICRON	PLUME PERCEPT-IBILITY E(L*A*B*)
1.	5.0	15.5	0.967	-.022	2.46
2.	5.0	13.3	0.936	-.037	4.35
5.	5.0	10.3	0.917	-.047	5.48
10.	5.0	8.4	0.915	-.047	5.59
15.	5.0	7.5	0.914	-.046	5.60
20.	5.0	7.0	0.913	-.046	5.63
30.	6.0	6.8	0.937	-.039	4.29
40.	8.0	6.9	0.968	-.027	2.42
50.	9.9	7.0	0.985	-.019	1.39
75.	14.9	7.2	0.998	-.003	0.40
100.	19.9	3.0	1.000	-.003	0.15
150.	29.8	0.0	1.000	-.000	0.03
200.	39.8	0.0	1.000	-.000	0.00
250.	49.7	0.0	1.000	-.000	0.00
300.	59.7	0.0	1.000	-.000	0.00
350.	69.6	0.0	1.000	-.000	0.00

2000MW COAL-FIRED PLANT
PASQUILL-GIFFORD F
WIND SPEED = 2.5 M/S
BACKGROUND VISUAL RANGE = 50. KM

DOWNWIND DISTANCE (KM)	PLUME-OBSERVER DISTANCE (KM)	VISUAL RANGE REDUCTION (%)	BLUE-RED RATIO	PLUME CONTRAST AT 0.55 MICRON	PLUME PERCEPT-IBILITY E(L*A*B*)
1.	5.0	14.7	0.902	-.051	5.10
2.	5.0	12.2	0.821	-.076	8.96
5.	5.0	9.1	0.774	-.090	11.33
10.	5.0	7.2	0.763	-.089	11.55
15.	5.0	6.4	0.763	-.088	11.54
20.	5.0	5.9	0.766	-.088	11.61
30.	6.0	5.6	0.793	-.083	10.42
40.	8.0	5.6	0.843	-.072	8.17
50.	9.9	5.8	0.881	-.064	6.42
75.	14.9	6.2	0.942	-.045	3.55
100.	19.9	6.6	0.973	-.032	2.00
150.	29.8	7.2	0.996	-.016	0.71
200.	39.8	7.2	1.000	-.007	0.31
250.	49.7	3.1	1.001	-.004	0.15
300.	59.7	0.2	1.001	-.002	0.08
350.	69.6	0.0	1.001	-.001	0.04

2000MW COAL-FIRED PLANT
PASQUILL-GIFFORD F
WIND SPEED = 2.5 M/S
BACKGROUND VISUAL RANGE = 100. KM

DOWNWIND DISTANCE (KM)	PLUME-OBSERVER DISTANCE (KM)	VISUAL RANGE REDUCTION (%)	BLUE-RED RATIO	PLUME CONTRAST AT 0.55 MICRON	PLUME PERCEPT-IBILITY E(L*A*B*)
1.	5.0	13.9	0.851	-.080	6.89
2.	5.0	11.4	0.741	-.106	11.80
5.	5.0	8.3	0.679	-.120	14.86
10.	5.0	6.5	0.674	-.117	15.10
15.	5.0	5.6	0.673	-.114	15.06
20.	5.0	5.2	0.672	-.113	15.14
30.	6.0	4.8	0.690	-.110	14.40
40.	8.0	4.8	0.732	-.104	12.70
50.	9.9	4.8	0.768	-.098	11.20
75.	14.9	5.1	0.841	-.085	8.17
100.	19.9	5.5	0.892	-.072	5.94
150.	29.8	6.2	0.953	-.052	3.19
200.	39.8	6.8	0.981	-.036	1.81
250.	49.7	7.3	0.994	-.025	1.10
300.	59.7	7.6	0.999	-.017	0.73
350.	69.6	8.0	1.001	-.012	0.50

2000MW COAL-FIRED PLANT
PASQUILL-GIFFORD F
WIND SPEED = 2.5 M/S
BACKGROUND VISUAL RANGE = 200. KM

DOWNWIND DISTANCE (KM)	PLUME-OBSERVER DISTANCE (KM)	VISUAL RANGE REDUCTION (%)	BLUE-RED RATIO	PLUME CONTRAST AT 0.55 MICRON	PLUME PERCEPT-IBILITY E(L*A*B*)
1.	5.0	12.9	0.796	-.118	8.60
2.	5.0	10.4	0.675	-.141	14.15
5.	5.0	7.4	0.603	-.150	17.62
10.	5.0	5.7	0.605	-.142	17.81
15.	5.0	5.0	0.606	-.138	17.73
20.	5.0	4.5	0.605	-.136	17.80
30.	6.0	4.1	0.616	-.133	17.44
40.	8.0	4.0	0.645	-.130	16.37
50.	9.9	4.0	0.672	-.127	15.36
75.	14.9	4.1	0.733	-.120	13.00
100.	19.9	4.4	0.786	-.112	10.90
150.	29.8	5.0	0.865	-.097	7.63
200.	39.8	5.5	0.917	-.083	5.40
250.	49.7	6.1	0.949	-.070	3.91
300.	59.7	6.5	0.970	-.059	2.93
350.	69.6	7.0	0.982	-.049	2.27

2000MW COAL-FIRED PLANT
PASQUILL-GIFFORD F
WIND SPEED = 5.0 M/S
BACKGROUND VISUAL RANGE = 20. KM

DOWNWIND DISTANCE (KM)	PLUME-OBSERVER DISTANCE (KM)	VISUAL RANGE REDUCTION (%)	BLUE-RED RATIO	PLUME CONTRAST AT 0.55 MICRON	PLUME PERCEPT-IBILITY E(L*A*B*)
1.	5.0	8.9	0.984	-.012	1.24
2.	5.0	6.8	0.975	-.014	1.74
5.	5.0	4.7	0.968	-.016	2.08
10.	5.0	3.8	0.964	-.017	2.29
15.	5.0	3.4	0.960	-.018	2.50
20.	5.0	3.2	0.957	-.020	2.69
30.	6.0	3.2	0.965	-.018	2.26
40.	8.0	3.3	0.982	-.014	1.35
50.	9.9	3.4	0.991	-.010	0.80
75.	14.9	3.6	0.999	-.004	0.23
100.	19.9	1.7	1.000	-.002	0.08
150.	29.8	0.0	1.000	-.000	0.01
200.	39.8	0.0	1.000	-.000	0.00
250.	49.7	0.0	1.000	-.000	0.00
300.	59.7	0.0	1.000	-.000	0.00
350.	69.6	0.0	1.000	-.000	0.00

2000MW COAL-FIRED PLANT
PASQUILL-GIFFORD F
WIND SPEED = 5.0 M/S
BACKGROUND VISUAL RANGE = 50. KM

DOWNWIND DISTANCE (KM)	PLUME-OBSERVER DISTANCE (KM)	VISUAL RANGE REDUCTION (%)	BLUE-RED RATIO	PLUME CONTRAST AT 0.55 MICRON	PLUME PERCEPT-IBILITY E(L*A*B*)
1.	5.0	3.5	0.952	-.028	2.59
2.	5.0	6.3	0.923	-.031	3.54
5.	5.0	4.3	0.911	-.033	4.19
10.	5.0	3.3	0.902	-.034	4.59
15.	5.0	3.0	0.893	-.036	5.00
20.	5.0	2.8	0.884	-.038	5.38
30.	6.0	2.6	0.887	-.039	5.34
40.	8.0	2.7	0.909	-.036	4.49
50.	9.9	2.8	0.928	-.033	3.70
75.	14.9	3.1	0.963	-.025	2.19
100.	19.9	3.4	0.982	-.018	1.26
150.	29.8	3.7	0.997	-.009	0.44
200.	39.8	3.9	1.000	-.004	0.18
250.	49.7	1.8	1.000	-.002	0.08
300.	59.7	0.1	1.000	-.001	0.04
350.	69.6	0.0	1.000	-.000	0.02

2000MW COAL-FIRED PLANT
PASQUILL-GIFFORD F
WIND SPEED = 5.0 M/S
BACKGROUND VISUAL RANGE = 100. KM

DOWNWIND DISTANCE (KM)	PLUME-OBSERVER DISTANCE (KM)	VISUAL RANGE REDUCTION (%)	BLUE-RED RATIO	PLUME CONTRAST AT 0.55 MICRON	PLUME PERCEPT-IBILITY E(L*A*B*)
1.	5.0	8.0	0.925	-.046	3.55
2.	5.0	5.9	0.894	-.047	4.65
5.	5.0	4.0	0.873	-.046	5.41
10.	5.0	3.0	0.861	-.046	5.90
15.	5.0	2.6	0.849	-.047	6.40
20.	5.0	2.4	0.838	-.050	6.89
30.	6.0	2.3	0.832	-.052	7.24
40.	8.0	2.3	0.846	-.052	6.83
50.	9.9	2.3	0.861	-.051	6.32
75.	14.9	2.5	0.898	-.046	4.97
100.	19.9	2.8	0.928	-.041	3.76
150.	29.8	3.2	0.967	-.030	2.06
200.	39.8	3.5	0.987	-.021	1.13
250.	49.7	3.7	0.995	-.014	0.65
300.	59.7	3.8	0.999	-.009	0.40
350.	69.6	3.9	1.000	-.006	0.26

2000MW COAL-FIRED PLANT
PASQUILL-GIFFORD F
WIND SPEED = 5.0 M/S
BACKGROUND VISUAL RANGE = 200. KM

DOWNWIND DISTANCE (KM)	PLUME-OBSERVER DISTANCE (KM)	VISUAL RANGE REDUCTION (%)	BLUE-RED RATIO	PLUME CONTRAST AT 0.55 MICRON	PLUME PERCEPT-IBILITY E(L*A*B*)
1.	5.0	7.4	0.892	-.071	4.52
2.	5.0	5.4	0.861	-.067	5.63
5.	5.0	3.5	0.841	-.061	6.38
10.	5.0	2.7	0.829	-.058	6.88
15.	5.0	2.3	0.816	-.059	7.43
20.	5.0	2.1	0.804	-.061	7.99
30.	6.0	2.0	0.792	-.064	8.63
40.	8.0	1.9	0.796	-.065	8.65
50.	9.9	1.9	0.804	-.066	8.49
75.	14.9	2.0	0.831	-.065	7.74
100.	19.9	2.2	0.859	-.063	6.78
150.	29.8	2.5	0.908	-.056	4.90
200.	39.8	2.8	0.943	-.047	3.44
250.	49.7	3.0	0.966	-.039	2.41
300.	59.7	3.2	0.980	-.032	1.72
350.	69.6	3.4	0.988	-.026	1.27

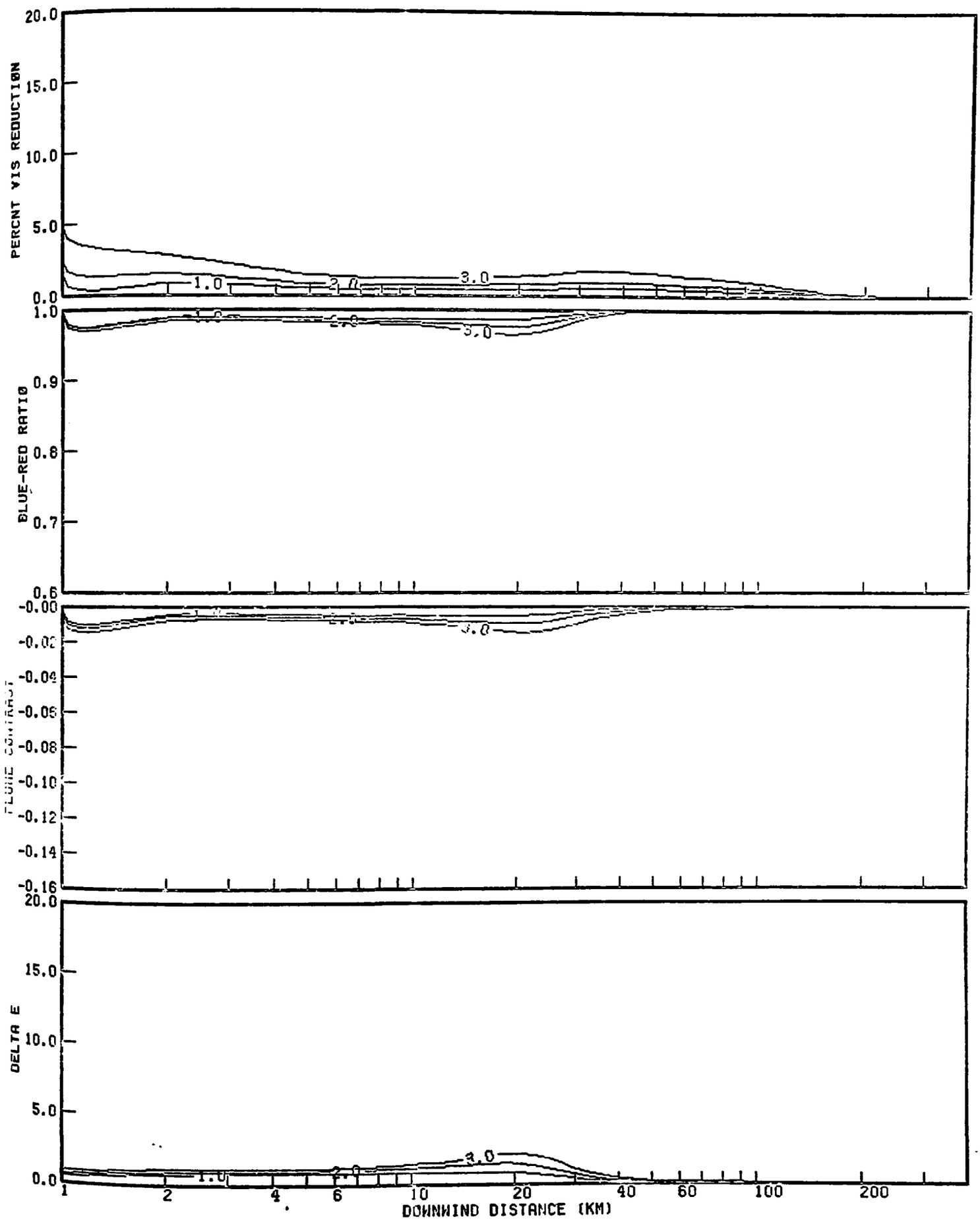

VISUAL IMPACTS ØF PØWER PLANTS ØF INDICATED SIZE
STABILITY CLASS C
2.5 M/S WIND SPEED
20.0 KM VISUAL RANGE

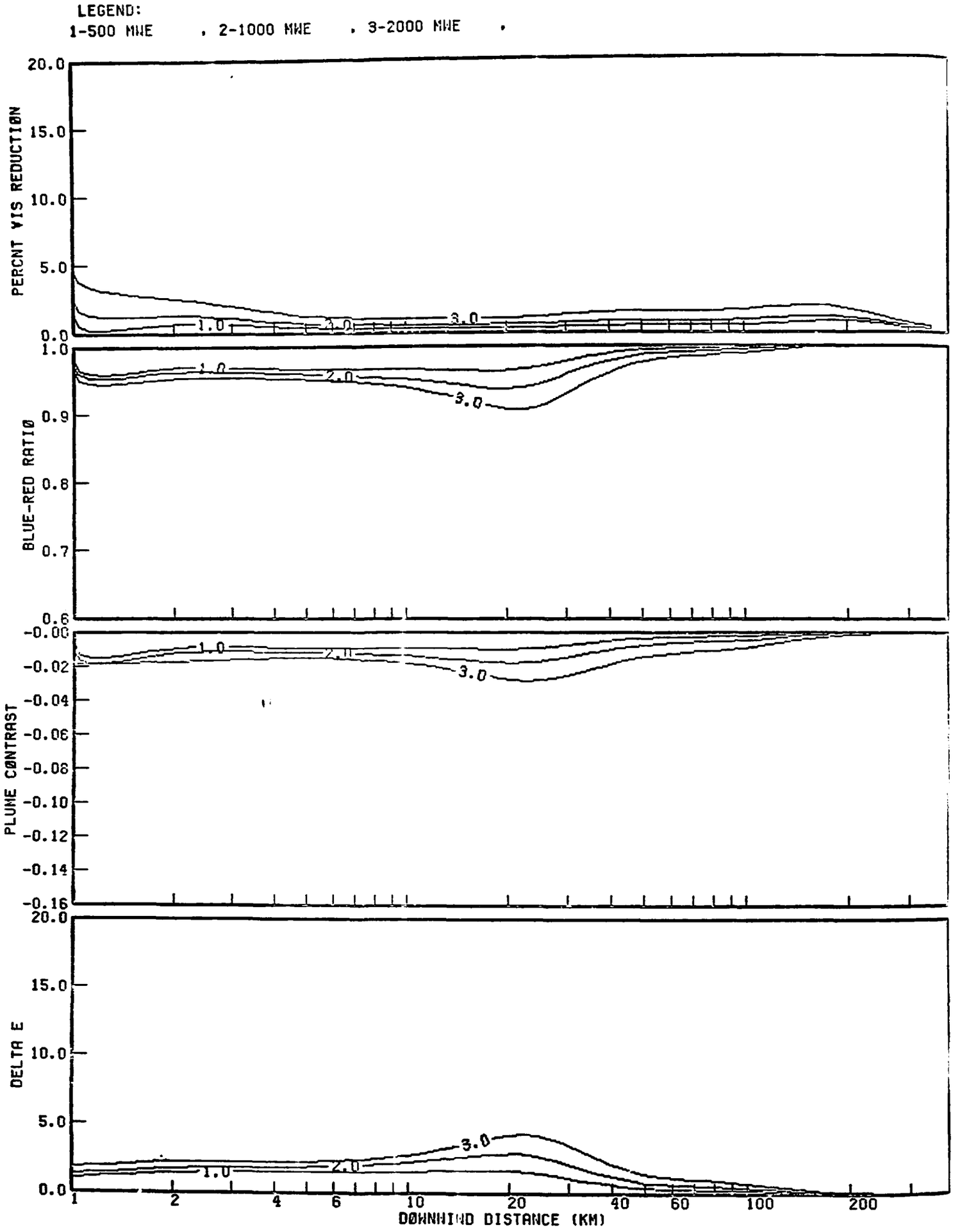

VISUAL IMPACTS OF POWER PLANTS OF INDICATED SIZE
STABILITY CLASS C
2.5 M/S WIND SPEED
50.0 KM VISUAL RANGE

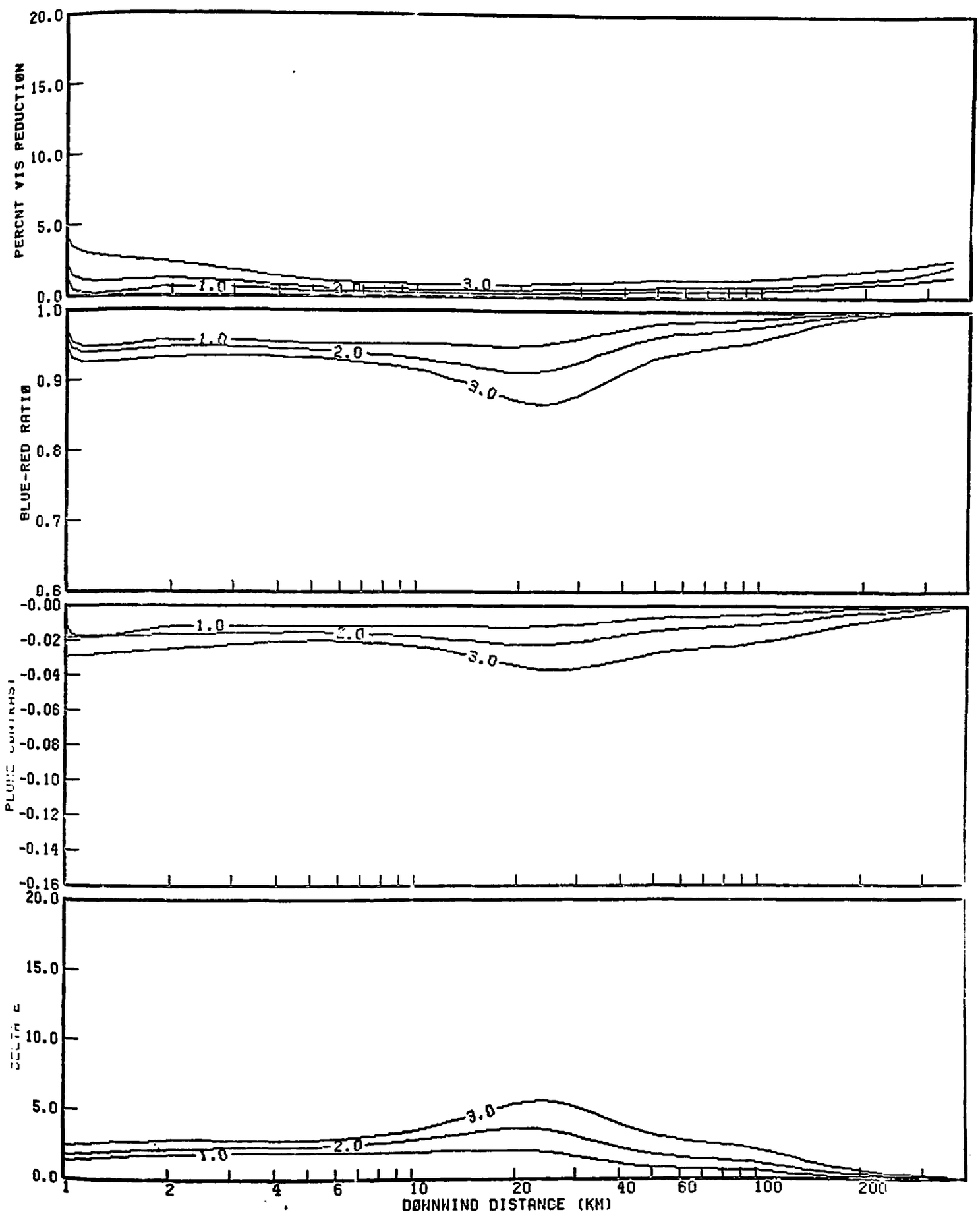

VISUAL IMPACTS OF POWER PLANTS OF INDICATED SIZE
STABILITY CLASS C
2.5 M/S WIND SPEED
100.0 KM VISUAL RANGE

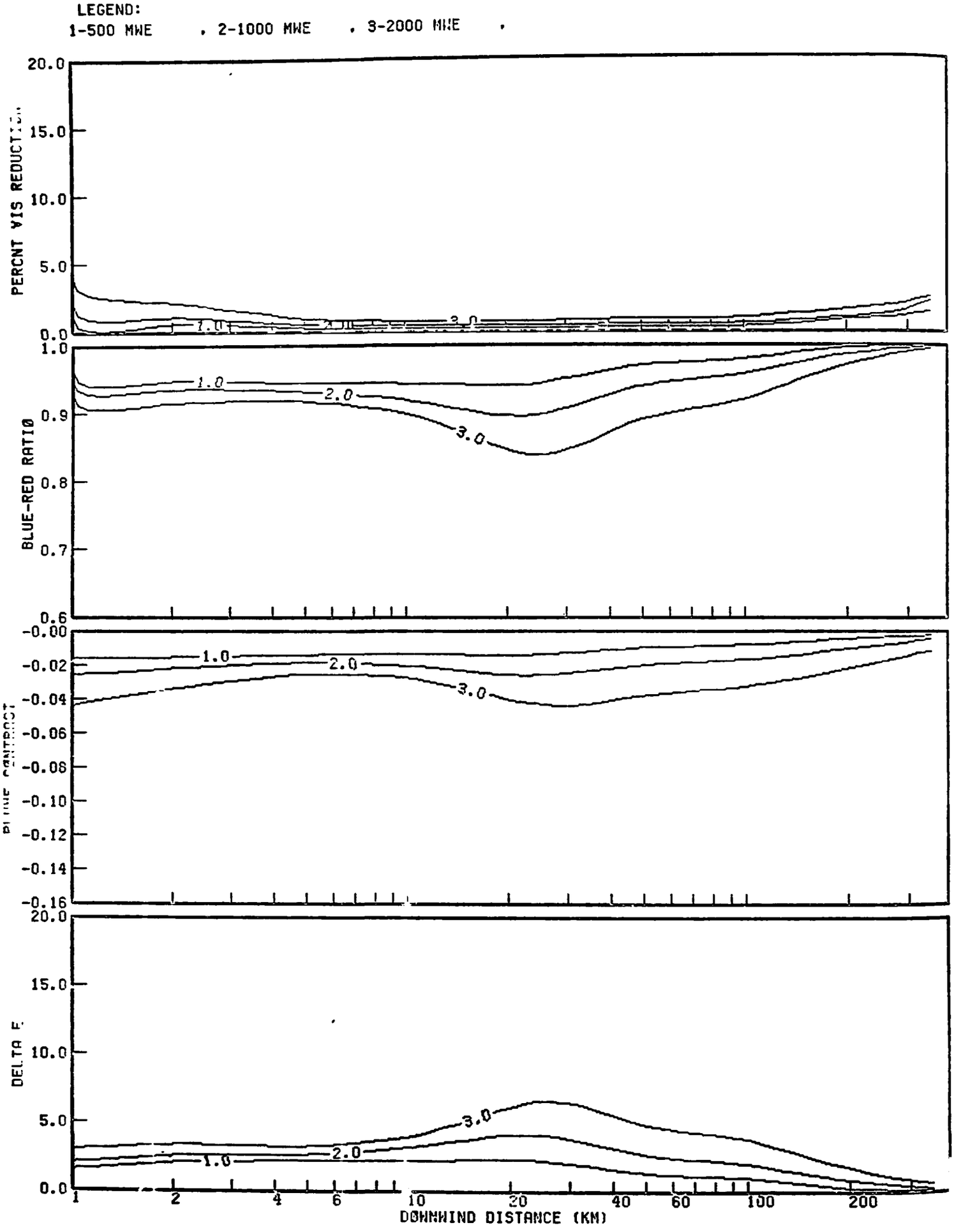

VISUAL IMPACTS OF POWER PLANTS OF INDICATED SIZE
STABILITY CLASS C
2.5 M/S WIND SPEED
200.0 KM VISUAL RANGE

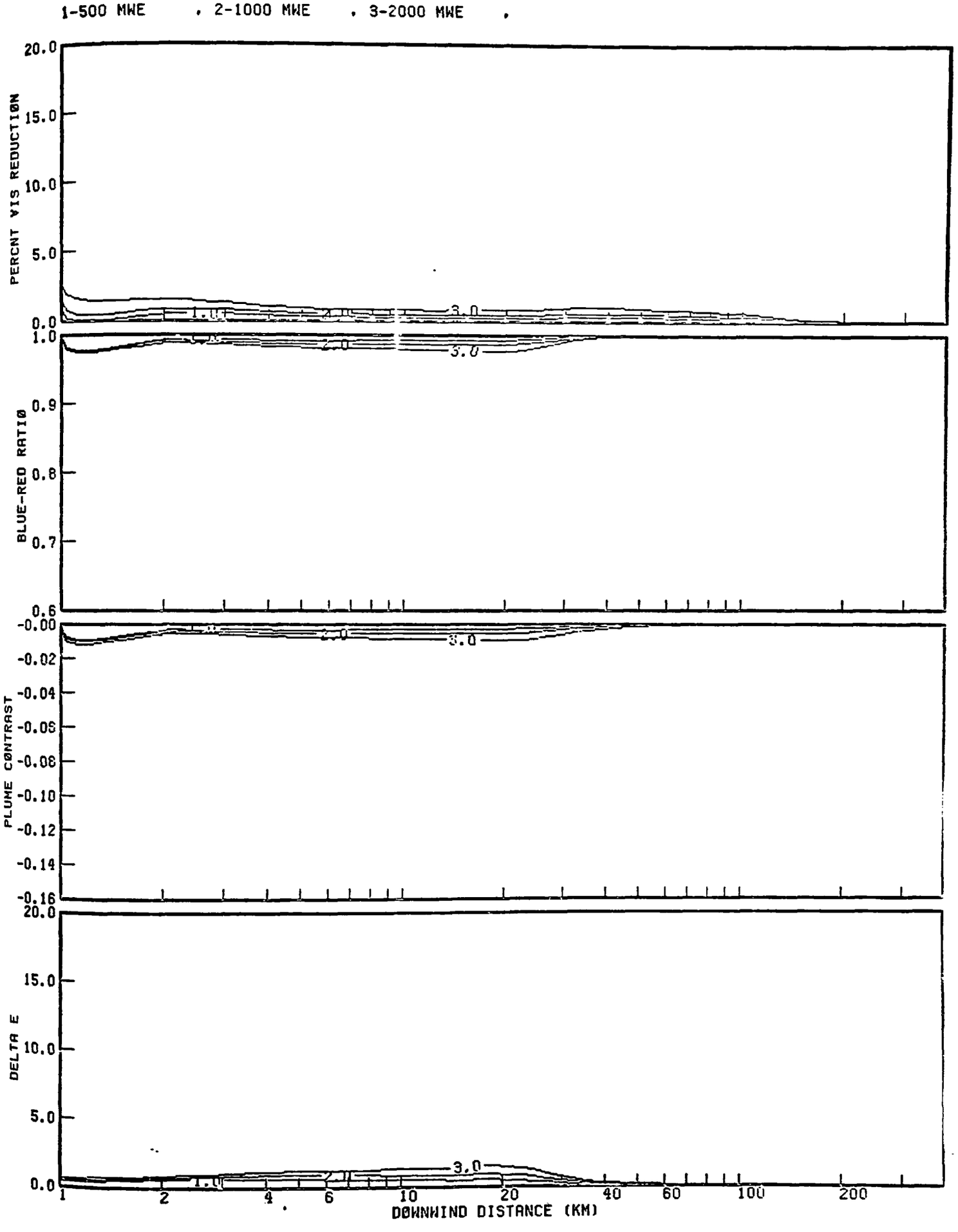

VISUAL IMPACTS OF POWER PLANTS OF INDICATED SIZE
STABILITY CLASS C
5.0 M/S WIND SPEED
20.0 KM VISUAL RANGE

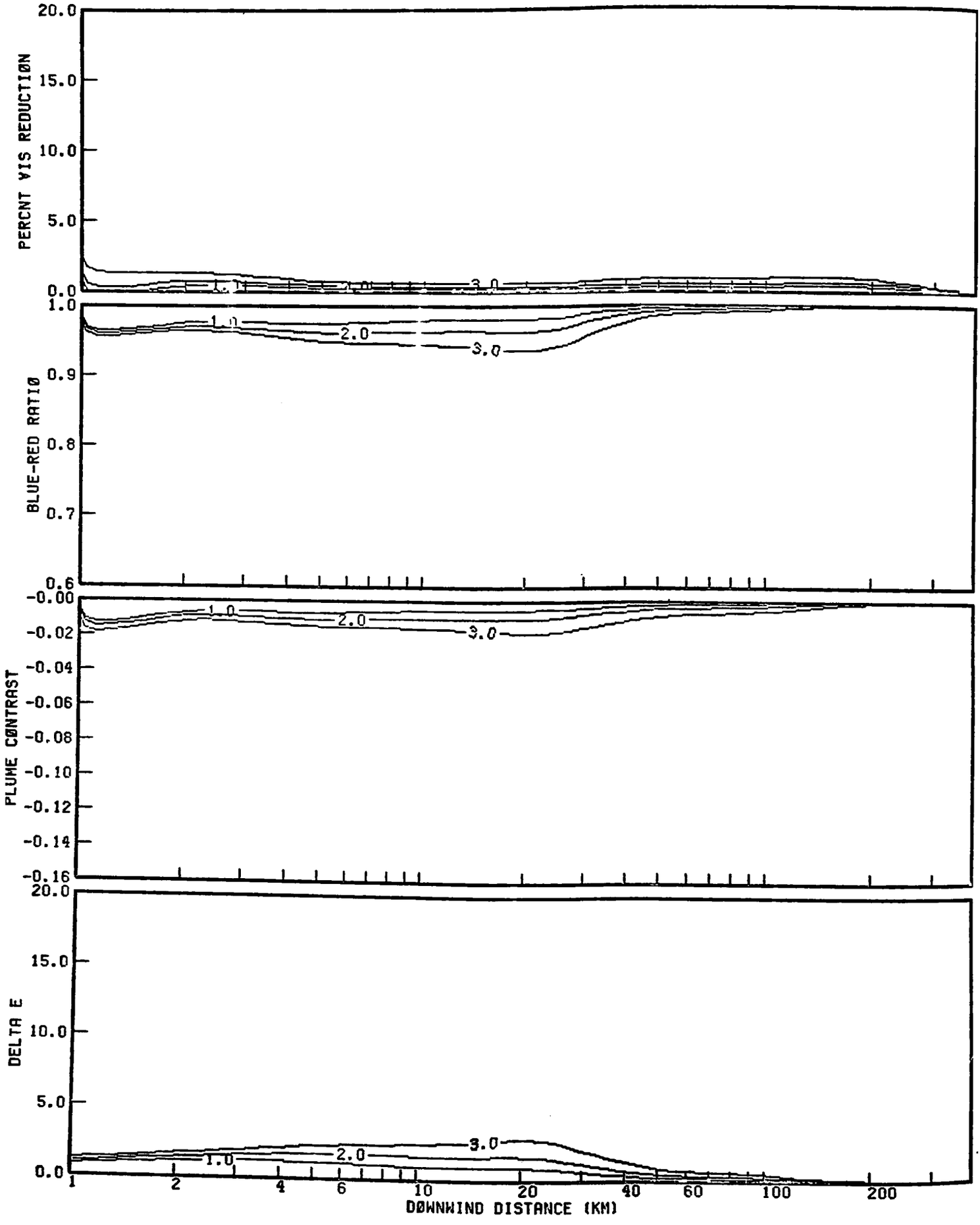

VISUAL IMPACTS OF POWER PLANTS OF INDICATED SIZE
STABILITY CLASS C
5.0 M/S WIND SPEED
50.0 KM VISUAL RANGE

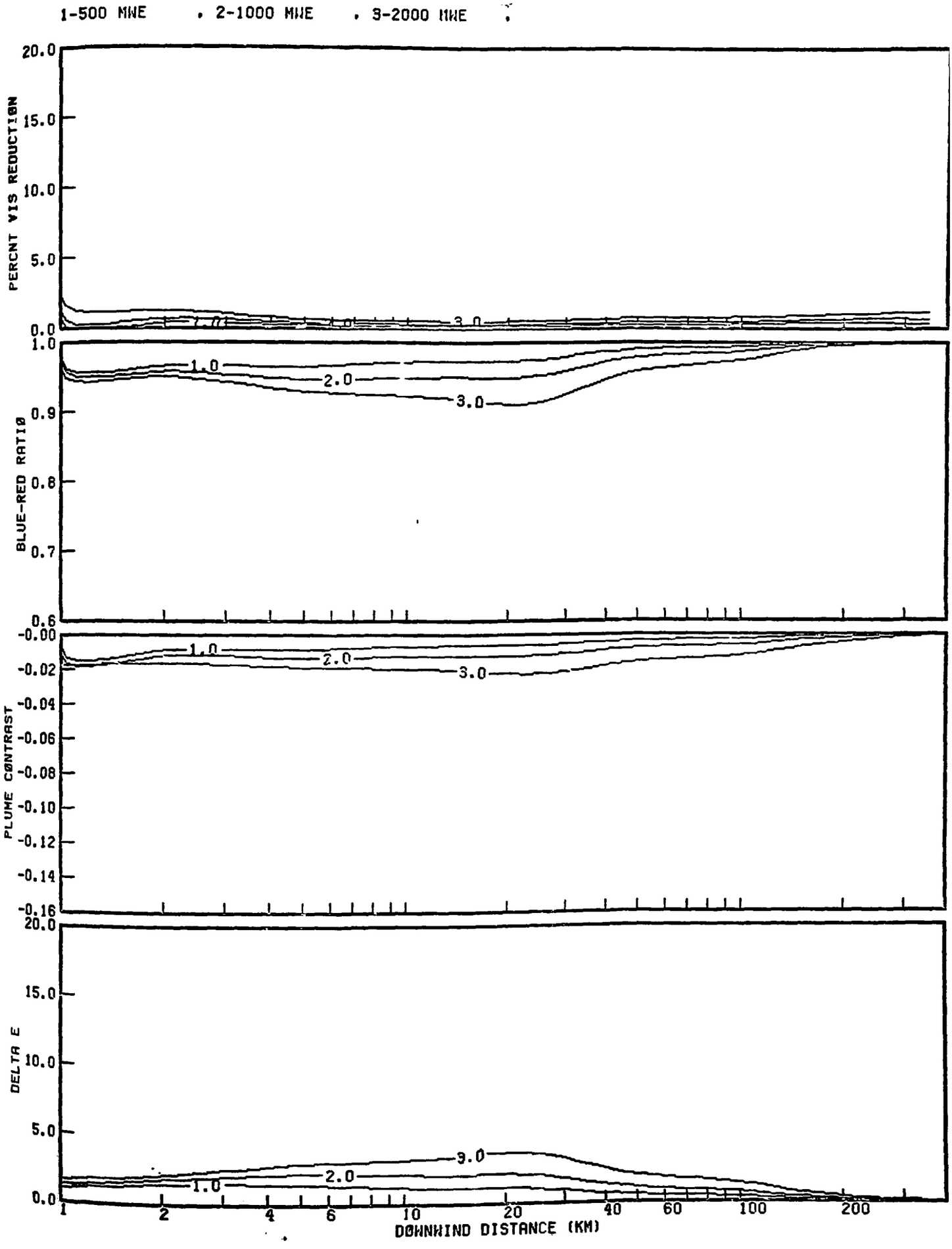

VISUAL IMPACTS OF POWER PLANTS OF INDICATED SIZE
STABILITY CLASS C
5.0 M/S WIND SPEED
100.0 KM VISUAL RANGE

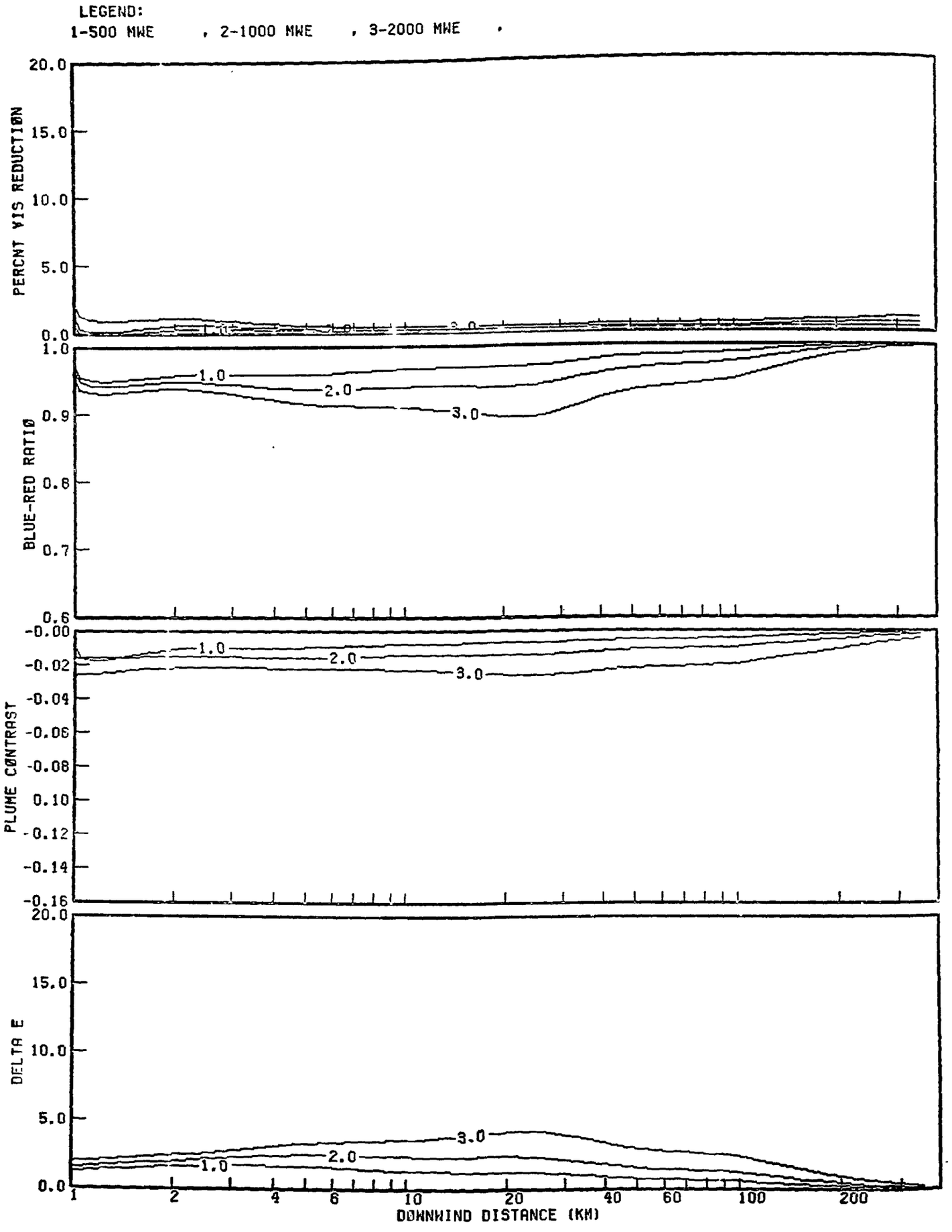

VISUAL IMPACTS OF POWER PLANTS OF INDICATED SIZE
STABILITY CLASS C
5.0 M/S WIND SPEED
200.0 KM VISUAL RANGE

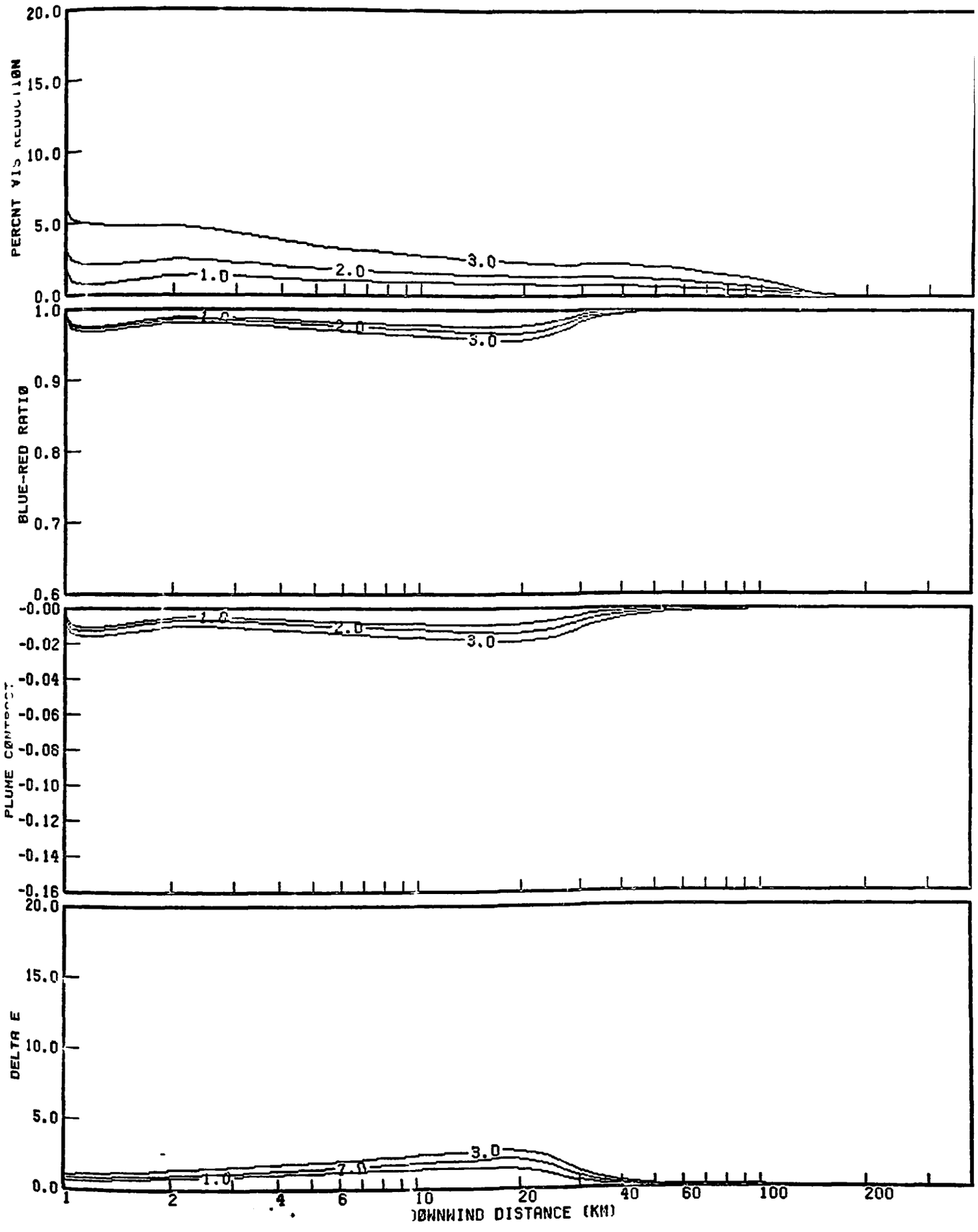

VISUAL IMPACTS ØF PØWER PLANTS ØF INDICATED SIZE
STABILITY CLASS D
2.5 M/S WIND SPEED
20.0 KM VISUAL RANGE

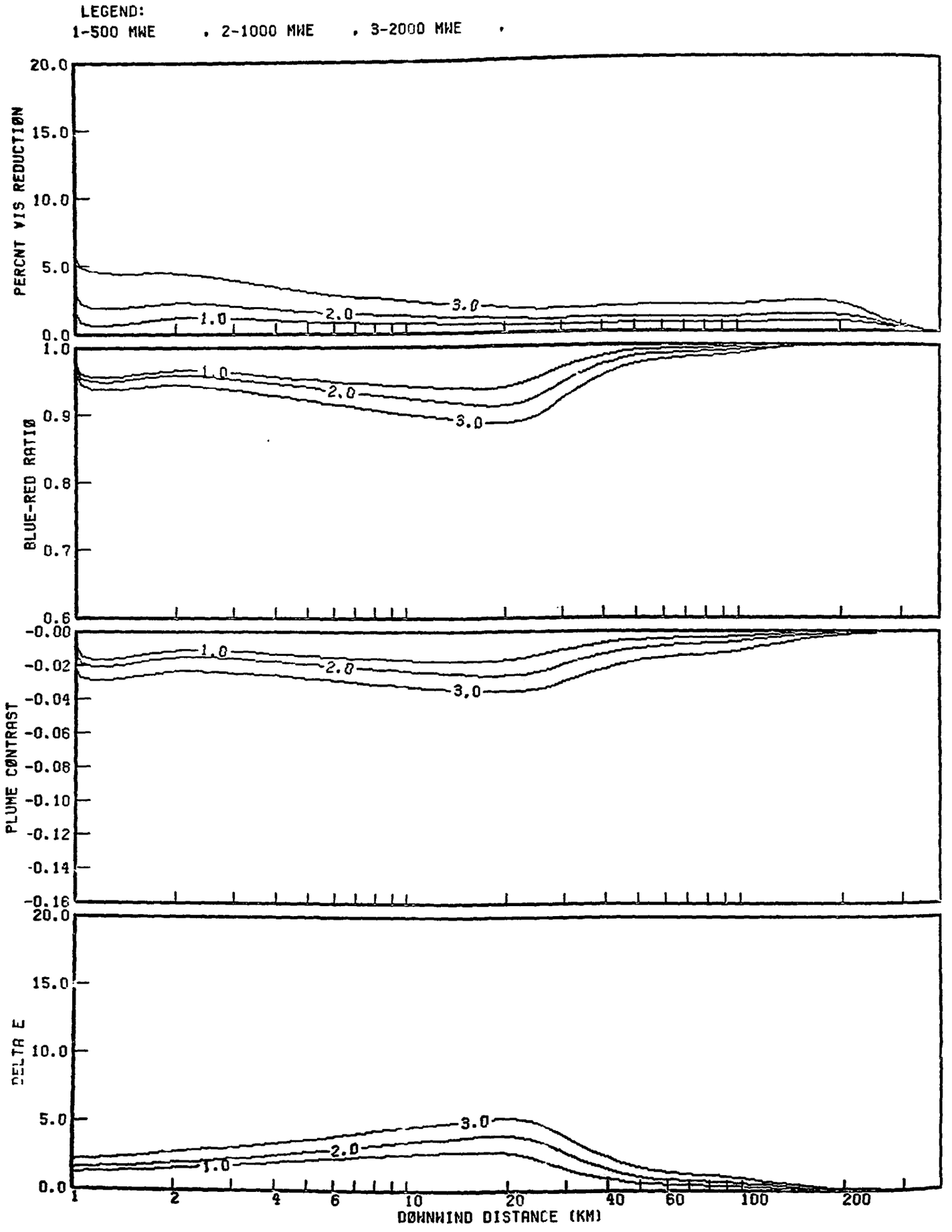

VISUAL IMPACTS OF POWER PLANTS OF INDICATED SIZE
STABILITY CLASS D
2.5 M/S WIND SPEED
50.0 KM VISUAL RANGE

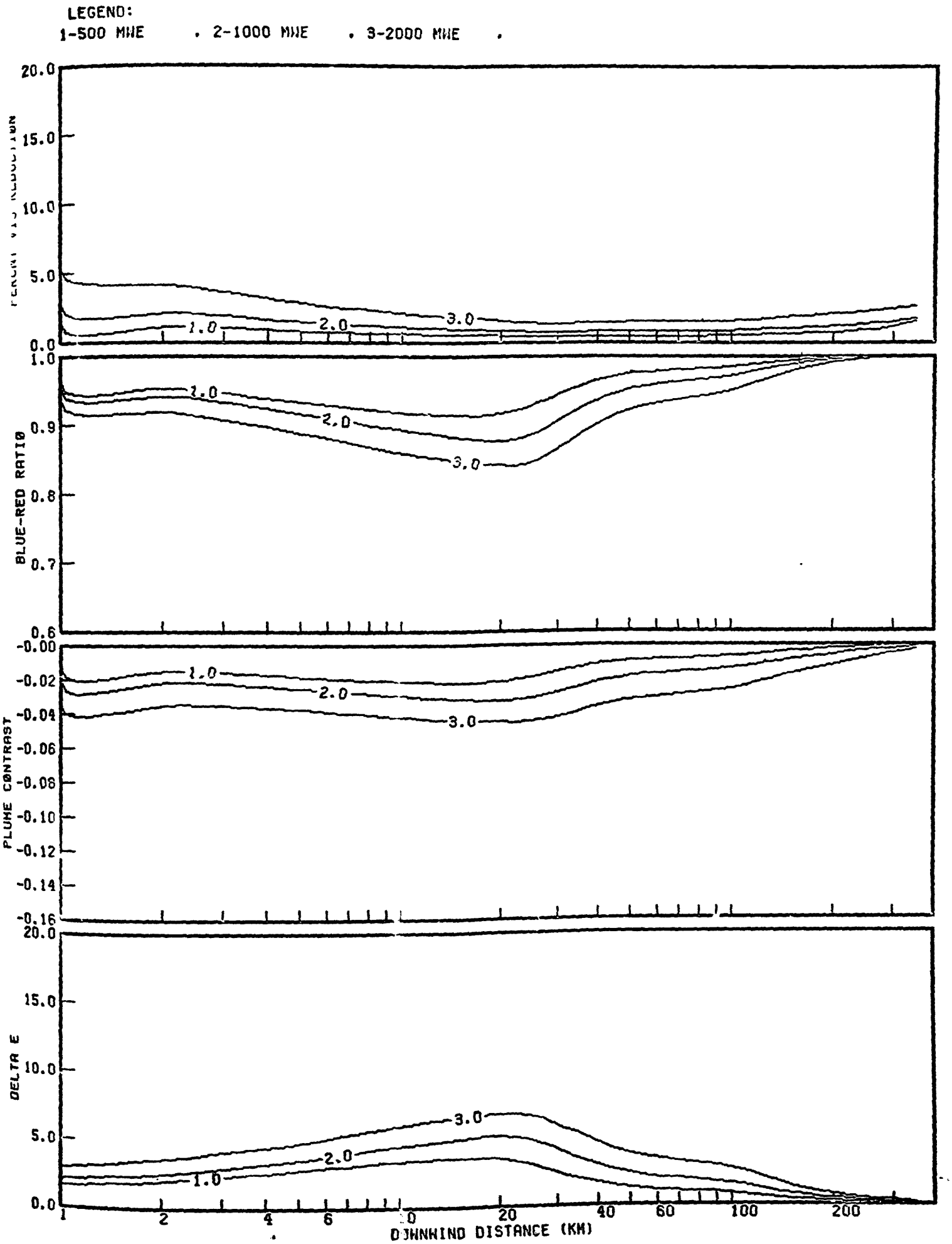

VISUAL IMPACTS OF POWER PLANTS OF INDICATED SIZE
STABILITY CLASS D
2.5 M/S WIND SPEED
100.0 KM VISUAL RANGE

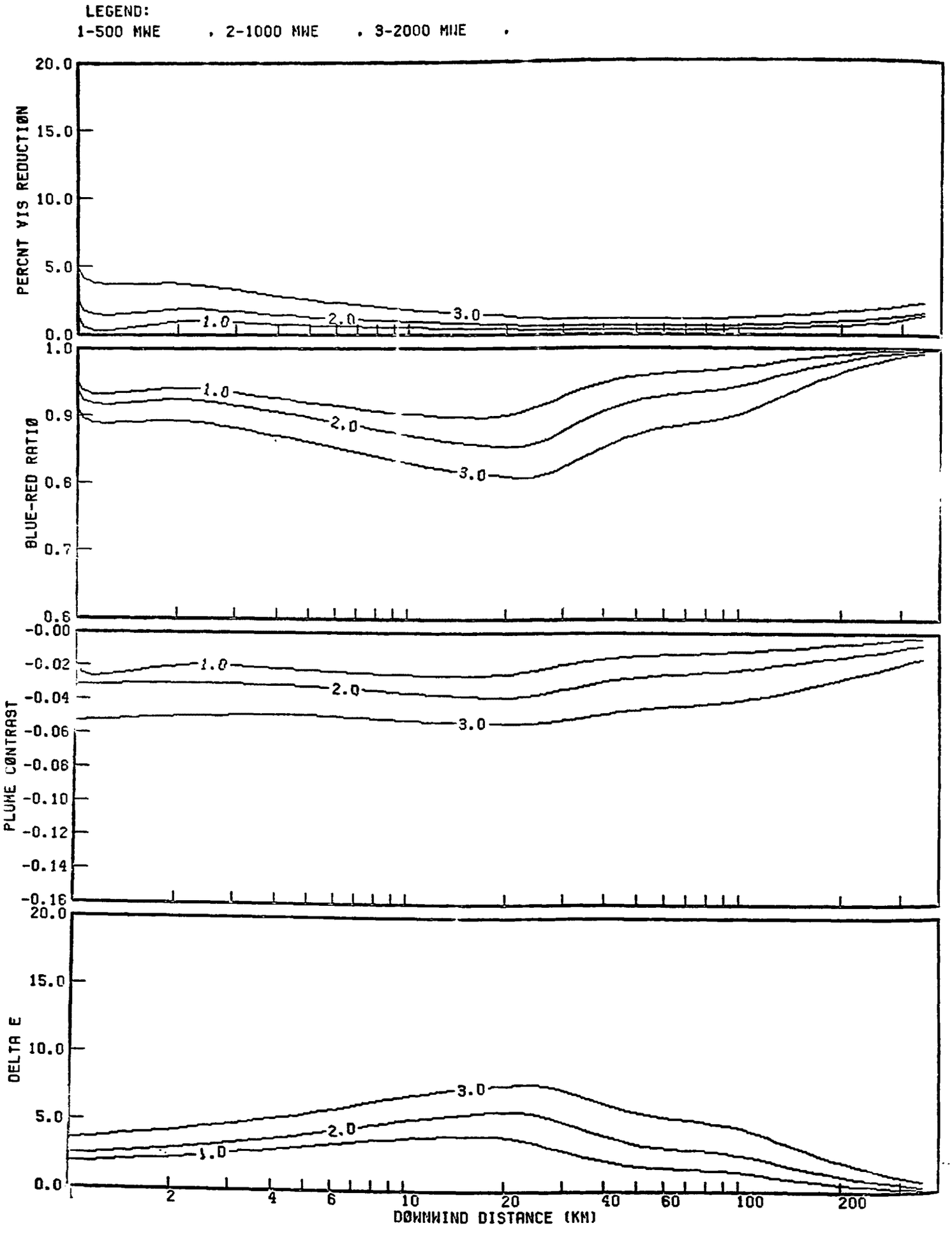

VISUAL IMPACTS OF POWER PLANTS OF INDICATED SIZE
STABILITY CLASS D
2.5 M/S WIND SPEED
200.0 KM VISUAL RANGE

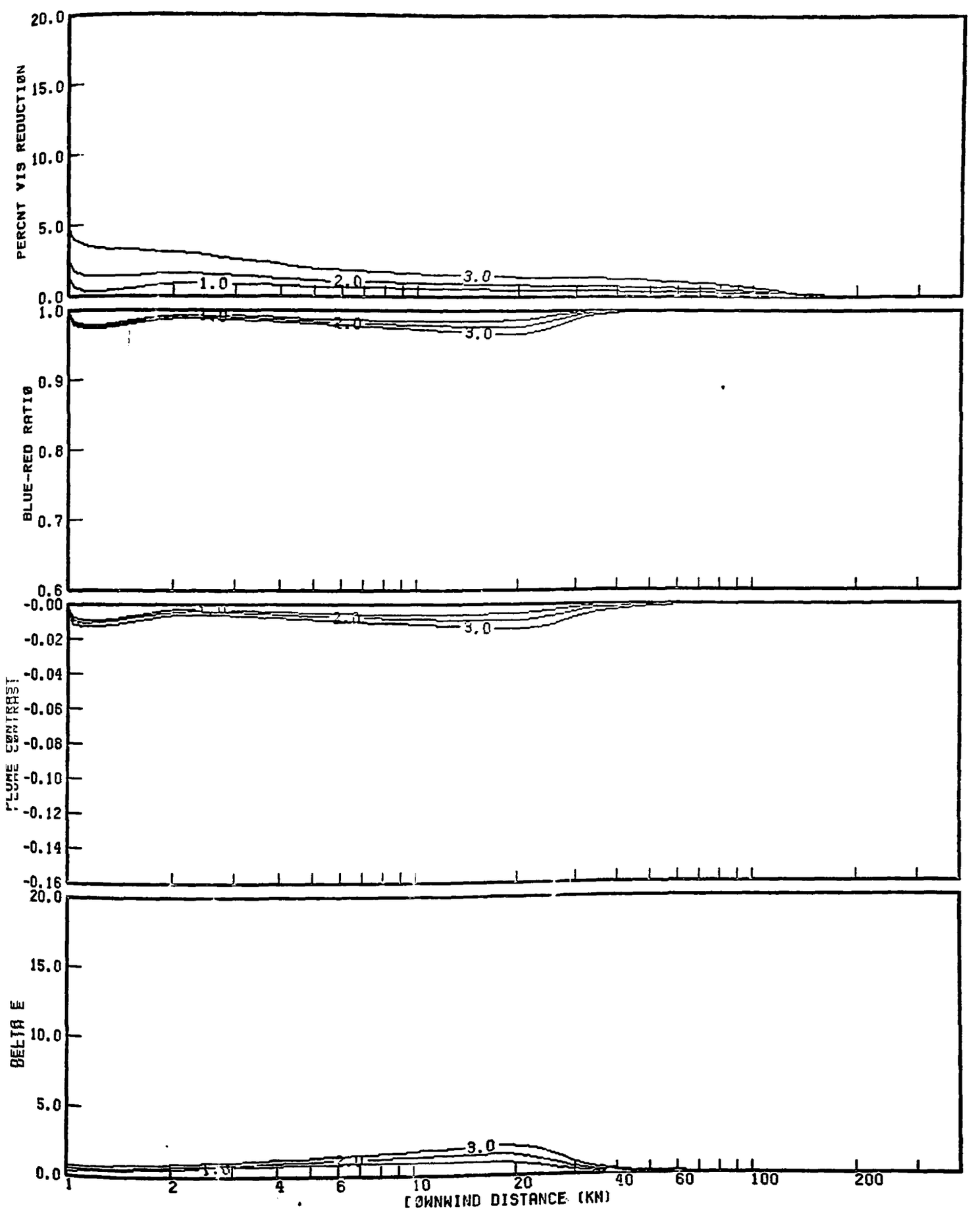

VISUAL IMPACTS OF POWER PLANTS OF INDICATED SIZE
STABILITY CLASS D
5.0 M/S WIND SPEED
20.0 KM VISUAL RANGE

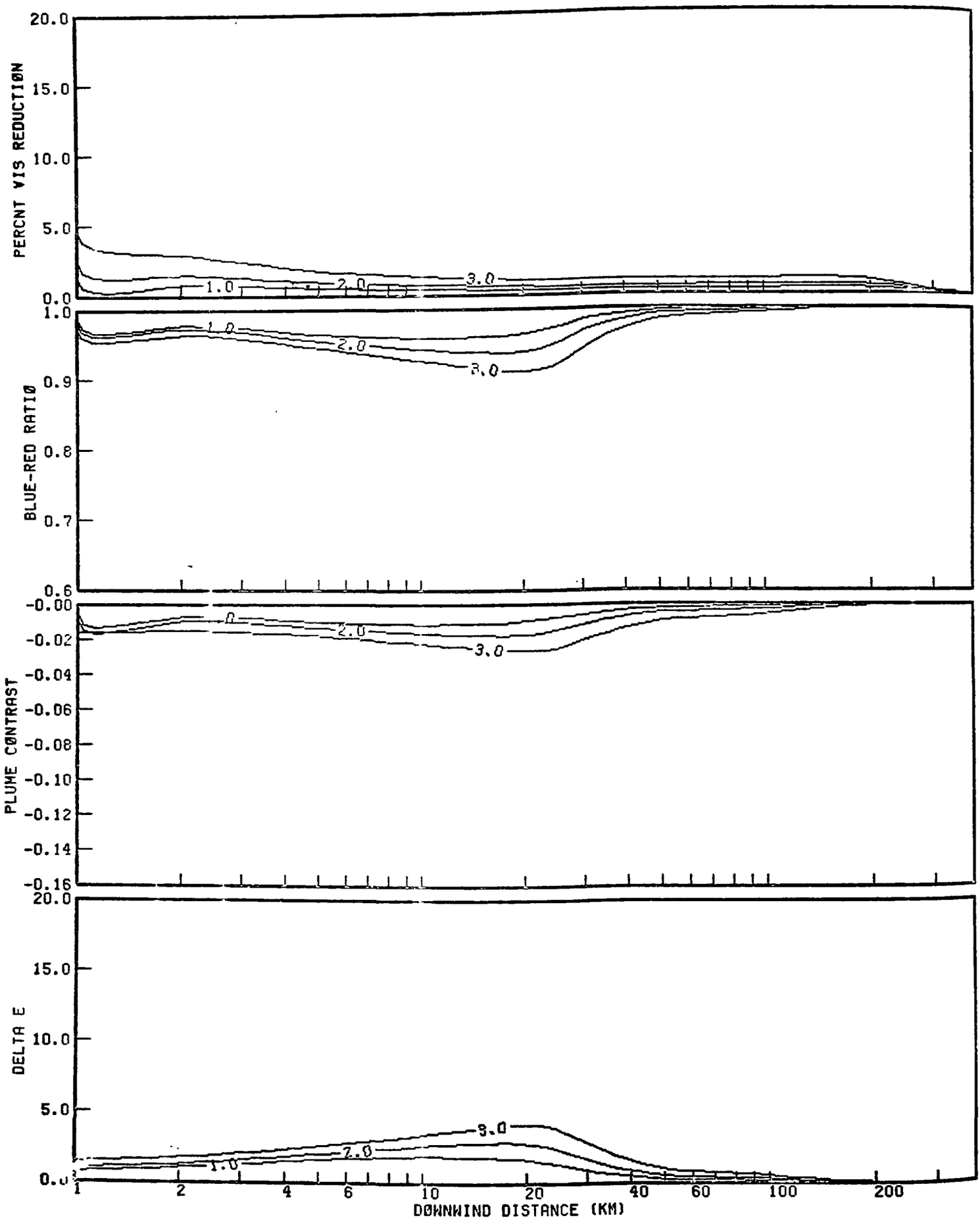

VISUAL IMPACTS OF POWER PLANTS OF INDICATED SIZE
STABILITY CLASS D
5.0 M/S WIND SPEED
50.0 KM VISUAL RANGE

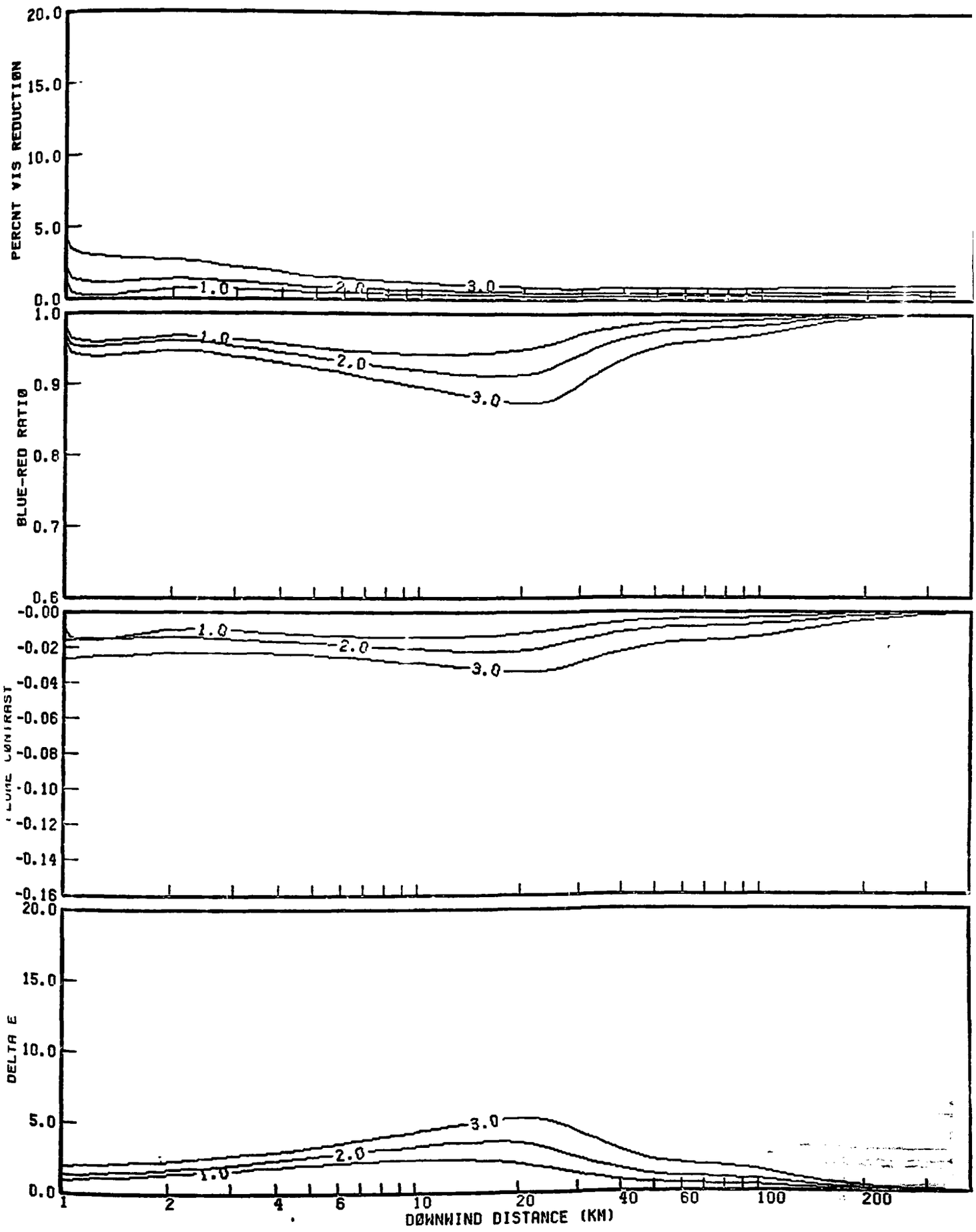

VISUAL IMPACTS OF POWER PLANTS OF INDICATED SIZE
STABILITY CLASS D
5.0 M/S WIND SPEED
100.0 KM VISUAL RANGE

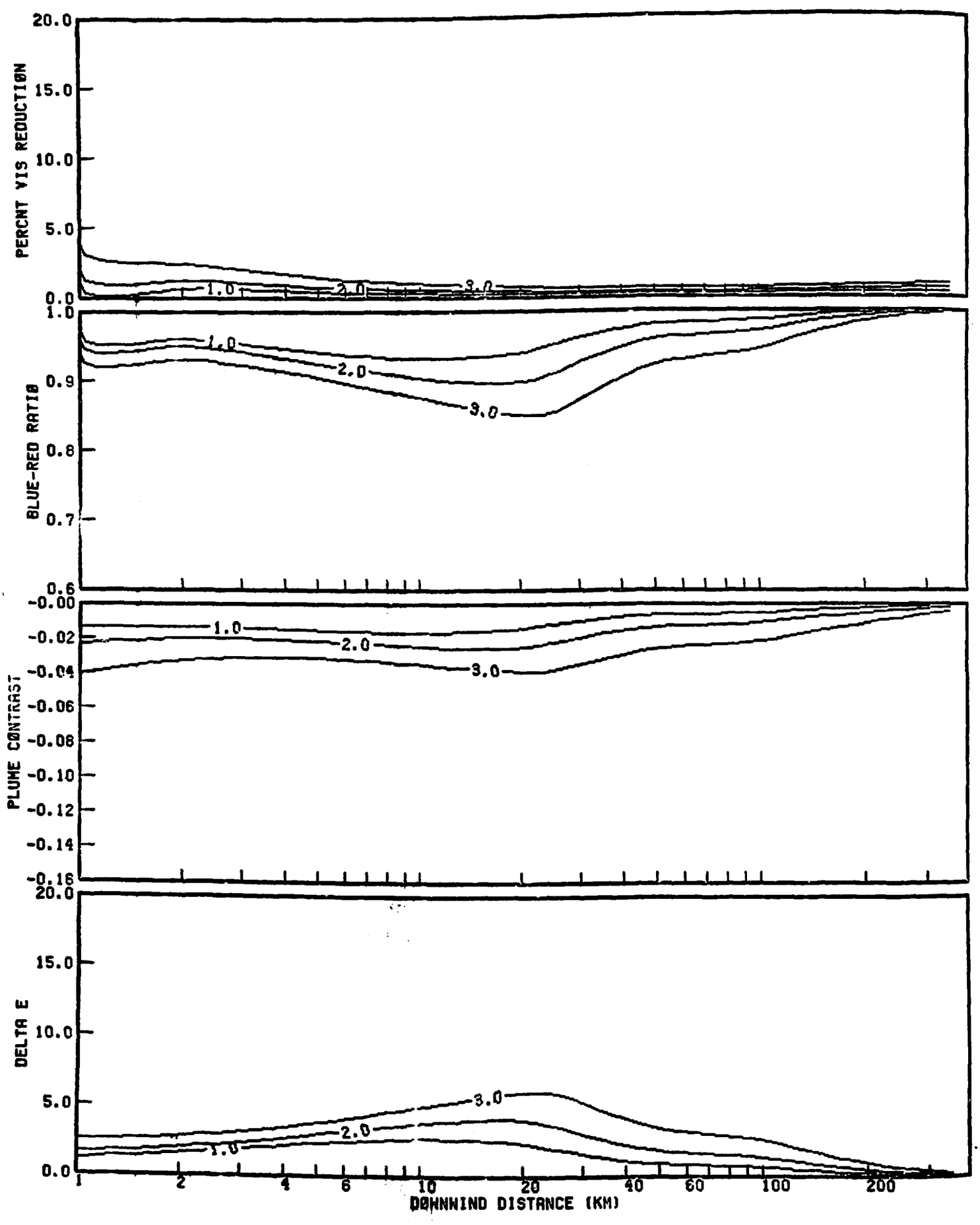

VISUAL IMPACTS OF POWER PLANTS OF INDICATED SIZE
STABILITY CLASS D
5.0 M/S WIND SPEED
200.0 KM VISUAL RANGE

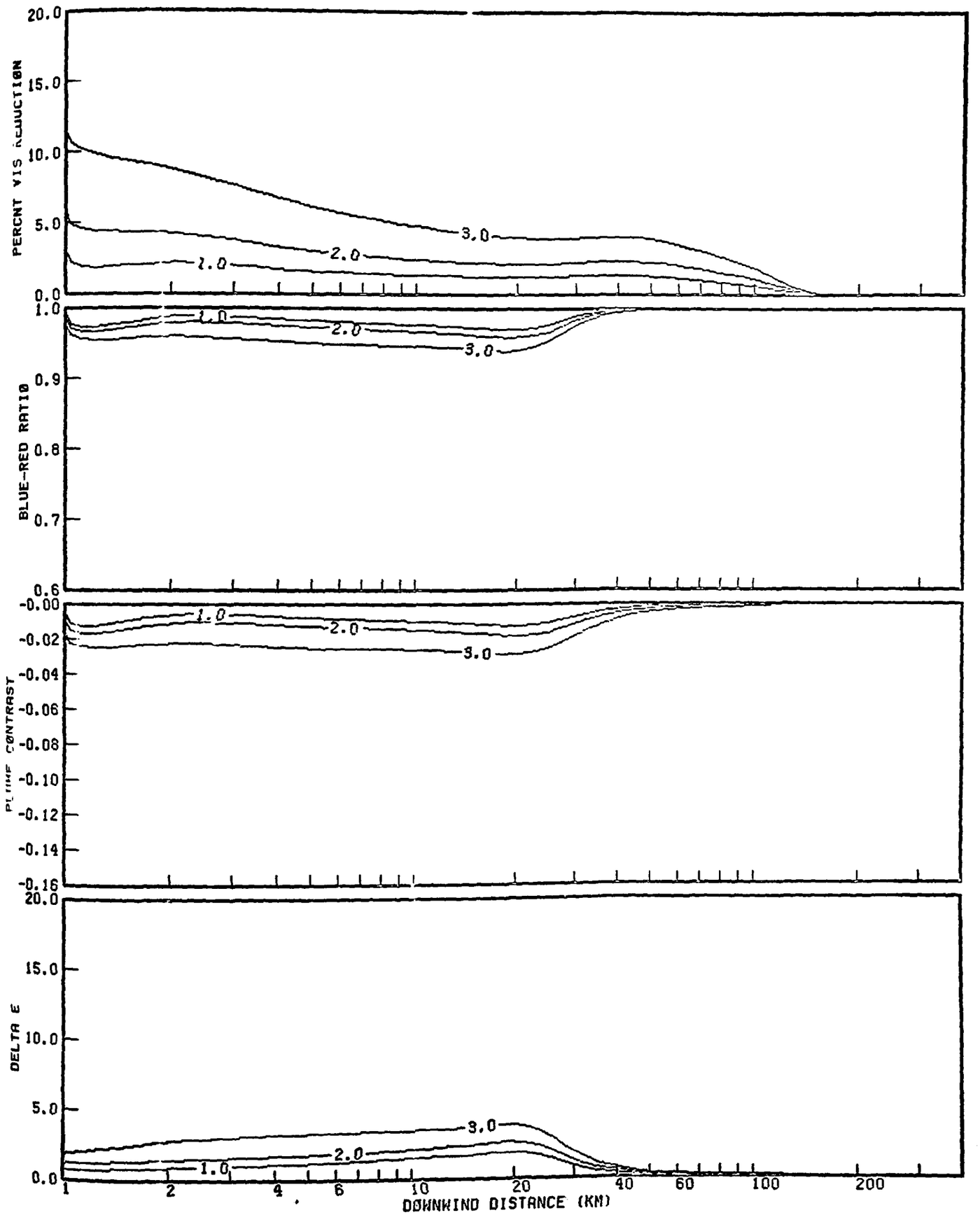

VISUAL IMPACTS ØF PØWER PLANTS ØF INDICATED SIZE
STABILITY CLASS E
2.5 M/S WIND SPEED
20.0 KM VISUAL RANGE

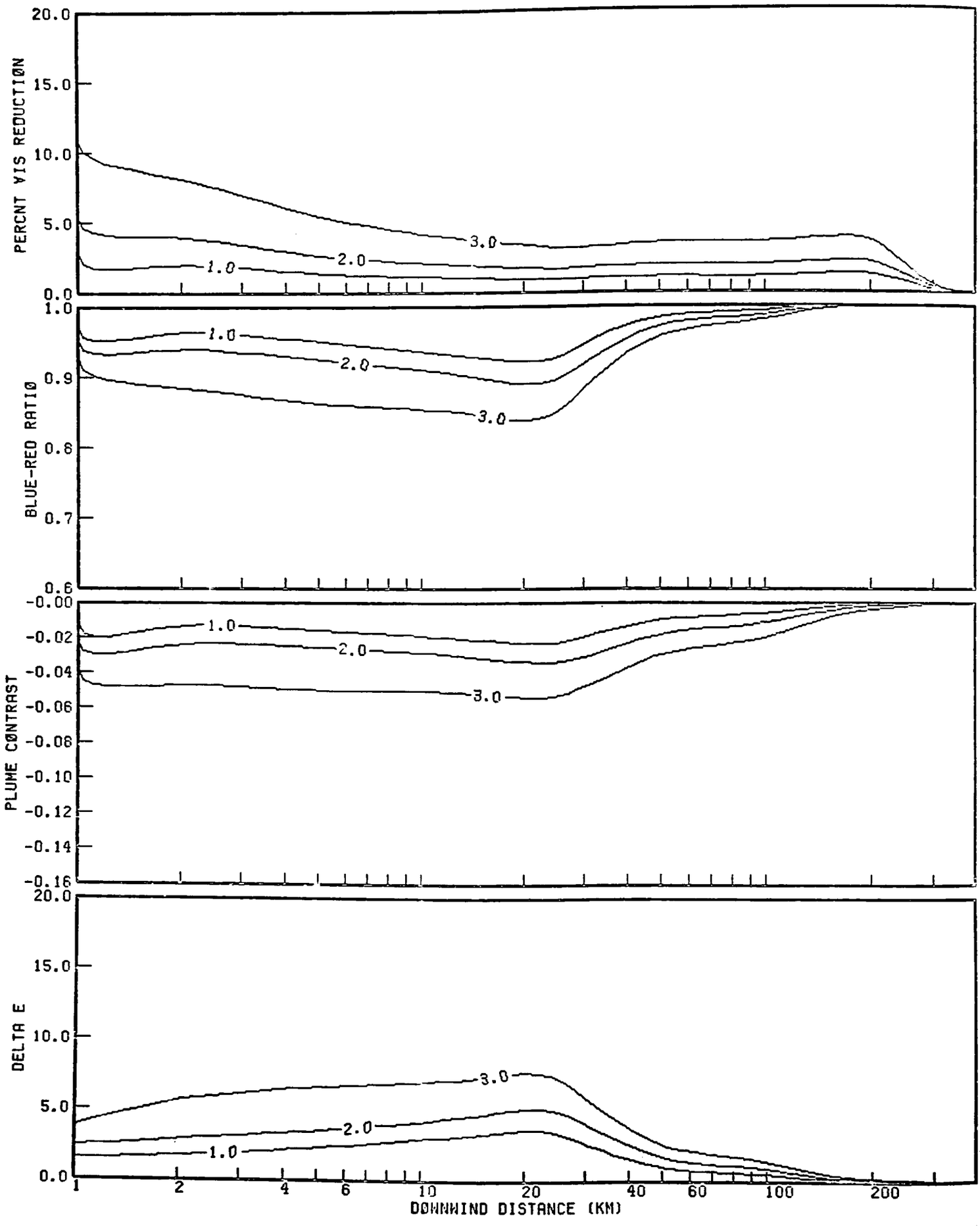

VISUAL IMPACTS ØF PØWER PLANTS ØF INDICATED SIZE
STABILITY CLASS E
2.5 M/S WIND SPEED
50.0 KM VISUAL RANGE

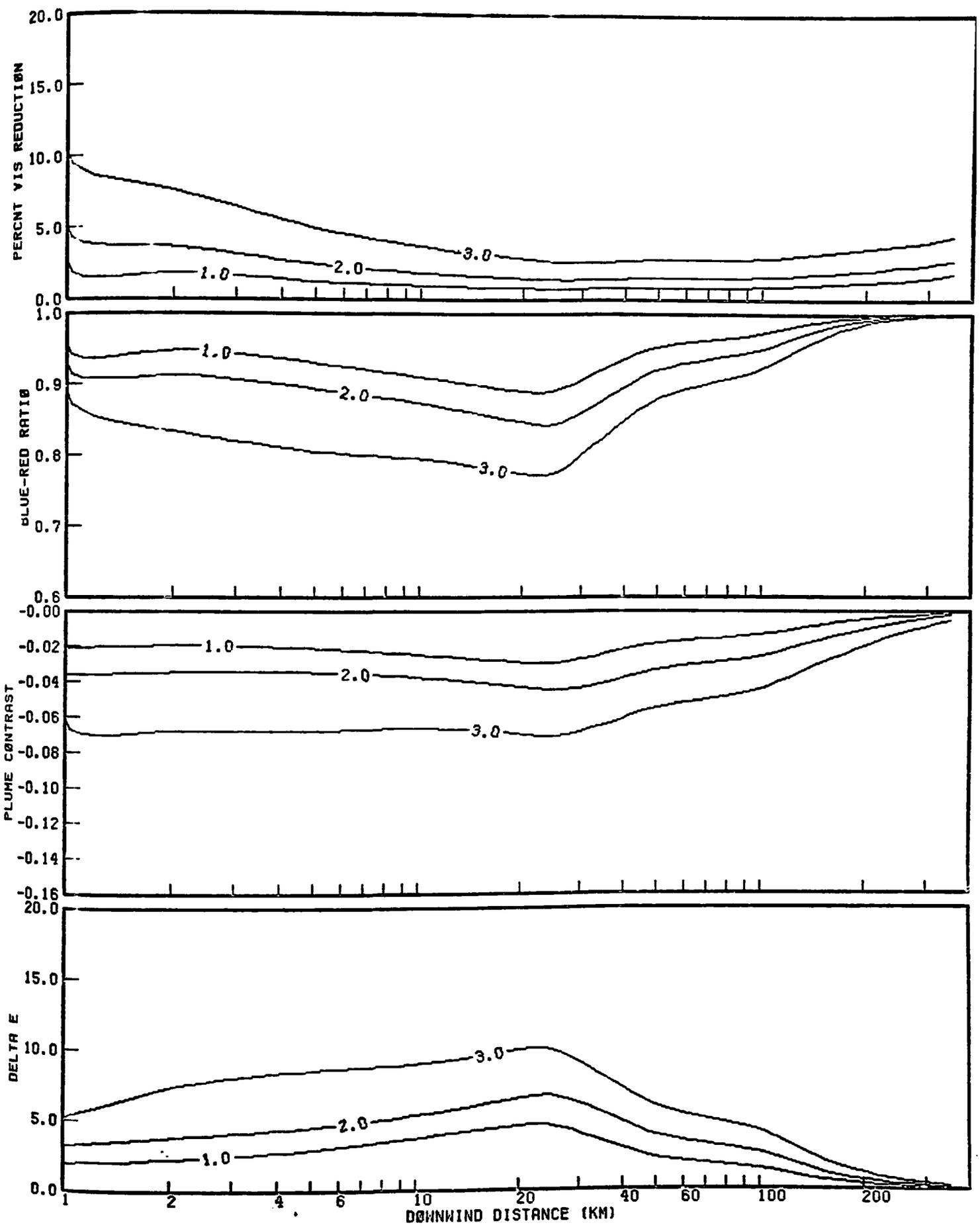

VISUAL IMPACTS OF POWER PLANTS OF INDICATED SIZE
STABILITY CLASS E
2.5 M/S WIND SPEED
100.0 KM VISUAL RANGE

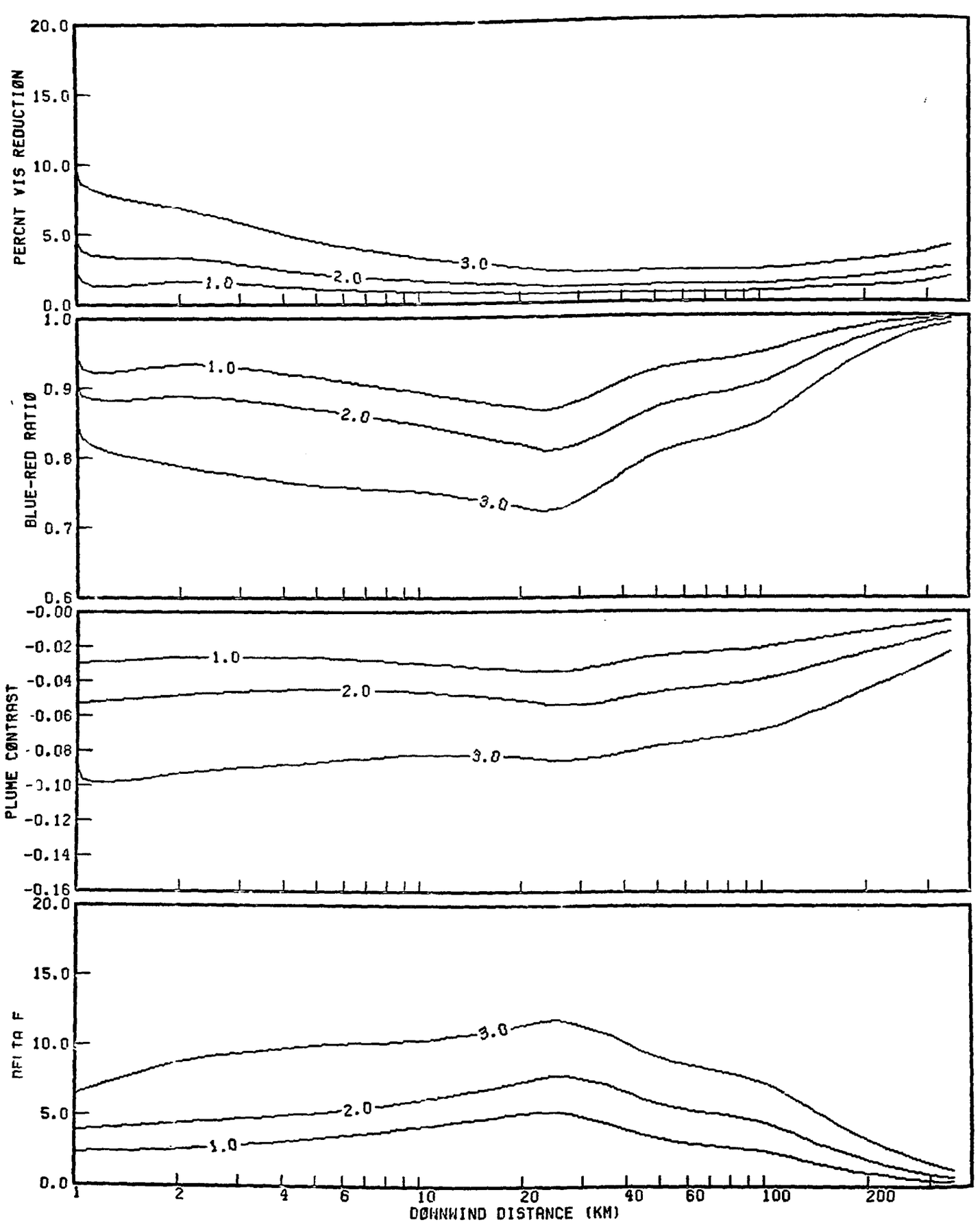

VISUAL IMPACTS OF POWER PLANTS OF INDICATED SIZE
STABILITY CLASS E
2.5 M/S WIND SPEED
200.0 KM VISUAL RANGE

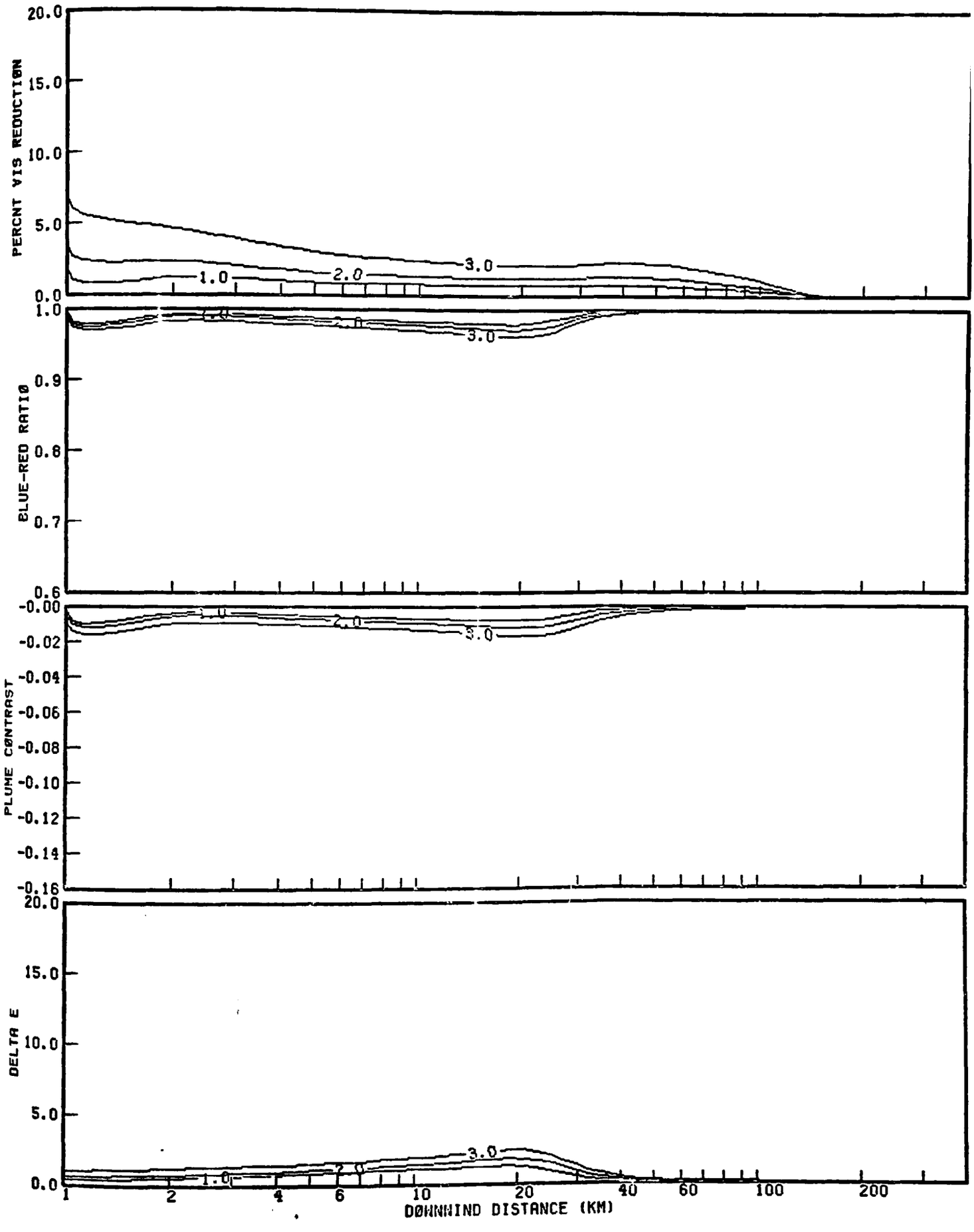

VISUAL IMPACTS OF POWER PLANTS OF INDICATED SIZE
STABILITY CLASS E
5.0 M/S WIND SPEED
20.0 KM VISUAL RANGE

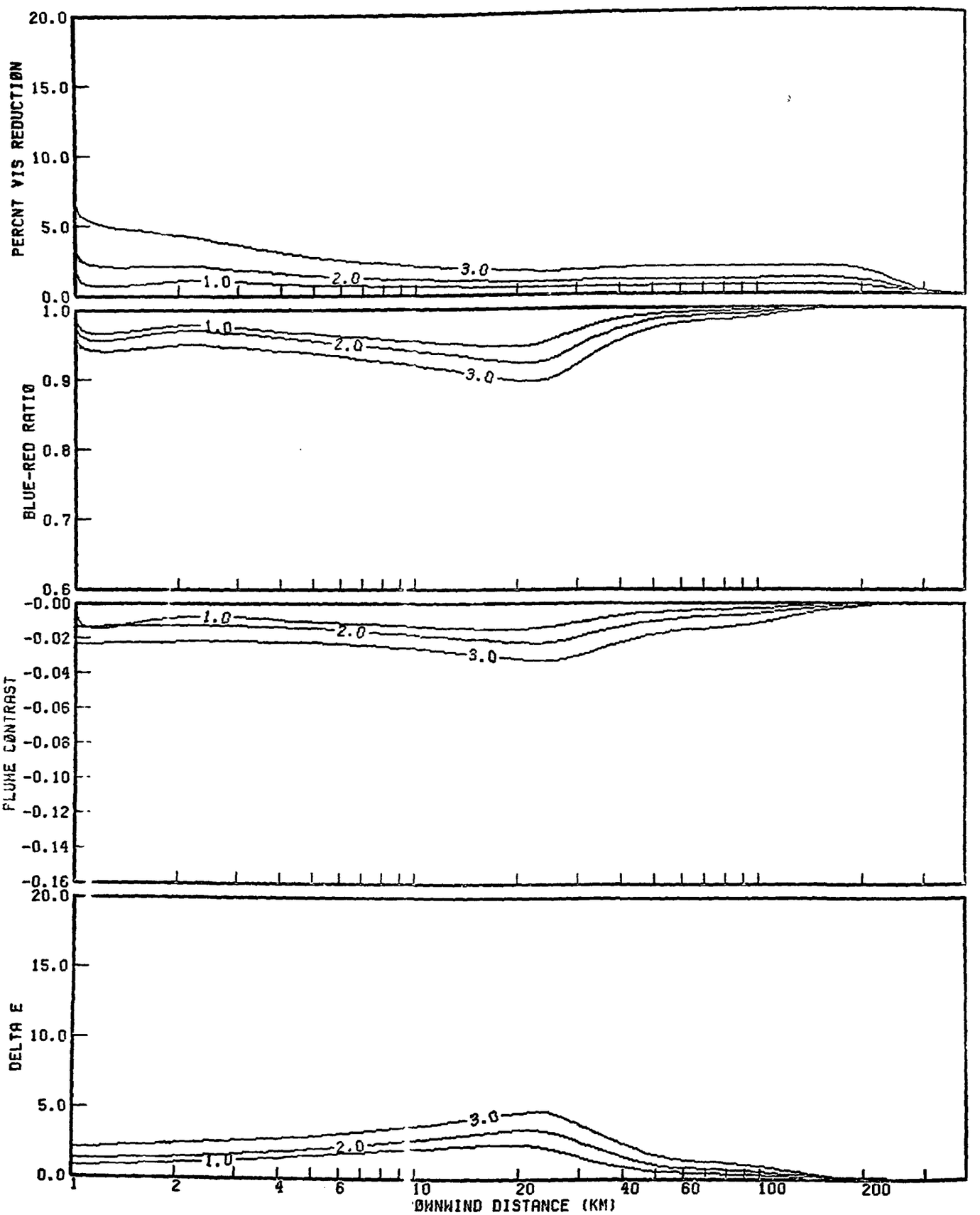

VISUAL IMPACTS OF POWER PLANTS OF INDICATED SIZE
STABILITY CLASS E
5.0 M/S WIND SPEED
50.0 KM VISUAL RANGE

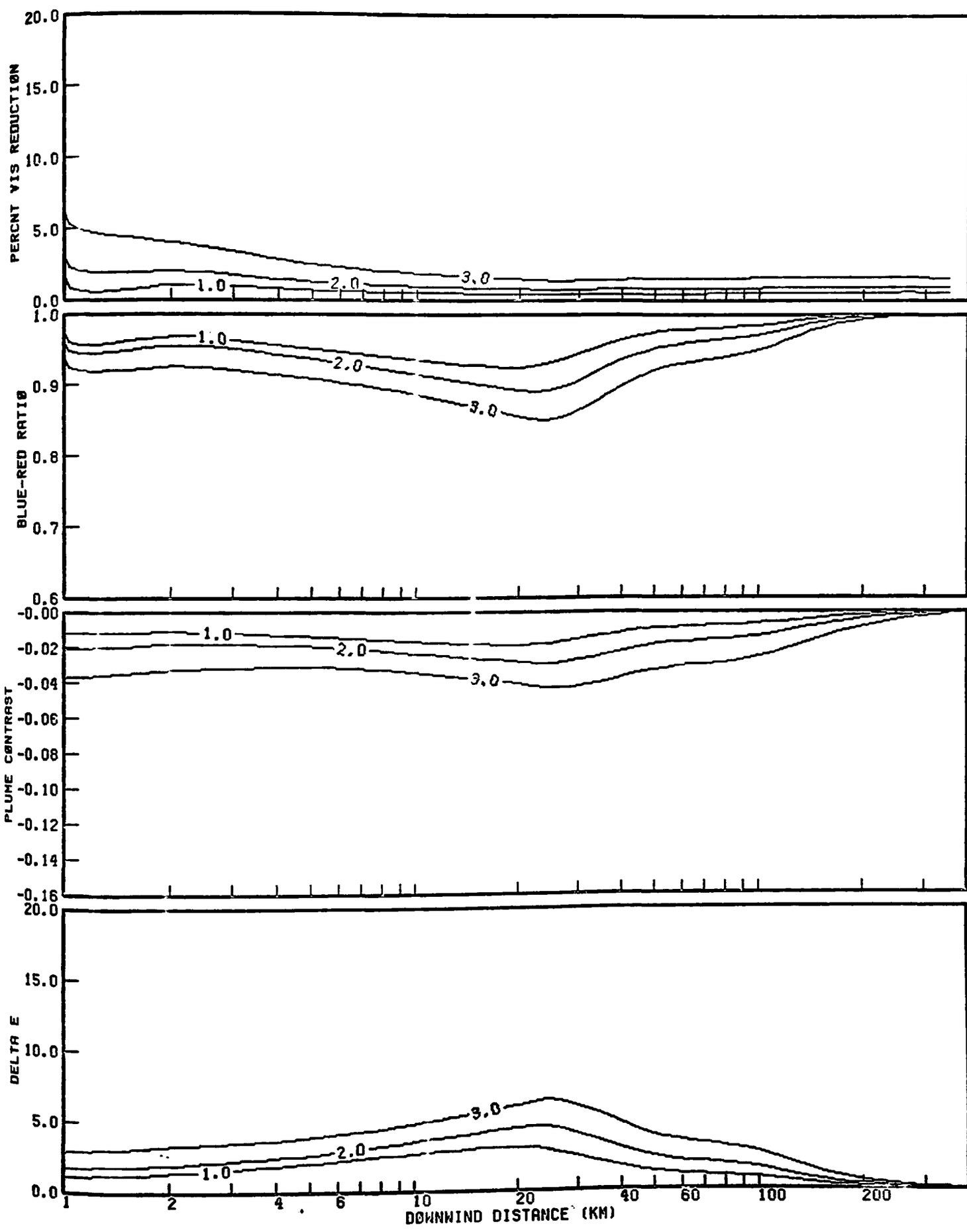

VISUAL IMPACTS OF POWER PLANTS OF INDICATED SIZE
STABILITY CLASS E
5.0 M/S WIND SPEED
100.0 KM VISUAL RANGE

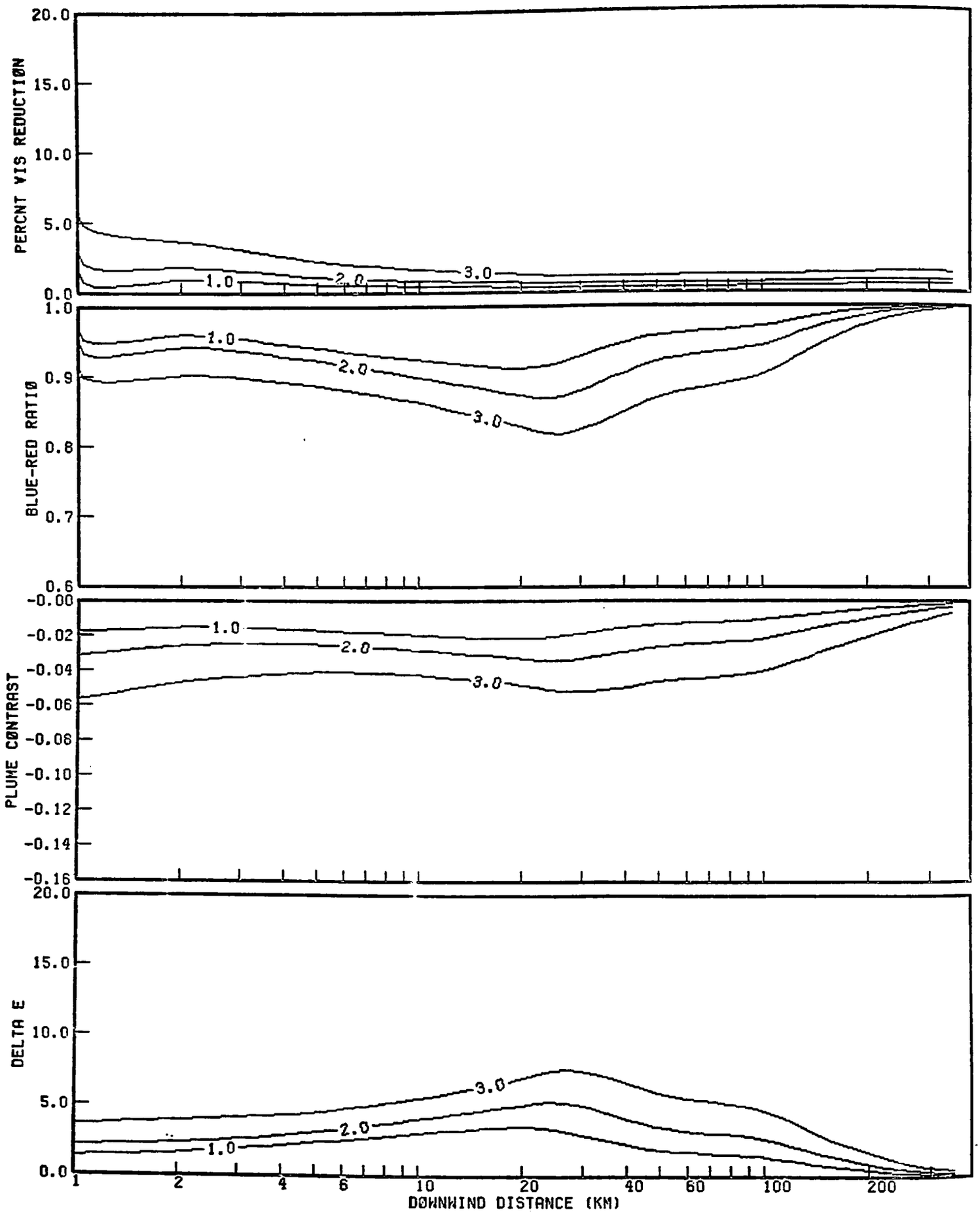

VISUAL IMPACTS OF POWER PLANTS OF INDICATED SIZE
STABILITY CLASS E
5.0 M/S WIND SPEED
200.0 KM VISUAL RANGE

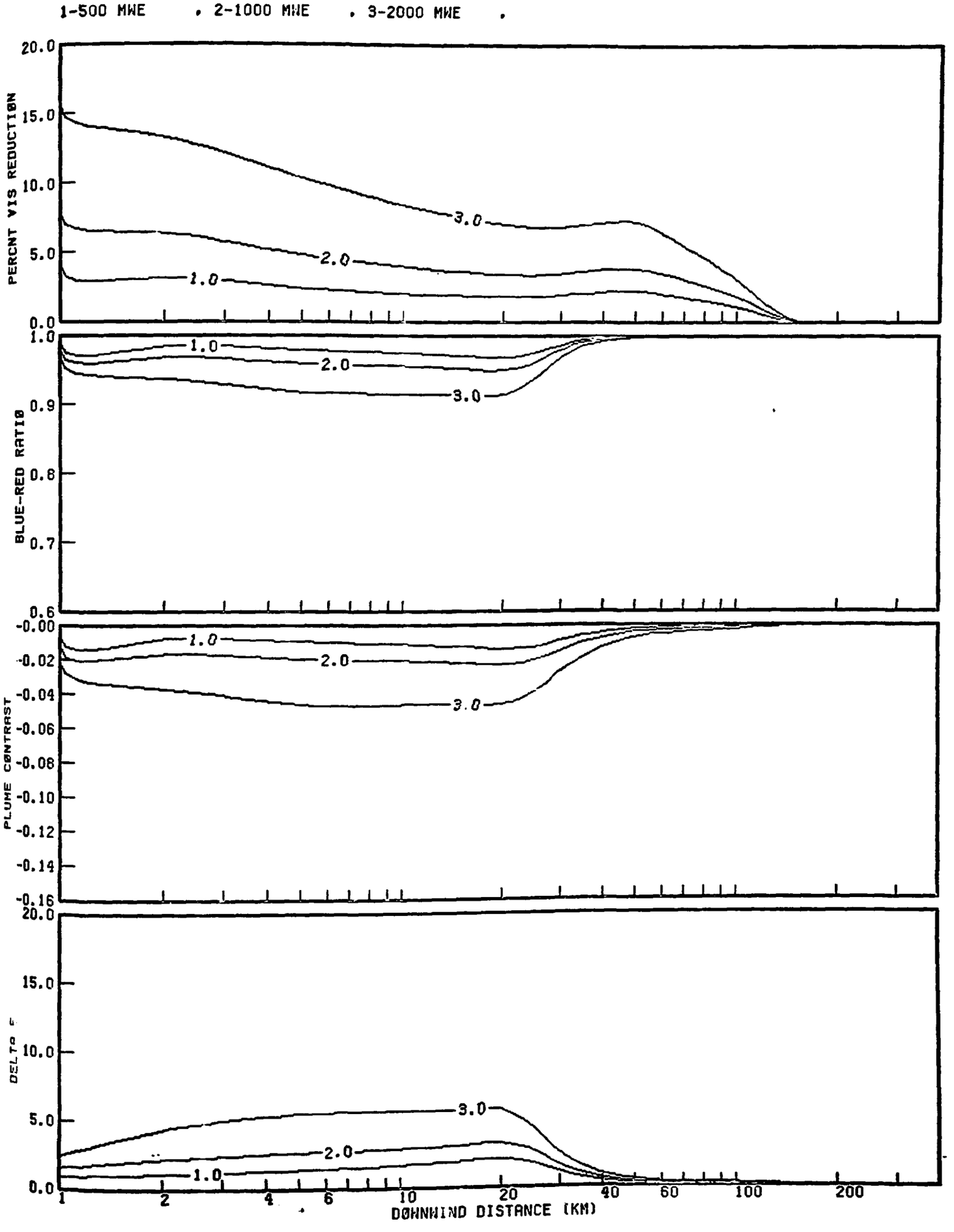

VISUAL IMPACTS OF POWER PLANTS OF INDICATED SIZE
STABILITY CLASS F
2.5 M/S WIND SPEED
20.0 KM VISUAL RANGE

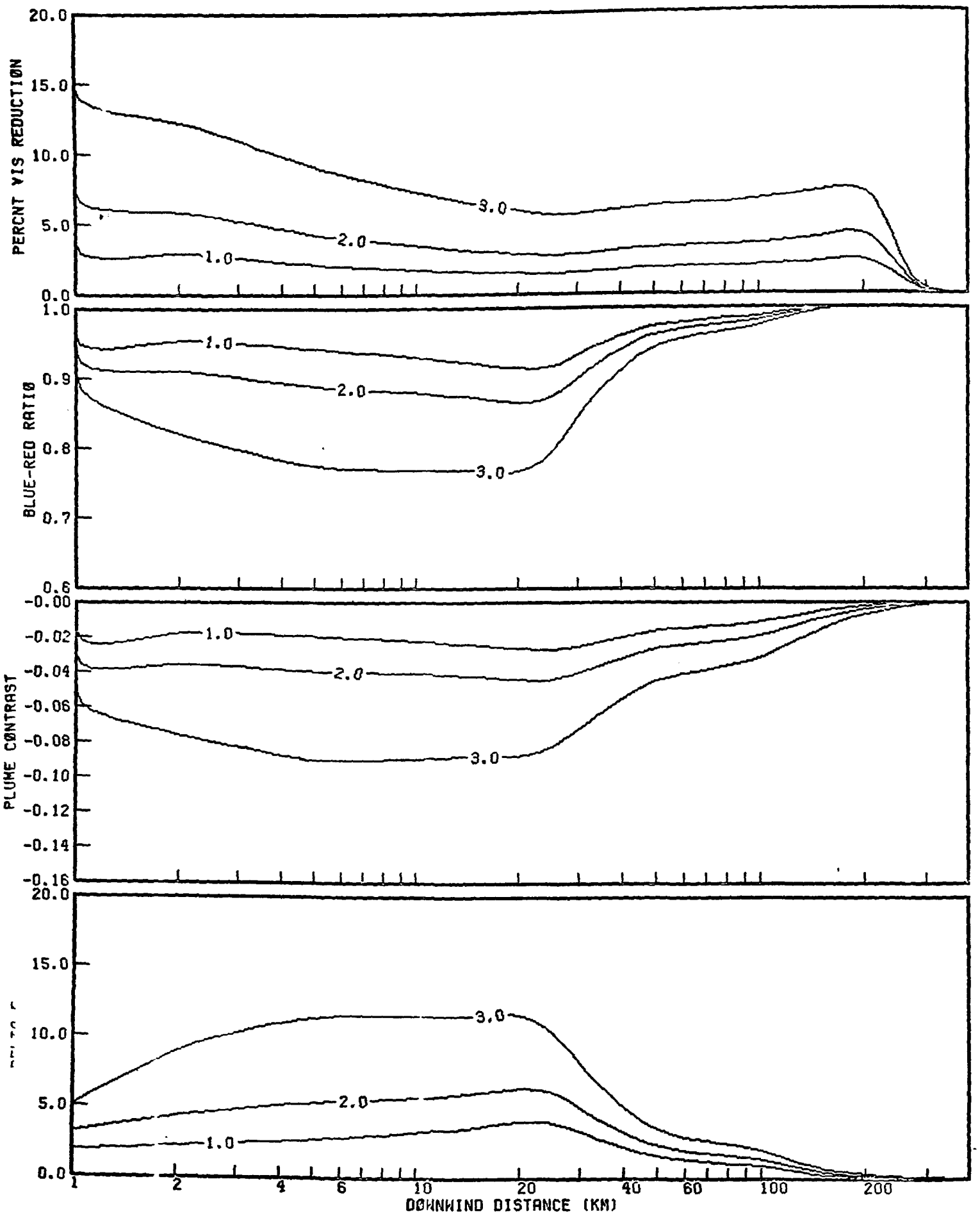

VISUAL IMPACTS OF POWER PLANTS OF INDICATED SIZE
STABILITY CLASS F
2.5 M/S WIND SPEED
50.0 KM VISUAL RANGE

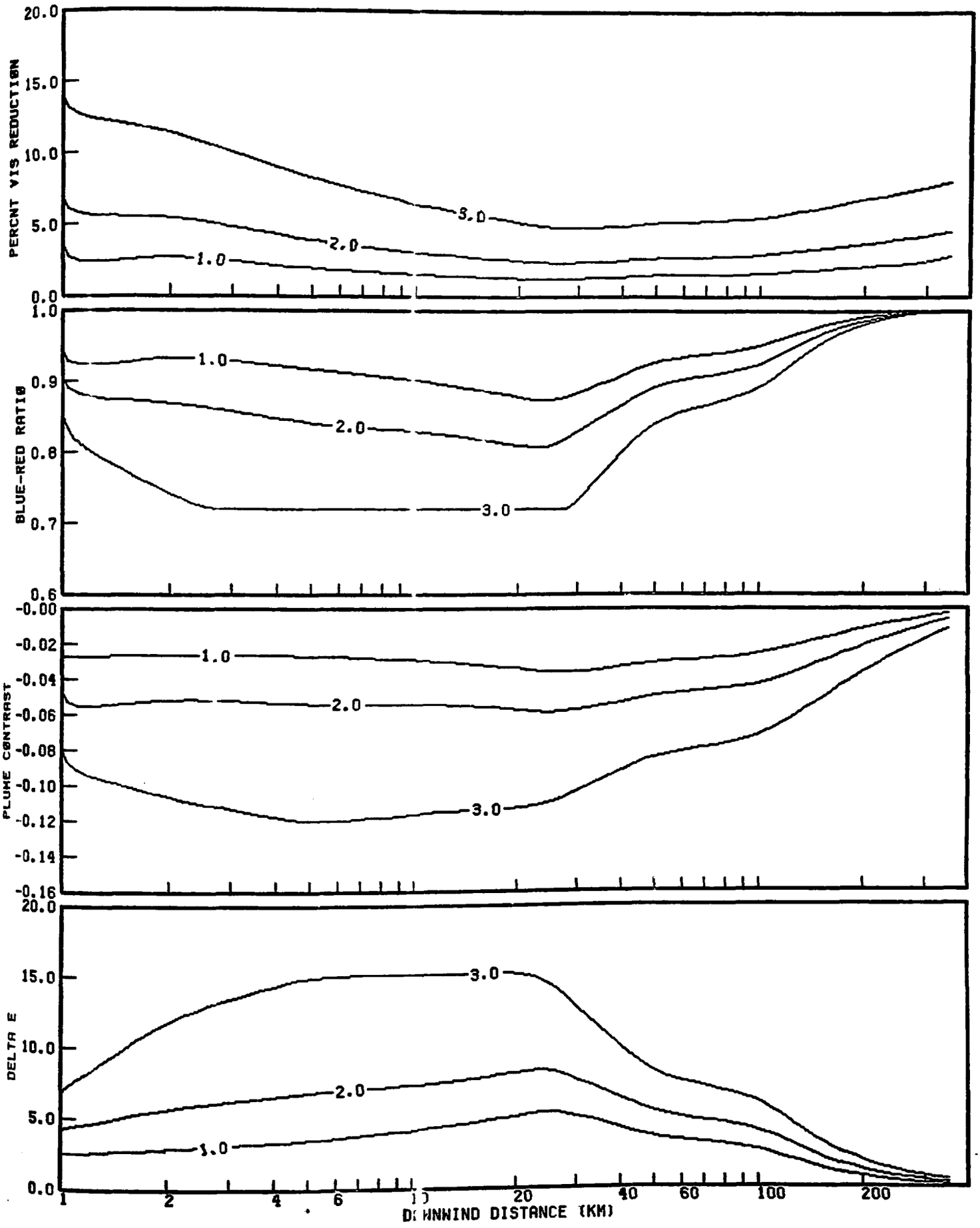

VISUAL IMPACTS ØF PØWER PLANTS ØF INDICATED SIZE
STABILITY CLASS F
2.5 M/S WIND SPEED
100.0 KM VISUAL RANGE

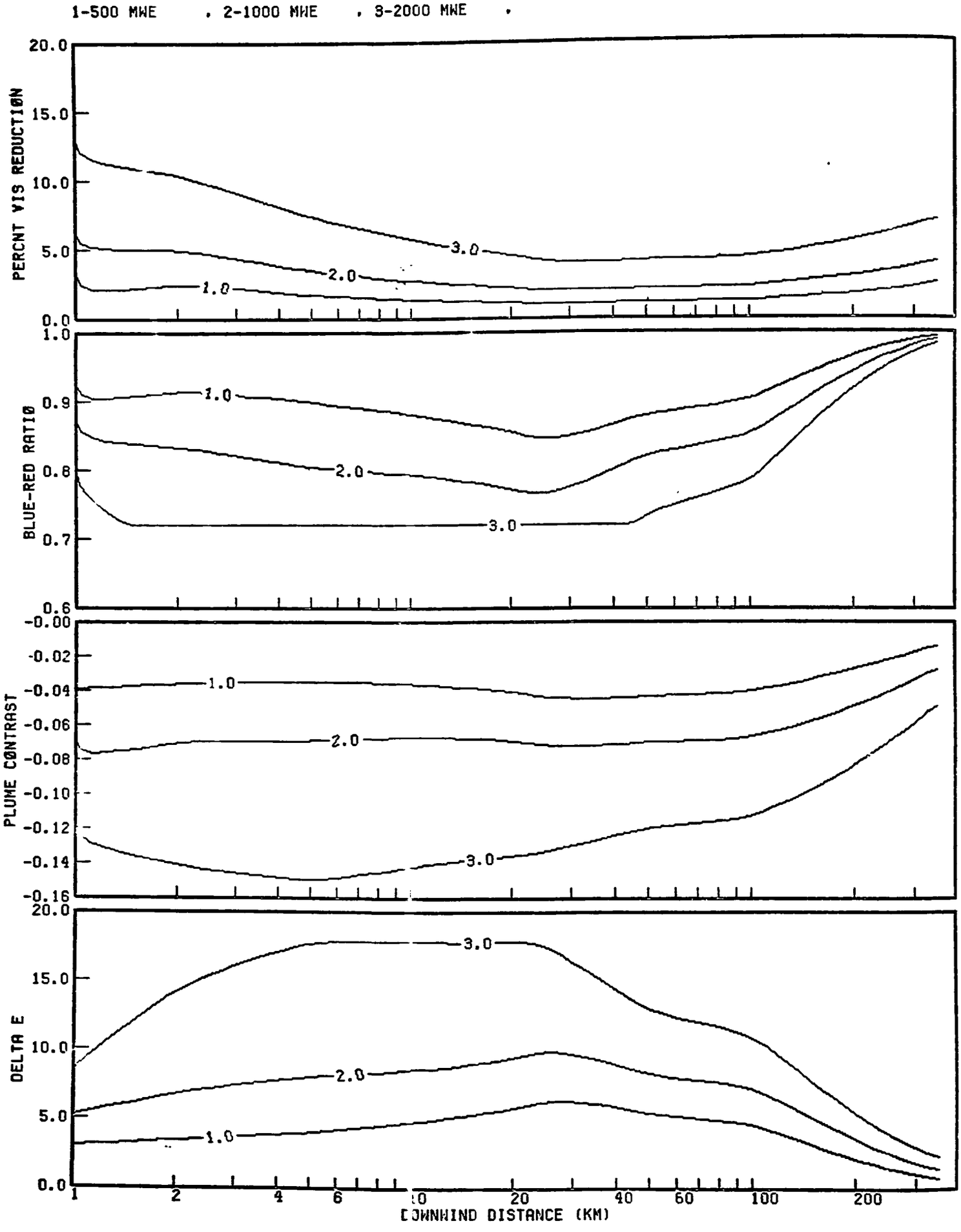

VISUAL IMPACTS ØF PØWER PLANTS ØF INDICATED SIZE
STABILITY CLASS F
2.5 M/S WIND SPEED
200.0 KM VISUAL RANGE

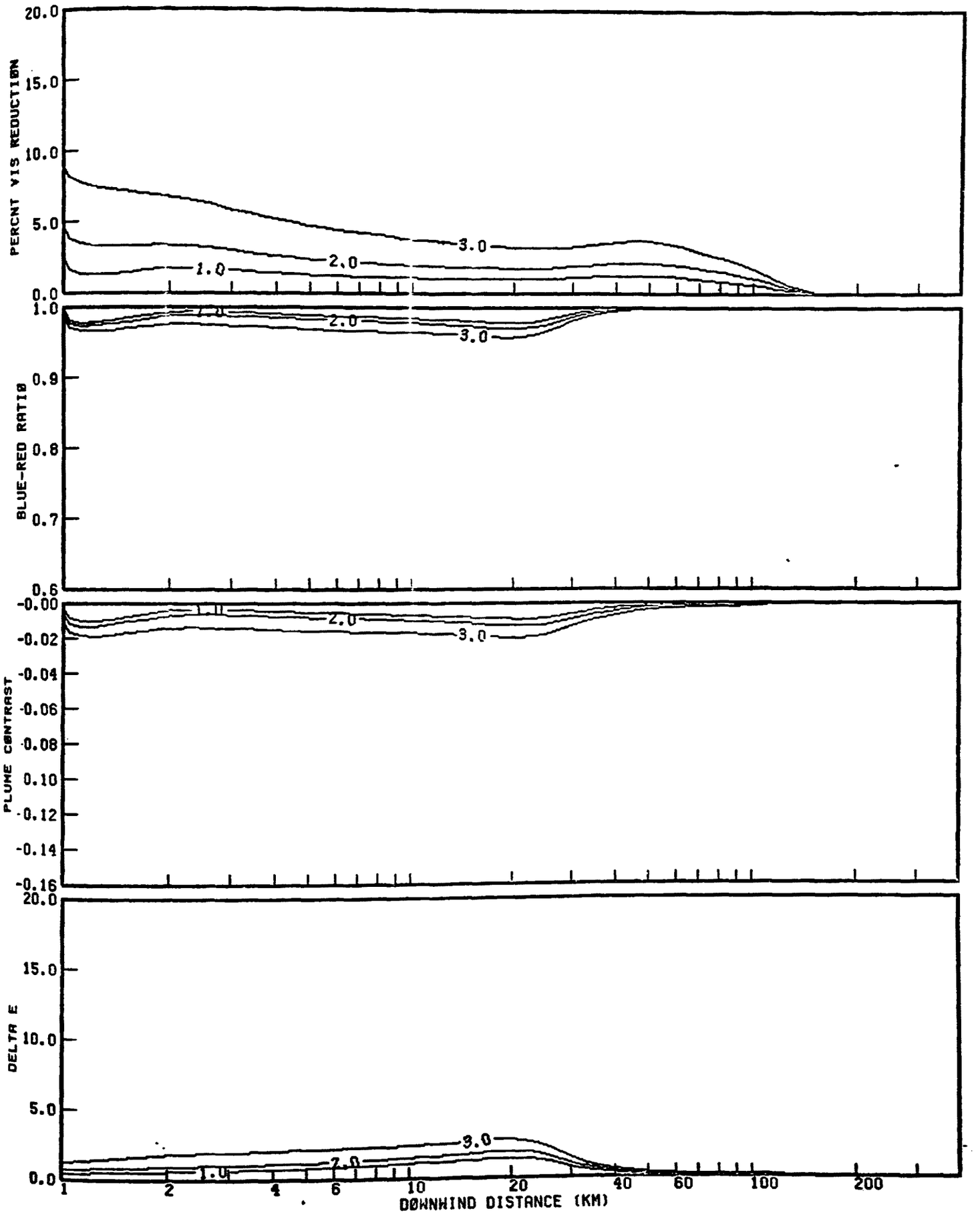

VISUAL IMPACTS OF POWER PLANTS OF INDICATED SIZE
STABILITY CLASS F
5.0 M/S WIND SPEED
20.0 KM VISUAL RANGE

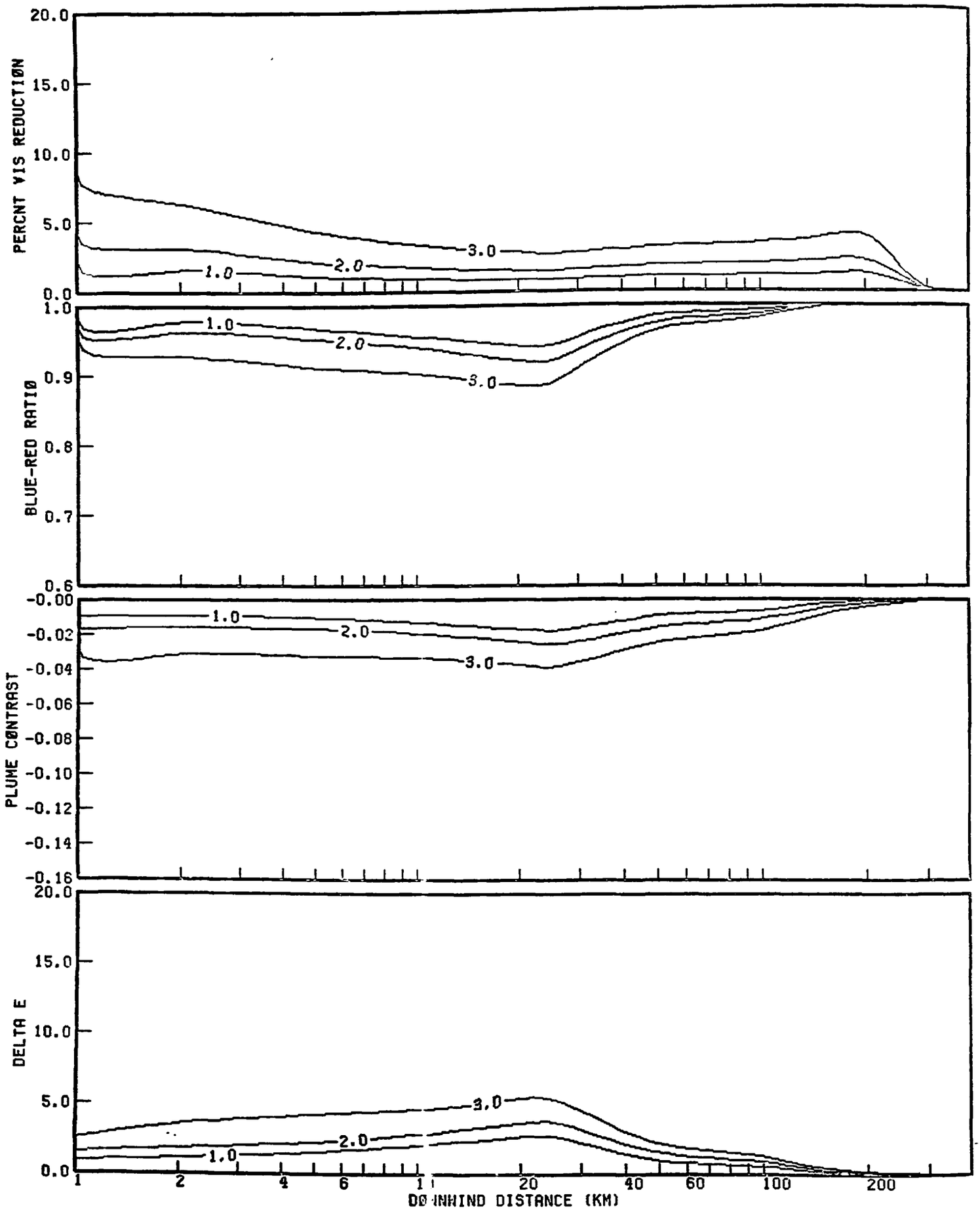

VISUAL IMPACTS OF POWER PLANTS OF INDICATED SIZE
STABILITY CLASS F
5.0 M/S WIND SPEED
50.0 KM VISUAL RANGE

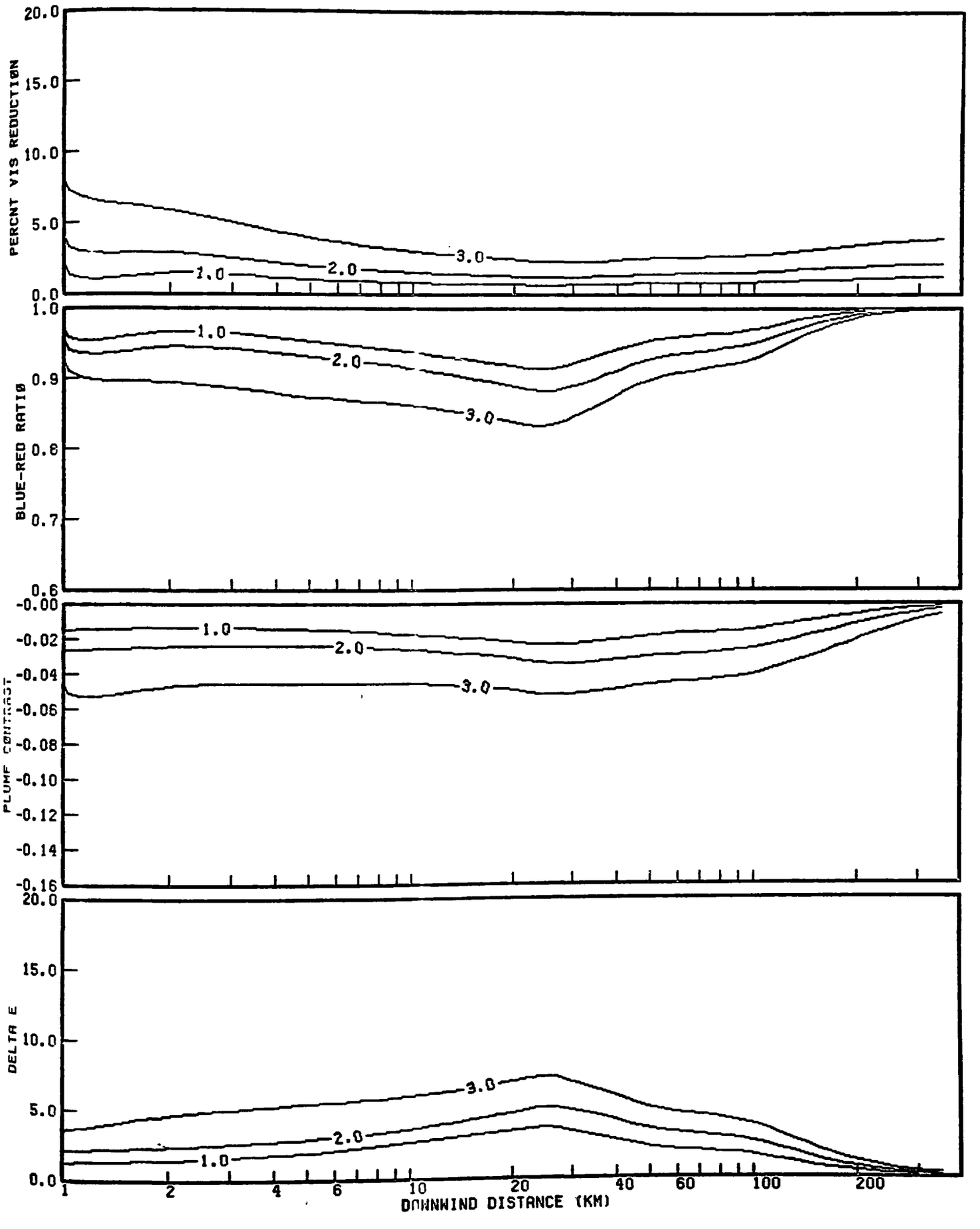

VISUAL IMPACTS OF POWER PLANTS OF INDICATED SIZE
STABILITY CLASS F
5.0 M/S WIND SPEED
100.0 KM VISUAL RANGE

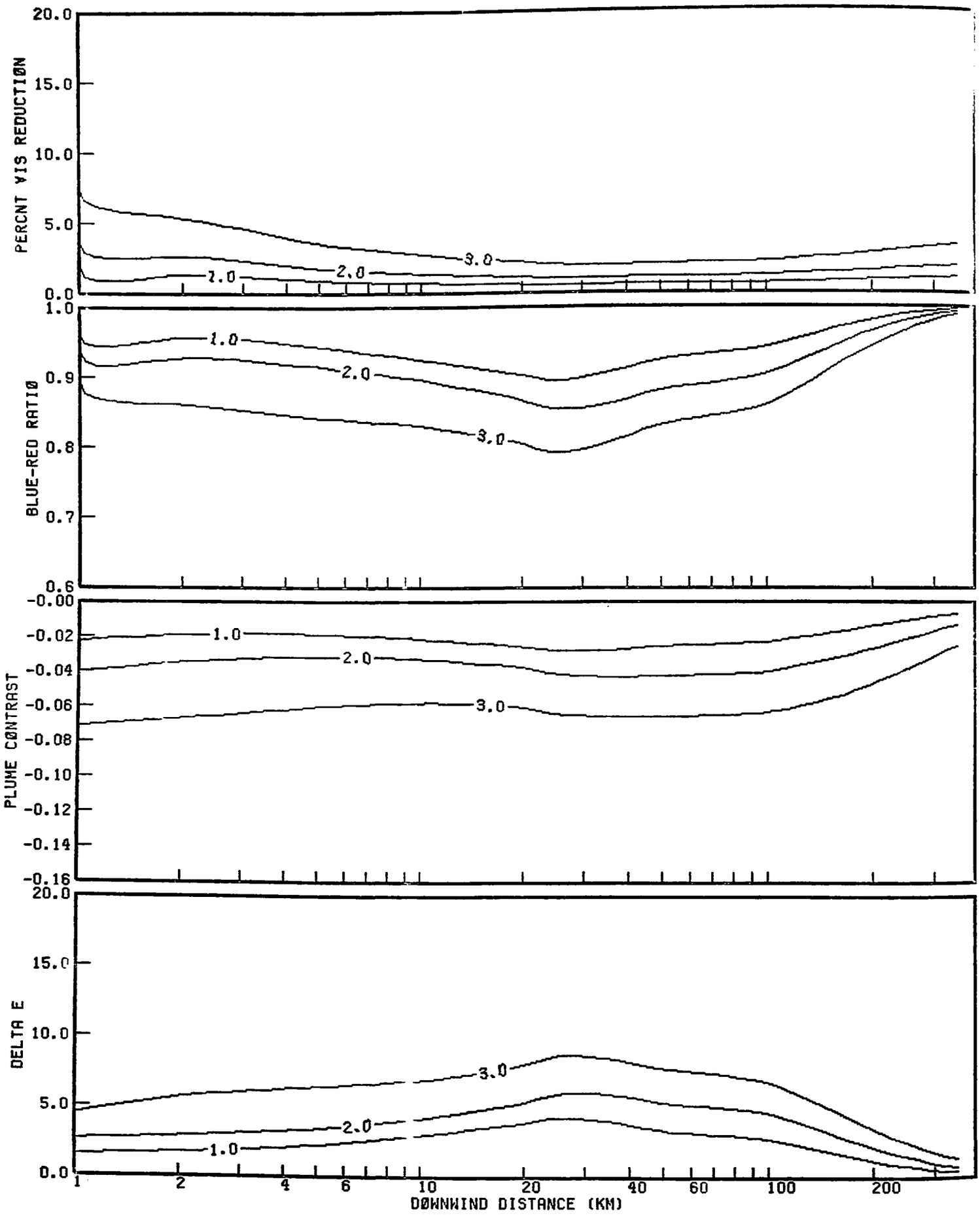

VISUAL IMPACTS ØF PØWER PLANTS ØF INDICATED SIZE
STABILITY CLASS F
5.0 M/S WIND SPEED
200.0 KM VISUAL RANGE

APPENDIX E

TWO EXAMPLE APPLICATIONS OF THE LEVEL-1 AND LEVEL-2 ANALYSES

E.1 EXAMPLE 1--COAL-FIRED POWER PLANT

E.1.1 Level-1 Analysis

This example is based on a hypothetical coal-fired power plant that has been proposed for a site approximately 70 km from a class I PSD area. The emission rates for this hypothetical power plant are projected to be 25 g/s of particulates, 380 g/sec of nitrogen oxides (as NO_2), and 120 g/sec of sulfur dioxide. Figure E-1 shows the relative locations of the proposed site and the class I area. The Federal Land Manager has identified the view toward the mountains to the west as integral to the visitors' experience of the class I area. The discussion below demonstrates the way in which potential visibility impairment in this situation would be evaluated with the level-1 procedure.

The level-1 procedure steps are carried out as follows:

1. $p = \frac{2.0 \times 10^8}{\sigma_z x}$

$x = 60$ km*

σ_{z_F} (60 km) = 83 m

$p = 4.0 \times 10^4$

2. $\tau_{part} = 1.0 \times 10^{-6} \cdot p \cdot Q_{part}$

$\tau_{NO_2} = 1.7 \times 10^{-7} \cdot p \cdot Q_{NO_x}$

* Distance from site to closest point of impact, which is the vista to the west.

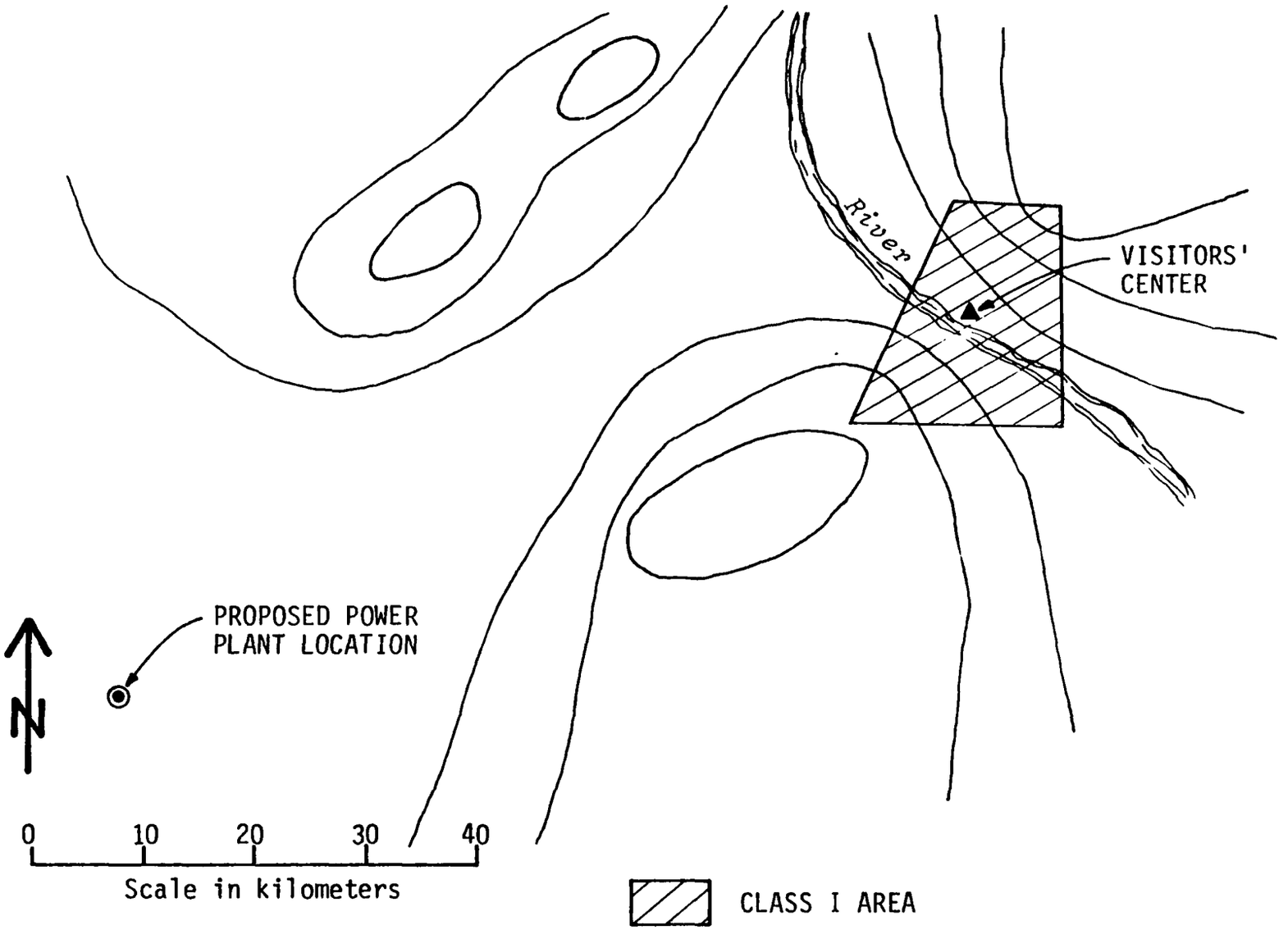

Figure E-1. Relative locations of the proposed power plant and class 1 area for example 1.

$$p = 4.0 \times 10^4$$

$$Q_{part} = 25 \text{ g/s} = 2.16 \text{ MT/day}$$

$$Q_{NO_x} = 380 \text{ g/s} = 32.8 \text{ MT/day}$$

$$\tau_{part} = 0.0864$$

$$\tau_{NO_2} = 0.223$$

3. $r_{v0} = 170$ km

(The proposed site is in the west-central United States.)

4. $$\tau_{aerosol} = (1.06 \times 10^{-5}) \cdot r_{v0} \cdot (Q_{part} + 1.31\, Q_{SO_2})$$

$$r_{v0} = 170 \text{ km}$$

$$Q_{part} = 2.16 \text{ MT/day}$$

$$Q_{SO_2} = 120 \text{ g/s} = 10.368 \text{ MT/day}$$

$$\tau_{aerosol} = 0.0284$$

5. $$C_1 = -\left[\frac{\tau_{NO_2}}{\tau_{part} + \tau_{NO_2}}\right]\left[1 - \exp(-\tau_{part} - \tau_{NO_2})\right]\left[\exp(-0.78\, x/r_{v0})\right]$$

$$C_2 = \left[1 - \frac{1}{(C_1 + 1)} \exp(-\tau_{part} - \tau_{NO_2})\right]\left[\exp(-1.56\, x/r_{v0})\right]$$

$$C_3 = 0.368\left[1 - \exp(-\tau_{aerosol})\right]$$

$\tau_{NO_2} = 0.223$

$\tau_{part} = 0.0864$

$x = 60$ km

$r_{v0} = 170$ km

$\tau_{aerosol} = 0.02837$

$C_1 = -0.146$

$C_2 = 0.0814$

$C_3 = 0.0103$

6. The absolute value of C_1 is greater than 0.10. Therefore, a level-2 analysis is indicated. Atmospheric discoloration due to NO_2 is expected to be the most serious problem.

E.1.2 Level-2 Analysis

The design parameters for the proposed power plant are:

Stack height	$h_{stack} = 150$ m
Stack inside diameter	$D = 8$ m
Stack gas velocity	$V_s = 15$ m/s
Stack temperature	$T_s = 350°K$
Particulate emissions rate	$Q_{part} = 25$ g/s = 2.16 MT/day
NO_x emissions rate (as NO_2):	$Q_{NO_x} = 380$ g/s = 32.8 MT/day
SO_x emissions rate (as SO_2):	$Q_{SO_2} = 120$ g/s = 10.4 MT/day
Site elevation	$Z_{site} = 940$ m MSL

E.1.2.1 Calculating Terrain Effects on Plume Transport

The level-2 analysis proceeds as described in the text. First, the potential for interference by terrain features on plume trajectories is identified by comparison with effective stack height.

The equation given for Δh in the text,

$$\Delta h = 1.6 \cdot F^{1/3} (3.5 x^*)^{2/3} \cdot u^{-1}$$

reduces to:

$$\Delta h = \begin{cases} 21.4\ F^{3/4} \cdot u^{-1} & \text{for } F < 55\ m^4 s^{-3} \\ 38.7\ F^{3/5} \cdot u^{-1} & \text{for } F > 55\ m^4 s^{-3} \end{cases} ,$$

where, as before,

$$F = g \frac{\dot{V}}{\pi} \left(1 - \frac{T_{ambient}}{T_{stack}}\right) ,$$

$$\dot{V} = \frac{v_s \pi d^2}{4} .$$

$h_{stack} = 150$ m
$u = 5$ m/s
$v_s = 15$ m/s
$d = 8$ m
$T_{ambient} = 10°C = 283°K$
$T_{stack} = 350°K$
$g = 9.8\ m/s^2$

$$\dot{V} = \frac{15\ m/s \cdot 3.14 \cdot 8^2\ m^2}{4}$$

$$\dot{V} = 754\ m^3/s$$

$$F = \frac{(9.8\ m/s^2)(754\ m^3/s)}{3.14} \cdot \left(1 - \frac{283°K}{350°K}\right)$$

$$F = 450\ m^4/s^3$$

$$\Delta h = \frac{38.7(450)^{3/5}}{5}$$

$$\Delta h = 302\ m$$

$$H = 150\ m + 302\ m$$

$$H = 452\ m$$

$$Z_{block} = Z_{site} + H + 500\ m$$

$$Z_{block} = 940\ m + 452\ m + 500\ m$$

$$Z_{block} = 1892\ m$$

Figure E-2 shows the area above Z_{block} in the vicinity of the class I area and the proposed power plant, along with trajectories affecting visibility in the class I area. Figure E-3 shows terrain elevation plots for several lines of sight from within the class I area.

E.1.2.2 Estimating Worst-Case Meteorological and Ambient Conditions

Worst-case conditions for plume discoloration--To characterize worst-case meteorological conditions, we obtained meteorological data from an airport 100 km west of the proposed power plant. Although the intervening terrain is not flat, we judged that the 850 mb wind and stability data are the best available data source. For the trajectory passing to the northwest of the class I area, we tabulated winds from the southwest and west-southwest for both morning and afternoon soundings. From these tabula-

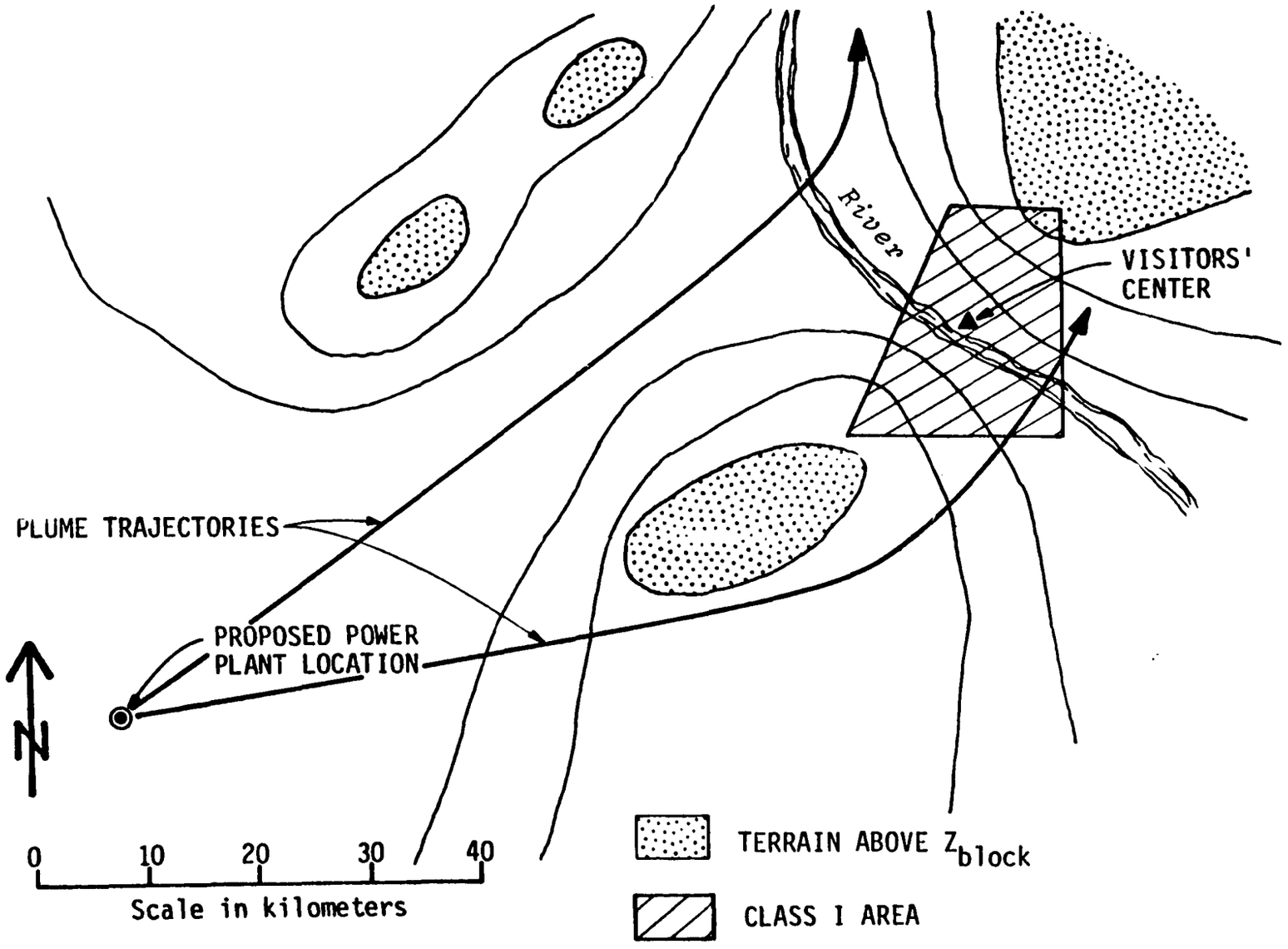

Figure E-2. Significant terrain features and possible plume trajectories.

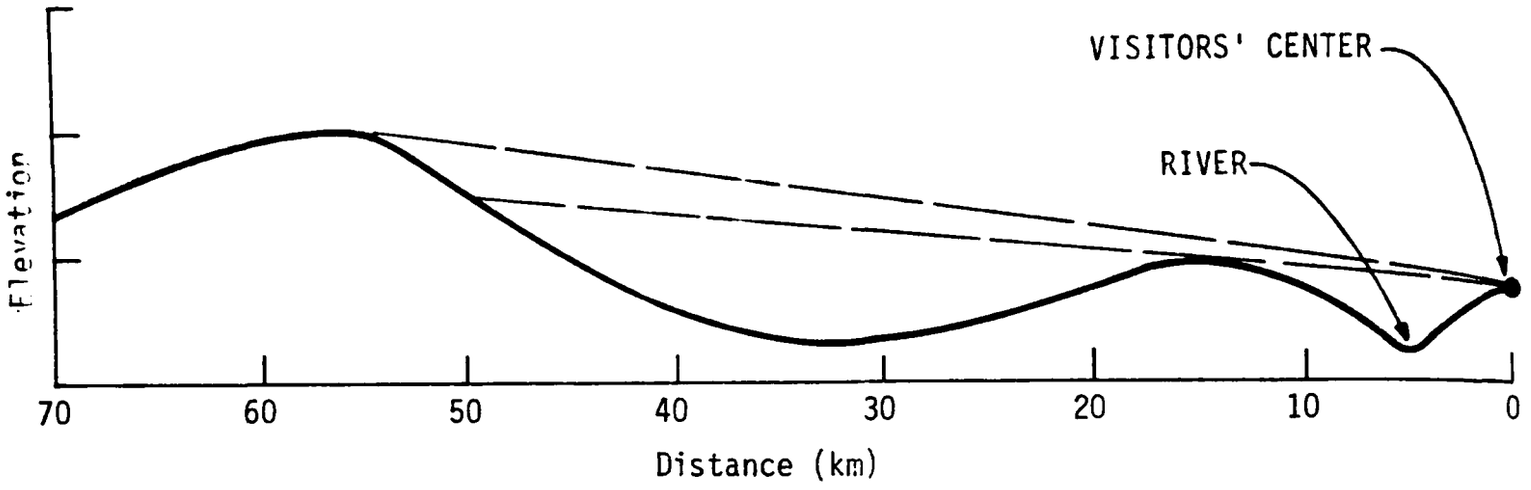

(a) View 1: To the west from Visitors' Center (A = 270°)

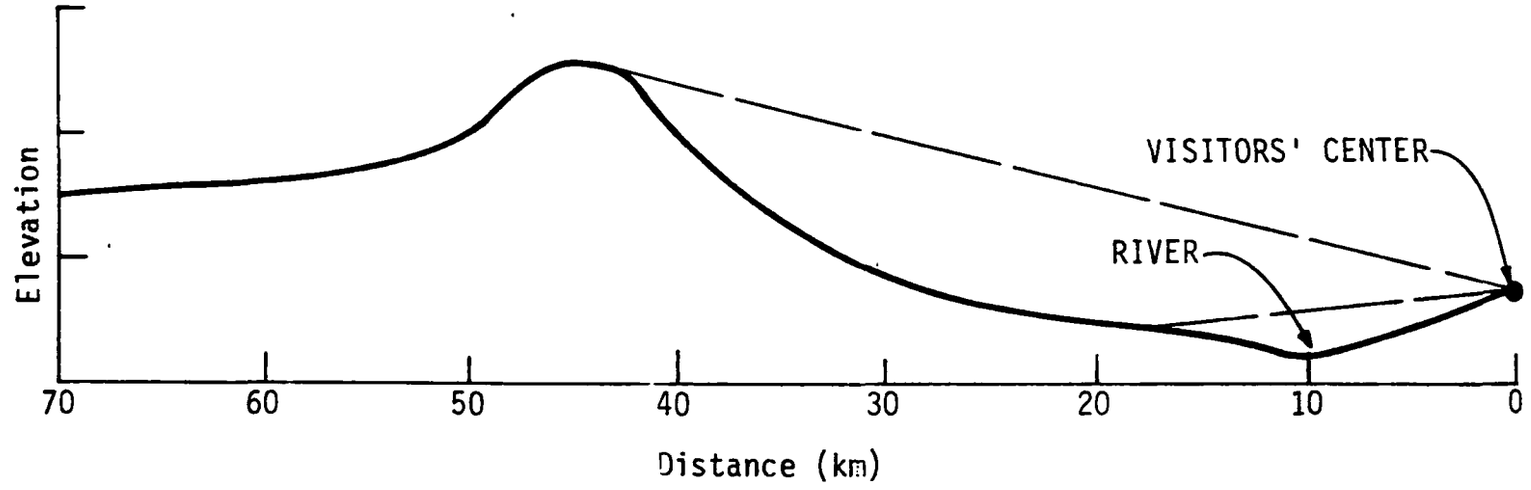

(b) View 2: To the west-northwest from Visitors' Center (A = 292.5°)

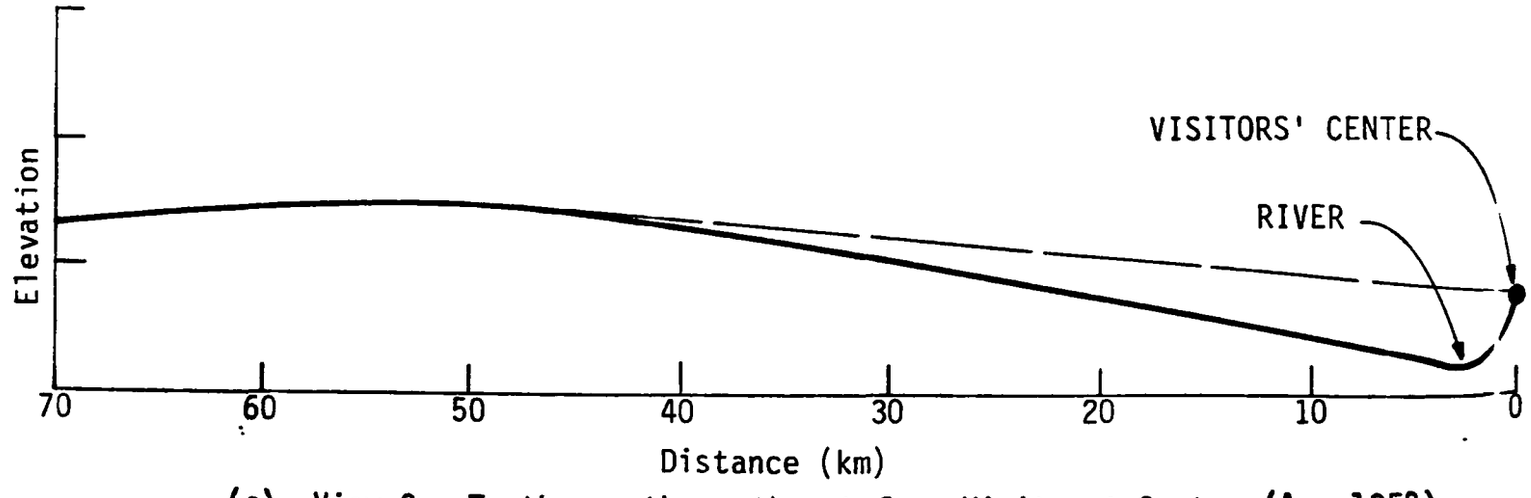

(c) View 3: To the south-southeast from Visitors' Center (A = 135°)

Figure E-3. Terrain elevation plots.

tions, a frequency of occurrence (table E-1) was developed. The cumulative frequency entries show that on three to four days per year conditions with $\sigma_z u$ values of 322 m^2/s (E stability, 2 m/s) can be expected. Note that the bulk of the contribution to the cumulative frequency (0.9% out of 1.0%) represents the 1200 GMT E,2 dispersion conditions. This corresponds to approximately 5 a.m. LST. Note also that the afternoon sounding frequency of E,2 dispersion conditions was relatively high (0.6 percent, or about two days per year).

Worst-case conditions for general haze*--Because of time and resource considerations, we decided to rely initially on Holzworth (1972) for the necessary data for the determination of episode frequency. A large scale map was obtained, on which circles of radii of integer multiples of 173 km (transport limit per 2 m/s of wind speed) were drawn, centered on the site of the proposed power plant. Class I areas were marked, and the wind sectors associated with transport to each area were noted, as shown in figure E-4. From this figure and the two-day-episode data for mixing height and wind speed in Holzworth (1972) (figures 51 through 62),† table E-2 was constructed. The worksheet in figure E-5 shows the extraction of the actual frequency of specific wind speeds and mixing depths for second-and-later episode days from the cumulative data presented in Holzworth. The four-day-per-year uH_m value is 4000 m^2/s. Note that the principal contribution to the frequency of occurrence of this condition derives from a high incidence of greater-than-two-day episodes of H_m between 500 and 1000 m and u between 2 and 4 m/s. This observation is confirmed by the five-day-episode data in figure 65 of Holzworth (1972), which show eight episodes lasting a total of 65 days for $H \leq 1000$ m and $u \leq 4$ m/s.

* Note that since C_3 was less than 0.1, we could have eliminated this step. However, for purposes of illustration this step is shown.

† The numerical values chosen here assume that Grand Junction, Colorado data best characterize the conditions affecting our hypothetical power plant.

TABLE E-1. FREQUENCY OF OCCURRENCE OF SW AND WSW WINDS BY DISPERSION CONDITION AND TIME OF DAY

Dispersion Condition	$\sigma_z u$ (m^2/s)	Transport Time (hrs)	Time of Day*		Frequency (%)	Cumulative Frequency (%)
			00Z	12Z		
F, 1	83	33	0	0	N/A	N/A†
E, 1	161	33	0	0	N/A	N/A†
D, 1	353	33	0	0	N/A	N/A†
F, 2	166	11	0.1	0	0.1	0.1
E, 2	322	11	0.6	0.9	0.9	1.0
D, 2	706	11	1.6	0.8	1.6	2.6
F, 3	249	7	0	0	0	2.6
E, 3	483	7	0.6	1.4	1.4	4.0
F, 4	332	5	0	0	0	4.0
D, 3	1060	7	3.4	1.2	3.4	7.4
F, 5	415	4	0	0.1	0.1	7.5
E, 4	644	5	0.4	1.2	1.2	8.7
D, 4	1410	5	2.4	1.5	2.4	11.1
F, 6	498	4	0	0	0	11.1
E, 5	805	4	0.2	1.8	1.8	12.9

* 00Z refers to midnight Greenwich mean time (GMT) and 12Z to noon GMT.

† Persistence of stable meteorological conditions for over 12 hours is not considered likely. Therefore, conditions requiring greater than 12-hour transport time are included in the cumulative frequency computation, but would not be selected as representative of the "1-percentile event."

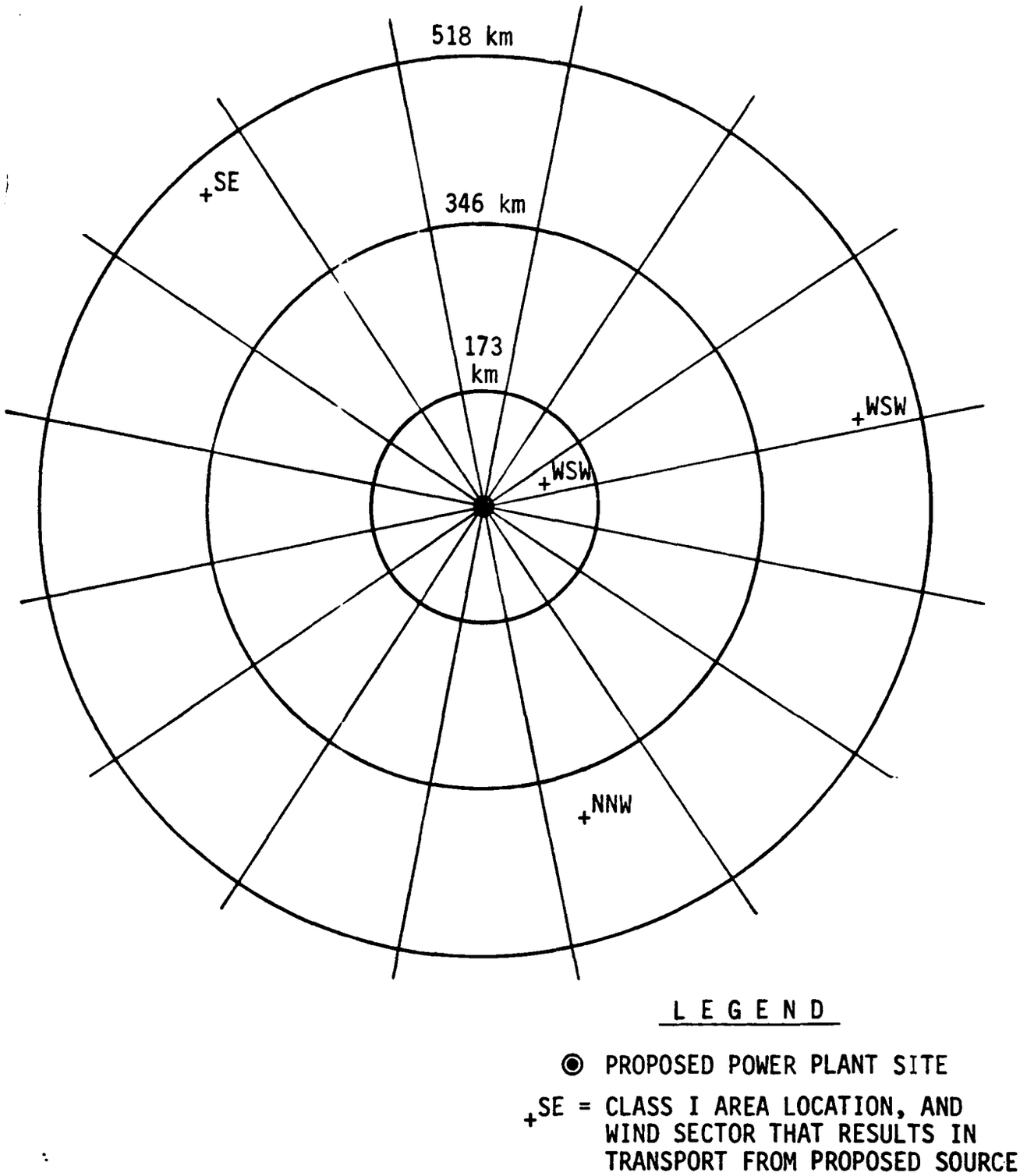

Figure E-4. Class I areas within 48-hour transport range at wind speeds up to 8 m/s.

TABLE E-2. FREQUENCY OF EPISODE DAYS BY MIXING DEPTH AND WIND SPEED*

u, H_m	u H (m^2/s)	f_{2+}† (Day 2+ frequency per five years)	Sectors with Class I Areas (n_s)	Number of Occurrences Affecting Class I Area Sectors per Year	
				f§	Cumulative
2, 500	1000	10	1	0.25	0.25
2, 1000	2000	3	1	0.075	0.325
4, 500	2000	15	3	1.125	1.45
2, 1500	3000	1	1	0.025	1.475
6, 500	3000	1	3	0.075	1.55
2, 2000	4000	0	1	0	1.55
4, 1000	4000	72	3	5.4	6.95
4, 1500	6000	49	3	3.675	10.625
6, 1000	6000	25	3	1.875	12.5
4, 2000	8000	23	3	1.725	14.225
6, 1500	9000	57	3	4.275	18.5
6, 2000	12000	37	3	2.775	21.275

* Example based on Grand Junction, Colorado.

† From frequency worksheet shown in figure E-5.

§ $f = \frac{f_{2+} \cdot n_s}{5 \cdot 16} = \frac{\text{Class 1 sector impact days}}{\text{year}}$.

(u, H)	5-year Cumulative (i.e., # ≤ u, ≤ H) No. of Episodes Lasting at Least 2 Days (f_e)	No. of Episode Days (f_d)	No. of 2nd and Later Days (f_d-f_e)	No. of 2nd and Later Days for Specific Conditions (from matrix below) (f_{2+})	
2, 500	7	17	10	10	
4, 500	12	37	25	15	
6, 500	12	38	26	1	
2, 1000	9	22	13	3	
4, 1000	29	129	100	72	Sum = 293
6, 1000	40	166	126	25	= f_d (6, 2000)
2, 1500	10	24	14	1	- f_e (6, 2000)
4, 1500	43	193	150	49	
6, 1500	64	297	233	57	
2, 2000	10	24	14	0	
4, 2000	51	224	173	23	
6, 2000	72	365	293	37	

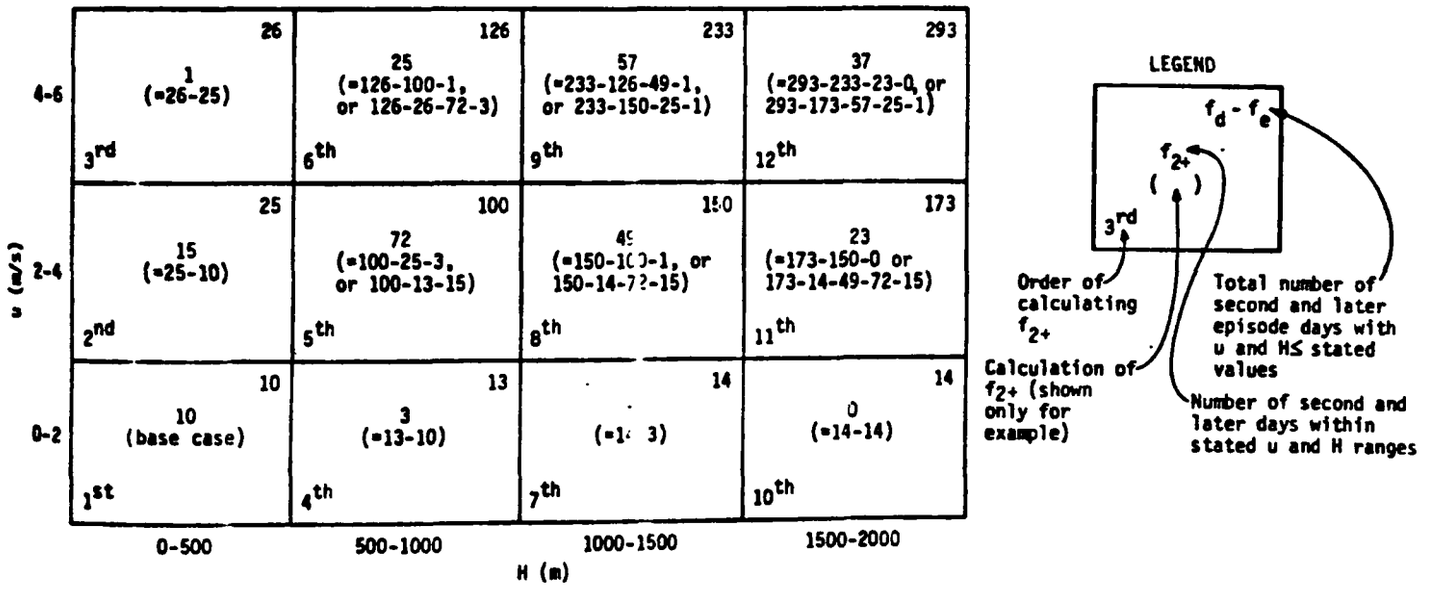

Figure E-5. Worksheet for the calculation of windspeed and mixing depth joint frequency distribution

Background Ozone Concentration--According to the "W" notation in figures 51 through 62 in Holzworth (1972), limited mixing episodes occur predominantly during winter months in the vicinity of Grand Junction, Colorado. Also, in the same reference, table B-1 gives seasonal mean mixing depths and wind speeds. According to this table, the uH value by season is most limiting for winter (uH = 3333, 19448, 22981, and 9011 m^2/s, respectively, for winter, spring, summer, and autumn). Therefore, in the absence of any other data for ozone aloft, a conservative winter median ozone estimate of 50 ppb (0.05 ppm) was taken from figure 19 of the text.

Background Visual Range--Telephotometer data for several months are available, and we have interpreted them as indicating a median r_{v0} of 140 km; however, this data set is relatively small. Therefore, the more conservative estimate of 170 km from figure 13 of the text was chosen for the initial level-2 analysis, based on our recognition that the analysis can be revised as more telephotometer data are generated.

E.1.2.3 Calculation of Worst-case Visual Impacts

The level-2 hand calculation procedure is demonstrated in this example. A comparison with the results obtained from reference tables and figures appears at the end of this example.

Determining plume-observer-object-sun geometry--Figure E-6 shows plume-observer orientations corresponding to the terrain elevation plots of figure E-3. Plan views of assumed geometries are shown in figures E-7 and E-8. From these figures, the following angles are determined:

Azimuth:

$A_1 = 270$
$A_2 = 292.5$
$A_3 = 157.5$

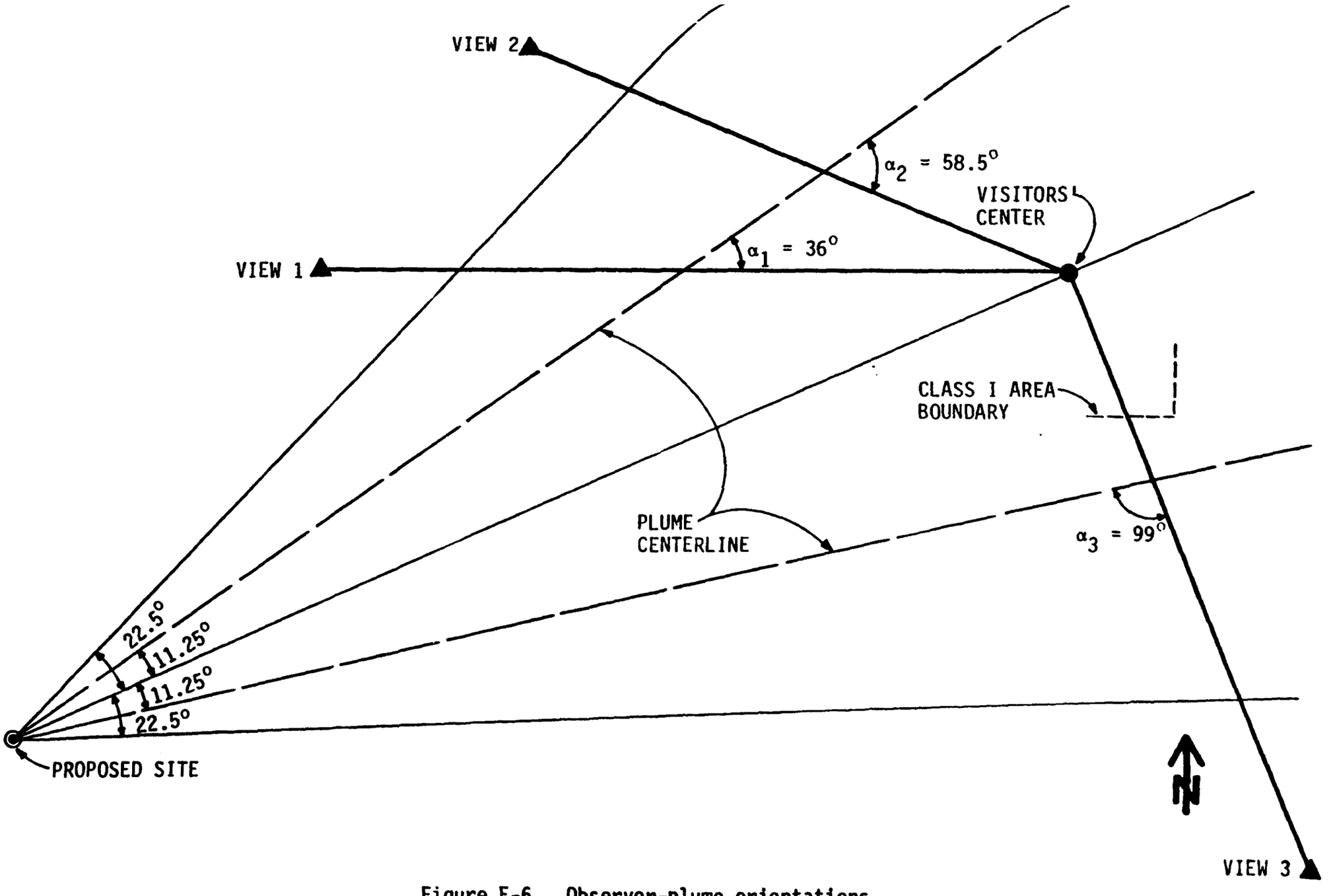

Figure E-6. Observer-plume orientations.

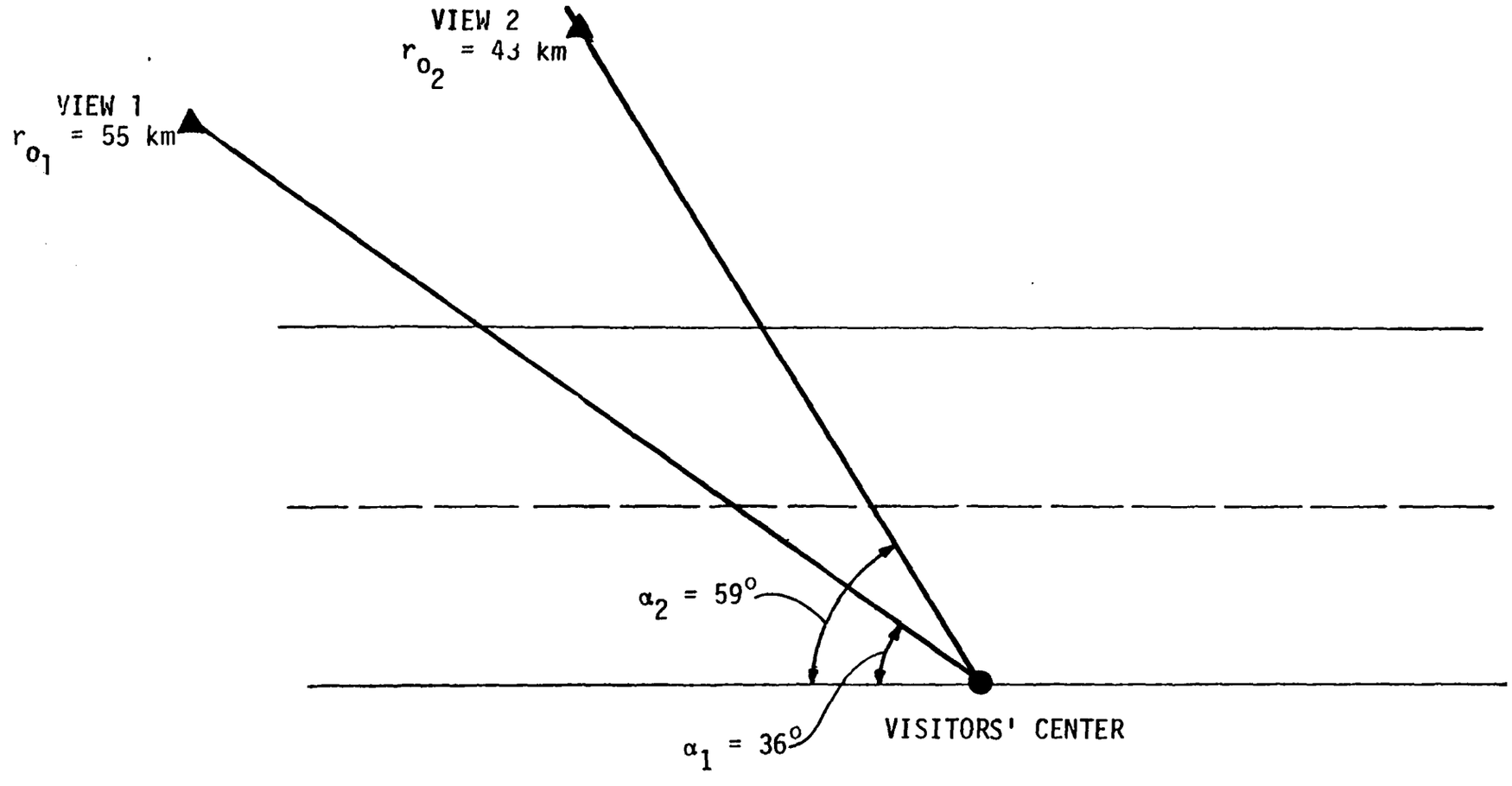

Figure E-7. Plan view of assumed geometries for views 1 and 2.

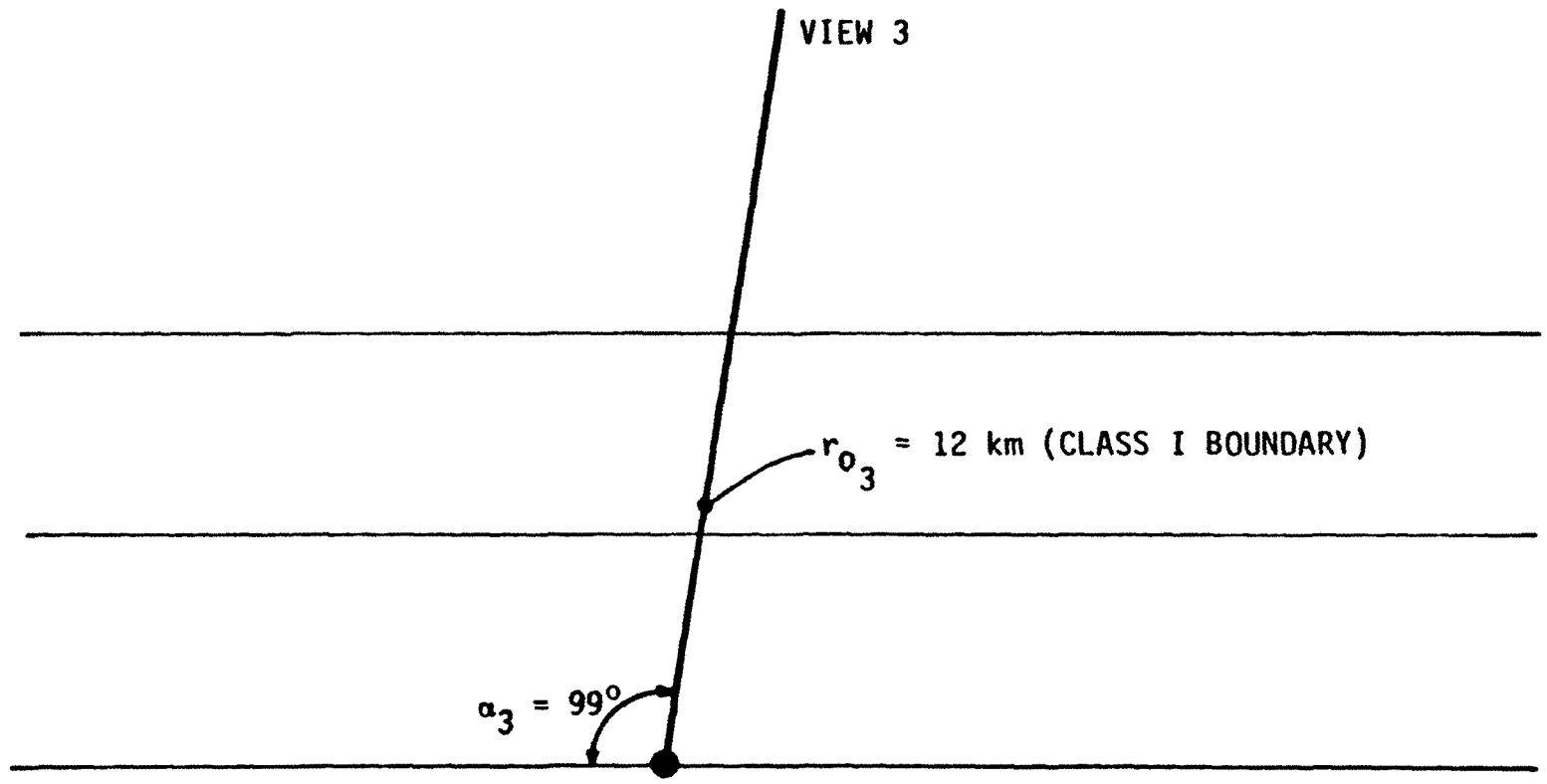

Figure E-8. Plan view of assumed geometry for view 3.

Angle to plume centerline:

$\alpha_1 = 36°$
$\alpha_2 = 58.5°$
$\alpha_3 = 99°$

We chose these lines of sight as the principal vistas for analysis because of the steep terrain and resulting obstructions surrounding the class I area. Therefore, rather than computing scattering angles for $\alpha = 30°$, 45°, 60°, 90°, 120°, 135°, and 150° for both plume centerlines, we chose to study azimuths including the three principal vistas plus three flanking lines of sight for each plume trajectory. Specifically, for the plume trajectory to the northwest of the class I area, azimuths corresponding to $\alpha = 30°$, 45°, and 90° are designated A_4, A_5, and A_6. For the plume trajectory passing to the south, azimuths A_7, A_8, and A_9 correspond to α values of 90°, 120°, and 135°. Thus, we computed azimuths for views 1 through 3 as follows:

Trajectory for views 1 and 2:

$\alpha_4 = 30° \rightarrow A_4 = 264°$
$\alpha_5 = 45° \rightarrow A_5 = 279°$
$\alpha_6 = 90° \rightarrow A_6 = 324°$

Trajectory for view 3:

$\alpha_7 = 90° \rightarrow A_7 = 166.5°$
$\alpha_8 = 120° \rightarrow A_8 = 136.5°$
$\alpha_9 = 135° \rightarrow A_9 = 121.5°$

We computed scattering angles for three scenarios corresponding to morning, midday, and late afternoon in early winter (December 21, Julian date 355). Values calculated for these scenarios are subscripted M, N, and A, respectively, in the calculations below:

$$\cos \theta_{ij} = -\cos \delta \sin \phi \cos A_i \cos H_j + \cos \delta \sin A_i \sin H_j + \sin \delta \cos \phi \cos A_i$$

$i = 1, 2, 3$

$j = M, N, A$

$$\delta = 23.45 \sin \left[360^\circ \frac{284 + n}{365}\right]$$

$n = 355$

ϕ = latitude = 39° N

$H_M = 45^\circ$ (for 9 a.m.)

$H_N = 0^\circ$ (for noon)

$H_A = -60^\circ$ (for 4 p.m.)

$A_1 = 270^\circ$

$A_2 = 292.5^\circ$

$A_3 = 157.5^\circ$

$A_4 = 264^\circ$

$A_5 = 279^\circ$

$A_6 = 324^\circ$

$A_7 = 166.5^\circ$

$A_8 = 136.5^\circ$

$A_9 = 121.5^\circ$

$$\delta = 23.45 \sin \left[360^\circ \left(\frac{284 + 355}{365}\right)\right]$$

$$= 23.45 \sin (270.2^\circ)$$

$$\delta = -23.45^\circ$$

$$\cos \theta_{1M} = -(\cos -23.45^\circ)(\sin 39^\circ)(\cos 270^\circ)(\cos 45^\circ) + (\cos -23.45^\circ)(\sin 270^\circ)(\sin 45^\circ) - (\sin -23.45^\circ)(\cos 39^\circ)(\cos 270^\circ)$$

$$\cos \theta_{1M} = -0.6487$$

$$\theta_{1M} = 130^\circ$$

Similarly, θ_{ij} values are derived for the other azimuth/time-of-day pairs, as shown in table E-3.

E.1.3 Calculation of Plume Optical Depth

The plume flux of scattering coefficient, $Q_{scat\text{-}part}$, is calculated with a particle-size distribution different from those used in the level-1 analysis. The values chosen here are expected to more accurately characterize emissions from this proposed project. Specifically:

$$Q_{scat\text{-}part} = \frac{1160\ Q_{part} \cdot \left(b_{scat}/V\right)}{\rho}$$

$$Q_{part} = 2.16 \text{ MT/day}$$
$$\rho = 2 \text{ g/cm}^3$$
$$DG = 1 \text{ } \mu\text{m}$$
$$\sigma_g = 2$$
$$b_{scat}/V = 0.05 \text{ (from figure 24)}$$

$$Q_{scat\text{-}part}\Big|_{0.55\ \mu m} = 63 \text{ m}^2/\text{s} \quad .$$

For the determination of NO_x concentration, we have

$$NO_x = \frac{6.17 \cdot Q_{NO_x}}{\sigma_z u x} \quad ,$$

TABLE E-3. VALUES OF θ_{ij}

	(A_i^j)								
j (H_j)	1 (270°)	2 (297.5°)	3 (157.5°)	4 (264°)	5 (279°)	6 (324°)	7 (166.5°)	8 (136.5°)	9 (121.5°)
M(45°)	130	151	24	125	139	164	32	15	22
N(0°)	90	110	35	85	98	136	30	50	62
A(60°)	37	60	76	32	46	91	67	97	111

Q_{NO_x} = 32.8 MT/day

σ_z u = 322 m^2/s (from table E-1)

x = 60 km

NO_x = 0.0105 ppm .

As the background ozone concentration (0.05 ppm) is greater than this calculated value for $[NO_x]$, we may assume complete conversion of NO to NO_2. Thus:

$$[NO_2]\Big|_{x = 60} = [NO_x]\Big|_{x = 60} = 0.0105 \text{ ppm} \quad .$$

Although we are concerned about nighttime stable transport of pollutants, as a check on the extent to which we may be overestimating $[NO_2]$ during daylight hours, we have also calculated $[NO_2]$ using the alternate formulation.

$$[NO_2] = 0.5\left[[NO_x] + h + j - \left\{([NO_x] + h + j)^2 - 4\,[NO_x]\,h\right\}^{1/2}\right] \quad .$$

Values of Z_s of 90°, 75°, 45° and 0° are computed, yielding the following:

Z_s	$[NO_2]$
90°	0.0105 ppm
75°	0.0093
45°	0.0080
0°	0.0077

Thus, even with the sun directly overhead (which would not occur for the latitude and season of concern), there is a relatively small difference in projected $[NO_2]$. For the remainder of the level-2 analysis, therefore, we will continue to use the more conservative value of 0.0105 ppm.

The optical thickness of the plume resulting from NO_2 is calculated for $\lambda = 0.40$, 0.55, and 0.70 μm, using the equation:

$$\tau_{NO_2} = 0.398\,[NO_2] \cdot x \cdot (b_{abs}/ppm)$$

$$[NO_2] = 0.0105 \text{ ppm}$$

$$x = 60 \text{ km}$$

$$(b_{abs}/ppm) = \begin{cases} 1.71 \text{ for } \lambda = 0.40 \text{ μm} \\ 0.31 \text{ for } \lambda = 0.55 \\ 0.017 \text{ for } \lambda = 0.70 \end{cases}$$

$\tau_{NO_2} = 0.429$ at $\lambda = 0.4$ μm

$\tau_{NO_2} = 0.078$ at $\lambda = 0.55$ μm

$\tau_{NO_2} = 0.00426$ at $\lambda = 0.7$ μm

Light scattering by sulfate aerosol is calculated under the 40 percent relative humidity assumption for the western United States. Thus,

$$Q_{scat\text{-}SO_4} = \frac{43.4 \cdot k_f \cdot Q_{SO_2}}{(k_f + k_d)(1 - RH/100)} \left\{1 - \exp\left[-0.48\left(k_f + k_d\right)\right]\right\}$$

$$k_d = {}^{V_d}/_{H_m} \cdot 3600$$

$k_f = 0.1$ %/hr (winter)

$V_d = 0.5$ cm/s

$H_m = 2000$ m*

$Q_{SO_2} = 10.4$ MT/day

RH = 40%

* Note from table E-2 that either 1000 or 2000 m could be assumed for H_m. In this equation, the higher value of Hm yields the most conservative result. Therefore, 2000 m has been used.

Therefore,

$$k' = k_f + k_d = 1.0\%/\text{hour}$$

and

$$Q_{scat\text{-}SO_4}\Big|_{\lambda=0.55\ \mu m} = 28.7\ m^2/s \quad .$$

Next, Q_{scat} wavelength dependence is determined via the equation

$$Q_{scat}\Big|_{\lambda} = Q_{scat}\Big|_{0.55\ \mu m} \cdot \left(\frac{\lambda}{0.55}\right)^{-n(DG,\sigma_g)} \quad ,$$

which is based on the proportionality of Q_{scat} and b_{scat}. Thus,

$$Q_{scat\text{-}part}\Big|_{\lambda=0.4} = Q_{scat\text{-}part}\Big|_{\lambda=0.55} \cdot \left(\frac{0.4}{0.55}\right)^{-n\ (1,2)}$$

$$n\ (1,2) = 0.2 \text{ (from table 4)}$$

$$Q_{scat\text{-}part}\Big|_{\lambda=0.55} = 63\ m^2/s$$

$$Q_{scat\text{-}part}\Big|_{\lambda=0.4} = 67 \quad .$$

Similarly,

$$Q_{scat\text{-}part}\Big|_{\lambda=0.7} = 60 \quad .$$

For $Q_{scat\text{-}SO_4}$, the size distribution has an assumed mass median diameter of 0.3 μm and σ_g of 2. Thus,

$$Q_{scat\text{-}SO_4}\Big|_{\lambda=0.4\ \mu m} = Q_{scat\text{-}SO_4}\Big|_{\lambda=0.55}\left(\frac{0.4}{0.55}\right)^{-n(0.3,2)}$$

$$Q_{scat\text{-}SO_4}\Big|_{\lambda=0.55} = 28.7\ m^2/s$$

$$n\ (0.3,2) = 1.6$$

$$Q_{scat\text{-}SO_4}\Big|_{\lambda\ =\ 0.4} = 47.8\ m^2/s \quad .$$

Similarly,

$$Q_{scat\text{-}SO_4}\Big|_{\lambda=0.7} = 19.5\ m^2/s \quad .$$

Optical thickness (τ) calculations are made using the equation

$$\tau_{part} = \frac{Q_{scat\text{-}part}}{(2\pi)^{1/2}\ \sigma_z u} \quad ,$$

and

$$\tau_{aerosol} = \frac{Q_{scat\text{-}part} + Q_{scat\text{-}SO_4}}{uH_m} \quad ,$$

where $\sigma_z u = 322\ m^2/s$ and $uH_m = 4000\ m^2/s$

Below are the tabulated values for τ for particulates, general haze, and NO_2 shown as a function of wavelength.

	0.4 μm	0.55 μm	0.70 μm
τ_{part}	0.083	0.078	0.074
$\tau_{aerosol}$	0.0287	0.0229	0.0199
τ_{NO_2}	0.429	0.078	0.00426

E.1.4 Phase Function Calculations

The wavelength, scattering angle, and particle-size-dependent phase function calculations are performed next.

$$b_{ext}(\lambda = 0.55\ \mu m) = \frac{3.912}{r_{v0}}$$

$$r_{v0} = 170\ km$$

$$b_{ext}(\lambda = 0.55) = 0.023\ km^{-1}$$

$$b_{scat}(\lambda = 0.55\ \mu m) = 0.95\ b_{ext}$$

$$b_{scat}(\lambda = 0.55) = 0.022\ km^{-1}$$

$$b_{ap} = 0.05\ b_{ext}$$

$$b_{ap} = 0.0012\ km^{-1}$$

$$b_R(\lambda = 0.55) = (11.62 \times 10^{-6} m^{-1}) \exp\left(-\frac{Z + 500}{9800}\right)$$

$$Z = 940\ m$$

$$b_R(\lambda = 0.55) = 1.0 \times 10^{-5}\ m^{-1} = 0.010\ km^{-1}$$

$$b_{sp}(\lambda = 0.55) = b_{scat} - b_R$$

$$b_{sp}(\lambda = 0.55) = 0.012\ km^{-1}$$

The attribution of b_{sp} to coarse and fine particles in 1/3 : 2/3 proportions gives:

$$b_{sp\text{-}coarse} = 0.004\ km^{-1}$$

$$b_{sp\text{-}submicron} = 0.008\ km^{-1}$$

Wavelength dependence is calculated as before, using:

$$b_{sp}(\lambda) = b_{sp}(\lambda{=}0.55\ \mu m)\left(\frac{\lambda}{0.55\ \mu m}\right)^{-n}$$

where

$$n_{coarse} = 0$$
$$n_{submicron} = 1.6$$
$$n_{Rayleigh} = 4.1$$
$$n_{average} = 0.2$$

The wavelength-specific b_{sp} values thus calculated are shown in table E-4 along with phase functions calculated for Rayleigh scattering according to

$$p(\Theta) = 0.75\ [1 + \cos^2\Theta] \text{ for all } \lambda$$

and extracted from appendix B for Mie scattering by coarse (DG = 6 μm) and fine (DG = 0.3 μm) mode particles.

Average $p(\lambda,\Theta)$ values are calculated according to

$$p(\lambda,\Theta)\Big|_{background} = \frac{\sum_{\substack{\text{Rayleigh,}\\ \text{coarse,}\\ \text{fine}}} b_{sp}(\lambda) \cdot p(\lambda,\Theta)}{\sum_{\substack{\text{Rayleigh,}\\ \text{coarse,}\\ \text{fine}}} b_{sp}(\lambda)}$$

Plume phase function values have also been taken from appendix B, for DG = 1 μm and $\sigma_g = 2$.

TABLE E-4. PHASE FUNCTIONS AND SCATTERING COEFFICIENTS FOR BACKGROUND AND PLUME

Scattering Component	λ (μm)	b_{scat} (km^{-1})	Phase Function $p(\lambda,\Theta)$ for Indicated Θ		
			36°	90°	130°
BACKGROUND					
Rayleigh Scattering					
Due to air molecules	0.40	0.037			
at site elevation	0.55	0.01	1.24	0.75	1.06
(n = 4.1)	0.70	0.0037			
Mie Scattering					
Submicron aerosol	0.40	0.013	2.87	0.276	0.157
DG = 0.3 μm	0.55	0.008	2.90	0.318	0.189
σ_g = 2.0	0.70	0.005	2.88	0.357	0.211
(n = 1.6)					
Mie Scattering					
Coarse aerosol	0.40	0.004	1.56	0.147	0.0552
DG = 6 μm	0.55	0.004	1.44	0.161	0.0529
σ_g = 2.0	0.70	0.004	1.61	0.167	0.0825
(n = 0)					
Total (average)	0.40	0.054	1.66	0.591	0.768
	0.55	0.022	1.88	0.486	0.560
	0.70	0.013	1.96	0.402	0.408
PLUME					
DG = 1 μm	0.40		2.22	0.203	0.159
σ_g = 2	0.55		2.45	0.219	0.142
	0.70		2.58	0.224	0.156

E.1.5 Calculating Plume Contrasts

Impacts are calculated for the range of scenarios described below. To eliminate repetition, only the impacts on the view to the west (A_1 = 270°) are presented here.

Azimuth = A_1 = 270°
α = 36°
θ_M = 130°
θ_N = 90°
α_A = 37°*
x = 60 km†

Stable plume conditions:

$$\tau_{NO_2} = \begin{matrix} 0.429 & \lambda = 0.40\ \mu m \\ 0.078 & \lambda = 0.55 \\ 0.004 & \lambda = 0.70 \end{matrix}$$

$$\tau_{part} = \begin{matrix} 0.083 & \lambda = 0.40\ \mu m \\ 0.078 & \lambda = 0.55 \\ 0.074 & \lambda = 0.70 \end{matrix}$$

* As $p(\lambda, \theta)$ values are given in appendix B only for even degree values of θ, subsequent calculations assume a θ_A = 36°.

† For each transport/azimuth scenario, x is taken to be the transport distance to the intersection of the plume centerline and the line of sight.

(Sulfate is not considered for the stable plume scenarios.)

Values of $\overline{p}_{plume}$ are taken from appendix B:

	Scenario Θ		
	M	N	A
λ	130°	90°	36°
0.40 μm	0.159	0.203	2.22
0.55	0.142	0.219	2.45
0.70	0.156	0.224	2.58

$\overline{\omega}_{background} = 0.95$

The value of b_{ext} is determined by summing the values for b (units of km^{-1}) shown below:

λ	b_R	$b_{sp\text{-}submicron}$	$b_{sp\text{-}coarse}$	b_{ap}	b_{ext}
0.40	0.037	0.013	0.004	0.001	0.055
0.55	0.010	0.008	0.004	0.001	0.023
0.70	0.004	0.005	0.004	0.001	0.014

Also, for calculating sky/terrain contrast reduction:

$r_o = 55$ km*

$C_o = -0.9$

$f_{obj} = 1$†

* From terrain elevation plot (figure E-3a).

† i.e., the entire plume is assumed to be between the mountains of view 1 and the Visitors' Center.

Intermediate calculations are made for the following parameters:

$$\bar{\omega}_{plume} = \frac{\tau_{part}}{\tau_{NO_2} + \tau_{part}}$$

$$= \begin{cases} 0.162 & \lambda = 0.40\ \mu m \\ 0.501 & \lambda = 0.55 \\ 0.946 & \lambda = 0.70 \end{cases}$$

$$\tau_{plume} = \frac{\tau_{NO_2} + \tau_{part}}{\sin \alpha}$$

$$= \begin{cases} 0.871 & \lambda = 0.40\ \mu m \\ 0.265 & \lambda = 0.55 \\ 0.134 & \lambda = 0.70 \end{cases}$$

$$r_p = \frac{0.199\ x}{\sin \alpha} = 20\ km \quad .$$

Given the above, plume contrast is calculated according to:

$$C_{plume} = \left[\frac{(\bar{p}\ \bar{\omega})_{plume}}{(\bar{p}\ \bar{\omega})_{background}} - 1\right]\left[1 - \exp(-\tau_{plume})\right]\left[\exp(-b_{ext}\ r_p)\right] \quad .$$

Scenario 1A--Morning, $\lambda = 0.55\ \mu m$:

$$C_{plume} = \left[\frac{(0.142)(0.501)}{(0.560)(0.95)} - 1\right]\left[1 - \exp(-0.265)\right]\left[\exp\ (-0.0230) \cdot (20)\right]$$

$$C_{plume} = -0.127 \quad .$$

Scenario 1B--Morning, $\lambda = 0.40$:

$$C_{plume} = \left[\frac{(0.159)(0.162)}{(0.768)(0.95)} - 1\right]\left[1 - \exp(-0.87)\right]\left\{\exp\left[(-0.055) \cdot (20)\right]\right\}$$

$$C_{plume} = -0.187 \quad .$$

Scenario 1C--Morning, $\lambda = 0.70$:

$$C_{plume} = \left[\frac{(0.156)(0.946)}{(0.408)(0.95)} - 1\right]\left[1 - \exp(-0.124)\right]\left\{\exp\left[(-0.014) \cdot (20)\right]\right\}$$

$$C_{plume} = -0.059 \quad .$$

E.1.6 Calculating Reduction in Sky/Terrain Contrast Caused By Plume

Using the above data, we calculate ΔC_r according to:

$$\Delta C_r = -C_o \exp(-b_{ext} r_o)\left[1 - \frac{1}{C_{plume} + 1} \exp(-f_{obj} \tau_{plume})\right] .$$

Scenario 1A--Morning, $\lambda = 0.55$ μm:

$$\Delta C_r = -(-0.9) \exp\left[-(0.0230) \cdot 55\right]\left\{1 - \frac{1}{(-0.127 + 1)} \exp\left[-1 \cdot (0.265)\right]\right\}$$

$$\Delta C_r = 0.031 \quad .$$

Scenario 1B--Morning, $\lambda = 0.40$ μm:

$$\Delta C_r = -(-0.9) \exp[-(0.055)(55)]\left\{1 - \frac{1}{(-0.187 + 1)} \exp[-1 \cdot (0.87)]\right\}$$

$$\Delta C_r = 0.021 \quad .$$

Scenario 1C--Morning $\lambda = 0.70$ μm:

$$\Delta C_r = -(-0.9) \exp[-(0.014)(55)]\left\{1 - \frac{1}{(-0.059 + 1)} \exp[-1 \cdot (0.134)]\right\}$$

$$\Delta C_r = 0.030$$

For the stable transport situation, we may summarize our results for the morning view toward the west as shown:

λ	C_{plume}	ΔC_r
0.40	-0.187	0.021
0.55	-0.127	0.031
0.70	-0.059	0.030

These values indicate that though significant reduction in visual range is not expected ($|\Delta C_r| < 0.1$), a perceptible yellow-brown plume is likely to be visible in some situations ($|C_{plume}| > 0.1$).

E.1.7 General Haze Effects

The same values for many parameters are used for assessing general haze effects. Aside from the differences in calculated values for optical thickness, the principal differences are

$$\tau_{plume} = \tau_{aerosol} = 0.0229$$

$$r_p = 50 \text{ km}$$

$$f_{obj} = r_o/100 \text{ km} = 0.55$$

$$\omega = 1 \quad .$$

For the westerly morning view at 0.55 μm, we have

$$C_{plume} = \left[\frac{(0.142)(1)}{(0.560)(0.95)} - 1\right]\left[1 - \exp(-0.0229)\right]\left[\exp(-0.0230 \cdot 50)\right]$$

$$= -0.005 \quad .$$

Also,

$$\Delta C_r = -(0.9)\left[\exp(-0.023 \cdot 55)\right]\left[1 - \frac{1}{-0.005 + 1} \exp\ (-0.55 \cdot 0.0229)\right]$$

$$= 0.002 \quad .$$

E.1.8 Comparison of Results with Reference Tables

The example described above corresponds reasonably closely to the hypothetical 500 Mwe power plant of appendix D, as shown in table E-5.

TABLE E-5. COMPARISON OF EXAMPLE POWER PLANT EMISSIONS AND APPENDIX D POWER PLANT EMISSIONS

	Emissions	
	Hypothetical 500 Mwe Power Plant	Example Power Plant
Q_{part} (MT/day)	1.6	2.2
Q_{NO_x} (MT/day)	14.5	10.4
Q_{SO_2} (MT/day)	29.0	32.8

The scenario descriptions, though somewhat different, are still close enough to provide useful results, as shown in table E-6.

TABLE E-6. COMPARISON OF SELECTED SCENARIO DESCRIPTORS

	Appendix D	Example
RH	40%	40%
$[O_3]_{background}$	0.04 ppm	0.05 ppm
Simulation date/time	23 September/1000	21 December/0900
Scattering angle	90°	130°
Wind speed	2.5 m/s	2 m/s
Background visual range	100 and 200 km	170 km

At a downwind distance of 50 km, with a 200 km visual range, appendix D shows a blue-red ratio of 0.892, which indicates that the plume would probably be perceptible. This agrees quite favorably with the hand calculated value of 0.864. The modeled plume contrast of -0.031 at 0.55 μm is significantly lower than the hand calculated value of -0.13. This is due to the differences in input parameters between the hand calculation and the model. Also, the hand calculation procedure is conservative for this backward scatter case ($\theta = 130°$) since multiple scattering is ignored. The $\Delta E(L^*a^*b^*)$ value of 4.5 (dropping to 3.37 by the 75 km downwind distance) indicates a marginally perceptible plume. Visual range reduction is insignificant at 0.6 percent, a result which agrees with the hand calculation showing ΔC_r of 0.031 at 0.55 μm.

The downwind effect profiles shown in the plots in appendix D indicate that, at downwind distances of 50 to 75 km, model results are relatively insensitive to downwind distance for all parameters except blue-red ratio, which peaks fairly sharply at approximately 25 km. The difference in the blue-red ratio plots between the 2.5 and 5 m/s scenarios indicates a substantial sensitivity to wind speed, a factor that contributes to the difference in the magnitude of results between the hand calculations and appendix D results. The assumption of 100% NO-NO_2 conversion also contributes to this difference.

In general, the results above indicate a potential concern only for the visibility effects of NO_x emissions from the proposed facility. Particulate and SO_2 emissions appear unlikely to cause perceptible impairment of visibility in either general haze or coherent plume scenarios.

Additional (level-3) analysis is probably warranted for this facility, if design parameters (specifically NO_x emissions rates) remain as originally stated. In particular, the significance of potential effects can be better evaluated given a more thorough analysis of the frequency of occurrence of meteorological regimes associated with perceptible impacts in and around the class I area, and a more precise determination of anticipated NO_x chemistry in the plume.

E.2 EXAMPLE 2--CEMENT PLANT AND RELATED OPERATIONS

A cement plant has been proposed, along with related quarrying, materials handling, and transportation facilities, for a location 20 km away from a class I area. Terrain in the vicinity is relatively flat, and no external vistas from the class I area (a national park) are considered integral to park visitors' experiences. Visibility within the park boundaries is of concern, however.

The proposed project would cause both elevated emissions from numerous process points and ground-level emissions of fugitive dust. Estimated emissions rates and particle-size distributions are shown in table E-7.

For the level-1 screening, a downwind distance (x) of 20 km is used, along with the corresponding σ_z, for F stability of 46 m. As before, the calculations are carried out in sequence.

E.2.1 Level-1 Analysis

$$p = \frac{2.0 \times 10^8}{\sigma_z \; x}$$

$x = 20$ km

$\sigma_z = 60$ m

$$p = 1.67 \times 10^5$$

$$\tau_{part} = 10^{-6} \; p \cdot Q_{part}$$

$Q_{part} = 4.93$ MT/day*

$(= 4.54 + .395)$

---

* For the initial screening, it is conservatively assumed that the emissions are released from a common point.

TABLE E-7. ESTIMATED PROJECT EMISSIONS

Emissions	Emissions Rates
Particulate Matter	
Process Sources	0.395 MT/day
(effective stack height = 50 m)	
DG = 1 μm	
σ_g = 2	
ρ = 2 gm/cm^3	
Fugitive Emissions	4.54 MT/day
DG = 10 μm	
σ_g = 2	
ρ = 2 gm/cm^3	
Sulfur Oxides	7.26 MT/day
(effective stack height = 50 m)	
Nitrogen Oxides	2.72 MT/day
(effective stack height = 50 m)	

$$\tau_{part} = 0.822$$

$$\tau_{NO_2} = 1.7 \times 10^{-7} \cdot p \cdot Q_{NO_x}$$

$$Q_{NO_x} = 2.72 \text{ MT/day}$$

$$\tau_{NO_2} = 0.0771$$

$$\tau_{aerosol} = 1.06 \times 10^{-5} \cdot r_{v0} \cdot (Q_{part} + 1.31 \cdot Q_{SO_2})$$

$$r_{v0} = 60 \text{ km}^*$$
$$Q_{part} = 4.93$$
$$Q_{SO_2} = 7.26$$

$$\tau_{aerosol} = 0.00918$$

$$C_1 = \frac{\tau_{NO_2}}{\tau_{part} + \tau_{NO_2}} \left[1 - \exp\left(-\tau_{part} - \tau_{NO_2}\right)\right] \left[\exp\ -0.78\ x/r_{v0}\right]$$

$$C_1 = -0.0392$$

$$C_2 = \left[1 - \frac{1}{C_1 + 1} \exp\left(-\tau_{part} - \tau_{NO_2}\right)\right]\left[\exp\left(-1.56\ x/r_{v0}\right)\right]$$

$$C_2 = 0.343$$

$$C_3 = 0.368\ [1 - \exp\ (-\tau_{aerosol})]$$

$$C_3 = 0.00336$$

---

* Taken from figure 12, text page 56, for the proposed location.

The values for C_1, C_2, and C_3 are characteristic of major particulate sources with relatively low NO_x and SO_x emissions. Both C_1 and C_3 (NO_2 discoloration and general haze indicators) are sufficiently low to indicate relatively little possibility of perceptible impact. However, C_2 indicates the potential for a perceptible particulate plume. It should be noted, however, that the level-1 calculations were based on the following two specific conservative assumptions:

> All particulate emissions are assumed to have been released from a common point, resulting in the creation of a single, coherent plume. Most of these emissions are, in fact, fugitive emissions released near ground level.

> Particle scattering efficiency is assumed to be significantly higher than would be expected for the DG = 10 μm fugitives.

Because level-1 procedures cannot address these issues, a level-2 assessment is indicated. It is worth noting, however, that plume discoloration resulting from NO_2 is unlikely, as are problems associated with general haze. Therefore, the level-2 analysis need only concentrate on those parameters related to estimation of particulate plume effects.

E.2.2 Level-2 Analysis

An analysis similar to that shown for example 1 (section E.1.2.2) indicates that a D stability 1 m/s wind speed scenario corresponds most closely to the 1-percentile worst-case diffusion. Because there are no terrain features that might affect the flow of pollutants toward the park, the transport distance for analysis remains at 20 km. Therefore, as σ_z for stability class D at 20 km is 200 m, the reasonable worst-case $\sigma_z u$ value is 200 m^2/s.

The park itself is also relatively flat, with sizable (20 km) internal open vistas. Because all internal vistas are potentially impacted at all times of the day, scattering angles between 0° and 180° are of potential concern. A range of angles covering backscatter, forward scatter, and side lighting of the plume are selected for analysis.

As a means of simplifying the level-2 screening calculations, it is assumed (as in level-1) that for calculation of visibility impacts, all emissions are released from a common point. General haze has been eliminated in the level-1 screening; therefore, SO_x emissions need not be considered, because the level-2 procedures do not incorporate short-term sulfate formation. NO_2 formation, on the other hand, must be considered, because of the effect of NO_2 on plume perceptibility.

Particulates constitute the major potential problem for the proposed project, as indicated by the C_2 value of 0.343. There are two major groups of particulate emissions, each of which warrants separate treatment. Process emissions constitute a relatively small proportion of the total mass emissions rate (< 10%); however, their size distribution (DG = 1, σ_g = 2) has a much greater scattering efficiency than the larger, fugitive emissions (DG = 10 σ_g = 2).* To distinguish between these emissions types, the calculations below have various parameters that are subscripted "proc" and "fug", to indicate the process (fine) emissions and fugitive (coarse) emissions, respectively.

The calculations of particulate impacts begin with determination of plume optical depth, based on the equation

---

* This example is based, in part, on cement plants, which will typically have bag-house controlled process emissions (and therefore no coarse particle emissions) and fugitive emissions, which are generally large particles. Fugitive emissions result from materials handling, quarrying, haul roads, and so on.

$$Q_{scat\text{-}part} = \frac{1160\ Q_{part}\ \ b_{scat}/v}{\rho} \quad .$$

Both Q_{part} and b_{scat}/v take different values for the different types of emissions. Therefore $Q_{scat\text{-}part}$ is determined separately for each type of emissions.

$$Q_{part\text{-}proc} = 0.395 \text{ MT/day}$$
$$DG_{proc} = 1 \text{ μm}$$
$$\sigma_{g\ proc} = 2$$
$$\rho_{proc} = 2 \text{ gm/cm}^3$$
$$(b_{scat}/v)_{proc} = 0.05^*$$

$$Q_{scat\text{-}part\ proc} = 11.5 \text{ m}^2/\text{s}$$

$$Q_{part_{fug}} = 4.54 \text{ MT/day}$$
$$DG_{fug} = 10 \text{ μm}$$
$$\sigma_{g_{fug}} = 2$$
$$\rho_{fug} = 2 \text{ gm/cm}^3$$
$$b_{scat}/v_{fug} = 0.004^*$$

$$Q_{scat\text{-}part\ fug} = 10.5 \text{ m}^2/\text{s}$$

Note that despite the relative difference in mass emission rates, the process emissions dominate the scattering coefficient flux at the assumed emissions point. For simplicity, it will be assumed that all emitted particles remain suspended in the plume. This conservative assumption need not be made; it is possible, though somewhat tedious, to calculate the settling of large particles from the plume.† On the other hand, if the

---

* From figure 24.

† Stokes settling velocities can be calculated, according to the equation $c_s = 3 \times 10^{-3}\ \rho d^2$, where c_s is the settling velocity (in cm/s), ρ is the particle density (in gm/cm^3), and d is the particle diameter (in μm). This equation is an approximation of the Stokes velocity equation, and it is approximately accurate for particles larger than about 2 μm.

less conservative meteorological scenarios of this level-2 analysis and the lower scattering efficiency of large particles result in calculated effects below perceptible levels, then no purpose is served by projecting settling effects. Should potential effects be projected under assumed conditions, then the decision can be made either to rework the level-2 analysis with consideration for settling or to go to a level-3 analysis.

Consideration of table 4 also indicates a possible simplification of calculations. Because of the size of particles emitted, there is little wavelength dependence of scattering coefficients. Therefore, we may restrict consideration of scattering effects to a single wavelength, $\lambda = 0.55$ μm.

Proceeding with the analysis, we have:

$$[NO_x] = \frac{6.17\ Q_{NO_x}}{\sigma_z u\ x}$$

$Q_{NO_x} = 2.72$ MT/day
$\sigma_z u = 200\ m^2/s$
$x = 20$ km

$[NO_x] = 0.0042$ ppm

Even at extremely low background $[O_3]$, it should be assumed that total conversion of NO to NO_2 will occur at concentrations below 0.02 ppm. Therefore,

$[NO_2] = 0.0042$ ppm

Continuing, we have:

$$\tau_{NO_2} = 0.398\ [NO_2]\ (b_{abs}/ppm)$$

$$b_{abs}/ppm\big|_{0.55} = 0.31$$

$$\tau_{NO_2} = 0.010$$

As stated previously, sulfate impacts need not be considered. Therefore, we need consider only τ_{part}.

$$\tau_{part} = \frac{Q_{scat\text{-}part}}{(2\pi)^{1/2}\sigma_z u}$$

$$= \frac{Q_{scat\text{-}part\ proc} + Q_{scat\text{-}part\ fug}}{(2\pi)^{1/2}\sigma_z u}$$

$$Q_{scat\text{-}part\ proc} = 11.5\ m^2/s$$
$$Q_{scat\text{-}part\ fug} = 10.5\ m^2/s$$
$$\sigma_z u = 200\ m^2/s$$

$$\tau_{part} = 0.0439$$

$$b_{ext}\ (\lambda=0.55\ \mu m) = \frac{3.912}{r_{v0}}$$

$$r_{v0} = 60$$

$$b_{ext}\big|_{0.55} = 0.065$$

$$b_{scat} = 0.95\ b_{ext}$$

$$b_{scat} = 0.062\ km^{-1}$$

$$b_{sp} = b_{scat} - b_R$$

$$b_R\Big|_{z = 400\ m} \tilde{=} 1.06 \times 10^{-5} m^{-1}$$

$$\tilde{=} 0.011\ km^{-1}$$

$$b_{sp} = 0.051$$

$$b_{sp_{submicron}} = 0.67\ b_{sp} = 0.034\ km^{-1}$$

$$b_{sp_{coarse}} = 0.33\ b_{sp} = 0.017\ km^{-1}$$

Phase functions are determined for the background air mass and the plume at scattering angles of 22°, 44°, 90°, and 136°, as shown in table E-8. Because of the assumed bimodal particle-size distribution, average values for the plume phase function are calculated. These plume average values are weighted using the values of $Q_{scat\text{-}part\ proc}$ and $Q_{scat\text{-}part\ fug}$ according to the equation

$$p(\lambda,\Theta)_{\text{av plume}} =$$

$$\frac{Q_{scat\text{-}part\ proc}\ p(\lambda,\ \theta)_{proc} + Q_{scat\text{-}part\ fug}\ p(\lambda,\ \theta)_{fug}}{Q_{scat\text{-}part\ proc} + Q_{scat\text{-}part\ fug}}$$

Finally, we determine C_{plume} and ΔC_r using the following values:

$$\alpha = 90°$$

$$\tau_{part} = 0.044$$

$$\tau_{NO_2} = 0.010\ .$$

TABLE E-8. BACKGROUND AND PLUME ATMOSPHERE PHASE FUNCTIONS AND SCATTERING COEFFICIENTS (λ = 0.55 μm)

Background Atmosphere Scattering Component	b_{scat} (km^{-1})	Phase Function $p(\lambda,\Theta)$ for Indicated Θ			
		22°	44°	90°	136°
Rayleigh Scattering Due to air molecules at site elevation	0.011	1.39	1.12	0.75	1.125
Mie Scattering					
Submicron Aerosol DG = 0.3 μm σ_g = 2.0	0.034	5.36	2.01	0.318	0.188
Coarse Aerosol DG = 6 μm σ_g = 2.0	0.017	3.20	1.08	0.160	0.0740
Total (average)	0.062	4.06	1.60	0.351	0.323

Plume Scattering Component	$Q_{scat-part}$	Phase Function $p(\lambda,\Theta)$ for Indicated Θ			
		22°	44°	90°	136°
Process Emissions DG = 1 μm σ_g = 2	11.5	5.92	1.57	0.218	0.175
Fugitive Emissions DG = 10 μm σ_g = 2	10.5	2.70	1.28	0.138	0.0344
Plume average	22	4.38	1.43	0.180	0.108

$$\tau_{plume} = \frac{\tau_{NO_2} + \tau_{part}}{\sin \alpha} = 0.054$$

$$r_p = \frac{0.199x}{\sin \alpha} = 4 \text{ km}$$

$$b_{ext} = 0.065$$

$$r_o = 5 \text{ km}$$

$$C_o = -0.9$$

$$f_{obj} = 1$$

$$\omega_{plume} = \frac{\tau_{part}}{\tau_{NO_2} + \tau_{part}} = 0.814$$

$$\omega_{bkg} = 0.95$$

C_{plume} and ΔC_r are determined according to:

$$C_{plume} = \left[\frac{(p\omega)_{plume}}{(p\omega)_{bkg}} - 1\right]\left[1 - \exp\left(-\tau_{plume}\right)\right]\left[\exp\left(-b_{ext} r_p\right)\right]$$

$$\Delta C_r = -C_o\left[\exp\left(-b_{ext} r_o\right)\right]\left[1 - \frac{1}{C_{plume} + 1}\exp\left(-f_{obj}\tau_{plume}\right)\right]$$

On the basis of these equations, and the $p(\lambda, \Theta)$ from table E-8, we compute the impact projections shown in table E-9.

TABLE E-9. PROJECTED PLUME CONTRAST AND CONTRAST REDUCTION FOR EXAMPLE 2 (λ = 0.55 μm)

	Scattering Angle (Θ)			
	22°	44°	90°	136°
C_{plume}	-0.003	-0.009	-0.023	-0.029
ΔC_r	0.032	0.028	0.020	0.016

These results show that visibility impacts would probably be imperceptible for the situation described. Therefore, further analysis is not warranted. Note that the combined effects of the less conservative meteorology (D,1 versus F,2), the consideration of particle-size distribution, and the more precise formulation of visibility impact parameters in level-2 have provided a substantially different description of expected impacts from that which might be extracted from the level-1 results.

REFERENCES

Altshuller, A. P. (1979), "Model Predictions of the Rates of Homogeneous Oxidation of Sulfur Dioxide to Sulfate in the Troposphere," Atmos. Environ., Vol. 13, pp. 1653-1661.

Briggs, G. A. (1972), "Discussion on Chimney Plumes in Neutral and Stable Surroundings," Atmos. Environ., Vol. 6, pp. 507-610.

Briggs, G. A. (1969), "Plume Rise," U.S. Atomic Energy Commission Critical Review Series, TID-25075, National Technical Information Service, Springfield, Virginia.

Briggs, G. A. (1971), "Some Recent Analyses of Plume Rise Observations," Proc. of the Second International Clean Air Congress, H. M. Englund and W. T. Berry, eds., (Academic Press, New York, New York), pp. 1029-1032.

Dixon, J. K. (1940), "Absorption Coefficient of Nitrogen Dioxide in the Visible Spectrum," J. Chem. Phys., Vol. 8, pp. 157-160.

Duffie, J. A., and W. A. Beckman (1974), Solar Energy Thermal Processes, (John Wiley and Sons, New York, New York).

Holzworth, G. C. (1972), "Mixing Heights, Wind Speeds, and Potential for Urban Air Pollution throughout the Contiguous United States," AP-101, Office of Air Programs, Environmental Protection Agency, Research Triangle Park, North Carolina.

Land, E. H. (1977), "The Retinex Theory of Color Vision," Sci. Am., Vol. 237, pp. 108-128.

Latimer, D. A., et al. (1978), "The Development of Mathematical Models for the Prediction of Anthropogenic Visibility Impairment," EPA-450/3-78-110a, b, and c, available from NTIS as PB 293118 SET.

Latimer, D. A., T. C. Daniel, and H. Hogo (1980), "Relationships between Air Quality and Human Perception of Scenic Areas," Publication no. 4323, American Petroleum Institute, Washington, D.C.

Latimer, D. A., et al. (1980a), "Modeling Visibility," invited paper presented at American Meteorological Society/Air Pollution Control Association, Second Joint Conference on Applications of Air Pollution Meteorology, 24-27 March, New Orleans, Louisiana.

Latimer, D. A., et al. (1980b), "An Assessment of Visibility Impairment in Capitol Reef National Park Caused by Emissions from the Hunter Power Plant," EF80-43, Systems Applications, Incorporated, San Rafael, California.

Liu, M. K., and D. R. Durran (1977), "The Development of a Regional Air Pollution Model and Its Application to the Northern Great Plains," EPA-908/1-77-001, U.S. Environmental Protection Agency, Region VII, Denver, Colorado.

Malm, W. C., et al. (1979), "Visibility in the Southwest," unpublished manuscript.

Middleton, W.E.K. (1952). Vision Through the Atmosphere (University of Toronto Press, Toronto, Canada

Randerson, D. (1972), "Temporal Changes in Horizontal Diffusion Parameters of a Single Nuclear Debris Cloud," J. Appl. Meteor., Vol. 11, pp. 670-673.

Schulz, E. J., R. B. Engdahl, and T. T. Frankenberg (1975), "Submicron Particles from a Pulverized Coal Fired Boiler," Atmos. Environ., Vol. 9, pp. 111-119.

Singh, H. B., F. L. Ludwig, and W. B. Johnson (1978), "Tropospheric Ozone: Concentrations and Variabilities in Clean Remote Areas," Atmos. Environ., Vol. 12, pp. 2185-2196.

Trijonis, J., and D. Shapland. (1979), "Existing Visibility Levels in the U.S.," EPA-450/5-79-010, U.S. Environmental Protection Agency, Research Triangle Park, North Carolina.

Turner, D. B. (1969), "Workbook of Atmospheric Dispersion Estimates," U.S. Department of Health, Education, and Welfare, Public Health Service Publication No. 999-AP-26.

Whitby, K. T., and G. M. Sverdrup (1978), "California Aerosols: Their Physical and Chemical Characteristics," ACHEX Hutchinson Memorial Volume, Particle Technology Laboratory Publication Number 347, University of Minnesota, Minneapolis, Minnesota.

Williams, M. D., E. Treiman, and M. Wecksung (1980), "Plume Blight Visibility Modeling with a Simulated Photograph Technique," J. Air Pollut. Contr. Assoc., Vol. 30, pp. 131-134.

TECHNICAL REPORT DATA
(Please read Instructions on the reverse before completing)

1. REPORT NO.	2.	3. RECIPIENT'S ACCESSION NO.
EPA-450/4-80-031		

4. TITLE AND SUBTITLE	5. REPORT DATE
WORKBOOK FOR ESTIMATING VISIBILITY IMPAIRMENT	November 1980
	6. PERFORMING ORGANIZATION CODE

7. AUTHOR(S)	8. PERFORMING ORGANIZATION REPORT NO.
Douglas A. Latimer and Robert G. Ireson	

9. PERFORMING ORGANIZATION NAME AND ADDRESS	10. PROGRAM ELEMENT NO.
Systems Applications, Inc. 950 Northgate Drive San Rafael, California 94903	11. CONTRACT/GRANT NO. 68-02-0337

12. SPONSORING AGENCY NAME AND ADDRESS	13. TYPE OF REPORT AND PERIOD COVERED
Office of Air Quality Planning and Standards U. S. Environmental Protection Agency Research Triangle Park, North Carolina 27711	14. SPONSORING AGENCY CODE

15. SUPPLEMENTARY NOTES

16. ABSTRACT

This workbook is designed to provide three screening procedures to assist in determining the potential impacts of an emissions source on a Federal Class I area's visibility. It does not address the cumulative impacts of multiple sources on regional haze. A level-1 analysis involves a series of conservative screening tests to eliminate sources with little potential for visibility impairment during hypothetical worst-case meteorological conditions. If impairment is indicated, a more resource intensive level-2 analysis is warranted. If both analyses indicate impairment, a level-3 analysis using a plume visibility model should be used. Two examples applications are provided; for a coal-fired power plant and a cement plant.

17. KEY WORDS AND DOCUMENT ANALYSIS

a. DESCRIPTORS	b. IDENTIFIERS/OPEN ENDED TERMS	c. COSATI Field/Group
Air Pollution Meteorology Atmospheric Diffusion Air Quality Modeling Visibility Sulfates Aerosols	New Source Review Point Sources	13 B 4 A 4 B

18. DISTRIBUTION STATEMENT	19. SECURITY CLASS *(This Report)*	21. NO. OF PAGES
RELEASE TO THE PUBLIC	None	390
	20. SECURITY CLASS *(This page)*	22. PRICE

EPA Form 2220-1 (Rev. 4-77) PREVIOUS EDITION IS OBSOLETE